Max-Planck-Institut für Biochemie
Abteilung Strukturforschung

Structural Investigations of Coagulation Factors

Pablo Fuentes-Prior

Vollständiger Abdruck der von der Fakultät für Chemie der Technischen Universität München zur Erlangung des akademischen Grades eines

Doktors der Naturwissenschaften

genehmigten Dissertation.

Vorsitzender: Univ.-Prof. Dr. Johannes Buchner

Prüfer der Dissertation:

1. apl. Prof. Dr. Dr. h.c. Robert Huber
2. Univ.-Prof. Dr. Wolfgang Hiller
3. apl. Prof. Dr. Wolfram Bode,
   Ludwig-Maximilians-Universität München

Die Dissertation wurde am 15.11.2000 bei der Technischen Universität München eingereicht und durch die Fakultät für Chemie am 17.05.2001 angenommen.

a los cubanos, en su mayoría anónimos, que hicieron mucho o poco
para que la ley ley primera de la república cubana
fuera “el culto de los cubanos a la dignidad plena del hombre”
–a mis padres,

a los que –quizás– puedan hacer realidad el sueño de martí
–para mi hijo,

y para maría del pilar

Chapter 2: Structural Basis for the Membrane Binding Ability of Coagulation Factor V: Crystal Structures of Human Factor V C2 Domain

Chapter 3: Thrombin Inhibition: Crystal Structure of the Thrombin-Triabin Complex

Chapter 4: Structural Basis for the Anticoagulant Activity of Thrombomodulin–Bound Thrombin: Crystal Structure of the Human α-Thrombin–TME456 Complex

ABP: actin-binding protein
AMP, ADP, ATP: adenosine mono-, di- and triphosphate
AT: antithrombin
BBP: bilin binding protein
BPTI: bovine pancreatic trypsin inhibitor
ECM: extracellular matrix
EGF: epidermal growth factor
EGR: L-Glu-Gly-L-Arg chloromethyl ketone
F1, F2: (pro)thrombin activation fragments 1 and 2
FIX, FIXa: coagulation factor IX, activated factor IX
FV, FVa: coagulation factor V, activated factor V
FVII, FVIIa: coagulation factor VII, activated factor VII
FVIII, FVIIIa: coagulation factor VIII, activated factor VIII
FX, FXa: coagulation factor X, activated factor X
FXI, FXIa: coagulation factor XI, activated factor XIa
FXII, FXIIa: coagulation factor XI, activated factor XIa
FXIII, FXIIIa: coagulation factor XIII, activated factor XIIIa
Gas6, Gas6: growth-arrest specific gene 6 and product thereof
GP: glycoprotein
HMWK: high molecular weight kininogen
MAD: multiple-wavelengths anomalous diffraction
NMR: nuclear magnetic resonance
NO: nitric oxide
NP: nitrophorin
OBP: odorant binding protein
PAI: plasminogen-activator inhibitor
PAR: protease activated receptor
PC, APC, PCI: protein C, activated protein C, protein C inhibitor
PEG: polyethylene glycol
PKC: protein kinase C
PLA_2: phospholipase A_2
PLC: phospholipase C
PPACK: D-Phe-Pro-L-Arg chloromethyl ketone
PS, (P_LS, P_DS): phosphatidylserine, (phosphatidyl-L-serine, phosphatidyl-D-serine)
RBP: retinol binding protein
r.m.s.d.: root-mean-square deviation
TF, TFPI: tissue factor, tissue factor pathway inhibitor
TM: thrombomodulin
t-PA: tissue-type plasminogen activator
TXA_2: thromboxane A_2
u-PA: urokinase-type plasminogen activator
vWf: von Willebrand factor

Chapter 1

The Coagulation Cascade

"Blut ist ein ganz besondrer Saft."

Johann Wolfgang Goethe, "Faust – Der Tragödie Erster Teil"

"Кровъ – великое дело, –неизвестно к чему весело сказал Воланд…"

Михаил Булгаков, "Мастер и Маргарита"

1.1. The Coagulation Cascade – An Overview

Life of higher organisms depends on the presence of a finely branched-out (fractal) circulatory system capable of rapidly delivering oxygen and nutrients to all body cells, and collecting their catabolites. In response to vascular injury, the body must therefore tightly regulate the formation of a **hemostatic plug** while preventing unrestrained intravascular clot development and vessel occlusion. Central to this complex and vital process is the interplay of the blood vessel wall, **platelets** and other blood cells, as well as many soluble plasma proteins. Their coordinated interactions allow **hemostasis** (closure of the injured site with prevention of further blood loss), **thrombosis** (formation of blood clots) and **fibrinolysis** (dissolution of the fibrin clot). (For reviews see (Davie et al., 1991; Furie and Furie, 1988; Kalafatis et al., 1997; Mann and Lorand, 1993)).

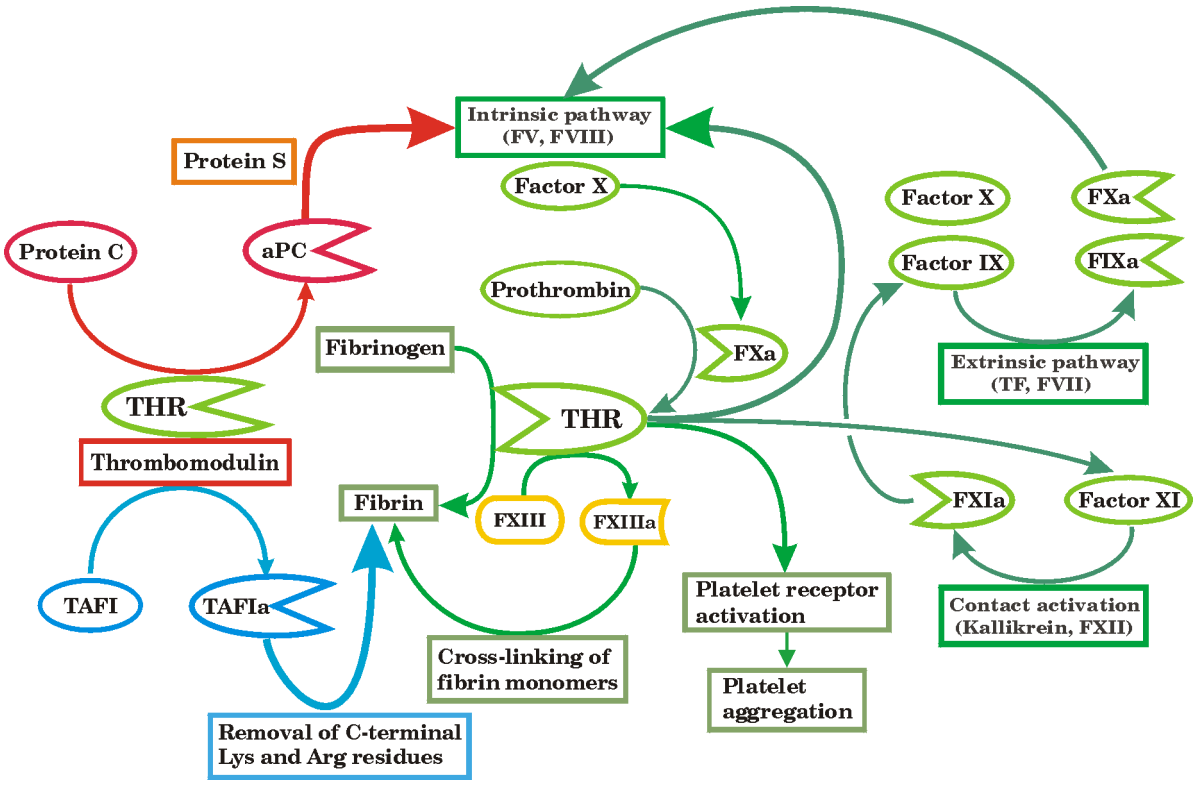

Fig. 1.1: Schematic representation of the coagulation cascade. Only the major reactions resulting in the generation or stabilization of the blood clot (green arrows), the antifibrinolytic pathway initiated with the activation of TAFI (blue arrows), and the anticoagulant protein C pathway (red arrows) are indicated in this figure. THR: thrombin. See text for details.

Resting platelets are small (approximately 2 μm in diameter, surface area about 20 μm^2) non-nucleated blood cell particles with a characteristic discoid shape. In resting platelets, a striking asymmetry in the phospholipid composition is generated by an **aminophospholipid translocase**, a putative Mg^{2+}-dependent ATPase that specifically transports the aminophospholipids **phosphatidylserine** (PS) and **phosphatidylethanolamine** to the inner (cytosolic) bilayer leaflets (Devaux, 1991; Seigneuret and Devaux, 1984); for reviews see (Devaux, 1992; Dolis et al., 1997). Following injury to a blood vessel, platelets rapidly adhere to **collagen** fibers at the site of exposed subendothelial matrix in the vessel wall and aggregate to form a temporary, loose platelet plug (for a recent review see (Shattil et al., 1998)). Upon aggregation, platelets become activated and secrete molecules from large intracellular vesicles termed **granules**. The **α granules** contain among other active substances the major soluble adhesion molecules **fibrinogen** (section 1.5.1.) and **thrombospondin**, as well as coagulation **factor V** (1.3.4.); the **dense granules** release **adenosine diphosphate** (ADP), **thromboxane A_2** (TXA_2) and **serotonin**, which have an autocrine/paracrine effect in amplifying platelet activation (see also sections 1.4.1. and 1.4.2.).

Activation brings about profound changes in the form and phospholipid composition of platelets, which become more spherical and form **filodopodia**-like structures (Siess, 1989; Zucker and Nachmias, 1985), with a concomitant two- to fourfold increase in their surface areas (Bevers et al., 1985; Zwaal et al., 1998). Mostly relevant for the subsequent reactions that result in blood clot formation, an intracellular membrane-associated protein known as "**scramblase**" destroys the asymmetry in the phospholipid composition by translocating the procoagulant aminophospholipids –in particular phosphatidylserine– to the outer membrane surface (Basse et al., 1996); for recent reviews see (Bevers et al., 1999; Zwaal et al., 1998; Zwaal and Schroit, 1997). Enrichment in phosphatidylethanolamine is also achieved by direct phospholipid transfer from the monolayer that surrounds plasma lipoproteins to the outer leaflet of the plasma membrane (Engelmann et al., 1996; Engelmann et al., 1998).

The negatively charged surfaces of activated platelets set the stage for a series of stepwise reactions involving only proteins circulating in blood in a

precursor (inactive) form, the **intrinsic pathway** of the coagulation cascade, which culminates in **fibrin** formation (Fig. 1.1). Current evidence indicates that the intrinsic pathway plays an important role in the growth and maintenance of the fibrin clot, while a second overlapping mechanism, called the **extrinsic pathway**, is critical for initiation of fibrin formation (Davie et al., 1991; Mann and Lorand, 1993).

The extrinsic pathway is triggered when an integral membrane glycoprotein located in the tissue adventitia, **tissue factor** (TF) comes in contact with blood. TF has a high affinity for the trypsin-like **serine proteinase** (section 1.2.4.) known as **factor VIIa** (FVIIa, section 1.2.8.) that circulates at low levels in blood (Davie et al., 1991; Furie and Furie, 1988). The stoichiometric TF-FVIIa complex (also termed **extrinsic Xase complex**) converts the zymogens of two other serine proteinases, factor IX and factor X, to the active enzymes **activated factor IX** (FIXa, section 1.2.7.) and **activated factor X** (FXa, section 1.2.6.), in the environment of the TF-bearing cell. Binding of the zymogen FVII to tissue factor also stimulates its activation to FVIIa, in a process known as **autoactivation** (Nakagaki et al., 1991; Neuenschwander et al., 1993).

The generated proteinases FIXa and FXa associate then with the non-enzymatic cofactors **activated factor V** (FVa, section 1.3.4.) and **activated factor VIII** (FVIIIa, section 1.3.5.) on the surface of activated platelets to form the activation complexes **intrinsic Xase** (FIXa + FVIIIa) and **prothrombinase** (FXa + FVa). These calcium- and phospholipid-dependent macromolecular complexes catalyze the additional conversion of factor X to FXa and of **prothrombin** (factor II) to the serine proteinase **α-thrombin** (section 1.2.5.), respectively. Thus, the complex cascade of reactions initiated with the blood exposure of tissue factor amplifies the clotting stimulus manifold and assures that formation of a hemostatic plug is largely confined, under physiological conditions, to sites of vascular tissue injury (for reviews see (Davie et al., 1991; Kane and Davie, 1988; Mann and Lorand, 1993)).

In the final step of the coagulation cascade, α-thrombin is liberated into the blood stream, where it performs several essential procoagulant functions (Fig. 1.1). Free α-thrombin converts soluble **fibrinogen** (section 1.5.1.) to fibrin, which spontaneously polymerizes to form the fibrillar matrix of the blood clot.

Thrombin also activates the transglutaminase known as **factor XIII** (section 1.5.2.), which thereafter cross-links fibrin monomers into an insoluble clot (Doolittle, 1984; Doolittle et al., 1998) (Fig. 1.1). By cleaving **G protein–coupled protease–activated receptors** (PARs, section 1.4.1.) on the platelet surface, thrombin strongly promotes additional platelet stimulation and aggregation (Coughlin, 1999). Furthermore, thrombin induces translocation of the most active **glucose transporter** isoform (GLUT3) to the plasma membrane, to fulfill the increased energy demands associated with activation (Sorbara et al., 1997). As an essential positive feed-back mechanism, thrombin amplifies its own generation by activating the non-proteolytic precursors factor V and factor VIII (Kane and Davie, 1988; Mann and Lorand, 1993), as well as **factor XI** (Gailani and Broze, 1991) (see Fig. 1.1 and sections 1.3.4., 1.3.5., 1.2.7. and 1.2.10.).

Several properties of the major proteins involved in the process of clot formation and of the genes encoding them are summarized in Tables 1.1 and 1.2. Knockout mice have been reported for most coagulation factors. The results of these investigations are summarized in Appendix A1; for a comprehensive review see reference (Carmeliet and Collen, 1996). Unexpectedly, besides their roles in hemostasis, alternative functions in embryonic development have been inferred for some of these proteins. Involvement of tissue factor (Bugge et al., 1996; Carmeliet et al., 1996; Rosen et al., 1997), factor V (Cui et al., 1996), prothrombin (Sun et al., 1998; Xue et al., 1998) and of the endothelial thrombin receptor **thrombomodulin** (TM, section 1.2.9.) (Healy et al., 1995; Weiler-Guettler et al., 1998) in other cell-signaling pathways seems particularly relevant.

Structural analysis of coagulation factors and fragments thereof has provided an important step forward in our understanding of the complex biochemical processes underlying clot formation and degradation (reviewed by (Bode et al., 1997; Stubbs and Bode, 1994). Elucidation of the three-dimensional crystal structures of the serine proteinases α-thrombin (Bode et al., 1989; Bode et al., 1992), factor IXa (Brandstetter et al., 1995), factor VIIa (Kemball-Cook et al., 1999; Pike et al., 1999), factor Xa (Brandstetter et al., 1996; Kamata et al., 1998; Padmanabhan et al., 1993), and of the anticoagulant proteinase **activated protein C** (section 1.2.9.) (Mather et al., 1996) has been essential for a better

understanding of their specificity. Moreover, the crystal structure of FVIIa bound to its cofactor (TF) has been determined (Banner et al., 1996).

Table 1.1: Major Soluble Human Coagulation Factors

Protein	Conc. (nM)	M_r (kDa)	Amino acids	Gene (kb)	mRNA (kb)	Exons	References[a]
Factor VII	10	50.0	406	12.8	2.4	8	(Furie and Furie, 1988; Kalafatis et al., 1997; Stenflo, 1999)
Factor IX (Christmas factor)	90	55.0	415	34.0	2.8	8	(Furie and Furie, 1988; Kalafatis et al., 1997; Stenflo, 1999)
Factor X (Stuart factor)	170	59.0	448 / 445[b]	27.0	1.5	8	(Furie and Furie, 1988; Kalafatis et al., 1997; Stenflo, 1999)
Prothrombin (Factor II)	1,400	72.0	579	21.0	2.0	14	(Furie and Furie, 1988; Kalafatis et al., 1997; Stenflo, 1999)
Protein C	60	62.0	419 / 417[b]	11.2	1.8, 1.6	9	(Furie and Furie, 1988; Stenflo, 1999)
Protein S	330/ 145[c]	75.0	635	>80.0	4.0, 3.1, 2.6	15	(Furie and Furie, 1988; Stenflo, 1999)
Fibrinogen (Factor I)	7,000	340.0	2,864[d]	–	–	–	(Doolittle, 1984; Doolittle et al., 1998; Herrick et al., 1999)
Aα:	–	70.0	610[d]	5.5	2.2	6	
Bβ:	–	56.0	461	8.0	1.9	8	
γ:	–	48.0	411[d]	8.5	1.6	10	
Factor V	20	330.0	2,196	80.0	6.8	25	(Kalafatis et al., 1997; Kane and Davie, 1988)
Factor VIII	0.7	280.0	2,332	187.0	9.0	26	(Kalafatis et al., 1997; Kane and Davie, 1988; Vlot et al., 1998)
Factor XI	30	160.0	1,214	23.0	2.1	15	(Kalafatis et al., 1997; Walsh, 1999)
Factor XII (Hageman factor)	375	80.0	596	12.0	2.4	14	(Colman and Schmaier, 1997; Tans and Rosing, 1987)
Factor XIII	70	360.0	2,744	–	–	–	(Kalafatis et al., 1997; Muszbek et al., 1999; Ruggeri and Ware, 1993)
A chain:		75.0	731	>160.0	3.8	15	
B chain:		80.0	641	28.0	2.6	12	
von Willebrand factor	50	270.0[e]	2,050[e]	178.0	8.7	52	(Sadler, 1998; Vlot et al., 1998)

[a]The cited references are review articles. Refer to work cited therein for the original publications.
[b]Single chain / circulating two-chain molecule.
[c]Total / free concentration.
[d]In the predominant Aα / γ chains of circulating fibrinogen.
[e]Corresponds to the mature monomer. vWf circulates as a multimer (see section 1.3.5.).

From the proteinases involved in fibrinolysis, the catalytic domain of **plasmin** (EC 3.4.21.7), the enzyme responsible for dissolution of fibrin clots, has been independently solved in complexes with the bacterial activators **streptokinase** (Wang et al., 1998) and **staphylokinase** (Parry et al., 1998). Structures of the catalytic domains of the physiological plasminogen activators **tissue-type plasminogen activator** (t-PA, EC 3.4.21.68) (Lamba et al., 1996;

Renatus et al., 1997) and **urokinase-type plasminogen activator** (u-PA, EC 3.4.21.73) (Spraggon et al., 1995) have also been reported.

Table 1.2: Major Human Membrane Proteins Involved and Thrombosis and Hemostasis

Protein	Molecules	M_r (kDa)	Amino acids	Gene (kb)	mRNA (kb)	Exons	References[a]
Tissue factor (Factor III)	?	37.0	263	12.0	2.3	6	(Davie et al., 1991; Kalafatis et al., 1997)
GP IIb–IIIa	50,000–80,000	226.0	1,770	–	–	–	(Bennett, 1996; Calvete, 1999)
GP IIb (αIIb)	–	160.0[b]	1,008[b]	60.0	3.4	14	
GP IIIa (β3)	–	90.0	762	46.0	6.1	14	
GP Ia–IIa	1,500–3,500	280.0	1,930	–	–	–	(Moroi and Jung, 1997; Sixma et al., 1997; Sixma et al., 1995)
GP Ia (α2)	–	150.0	1,152	?	5.4	?	
GP IIa (β1)	–	130.0	778	?	?	?	
GP Ib–IX–V	25,000–28,000	450.0[c]	2,446[c]	–	–	–	(Jandrot-Perrus et al., 1996; Lopez et al., 1998; Lopez and Dong, 1997)
GP Ibα	–	135.0	610	> 3.5	2.5	2	
GP Ibβ	–	25.0	181	> 1.4	1.0	2	
GP IX	–	22.0	160	3.2	1.0	3	
GP V	–	83.0	544	7.5	4.5	2	
PAR1	1,000–2,000	48.0	400	27.0	3.5	2	(Coughlin, 1999; Vu et al., 1991)
PAR4	1,000–2,000(?)	41.2[d]	368	?	2.7	?	(Kahn et al., 1998; Xu et al., 1998)
Thrombomodulin	30,000–100,000	75.0–100.0	559	3.7	3.7	1	(Suzuki, 1988; Suzuki et al., 1987; Wen et al., 1987)

[a]Most of the cited references are review articles. Refer to work cited therein for the original publications.
[b]Actually a disulfide-linked dimer, derived by proteolytic cleavage of a precursor (section 1.4.2.).
[c]Assuming a 2:2:2:1 stoichiometry.
[d]Theoretical mass.

The structures of the non-catalytic domains of coagulation factors (sections 1.2.1 – 1.2.3.) have also been intensively studied by X-ray and/or NMR methods. For instance, crystal structures have been reported for residues Ala1 to Arg156 of bovine prothrombin comprising the N-terminal **γ–carboxyglutamic** (**Gla**)-rich domain (see section 1.2.1.) and the first **kringle** domain (section 1.2.3.) (Seshadri et al., 1991; Tulinsky et al., 1985; Tulinsky et al., 1988). Moreover, the structure of **desF1-meizothrombin** (comprising residues Ser165 to Ser582; see section 1.2.5.) has been solved at medium resolution (Martin et al., 1997). Finally, several isolated **epidermal growth factor** (EGF)-like (section 1.2.2.) and kringle domains of proteinases involved in clot formation and dissolution have been studied by either X-ray crystallography and/or nuclear magnetic resonance (NMR) in solution. In the following sections, we summarize the main results of these investigations.

1.2. The Proteinases

Stepwise activation of circulating zymogens of **serine proteinases** *via* limited proteolysis is a common feature of several important physiological processes. The term **cascade** or waterfall was first coined to describe the complex set of reactions culminating in clot formation after tissue injury (Davie and Ratnoff, 1964; Macfarlane, 1964); reviewed by (Davie et al., 1991; Furie and Furie, 1988; Mann and Lorand, 1993), but has also been utilized to summarize the activation of the immune **complement system** (for reviews see (Müller-Eberhard, 1988; Reid, 1983). Indeed, sequence analysis of the constituents of blood coagulation and complement cascades suggests that they are descendants of an ancestral defense system that served the dual role of immobilization and destruction of invading bacteria and prevented loss of body fluids (Patthy, 1990). Concerted activation of serine proteinase zymogens is also central to the establishment of dorsal-ventral polarity in the *Drosophila* embryo (Chasan et al., 1992; DeLotto and Spierer, 1986; Stein and Nusslein-Volhard, 1992); for a recent review see (LeMosy et al., 1999).

Because of the notable sequence similarities of the serine proteinase moieties (1.2.4.) making up the C-terminal domains of the proteolytic cofactors involved in these processes, they are grouped together in the **S1** or (**chymo)trypsin family** of **endopeptidases** (Rawlings and Barrett, 1994), which also includes digestive enzymes such as trypsin and chymotrypsin. The linear order of residues forming the **catalytic triad** of these proteinases is conserved as His, Asp, Ser, and the mechanism of catalysis has been extensively characterized (section 1.2.4.).

Fig. 1.2 (next page): Schematic domain organization of the serine proteinases involved in coagulation and fibrinolysis. The open arrows mark activation cleavage sites; additional cleavage sites within prothrombin, factor IX, factor XII and u-PA are also indicated (→). With the only exceptions of factor X and protein C, zymogens circulate in plasma as single-chain molecules.

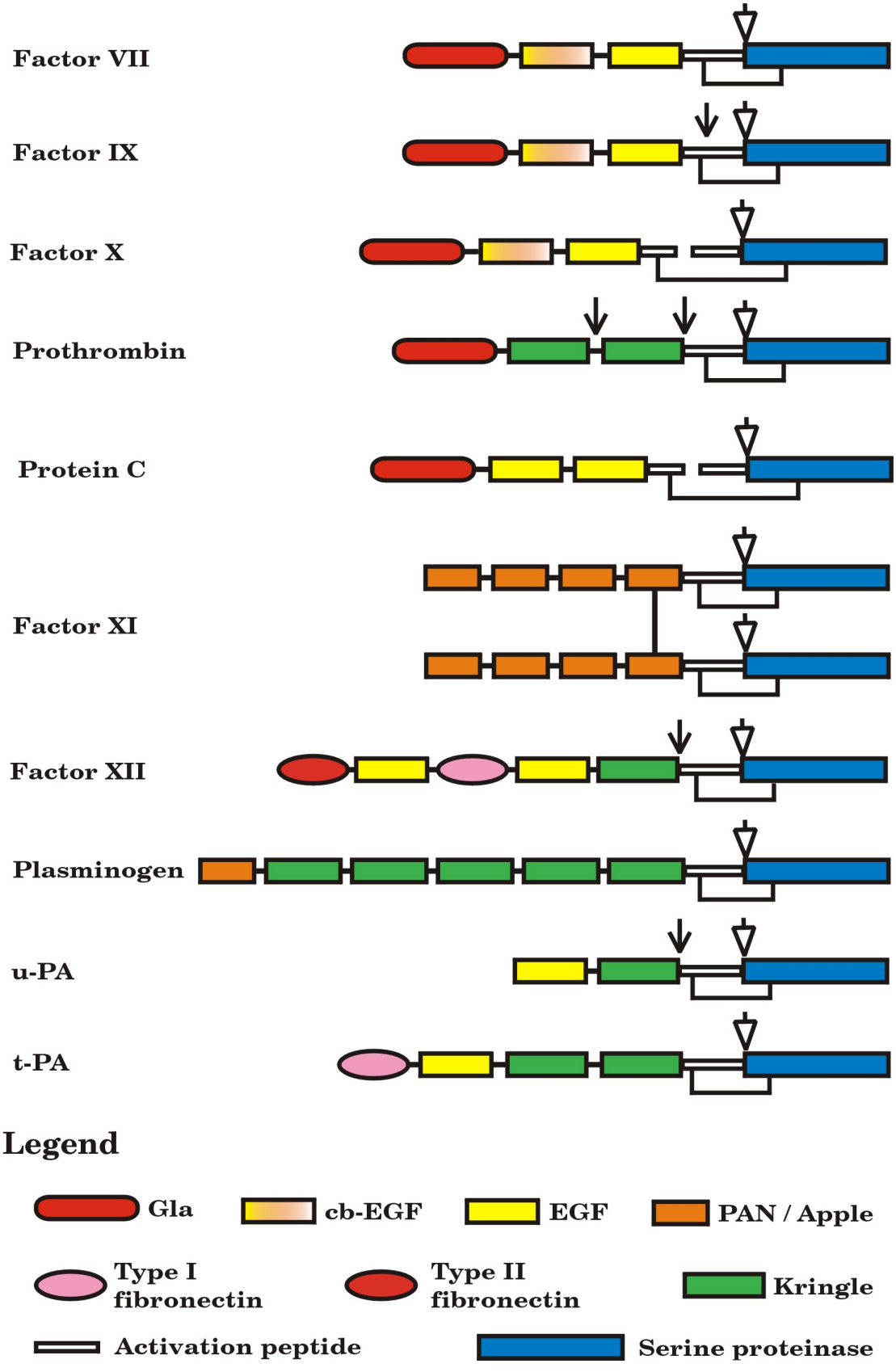

In contrast to the digestive enzymes, serine proteinases involved in the processes of thrombosis and fibrinolysis are chimeric proteins, with modules inserted N-terminally to the site of proteolytic activation (1.2.4.1.). Coagulation

factors VII, IX and X and protein C share the same domain structure (Fig. 1.2), as they consist of a Gla-rich domain (1.2.1.), followed by two EGF-like repeats (1.2.2.) and the actual trypsin-like, serine proteinase catalytic domain (1.2.4.). The precursor of thrombin, prothrombin (1.2.5.), differs from these proenzymes in that the Gla-domain is followed by two kringle domains instead (1.2.3.). Kringle domains have also been identified in factor XII (FXII, see section 1.2.10.) as well as in the proteins involved in the degradation of the fibrin clot. Five kringle domains form the N-terminal heavy chain of plasmin (Novokhatny et al., 1984; Petersen et al., 1990; Ponting et al., 1992; Wiman and Wallen, 1975); the plasminogen activators u-PA (Gunzler et al., 1982; Kasai et al., 1985) and t-PA (Harris et al., 1986; Ny et al., 1984) contain one and two kringle domains in their regulatory chains, respectively. (For reviews on the plasminogen (fibrinolytic) system see (Harris, 1987; Plow et al., 1995)). The domain organization of all serine proteinases involved in coagulation and fibrinolysis is presented in Fig. 1.2. In the next sections (1.2.1. to 1.2.4.) we describe the common structural features of the independent domains, before introducing the proteinases involved in clot formation in sections 1.2.5. to 1.2.10.

1.2.1. Gla Domains Mediate Binding to Phospholipid Membranes

The N-terminal domains of coagulation factors VII, IX, X and prothrombin, as well as those of protein C and of its cofactor, **protein S** (1.3.6.), are post-translationally modified by the action of a microsomal protein, a **vitamin K-dependent carboxylase** that converts several (from 9 to 12) glutamic acid residues to **γ-carboxyglutamic** (Gla) residues. These proteins are therefore termed **vitamin K-dependent coagulation factors**, and the modified domains (containing 46 or 47 residues) are known as **Gla domains** (for recent reviews see (Furie and Furie, 1997; Stenflo, 1999); see Fig. 1.3 for a sequence comparison). The enzymatic carboxylation is directed by the propeptide on the precursor form of the proteinase (Jorgensen et al., 1987).

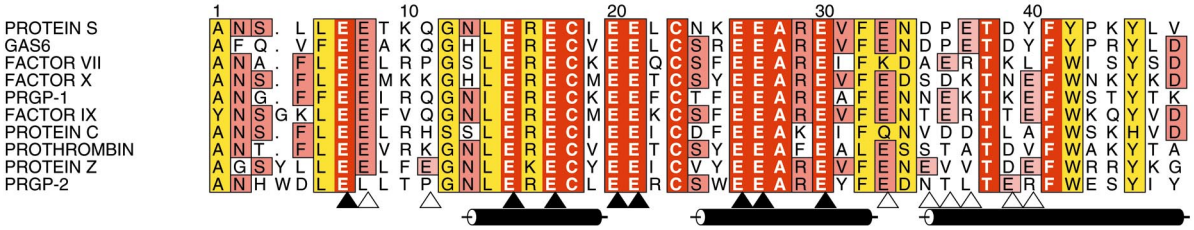

Fig. 1.3 (previous page): Sequence alignment of human Gla domains. Conserved residues are given in red boxes, conservative substitutions are shadowed yellow. Other residues conserved in at least half of the proteins included in this alignment (coagulation factors VII, IX, and X, prothrombin, protein C, protein S, protein Z, as well as Gas6 and the two proline-rich Gla-containing proteins PRGP-1 and -2) are shadowed in salmon color. Glutamic acid residues converted to γ-carboxyglutamic acid in all Gla-domains are indicated with closed triangles, those modified only in some of the proteins with open triangles and shadowed pink. Numbering corresponds to the sequence of factor IX.

Also included in this family is the pseudoenzyme **protein Z** (Broze and Miletich, 1984; Petersen et al., 1980), whose structure is similar to that of factors VII, IX and X, but lacks the His57 and Ser192 residues of the catalytic triad (compare section 1.2.4.). Instead, protein Z appears to modulate factor Xa activity by serving as a cofactor for its inactivation by a **ser**ine **p**roteinase **in**hibitor (**serpin**) (1.5.5.) called protein Z-dependent protease inhibitor (Han et al., 1999). A protein S homologue (termed **Gas6**) has been identified as a product of the **g**rowth **a**rrest-**s**pecific gene **6** (Manfioletti et al., 1993). Gas6, which shares all by the thrombin-sensitive module with protein S (see section 1.3.6.), is released from activated platelets and might thus also be involved in the regulation of the coagulation cascade (Ishimoto and Nakano, 2000; Manfioletti et al., 1993). Two novel transmembrane **p**roline-**r**ich **G**la-containing **p**roteins (PRGP-1 and -2) have been recently identified, but their physiological relevance remains unclear (Kulman et al., 1997).

Several independent investigations have revealed the overall structure of Gla domains (summarized in Table 1.3). Figure 1.4 presents ribbon models of the factor VIIa Gla domain, as seen in the crystal structure of its complex with soluble tissue factor ((Banner et al., 1996), see also section 1.2.8.).

Fig. 1.4 (next page): Three-dimensional structure of Gla domains. Ribbon plots showing two approximately perpendicular views of factor VIIa Gla domain, as seen in the crystal structure of its complex with TF (Banner et al., 1996). Seven bound Ca^{2+} ions are shown as blue spheres. Side chains of all γ-carboxyglutamic residues (compare Fig. 1.3) are shown, as well as aromatic side chains in the α-helical "stack region". Notice also the presence of three solvent-exposed hydrophobic residues in the N-terminal loop.

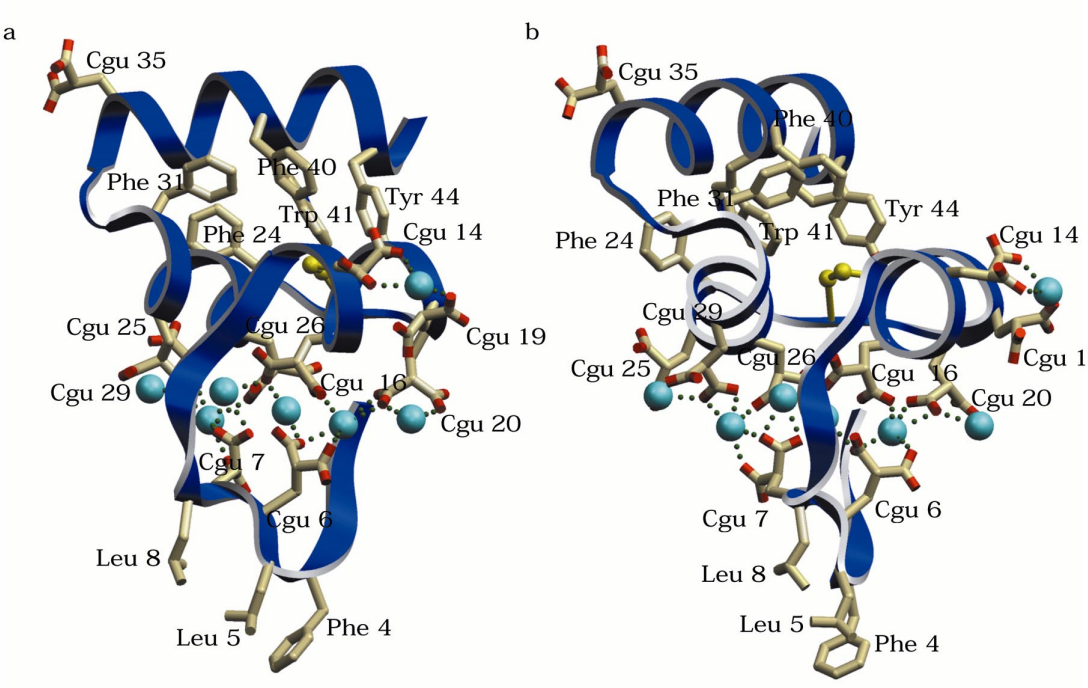

Table 1.3: Structural Investigations of Gla Domains of Vitamin K-Dependent Cofactors

Protein	Organism	Method	PDB Code	Description	Reference
Factor VIIa	*Homo sapiens* (recombinant)	X-ray / 2.0 Å	1DAN	Complex of the whole proteinase with soluble TF. Ca^{2+}-bound.	(Banner et al., 1996)
Factor IXa	*Homo sapiens* (synthetic)	NMR / n.a.	1CFH	Residues Tyr1–Asp47 (Gla domain). Metal-free. 15 structures.	(Freedman et al., 1996; Freedman et al., 1995)
Factor IXa	*Homo sapiens* (synthetic)	NMR / n.a.	1CFI	Gla domain. Ca^{2+}-bound. 17 structures.	(Freedman et al., 1996; Freedman et al., 1995)
Factor IXa	*Homo sapiens* (synthetic)	NMR / n.a.	1MGX	Gla domain. Mg^{2+}-bound. 7 structures.	(Freedman et al., 1996)
Factor Xa	*Bos taurus* (plasma)	NMR / 683 NOEs	1WHE	Residues Ala1–Arg86 (Gla + EGF1). Ca^{2+}-free. 20 structures.	(Sunnerhagen et al., 1995; Sunnerhagen et al., 1996)
Factor Xa	*Bos taurus* (plasma)	NMR / n.a.	1WHF	Gla + EGF1. Ca^{2+}-bound. 15 structures.	(Sunnerhagen et al., 1995; Sunnerhagen et al., 1996)
Prothrombin	*Bos taurus* (plasma)	X-ray / 2.25 Å	2PF1	Residues Ala1–Arg155 (Gla + kringle 1). Ca^{2+}-free, residues 1–35 not defined.	(Seshadri et al., 1991)
Prothrombin	*Bos taurus* (plasma)	X-ray / 2.8 Å	2PF2	Gla + kringle 1. Ca^{2+}-bound.	(Tulinsky et al., 1985; Tulinsky et al., 1988)

Detailed NMR studies in solution conducted with a proteolytic factor X fragment comprising both the Gla- and the first EGF-like domain indicated that Gla domains are essentially disordered in the absence of calcium (Stenflo, 1999; Sunnerhagen et al., 1995). Also along these lines, no density has been observed for the N-terminal residues Ala1–Leu35 of bovine prothrombin (Seshadri et al., 1991) and Tyr1–Thr35 of porcine factor IXa (Brandstetter et al., 1995), when

crystallized in the absence of calcium ions. Calcium binding causes a folding transition, resulting in the exposure of three hydrophobic residues located in the hook-shaped N-terminal loop (Fig. 1.5). These hydrophobic residues may constitute major determinants for insertion into the apolar phospholipid membrane core (Stenflo, 1999; Sunnerhagen et al., 1995). Similar results have been obtained from an independent NMR investigation conducted with the synthetic factor IX Gla domain (Freedman et al., 1996); these researchers detected interactions between side chains of specific hydrophobic residues of the N-terminal loop (Leu6, Phe9) and phospholipid membranes. However, hydrophobic interactions mediated by these exposed side chains cannot account for the large differences (as much as two orders of magnitude) in membrane affinity of vitamin K-dependent proteins. This and other observations point to a more subtle mechanism of membrane association by Gla domains, which seems to involve recognition of specific phospholipid head-groups by the side chains of residues at positions 11, 33 and 34 (factor IX numbering, Fig. 1.3) (McDonald et al., 1997; McDonald et al., 1997; Zwaal et al., 1998).

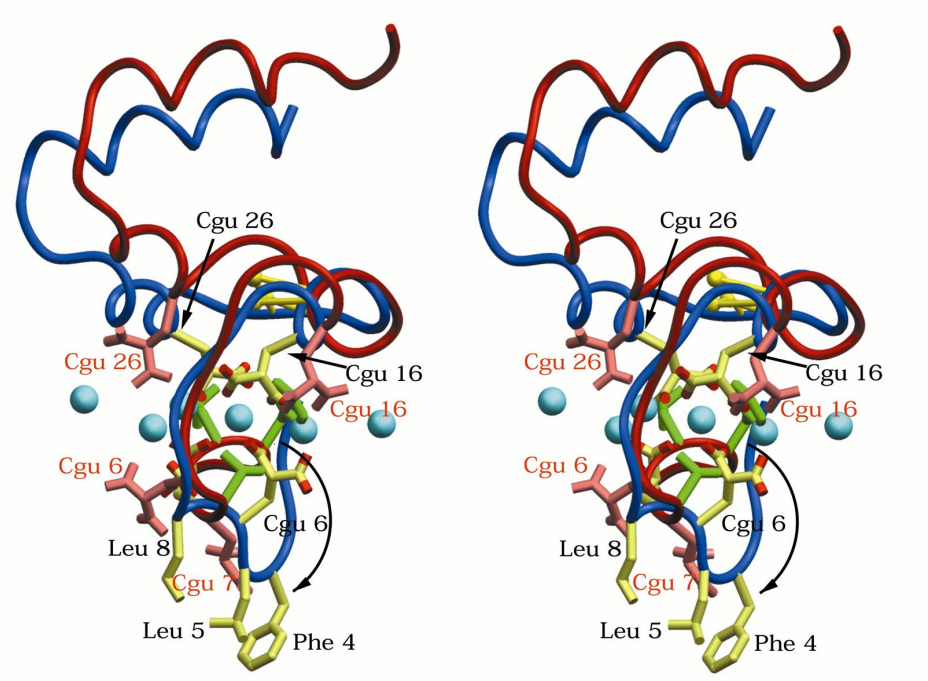

Fig. 1.5: Putative mechanism of membrane binding by Gla domains. Stereo view of the overlay between the apo (Ca^{2+}-free) less-energy solution structure of the factor Xa Gla domain (red; Gla residues light red, hydrophobic residues green) and the crystal structure of calcium-bound FVIIa (blue, side chains color-coded). Only a few side chains of both modules are shown. Notice the concerted movements of Gla- and hydrophobic residues upon calcium binding (indicated with an arrow for Phe4).

1.2.2. EGF-Like Domains Are Involved in Protein-Protein Interactions

The structural motif of 40-50 amino acid residues first identified in the soluble **epidermal growth factor** (EGF) ((Savage et al., 1972), and references therein), has been subsequently found in a multitude of both transmembrane and extracellular matrix proteins, where it forms contiguous arrays up to 36 modules long (Campbell and Bork, 1993). EGF-like repeats are also important structural and functional elements of several coagulation factors (Fig. 1.2). About 25% of EGF modules possesses calcium-binding capability; these domains are characterized by the presence of a signature (D/N)-X-(D/N)-(E/Q)-X_m-(D/N)*-X_n-(Y/F) (where m and n are variable, and an asterisk indicates possible **β–hydroxylation**. (See appendix A2 for a list posttranslational modifications found in coagulation factors).

Besides the almost strict conservation of the disulfide pairing ([Cys1-Cys3, Cys2-Cys4, Cys5-Cys6]) in these small protein modules, they possess few conserved amino acid residues. This point is illustrated in Fig. 1.6, showing the sequence alignment of **c**alcium-**b**inding (cb) EGF domains identified in human coagulation factors, and contrasts with the high sequence identity between Gla domains (compare Fig. 1.3). The sequence conservation is much lower if also other EGF-like repeats are included in the comparison. Curiously, the only known exception to the conserved disulfide pairing has been found in the fifth EGF-like repeat of thrombomodulin (Sampoli Benitez et al., 1997; White et al., 1996); see also chapter 4).

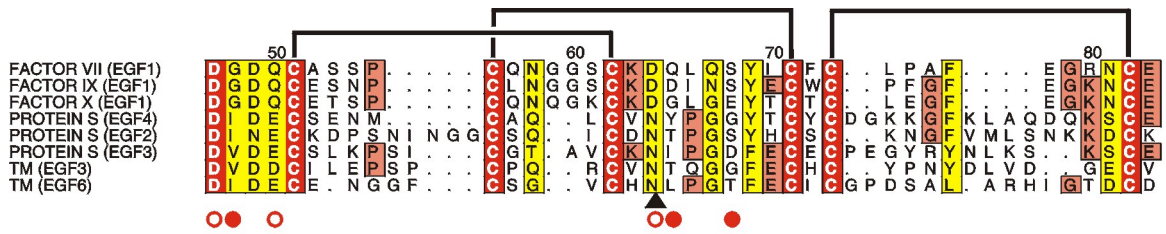

Fig. 1.6: Sequence alignment of calcium-binding EGF-like domains. Conserved residues are given in red boxes, conservative substitutions are shadowed yellow. Residues involved in Ca^{2+} binding are indicated with closed (if the main chain carbonyl contacts the calcium ion) or open red circles (by Ca^{2+} contacts with a side-chain oxygen atom). The site of β-hydroxylation is shown with a full arrow. Numbering corresponds to the sequence of human factor IX.

The three-dimensional structures of most EGF-like repeats of coagulation factors have been revealed, either isolated or together with the catalytic domains of the serine proteinase moieties (Table 1.4). The three-dimensional structures of the N-terminal EGF-like domains of factors VIIa, IXa and Xa are compared in Fig. 1.7. The fourth (Meininger et al., 1995) and fifth (Sampoli Benitez et al., 1997) EGF-like repeats of TM have been studied by NMR. In chapter 4, we compare the solution structures of these isolated modules with the crystal structure of the three C-terminal EGF-like domains of this thrombin receptor.

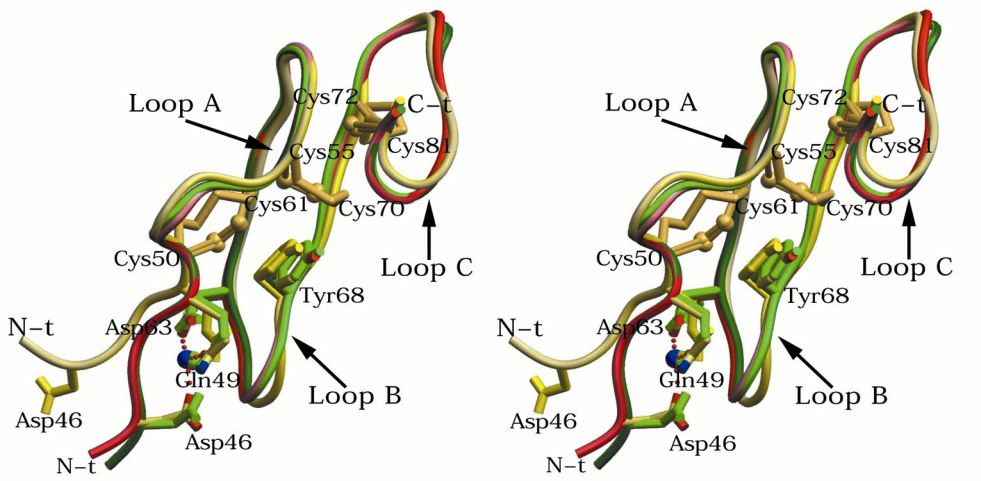

Fig. 1.7: The three-dimensional structure of calcium-binding EGF-like domains is highly conserved. The structures of the N-terminal EGF domain of TF-bound factor VIIa (red, side chains color-coded; (Banner et al., 1996)), the isolated EGF1 domain of factor IXa (green; (Rao et al., 1995)) and the less-energy solution structure of isolated factor Xa EGF1 domain (yellow; (Ullner et al., 1992)) are depicted after least-square minimization. The bound calcium ions are shown as a blue (factor VIIa) or green (factor IXa) sphere. The structures enclosed by cysteine residues Cys1-Cys3, Cys2-Cys4 and Cys5-Cys6 are occasionally termed loops A, B and C, respectively, and are also labeled. Side chains of residues involved in calcium binding are shown, as well as the structurally important Tyr68 (Tyr69 in FIXa; addition of 1 to the indicated residue numbering gives the FIX numbering). Notice the different conformation of disulfide bridges in solution.

Table 1.4: Structural Investigations of EGF-Like Domains From Coagulation Factors

Factor	Organism	Method	PDB Code	Description	Reference
VIIa	*Homo sapiens* (recombinant)	X-ray / 2.0 Å	1DAN	Complex of D-Phe-Phe-Arg-inhibited FVIIa with soluble TF. Ca^{2+}-bound.	(Banner et al., 1996)
VIIa	*Homo sapiens* (recombinant)	X-ray / 2.1 Å	1FAK	Ternary complex FVIIa-sTF-BPTI mutant. Ca^{2+}-free.	(Zhang et al., 1999)
VIIa	*Homo sapiens* (recombinant)	X-ray / 2.8 Å	1QFK	Residues Ser45 to Arg152 + Ile153 to Pro406 (Gla-less FVIIa). Inhibited with D-Phe-Phe-Arg.	(Pike et al., 1999)
VIIa	*Homo sapiens* (recombinant)	X-ray / 2.28 Å	1CVW	Gla-less FVIIa, inhibited with 1,5-dansyl-Glu-Gly-Arg. EGF1 flexibly disordered.	(Kemball-Cook et al., 1999)
VIIa	*Homo sapiens* (synthetic)	NMR / 521 NOEs	1BF9	Residues Ser45 to Lys85 (EGF1). Ca^{2+}-free. 23 structures.	(Muranyi et al., 1998)
VIIa	*Homo sapiens* (recombinant)	NMR / n.a.	1F7E / 1F7M	EGF1 (non-glycosylated). Ca^{2+}-bound. 20 structures / average structure.	(Kao et al., 1999)
VIIa	*Homo sapiens* (recombinant)	NMR / n.a.	1FF7 / 1FFM	EGF1 (fucosylated at Ser60). Ca^{2+}-bound. 20 structures / average structure	(Kao et al., 1999)
IXa	*Sus scrofa* (plasma)	X-ray / 3.0 Å	1PFX	Residues Tyr1 to Arg146 + Ile181 to Thr415. (PPACK-inhibited proteinase). Ca^{2+}-free.	(Brandstetter et al., 1995)
IXa	*Homo sapiens* (recombinant)	X-ray / 2.8 Å	1RFN	Residues Asp85 to Arg145 and Val181 to Thr415 (desGla-desEGF1 FIXa). Inhibited with *p*-aminobenzamidine.	(Hopfner et al., 1999)
IXa	*Homo sapiens* (recombinant)	NMR / n.a.	1IXA	Residues Val46 to Leu84 (EGF1). Ca^{2+}-free. Average structure.	(Baron et al., 1992)
IXa	*Homo sapiens* (recombinant)	X-ray / 1.5 Å	1EDM	EGF1. Ca^{2+}-bound.	(Rao et al., 1995)
Xa	*Homo sapiens* (plasma)	X-ray / 2.2 Å	1HCG	Residues Asp46 to Arg139 + Ile195 to Lys448 (Gla-less FXa). Ca^{2+}-free.	(Padmanabhan et al., 1993)
Xa	*Homo sapiens* (plasma)	X-ray / 3.0 Å	1FAX	Gla-less FXa. Inhibited with DX-9065a. Ca^{2+}-bound.	(Brandstetter et al., 1996)
Xa	*Homo sapiens* (plasma)	X-ray / 2.3 Å	1XKA	Gla-less FXa. Inhibited with FX-2212A.	(Kamata et al., 1998)
Xa	*Homo sapiens* (plasma)	X-ray / 2.4 Å	1XKB	Gla-less FXa. Inhibited with FX-2212A.	(Kamata et al., 1998)
Xa	*Bos taurus* (plasma)	NMR / 683 NOEs	1WHE	Residues Ala1 to Arg86 (Gla + EGF1). Ca^{2+}-free. 20 structures.	(Sunnerhagen et al., 1995)
Xa	*Bos taurus* (plasma)	NMR / n.a.	1WHF	Gla + EGF1. Ca^{2+}-bound. 15 structures.	(Sunnerhagen et al., 1995)
Xa	*Bos taurus* (plasma)	NMR / 420 NOEs	1CCF	Residues Lys45 to Arg86 (EGF1). Ca^{2+}-bound. 15 structures.	(Selander-Sunnerhagen et al., 1992)
Xa	*Bos taurus* (plasma)	2D NMR / 370 NOEs	1APO	EGF1. Ca^{2+}-free. 13 structures.	(Ullner et al., 1992)
PC	*Homo sapiens* (plasma)	X-ray / 2.4 Å	1AUT	Residues Ser42 to Lys146 + Leu170 to Pro419 (Gla-less APC).	(Mather et al., 1996)
TM	*Homo sapiens* (synthetic)	NMR / 519 NOEs	1ZAQ	Residues Glu346 to Phe389 (EGF4). 12 structures.	(Meininger et al., 1995)
TM	*Homo sapiens* (synthetic)	NMR / 483 NOEs	1ADX/ 2ADX	Residues Gln387-Glu426 (EGF5). 14 structures / average structure.	(Sampoli Benitez et al., 1997)

BPTI: bovine pancreatic trypsin inhibitor; NOE: nuclear Overhauser enhancement; sTF: soluble tissue factor; FX-2212A: (2s)-2-(3'-amidino-3-biphenyl)-5-(4-pyridylamino) pentanoic acid

EGF-like domains play major physiological roles as mediators of protein-protein interactions (Campbell and Bork, 1993; Rebay et al., 1991). In particular, they provide highly specific interaction surfaces in the coagulation factors. (For a recent review see reference (Stenflo, 1999)). For instance, extensive interactions are made between the EGF domains of factor VIIa and tissue factor ((Banner et

al., 1996); see also section 1.2.8.). The second EGF domains of factors IXa / Xa mediate binding of cofactors VIIIa / Va and thus assembly of the macromolecular complexes intrinsic Xase / prothrombinase, respectively (Hertzberg et al., 1992; Skogen et al., 1984); see also sections 1.2.6. and 1.2.7.). Additionally, the second EGF-like repeat of human factor IXa appears to mediate binding to platelets (Wong et al., 1999). Finally, it should be mentioned that the C-terminal EGF domains of factors VII, IX, X, and protein C occupy very similar positions relative to the catalytic domain (compare sections 1.2.6. to 1.2.9.). Accordingly, residues clustered at the interface between the EGF and the serine proteinase domain are particularly conserved through evolution (Gaboriaud et al., 1998). Three highly conserved residues (Asn92, Phe98 and Leu117 in FIXa) are specifically associated with the EGF-serine proteinase domain pair. In addition, the consensus motif C-X-[P/S]-X_3-[Y/F]-P-C-G is characteristic of the region starting with the last cysteine of the EGF domain in this domain pair (Gaboriaud et al., 1998).

1.2.3. Kringle Domains Possess Lysine Binding Sites

S. Magnusson coined the term **kringle** (inspired in a Danish pastry) to design the small (about 80 residues) domains with a three disulfide three-looped pattern that were first identified at the sequence level in plasminogen and prothrombin (Magnusson et al., 1976). The structure of prothrombin's kringle 2 has been unveiled in its complex with the catalytic domain of the proteinase (Arni et al., 1993; Martin et al., 1997)); a fragment containing both kringle 1 and the N-terminal Gla domain has also been studied by X-ray diffraction ((Seshadri et al., 1991; Tulinsky et al., 1988); see also 1.2.5.). The structures of most individual plasminogen kringles have been determined in solution and/or by X-ray crystallography. Additionally, the sole kringle domain of u-PA and the second kringle domain of t-PA have been studied by either method (summarized in Table 1.5). The sequences of all kringle domains from human proteins involved in coagulation and fibrinolysis are aligned in Fig. 1.8. The three-dimensional structure of kringle domains is mainly defined by two antiparallel β-sheets, which are oriented approximately perpendicular to each other (Fig. 1.9).

Table 1.5: Structural Investigations of Kringle Domains of Proteins Involved in Coagulation and Fibrinolysis

Protein	Organism	Method	PDB Code	Description	Reference
Prothrombin	*Bos taurus* (plasma)	X-ray / 2.25 Å	2PF1	Residues Ala1–Arg156 (fragment 1). Ca^{2+}-free; residues 1–35 not defined.	(Seshadri et al., 1991)
Prothrombin	*Bos taurus* (plasma)	X-ray / 2.8 Å	2PF2	Fragment 1. Ca^{2+}-bound. Residues 148–156 not defined.	(Tulinsky et al., 1988)
Prothrombin	*Bos taurus* / *omo sapiens* (plasma)	X-ray / 3.3 Å	n.d.	Both human and bovine kringle 2, non-covalently bound to catalytic domain of the human proteinase.	(Arni et al., 1993)
Prothrombin	*Bos taurus* (plasma)	X-ray / 3.1 Å	1AOH	Residues Ser157–Arg323 + Ile324–Ser582 (Meizothrombin-desF1). PPACK-inhibited.	(Martin et al., 1997)
t-PA	*Homo sapiens* (recombinant)	NMR / n.a.	1PK2	Residues Ser174–Thr263 (kringle 2). Complex with εACA. Best structure.	(Byeon et al., 1991; Byeon and Llinas, 1991)
t-PA	*Homo sapiens* (recombinant)	X-ray / 2.4 Å	1TPK	Kringle 2. Apo form.	(de Vos et al., 1992)
t-PA	*Homo sapiens* (recombinant)	X-ray / 2.38 Å	1PML	Kringle 2. Apo form.	(Padmanabhan et al., 1994)
u-PA	*Homo sapiens* (recombinant)	NMR / 946 NOEs	1KDU	Residues Thr49–Asp133 (kringle domain).	(Li et al., 1994)
Plasminogen	*Homo sapiens* (plasma)	NMR / n.a.	1HPJ/ 1HPK	Residues Lys77–Glu165 (kringle 1). Complex with εACA. 12 structures / average structure.	(Rejante and Llinas, 1994)
Plasminogen	*Homo sapiens* (recombinant)	X-ray / 2.48 Å	1PKR	Kringle 1.	(Wu et al., 1994)
Plasminogen	*Homo sapiens* (recombinant)	X-ray / 2.1 Å	1CEA/ 1CEB	Kringle 1. Complexes with εACA / AMCHA.	(Mathews et al., 1996)
Plasminogen	*Homo sapiens* (recombinant)	NMR / n.a.	1B2I	Residues Glu164–Thr244 (kringle 2). Complex with AMCHA. 20 structures.	(Marti et al., 1997)
Plasminogen	*Homo sapiens* (plasma)	X-ray / 2.25 Å	1PMK	Residues Val355–Val442 (kringle 4). Apo form.	(Padmanabhan et al., 1994)
Plasminogen	*Homo sapiens* (plasma)	X-ray / 1.68 Å	1KRN	Kringle 4. Measured at 277 K.	(Stec et al., 1997)
Plasminogen	*Homo sapiens* (plasma)	X-ray / 1.9 Å	1PK4	Kringle 4. Apo form.	(Mulichak et al., 1991)
Plasminogen	*Homo sapiens* (plasma)	X-ray / 2.25 Å	2PK4	Kringle 4 (defined between Gln356 and Cys435). Complex with εACA.	(Wu et al., 1991)
Plasminogen	*Equus caballus* (plasma)	NMR/ n.a.	n.d.	Kringle 4. Complex with εACA. 10 structures.	(Cox et al., 1994)
Plasminogen	*Homo sapiens* (recombinant)	X-ray / 1.66 Å	5HPG	Residues Asp461–Pro544 (kringle 5).	(Chang et al., 1998)

AMCHA: trans-4-**a**mino**m**ethyl**c**yclo**h**exane-1-carboxylic **a**cid, εACA: 4-epsilon-**a**mino**c**aproic **a**cid (6-aminohexanoic acid), NOE: nuclear Overhauser enhancement, n.d.: not deposited.

Fig. 1.8 (next page): Sequence alignment of kringle domains found in proteins involved in thrombosis and hemostasis. Conserved residues are white with red underground, conservative substitutions are shadowed yellow. Other residues conserved in at least half of the domains are shadowed orange, some additional similarities are shadowed pink. Residues involved in ligand binding are indicated with a full arrow. Numbers refer to the plasminogen numbering system.

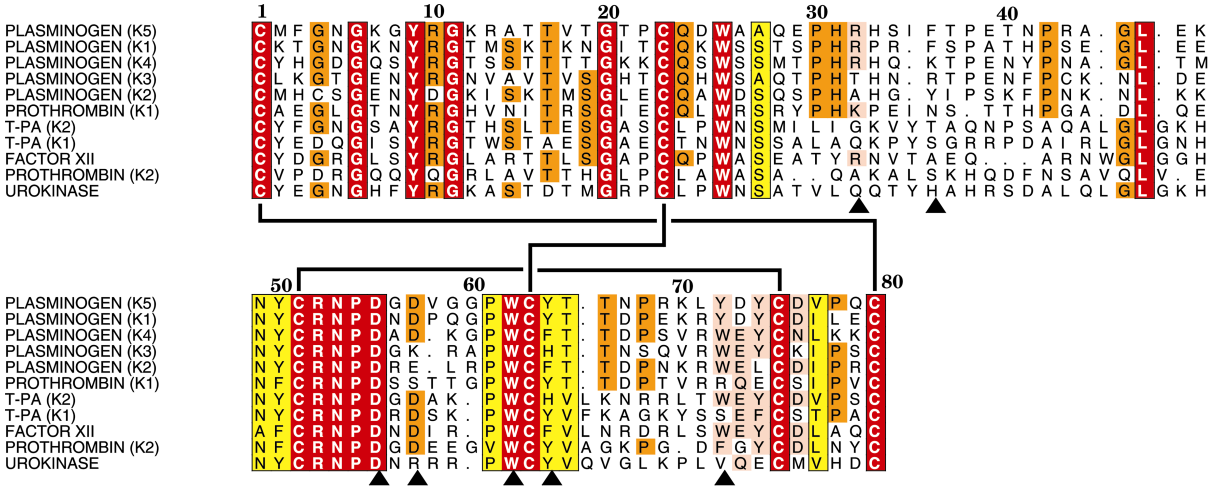

The ability of some kringle domains of plasmin(ogen) and t-PA to selectively bind lysine and/or arginine residues on the fibrin clot is essential for the process of fibrinolysis *in vivo*. The molecular basis of fibrin recognition by kringle domains has been explored by co-crystallization experiments using lysine analogs (Mathews et al., 1996; Wu et al., 1991). As shown in Fig. 1.9 for plasminogen kringle 4, the lysine binding site is a relatively open and shallow depression, that is lined by three aromatic rings (Trp62, Phe64 and Trp72 in the plasminogen numbering system). These aromatic side chains provide a highly nonpolar environment between doubly charged anionic and cationic centers formed by Asp55/Asp57 and Lys35/Arg71 (Wu et al., 1991).

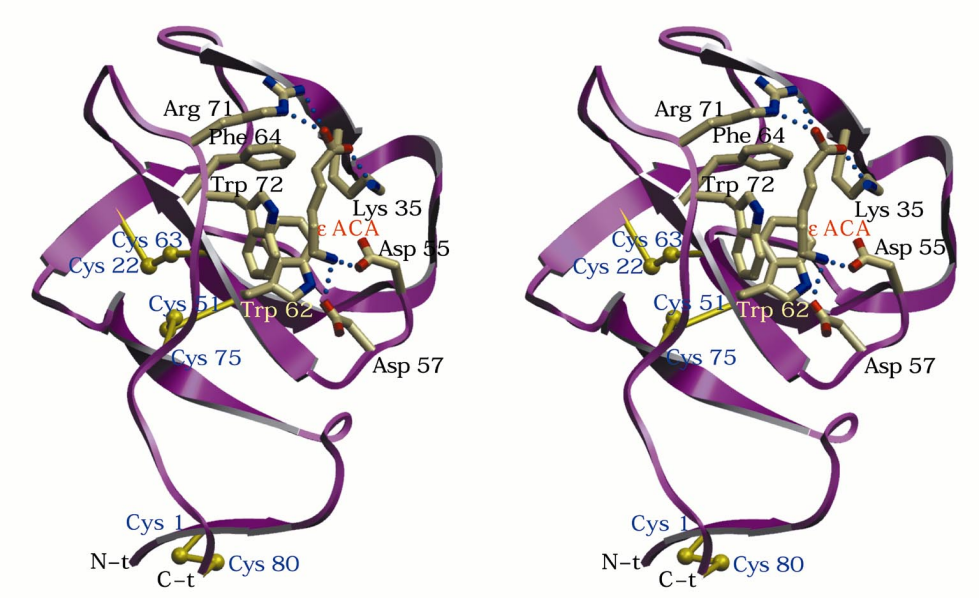

Fig. 1.9 (previous page): Structure of plasminogen kringle 4, highlighting its lysine-binding site. Notice that the zwitterionic εACA molecule lies in an extended conformation between the doubly charged anionic and cationic centers of the kringle domain, and is held by hydrogen-bonded ion pair interactions (blue dotted lines) and van der Waals contacts. The lysine-binding site appears to be preformed, and lysine binding does not require conformational changes of the module (Wu et al., 1991).

1.2.4. The Proteinases Involved in Thrombosis and Fibrinolysis Belong to the Trypsin Family

The large enzyme family of trypsin-like serine proteinases is among the most extensively investigated and thoroughly characterized protein families (Neurath, 1986; Perona and Craik, 1997; Steitz and Shulman, 1982). Because the digestive enzyme α-chymotrypsin was the first family member for which a three-dimensional structure was reported (by D. Blow and co-workers, (Matthews et al., 1967)), it constitutes the reference structure, and chymotrypsinogen numberings (starting with residue 16) have become standard in the field. This numbering system will be used for the catalytic domains of all serine proteinases throughout this work. In most cases, however, to avoid ambiguities the sequence of the mature protein will be used, with the (chymo)trypsin numbering given in curly brackets.

Structural investigations have revealed a common framework of two lobes of six-stranded antiparallel β-strands, folded into a so called **Greek key motif** (strands β1-β4) followed by an antiparallel hairpin motif (strands β5 and β6). (See appendix A3 for a structure-based alignment of the serine proteinase domains of human coagulation factors). The active site is located in a crevice between both subdomains. Subdomain 1 contributes two residues to the **catalytic triad** (His57 and Asp102), while the reactive Ser195 is part of the C-terminal subdomain (Kraut, 1988; Matthews et al., 1967; Neurath, 1986). Although both subdomains are intricately associated to form a single unit, calorimetric investigations revealed two unfolding transitions for the catalytic domains of several serine proteinases (Novokhatny et al., 1984; Novokhatny et al., 1993), in agreement with the structural evidence.

Common features of serine proteinases include the presence of a **specificity** (**S1**) **pocket**, which is important for recognition of the peptide to be cleaved (the P1 residue). (We adopt the nomenclature of Schechter and Berger

(Schechter and Berger, 1967), in which residues N-terminal to the cleavage site are denoted as P1, P2, ..., while those following the cleavage site are primed: P1', P2', ... The corresponding interaction subsites in the enzyme are accordingly termed S1, S2, ... and S1', S2', ..., respectively). The main chain amides of residue 193 and of the catalytic Ser195 form the **oxyanion hole**, which accommodates the substrate carbonyl oxygen (Fig. 1.10). The P1-P3 residues of serine proteinase inhibitors form a short antiparallel β-sheet interaction with residues Ser214-Gly216 of the proteinase, which includes three highly conserved hydrogen bonds between the two main chains (Fig. 1.10). It is believed that these inhibitors mimic the proteinase-substrate interaction. (For a recent critical study of this hypothesis, however, see reference (Coombs et al., 1999)). The entropy loss on substrate binding appears to provides the necessary energy for the increase in reaction rate (Blow, 2000).

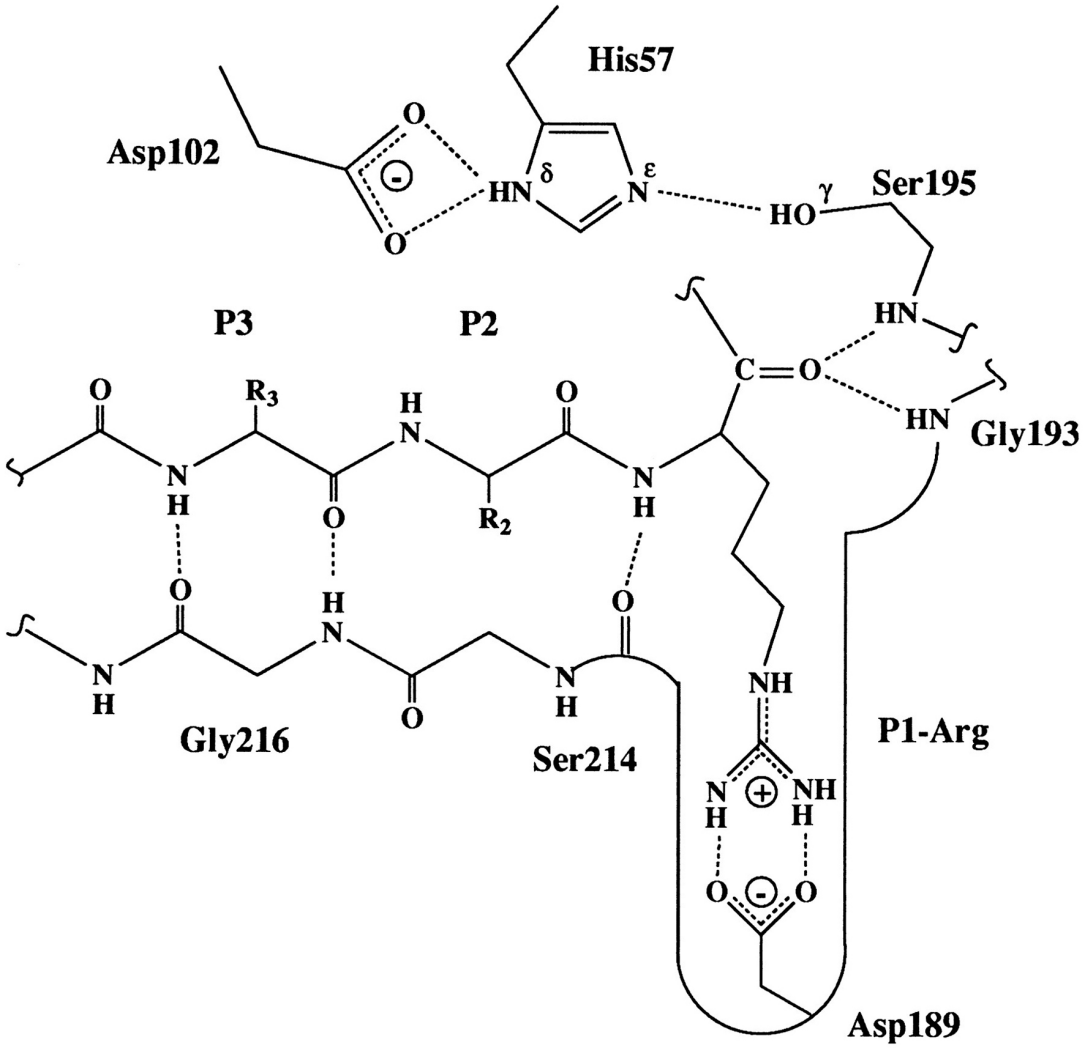

Fig. 1.10 (previous page): Substrate recognition and catalytic mechanism of serine proteinases. Schematic diagram of the major interactions between substrate and proteinase in trypsin-like serine proteinases (from reference (Perona and Craik, 1997)). Because of the polarization of the Ser-His-Asp catalytic triad, it is referred to as a **charge-relay system**. Peptide cleavage involves formation of a (negatively charged) **transition state intermediate** between the peptide carbon atom of the substrate and the hydroxyl group of Ser195. This carbon atom has a tetrahedral geometry in contrast to the planar geometry in peptide bonds. After cleavage of the peptide bond, the N-terminal peptide product remains attached to the catalytic serine as an **acyl-enzyme intermediate**, while the C-terminal peptide is released. Finally, the intermediate is hydrolyzed by a water molecule, again *via* formation of a tetrahedral transition state.

1.2.4.1. Zymogen Activation Follows Cleavage of a Single Peptide Bond

All zymogens of serine proteinases are activated *via* the same mechanism established for the chymotrypsin zymogen (**chymotrypsinogen**) by H. T. Wright and J. Kraut (Kraut, 1977; Wright, 1973; Wright, 1973) and for trypsinogen by W. Bode and R. Huber (Bode et al., 1978; Huber and Bode, 1978). Cleavage of the Arg15-Xxx16 peptide bond (chymotrypsinogen numbering; Xxx designs a branched aliphatic residue, usually Ile) allows insertion of the newly formed amino terminus into the main body of the protein, where it stabilizes the active enzyme conformation by making a strong salt-bridge with the carboxylate of Asp194. The studies on trypsin showed that the major structural changes resulting from the activation cleavages were limited to a rather small portion of the molecule, the "**activation domain**" (Huber and Bode, 1978). This region comprises basically the four segments 16–19, 142–152, 184–193, and 216–223 and possesses significantly lower crystallographic B-values in the proteinase. Cleavage of the correct peptide bond in zymogens of blood clotting factors and their substrates poses major biochemical and topological problems. Fig. 1.11 summarizes the activation cleavage sites of serine proteinases involved in clot formation, along with the activation sites of thrombin substrates factor V (section 1.3.4.), factor VIII (1.3.5.), the platelet receptor PAR1 (1.4.1.), fibrinogen (1.5.1.), factor XIII (1.5.2.), and the plasma procarboxypeptidase TAFI (1.5.3.).

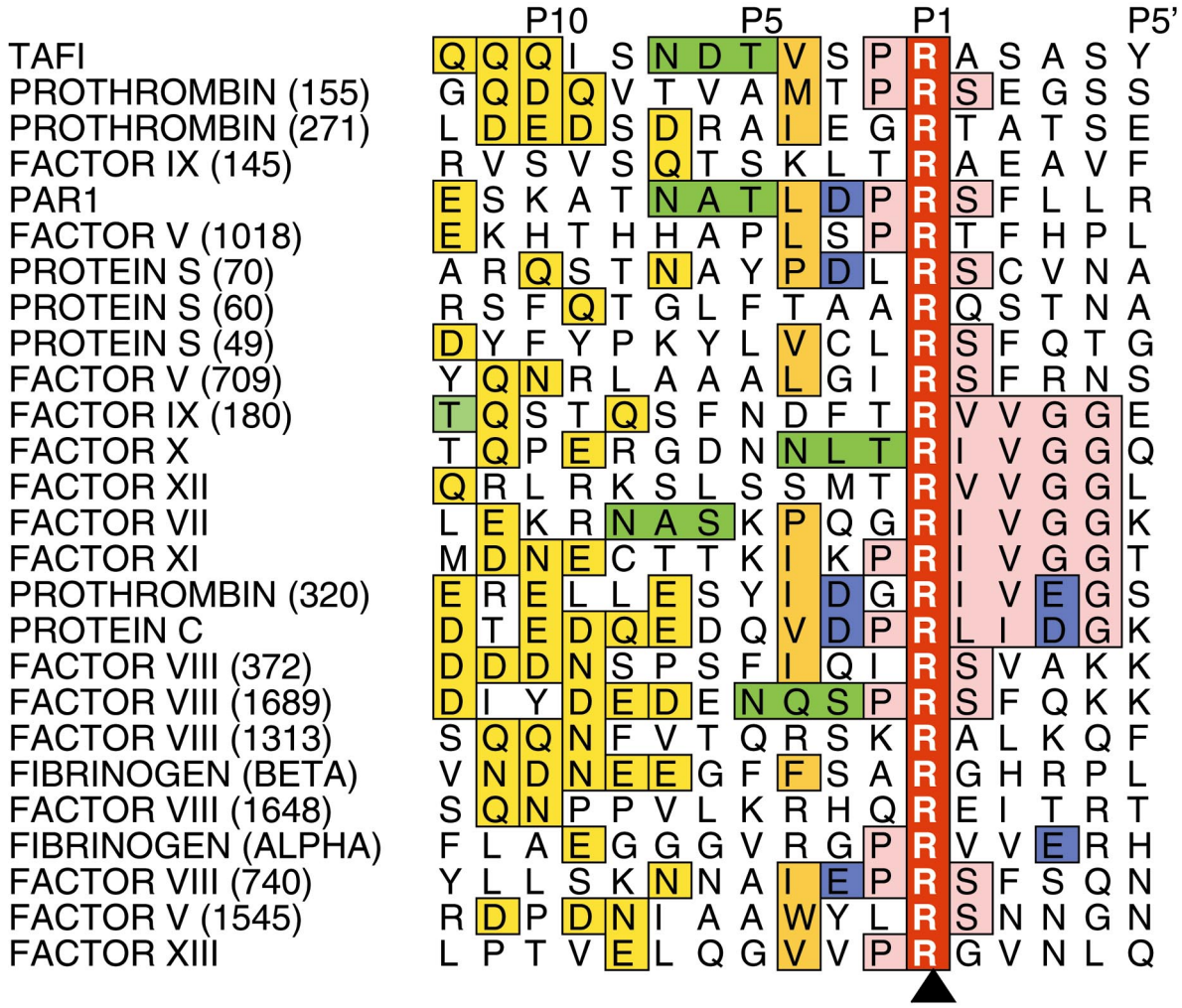

Fig. 1.11: Activation cleavage sites of serine proteinases and other factors involved in clot formation. Polypeptide sequences comprising positions P12 to P5' of the activation peptides have been included in the alignment. Notice the great sequence variability, even among substrates of the same proteinase. Glu/Gln and Asp/Asn residues are preferentially found at positions P7-P12 (shadowed yellow), position P4 is usually occupied by a hydrophobic residue (shadowed orange). Proline is most commonly found at position P2 (shadowed pink). Also shadowed pink are the conserved P1'-P4' residues of the serine proteinases. Notice that the P1' residue of other cofactors possess usually a short side chain (Ser, in most cases). Sites of *N*-glycosylation (Asn–Xxx–Ser/Thr) and the *O*-glycosydically modified Thr169 in factor IX are shadowed green. Negatively charged aspartate residues at positions P3 and P3' are shadowed blue.

1.2.5. Prothrombin, Meizothrombin, Thrombin

The proform of thrombin (**prothrombin**, EC 3.4.21.5) is synthesized primarily in the liver and secreted into the blood as a 579-residues glycoprotein, with carbohydrates attached to asparagines Asn78 and Asn100 (both in the first kringle domain), and Asn373{60G}. (For a recent review on the biology of

prothrombin synthesis see (Degen and Sun, 1998); see appendix A2 for a list of posttranslational modifications). The N-terminal Gla-domain (1.2.1.) of prothrombin contains 10 γ-carboxyglutamic residues (compare Fig. 1.3) and anchors the zymogen to phospholipid membranes upon calcium binding (Nelsestuen, 1976) (see also section 1.2.1.). The Gla domain is followed by two kringle domains (1.2.3.) and by the serine proteinase catalytic domain; these major structural elements are connected by relatively long peptides (see below).

As stated before, activation and concomitant release of active α-thrombin is performed *in vivo* by the membrane-bound prothrombinase complex (factors Va and Xa assembled on a phospholipid surface) and requires cleavages at positions Arg271–Thr272 and Arg320{15}–Ile321{16}. In addition, thrombin cleaves readily the peptide bond Arg155–Thr156 in the linker between both kringle domains (for a review see reference (Stubbs and Bode, 1993)). Fig. 1.12a presents a schematic drawing of the prothrombin domain organization, highlighting possible activation pathways. In the presence of both factor Va and factor Xa, prothrombin activation starts with the cleavage of the peptide bond Arg320–Ile321 (Krishnaswamy et al., 1987; Krishnaswamy et al., 1986), what generates an unstable membrane-bound intermediate form that is known as **meizothrombin** and possesses several distinguishing enzymatic properties (Cote et al., 1997; Doyle and Mann, 1990).

Following the initial structure determination of D-Phe-Pro-Arg chloromethyl ketone (PPACK)-inhibited human α-thrombin by W. Bode (Bode et al., 1989), the structures of a multitude of thrombin complexes have been solved. (There are currently over one-hundred thrombin structures deposited in the Protein Data Bank, most of which correspond to complexes with small synthetic inhibitors). Fig. 1.12b shows the electrostatic surface potential of the proteinase, as seen in the PPACK complex. Bovine fragment 1 has also been studied by X-ray crystallography, both in the presence and absence of calcium ions (Seshadri et al., 1991; Tulinsky et al., 1988); Fig. 1.13). The crystal structure of non-covalent complexes between bovine / human kringle 2 and the human catalytic domain has also been reported (Arni et al., 1993); the structure of the whole desF1-meizothrombin fragment slightly corrected the initial view and provided a more detailed picture of the association of fragment 2 with the catalytic domain

(Martin et al., 1997) (Fig. 1.14). Docking of this structure with that of the Gla-K1 tandem (Fig. 1.13) resulted in different models for the structures of pro– and meizothrombin (Arni et al., 1994; Martin et al., 1997), see also chapter 4). The three-dimensional structure of **prethrombin 2** (the zymogen form devoid of Gla and kringle domains) has also been reported (Vijayalakshmi et al., 1994).

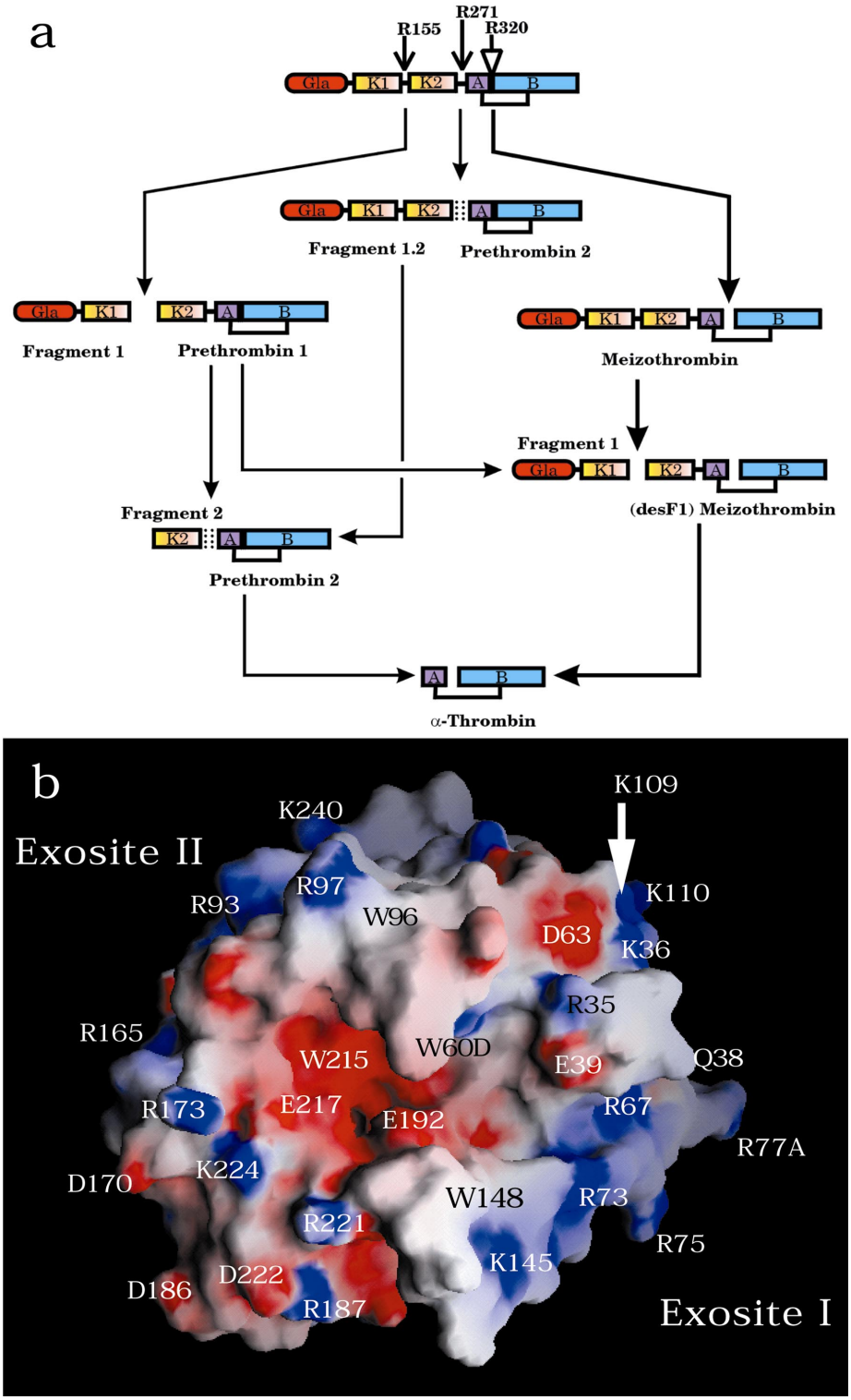

Fig. 1.12 (previous page): Domain organization of prothrombin and structure of α-thrombin. (**a**) Schematic drawing showing possible pathways of thrombin generation. For detailed kinetic analysis see references (Carlisle et al., 1990; Esmon et al., 1974). Fragment 1.2 and prethrombin 2 bind to each other with high affinity ($K_d \sim 10^{-10}$ M; (Myrmel et al., 1976; Nesheim et al., 1988)), and may remain associated, at least temporarily. (**b**) GRASP (Nicholls et al., 1993) surface representation of the electrostatic potential (red, negative; blue, positive) of human α-thrombin. Notice the unbalanced charge distribution: the negatively charged active-site region is surrounded by two regions of positive potential, the exosites.

One of the most remarkable features of the proteinases involved in coagulation and fibrinolysis is the presence of interaction surfaces distant from the immediate surroundings of the active-site residues. This feature is particularly relevant in the case of α-thrombin (Bode et al., 1989; Bode et al., 1992). Essential for the high specificity of thrombin are not only its prominent active-site cleft, which is narrowed to a deep canyon that limits access of macromolecular substrates and inhibitors to the catalytic center, but also two surface patches enriched in basic amino acid residues and termed **anion-binding exosites** (Fig. 1.12b).

Exosite I, also referred to as **fibrinogen-recognition exosite**, can be subdivided into a more proximal region consisting of the "eastern" part of the active-site cleft, and a more distal one where the active-site cleft passes over to the adjacent convex surface of thrombin ("standard orientation", see Fig. 1.12b). Anion-binding exosite I is utilized by thrombin for selective binding of macromolecular substrates and cofactors such as fibrinogen (Doolittle, 1984), see also section 1.5.1.), factors V and VIII (Dharmawardana and Bock, 1998; Dharmawardana et al., 1999; Esmon and Lollar, 1996); section 1.3.4.) and the thrombin platelet receptor PAR1 (Liu et al., 1991) (see section 1.4.1.). Exosite I is also crucial for the formation of thrombin-serpin complexes (Myles et al., 1998; Rezaie, 1998); see also 1.5.5.) and appears to mediate prothrombin dimerization on phospholipid membranes (Anderson, 1998).

A second patch of positively charged residues termed **anion binding exosite II** is centered on residues Arg93, Arg97, Arg101, Arg233 and Lys236 (Fig. 1.12b) and seems to serve as an anchoring region for the acidic glycosaminoglycan **heparin** (Olson and Bjork, 1991; Olson and Shore, 1982); see

also section 1.5.5.). This region is therefore called **heparin-binding exosite**, it seems to be involved also in the recognition of factors V and VIII (Esmon and Lollar, 1996). It is conceivable that additional (pro)thrombin surfaces are involved in intermolecular interactions with substrates and cofactors. In this regard, recent studies indicate that recognition of prothrombin by the prothrombinase complex involves a region(s) distinct from both exosites and also spatially removed from structures surrounding the scissile bond (Betz and Krishnaswamy, 1998); direct interactions between prothrombin's kringle 1 and factor Va has been reported (Deguchi et al., 1997), while factor Xa binds to kringle 2 (Taneda et al., 1994).

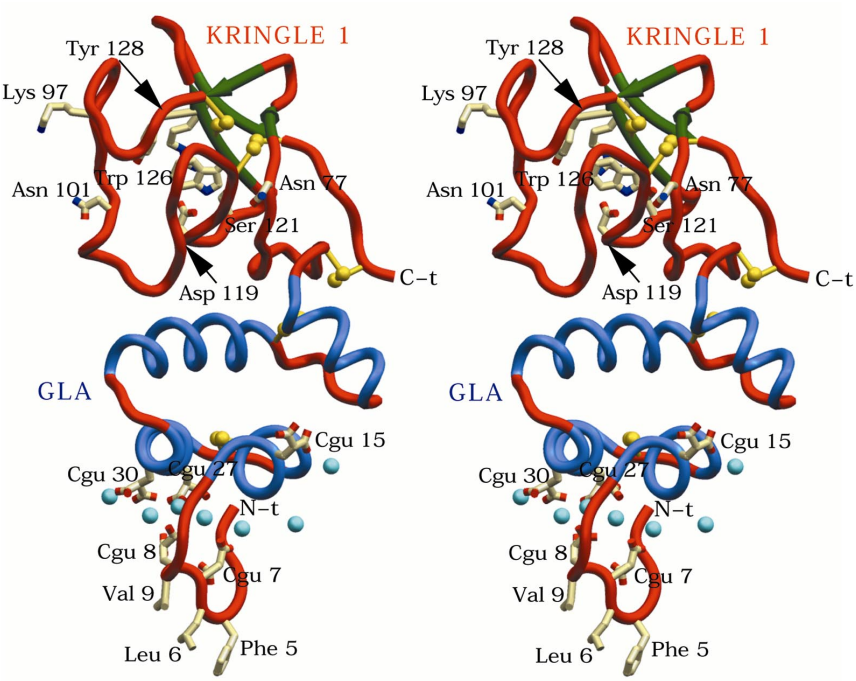

Fig. 1.13: Three-dimensional structure of bovine prothrombin fragment 1 (F1). The Ca^{2+}-bound form is represented as a ribbon plot, with α-helices in blue and hydrogen-bonded β-strands in kringle 1 in green. Only some of the γ-carboxyglutamic residues and the three hydrophobic residues exposed in the N-terminal loop are given in full length (compare 1.2.1. and Fig. 1.4). Glycosylated asparagine residues (corresponding to Asn78 and Asn100 in the human protein) are also indicated. Notice the absence of a lysine-binding site, at least partly because of the substitutions of critical residues (e.g., Tyr/Phe36 →Asn and Asp57 →Ser; compare Figs 1.8 and 1.9).

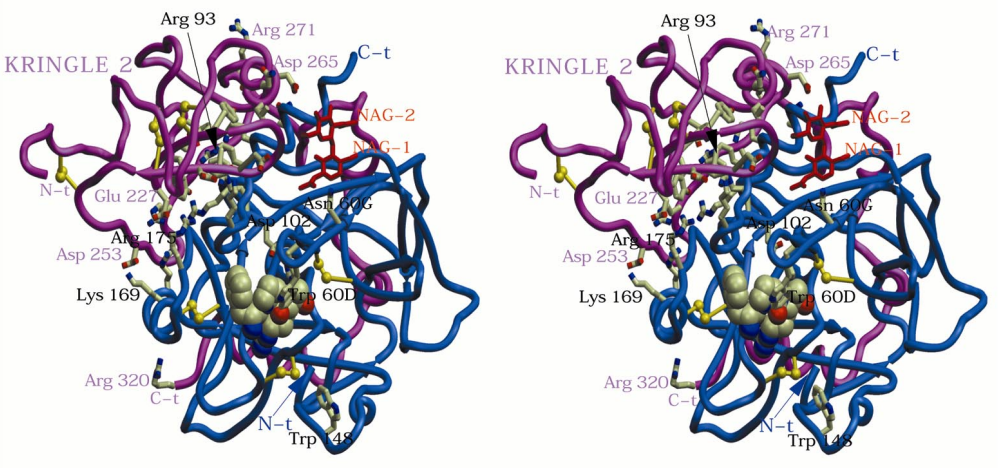

Fig. 1.14: Structure of desF1-meizothrombin. Both fragment 2 and the catalytic domain are presented as ribbon plots (pink and blue, respectively); the bound inhibitor (PPACK) is shown as color-coded van der Waals spheres. Notice that the kringle 2 domain occupies the heparin-binding exosite, protecting the enzyme from heparin-mediated antithrombin inhibition (see 1.5.5.). In particular, the important side chain of Arg93 is completely enclosed by kringle 2. Notice that both factor Xa cleavage sites are separated by about 40 Å.

Identification of a sodium ion bound to thrombin (Di Cera et al., 1995) and its effect on thrombin activity *in vitro* has raised speculations about the allosteric regulation of the proteinase *in vivo*. In particular, binding of a Na^+ ion to this single site converts thrombin from an anticoagulant form that preferentially cleaves protein C (the "slow" form) to a form that preferentially cleaves fibrinogen (the "fast" form) (for a review see (Di Cera et al., 1997). However, it must be stressed that at the constant sodium concentrations in plasma (about 150 mM), occupancy of the Na^+-binding site is unlikely to contribute to the regulation of thrombin activity (see also section 1.2.9. and chapter 4).

In addition to its manifold pro- and anticoagulant activities, thrombin is a potent activator of cellular events (Bar-Shavit et al., 1992; Bar-Shavit et al., 1983). For instance, thrombin induces angiogenesis *via* activation of the metalloproteinase zymogen **progelatinase A** in vascular endothelial cells (Zucker et al., 1995); a recent investigation suggests that this effect is elicited *via* protein C activation ((Nguyen et al., 2000); compare section 1.2.9.). Thrombin also possesses angiogenesis-promoting activity that is based on the sensitization of endothelial cell receptors for the key angiogenic factor, **vascular endothelial growth factor** (Tsopanoglou and Maragoudakis, 1999). On the other hand, the isolated kringle 2 domain possesses growth-inhibitory activity (Lee et al., 1998).

Further, thrombin induces thrombomodulin mRNA expression by cleaving protease-activated receptors (1.4.1.) on smooth muscle cells (Ma et al., 1997). Thrombin also cleaves specifically an essential physiological regulator of megakaryopoiesis and platelet production, **thrombopoietin** (Kato et al., 1997). Recently, thrombin has been identified as an extracellular "death signal" that induces apoptosis of neuronal cells, by a mechanism involving activation of its receptor (Smirnova et al., 1998); see section 1.4.1.).

1.2.5.1. Exosite Binding Induces Allosteric Rearrangements

Several independent observations indicate that binding of substrates, cofactors or inhibitors to exosites I and II promotes conformational changes in the active site of thrombin and/or affect the binding properties of the opposing exosite.

(1) Prothrombin fragment 2 produces fluorescence changes in probes linked to the catalytic residues (Bock, 1992), alters the calcium-dependency of protein C activation (section 1.2.9.) (Liu et al., 1994), and increases the k_{cat} for hydrolysis of tosyl-Arg-*O*-methyl ester (Myrmel et al., 1976) and tosyl-Gly-Pro-Arg-*p*-nitroanilide (Jakubowski et al., 1986) approximately 2-fold. More recently, it has been shown that not only F2 but also peptides thereof alter the rate of thrombin-mediated hydrolysis of chromogenic substrates (Liaw et al., 1998).

(2) A monoclonal antithrombin IgG recognizes an epitope that includes residues Arg101, Arg233 and Lys236 in exosite II (compare Figs 1.12b, 1.14) (Colwell et al., 1998). Binding of this antibody affects the rate at which thrombin cleaves various peptide *p*-nitroanilide substrates with arginine in the P1 position, but does not seem to alter the conformation of exosite I.

(3) Binding of the C-terminal tail of the thrombin inhibitor **hirudin** (see section 3.6.) to exosite I induces rearrangements in the 149-loop of thrombin, resulting in a six-fold reduction in the sensitivity of thrombin to limited proteolysis by elastase and chymotrypsin (Parry et al., 1993). Further, the affinity of thrombin for the C-terminal tail of hirudin (residues 54-65) decreases in the presence of a peptide corresponding to part of prothrombin fragment 2 (residues 218-271) and *vice versa* (Fredenburgh et al., 1997). An allosteric linkage between both exosites has also been inferred from studies conducted with **glycocalycin**, the extracellular portion of a thrombin platelet receptor, glycoprotein (GP) Ibα (de Cristofaro et al., 1998); see also section 1.4.2.).

1.2.6. Factor Xa: At the Cross-Point of the Intrinsic and Extrinsic Pathways

Human **factor X** (FX; also known as **Stuart factor**, EC 3.4.21.6) is synthesized primarily in the liver and subjected to manifold co- and posttranslational modifications (Appendix A2) before secretion into the blood (Davie et al., 1991; Leytus et al., 1986; Messier et al., 1991). Factor X circulates as an inactive two-chain molecule (M_r ~ 59 kDa) composed of a Gla domain followed by two EGF-like repeats (the **light chain**, residues Ala1 to Arg139), disulfide-linked to the serine proteinase domain (the **heavy chain**, residues Ser143–Lys448) *via* Cys132–Cys302{122}. During the coagulation process, the zymogen is converted to the serine proteinase factor Xa by cleavage of the peptide bond (Arg194{15}-Ile195{16}), with concomitant release of a small glycopeptide of 52 amino acids (Di Scipio et al., 1977; Inoue and Morita, 1993).

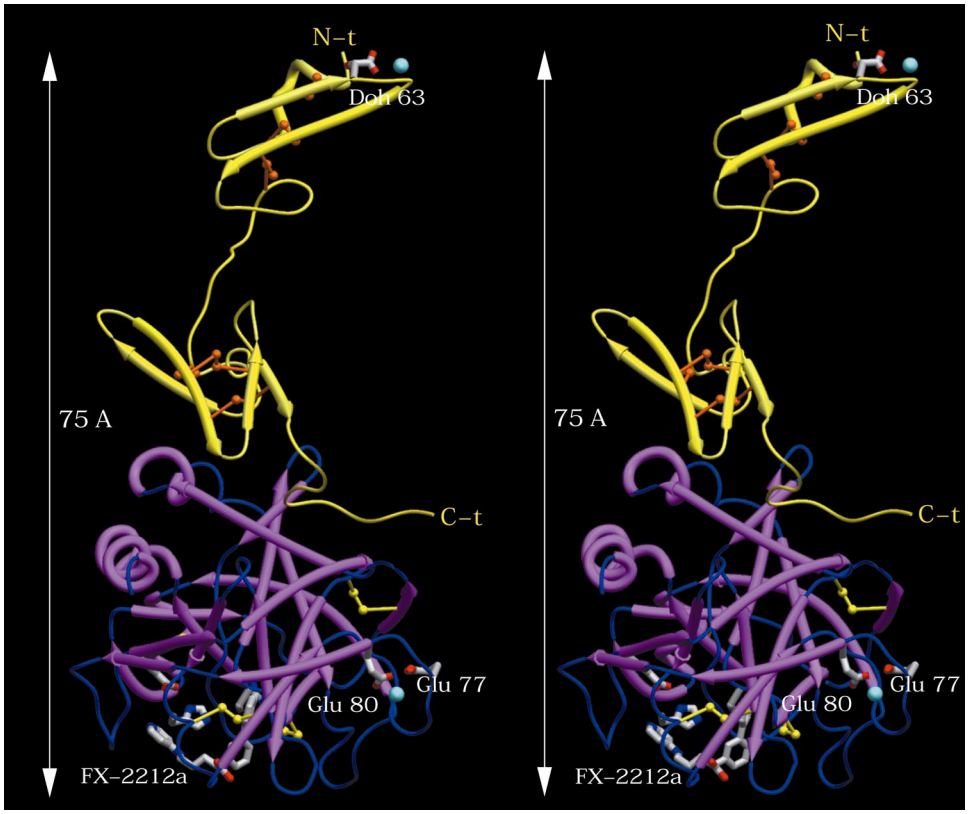

Fig. 1.15: The Gla-less factor Xa molecule. The proteinase is shown as seen in the crystal structure of its complex with the synthetic inhibitor FX-2212a (color-coded) (Kamata et al., 1998). (FX-2212a = *S*-isomer of (2*RS*)-(3'-amidino-3-biphenyl)-5-(4-pyrdylamino)pentanoic acid). Notice that the second EGF-like domain (EGF2) sits "behind" the molecule, in contrast to the position of second kringle domain in meizothrombin (compare with Fig. 1.14). The bound Ca^{2+} ions are shown as blue spheres.

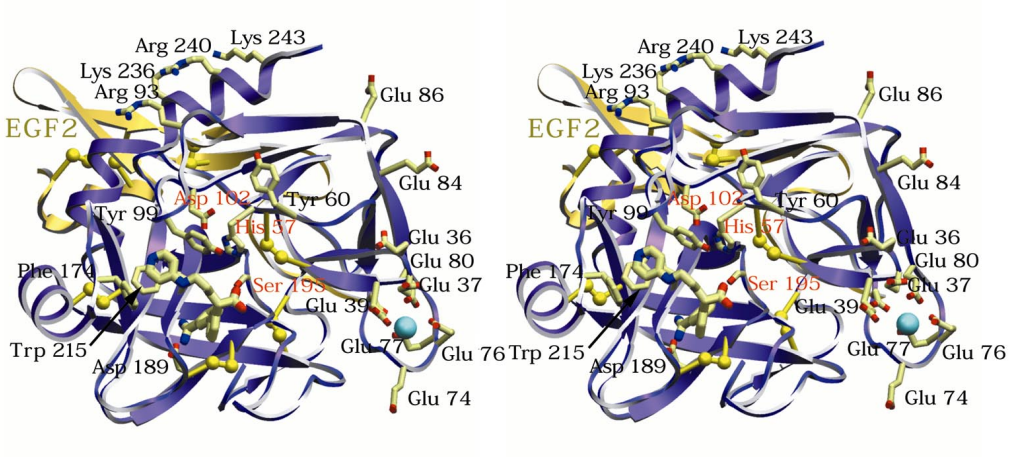

Fig. 1.16: Catalytic domain of factor Xa. Stereo plot showing the EGF2 and serine proteinase domain substructure in the "standard orientation", i.e., with substrates running from left to right. Exposed charged residues that roughly correspond to exosites I and II of thrombin are also given. Notice that the bound Ca^{2+} ion (shown as a blue sphere) is held by interactions with several acidic side chains of the 70-loop.

The structures of free factor Xa (Padmanabhan et al., 1993) and of two non-covalent inhibitor complexes (the Daiichi inhibitor DX-9065a (Brandstetter et al., 1996), and FX-2212a (Kamata et al., 1998)) have been solved by X-ray crystallography. The structure of the latter complex has been reported in two different crystal forms (one of which is shown in Figs 1.15-1.16), and is particularly interesting because both EGF-like domains and their linker peptide are well ordered in all three crystallographically independent molecules. The extended region between both EGF-like repeats (Leu83-Phe-Thr-Arg-Lys-Leu88) has been mapped to the binding site of the putative factor Xa receptor called **effector cell proteinase receptor-1** (EPR-1) (Ambrosini et al., 1997; Cirino et al., 1997), a 62-kDa protein that appears to be needed for factor Xa binding to activated platelets to form a functional prothrombinase complex (Altieri, 1995; Bouchard et al., 1997). EPR-1 may contribute to prothrombinase formation by binding and stabilizing the exposed linker peptide between both EGF domains (Kamata et al., 1998). It has been shown that factor Xa association with EPR-1 induces acute inflammation *in vivo*, which may amplify both coagulation and inflammatory cascades (Cirino et al., 1997). Indeed, targeting of EPR-1 with antisense oligonucleotide or with a monoclonal antibody resulted in the suppression of immune responses *in vivo* (Duchosal et al., 1996).

The lack of contacts between both EGF repeats indicates that the N-terminal Gla-EGF tandem is not constrained to a definite position in factor X / Xa, but possesses a certain degree of flexibility. (Different orientations between the two EGF domains are observed in the three independent molecules reported by Kamata and co-workers). Accordingly, no density has been observed for EGF1 in the crystals of both free (Padmanabhan et al., 1993) and DX–9065a–inhibited des-Gla-FXa (Brandstetter et al., 1996), indicating that the domain is flexibly disordered. In contrast, the second EGF-like domain, located at the molecular surface opposite to the active site cleft (Figs 1.15, 1.16), is intimately associated with the catalytic domain of the proteinase. Therefore, the two domains might be considered as a single unit.

Regarding the active site architecture of factor Xa, a comparison with thrombin shows a rather open active site cleft, which is more a groove than a canyon (Fig. 1.16). The S2 pocket is almost entirely blocked by the bulky side chain of Tyr99, in agreement with the preference of glycine at the P2 site of substrates (compare Fig. 1.11). A conspicuous feature is the presence of a "hydrophobic box" delineated by the side chains of Tyr99, Phe174 and Trp215, which is ideally suited to accommodate bulky hydrophobic P4 substrate residues (Stubbs and Bode, 1994) (Fig. 1.16). Similar to thrombin, the surface of FXa shows a distinctive pattern of surface charge distribution. Basic residues (e.g., Arg93, Lys236, Arg240, Lys243; see Fig. 1.16) cluster to a site topologically equivalent to the heparin-binding exosite of thrombin (compare with section 1.2.5. and Figs 1.12b, 1.14), although they might serve a different function in factor Xa, such as substrate binding (Padmanabhan et al., 1993; Stubbs and Bode, 1994). An acidic patch is found in the "northeast" part of the molecule (standard orientation, Fig. 1.16) that corresponds to the anion-binding exosite I of thrombin, and may represent a factor Va binding site within the prothrombinase complex (Stubbs and Bode, 1994) (see section 1.3.4.).

1.2.7. Factor IXa: An Age-Regulated Factor

The vitamin K-dependent **factor IX** (**Christmas factor**, EC 3.4.21.22) is secreted as a 415-residue single-chain molecule that is activated in a two-step process by the extrinsic Xase complex (section 1.2.8.) or by activated factor XI (FXIa, section 1.2.10.). Initial cleavage at the α-site Arg145-Ala146 produces a two-chain inactive intermediate (FIXα). Cleavage at Arg180{15}–Val181{16} generates the physiological active form FIXaβ (formed by a light chain of residues Tyr1 to Arg145, disulfide-linked to the catalytic domain *via* Cys132–Cys289{122}), and removes the glycopeptide Ala146–Arg180 (Davie et al., 1991; Kurachi et al., 1993). Human neutrophil elastase (HNE) cleaves FIX at positions Thr140/Thr144 and Thr172/Val181 close to the physiological α- and β-activation cleavage sites, respectively. These cleavages generate an inactive factor IX species, what might contribute to the disrupted regulation of hemostasis that occurs in diseases such as **disseminated intravascular coagulation** (Samis et al., 1997).

The crystal structure of PPACK-inhibited factor IXa has been determined at 3.0 Å resolution (Brandstetter et al., 1995). As a major divergence from factor Xa, important contacts between both EGF-like repeats result in a relatively rigid arrangement of both domains (Fig. 1.17). More recently, the structure of FIXa bound to negatively charged phospholipid surfaces has been determined by electron crystallographic analysis of two-dimensional crystals. In agreement with the crystal structure, lipid-bound FIXa appears to consist of a membrane-bound "stem" (a small domain with an average diameter of 3 nm), which is oriented perpendicularly to the lipid layer, connected in its upper half to the larger domain (4.2 x 7.4 nm) which is nearly parallel to the lipid surface and contains the catalytic site (Stoylova et al., 1998).

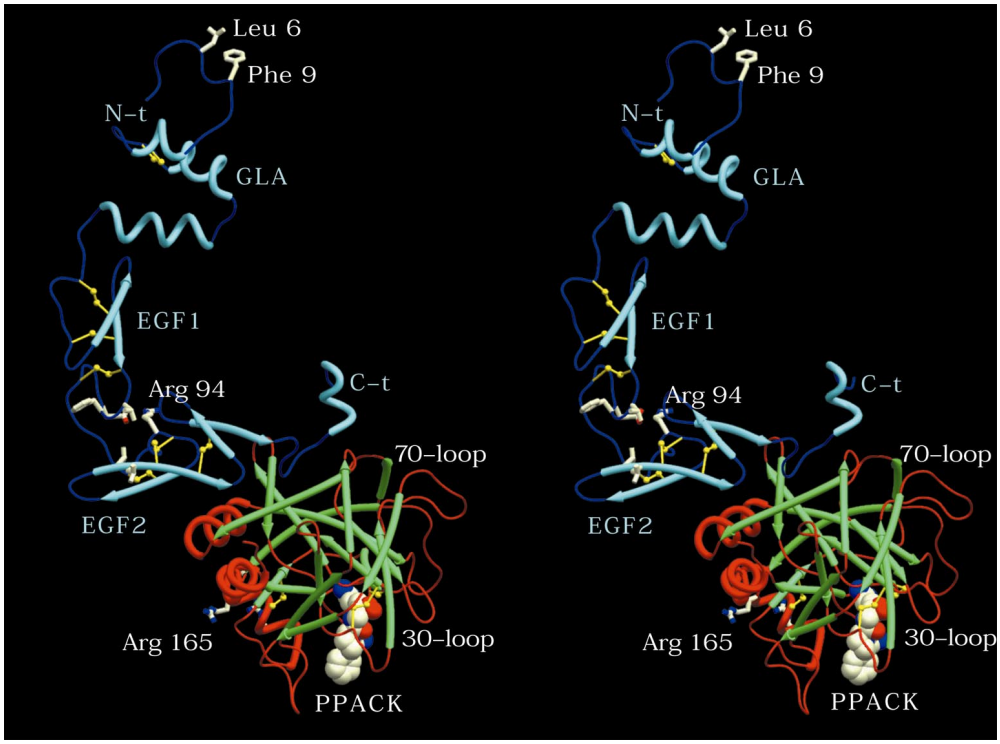

Fig. 1.17: Three-dimensional structure of factor IXa. The active-site bound inhibitor is shown as van der Waals spheres (color-coded). Residues Tyr1-Thr35 of the Gla domain were not visible in the electron density, and were modeled according to the conformation of the similar domain in prothrombin fragment 1 (compare Fig. 1.14). Several important side chains are given in full length; notice in particular the salt bridge Glu78-Arg94 joining EGF domains. Both this salt-bridge (Christophe et al., 1998) and the hydrophobic interdomain interactions (involving side chains of Phe75 and Phe77 (EGF1) as well as Val107 and Val108 (EGF2) in the human protein; (Celie et al., 2000)) are essential for binding of FIXa to its cofactor VIIIa and for factor VIIIa-mediated activation of factor X. Residues exposed within the α-helical stretch 162-170 (Kolkman et al., 1999; Mathur and Bajaj, 1999) (notice the position of Arg165) constitute another major FVIIIa binding site. This exosite corresponds approximately to the TF-binding region in factor VIIa (compare Figs 1.18, 1.19). The 30-loop (residues 199-204 of the mature proteinase) are involved in interactions with macromolecular substrates (Kolkman et al., 1999)).

Two unique features in the active site region of FIXa appear to be responsible for its low amidolytic efficiency (Castillo et al., 1983; Cho et al., 1984; McRae et al., 1981). First, the side chain of Tyr99 adopts an atypical conformation in the free factor in which the hydroxyl group occupies the region that corresponds to a canonically bound substrate P2 residue. Thus, to accommodate substrates Tyr99 has to be displaced to a higher energy conformation that simultaneously creates the S2 pocket and restricts the S4 pocket (Hopfner et al., 1999). It has been speculated that FVIIIa binding, perhaps to the intermediate helix (Fig. 1.17, see also section 1.2.8.), induces

rearrangements of the 99-loop to allow canonical substrate binding. Further, FIXa possesses a strictly conserved glutamate at position 219, which is occupied by a glycine in other serine proteinases (Greer, 1990). The glutamate side chain is located at the frame entrance of the S1 pocket, and might disturb proper formation of the active site machinery.

Blood coagulation potential is known to increase with age in healthy humans as well as in other mammals (Kurachi et al., 1996). This augmentation in coagulation potential is related to increases in plasma levels of procoagulant factors, specially factor IX, while the levels of anticoagulant and fibrinolytic factors are only marginally influenced (Lowe et al., 1997). Two age-regulatory elements (termed AE5', in the 5' upstream region of the factor IX gene and AE3', in the middle of the 3' untranslated region) are responsible for the age-associated elevation in plasma factor IX levels (Kurachi et al., 1999).

1.2.8. Factor VIIa and Tissue Factor

Coagulation **factor VII** (EC 3.4.21.21) is a 50-kDa vitamin K-dependent glycoprotein with an overall architecture similar to that of factors IX and X (compare sections 1.2.6 and 1.2.7. and Figs 1.14 – 1.16). It circulates in an inactive zymogen form in blood plasma at a concentration of approximately 0.5 mg/ml. Simultaneously, about 4 μg/ml of the activated proteinase (FVIIa) circulates in the blood (Howard et al., 1994; Wildgoose et al., 1992). Factor VIIa is unique among serine proteinases, however, because cleavage of the "standard" Arg15–Ile16 activation peptide bond (Arg152–Ile153 in the mature human protein) results in an incomplete zymogen-to-enzyme transition (Banner, 1997). Thus, the free enzyme is virtually inactive against its physiological substrates, factors IX and X.

The factor VIIa receptor **tissue factor** (TF) is a membrane-anchored type I glycoprotein that is constitutively expressed at high levels in tissues surrounding inner and outer bodily surfaces, but not in cells that are in direct contact with blood (Camerer et al., 1996). TF belongs to the family of **cytokine receptors** and is formed by two consecutive **fibronectin type III** (Fn-III) repeats. (For reviews see (Banner, 1997; Ruf and Edgington, 1994)). The crystal structure of the extracellular part of tissue factor has been determined both free (Harlos et al., 1994; Muller et al., 1994) and in complex with FVIIa (Banner et al., 1996)

(Fig. 1.18). Both Fn-III domains are held together through extensive contacts, resulting in a rigid assemble of the FVIIa interaction interface. This stiff structure allows positioning of the FVIIa active site above the membrane surface, even in the absence of the factor VIIa Gla domain (McCallum et al., 1997).

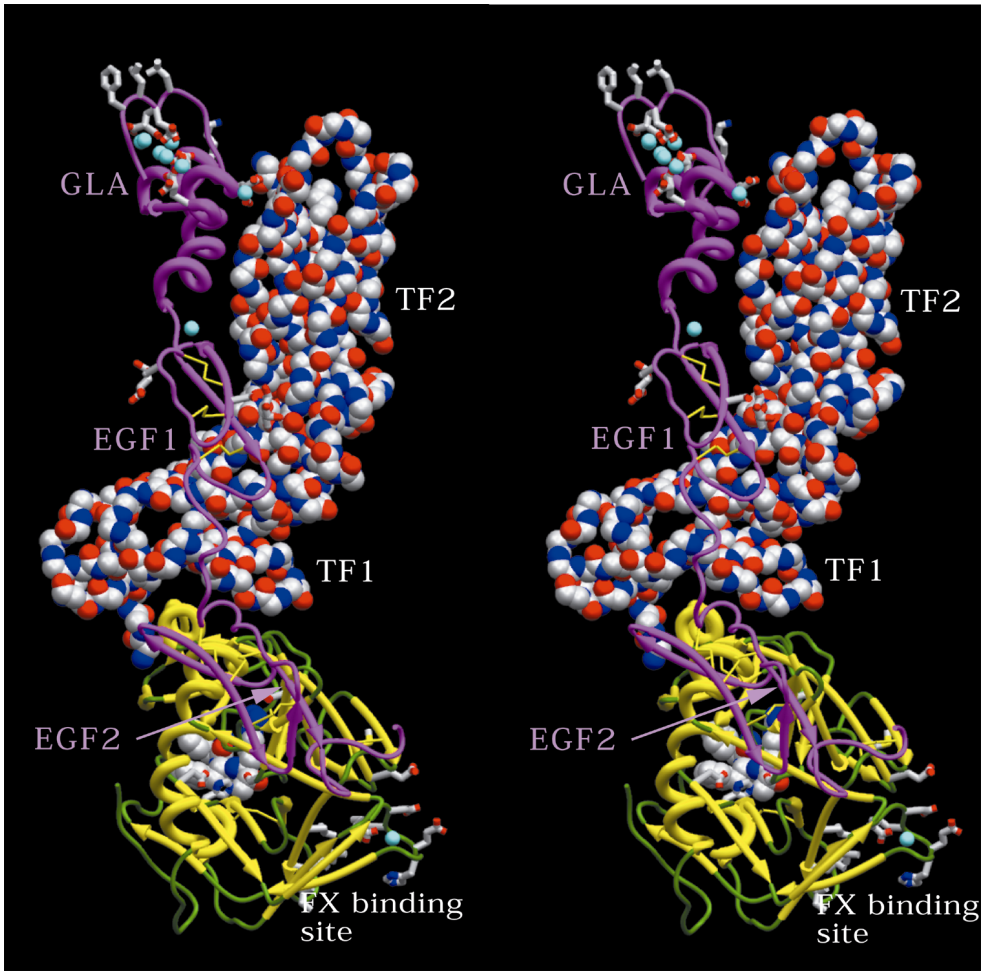

Fig. 1.18: Three-dimensional structure of the complex between soluble tissue factor and factor VIIa. The Cα traces of the two fibronectin III-like domains are given as van der Waals spheres (TF1, residues 1 to 101; TF2, residues 108 – 219); the factor VIIa moiety is shown as a ribbon plot. The N-terminal EGF-like domain is critical for alignment of TF with the catalytic domain of FVIIa, which in turn promotes optimal catalytic activities (Jin et al., 1999). Both TF and FVIIa are involved in the recognition of macromolecular substrates; the factor X binding site on FVIIa includes the neighboring residues Asp72, Glu75, Arg148, Glu154, Met156, and Asp185B (in agreement with mutagenesis studies (Dickinson et al., 1996)) as well as Leu32, Leu34, Ile65, Val67, Glu70, His76, and Leu153 (according to the structure of the bound exosite inhibitor (Dennis et al., 2000)), and is thus roughly equivalent to thrombin's exosite I.

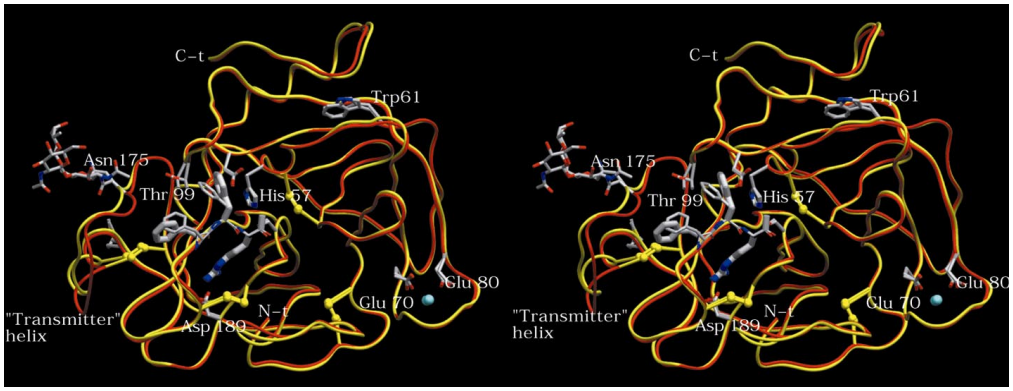

Fig. 1.19: Mechanism of factor VIIa modulation by tissue factor. Tissue factor appears to function as a cofactor in the activation of factor X by causing conformational changes in the active site of FVIIa. This is suggested by the structural rearrangements of the "transmitter" helix (165-170) between free and TF-bound FVIIa (red and yellow ribbons, respectively). It is considered that these changes might be conducted *via* disulfide bridge Cys168-Cys182 to the activation domain region 182-189 and stabilize the active enzyme conformation (Pike et al., 1999). Notice also the differences in the binding modes of the active site inhibitor D-Phe-L-Phe-L-Arg chloromethyl ketone in free and TF-complexed FVIIa.

In solution, FVIIa has an extended domain structure (Ashton et al., 1998), which appears to allow rapid interaction with TF over a large surface area (Fig. 1.18) to form the high affinity complex (K_d 2-5 nM; (Kelley et al., 1995; Martin et al., 1995)). The rigid scaffold provided by the tissue factor traps the FVIIa molecule, dampening the interdomain motions in the proteinase. This fastening of the proteinase conformation by its cofactor might be important for the recognition of the substrates, factors IX and X (Soejima et al., 1999). Perhaps more importantly, complex formation appears to induce subtle conformational changes that result in complete formation of the active site structure, as indicated by a recent crystallographic study (Pike et al., 1999). Residues Leu305{163}-Glu325{178} and in particular the short surface exposed "transmitter helix" 165–170 (residues 307–312 in the mature human protein) are thought to act as an allosteric control site by regulating the position of the activation domain loops Tyr184-Ser190 and Thr221-Phe225 (Pike et al., 1999) (see Fig. 1.19). Alternatively, TF binding might induce reorientation of the EGF-proteinase moieties to allow proper substrate positioning (Kemball-Cook et al., 1999).

Besides its role in the generation of initial amounts of factor IXa / Xa, the FVIIa-tissue factor complex produces a modified form of factor V which is highly

sensitive to inactivation by activated protein C (Safa et al., 1999), and an inactive factor VIII species no longer capable of activation by thrombin (Warren et al., 1999); see also sections 1.2.9. and 1.3.4.).

1.2.9. Protein C, Thrombomodulin and the Regulation of the Coagulation Cascade

The positive feed-back of thrombin generation promoted by the activation of FV and FVIII (see Fig. 1.1) would certainly result in an uncontrolled clot growth and in its downstream propagation in the absence of efficient down-regulation mechanisms. Initially, factor Xa generation is rapidly inhibited by **tissue-factor pathway inhibitor** (TFPI) (Broze, 1995) (section 1.5.4.). Several **serpins** (1.5.5.) readily inactivate the proteolytic cofactors FIXa, FXa and α-thrombin. Finally, thrombin complexation with the endothelial glycoprotein **thrombomodulin** (TM) triggers a major control mechanism that limits clot propagation (Esmon and Owen, 1981; Esmon et al., 1982).

Thrombomodulin binds α-thrombin with high affinity (K_d ~ 10^{-9} M), avoiding its diffusion from sites of tissue injury. Upon binding, procoagulant activities of α–thrombin are dramatically impaired because it is no longer able to productively interact with substrates such as fibrinogen and factor V (Esmon et al., 1982), or to activate platelets (Esmon et al., 1983). Moreover, thrombin's specificity is drastically changed in the presence of physiological concentrations of calcium ions towards the activation of the zymogen of another serine proteinase, **protein C** (formerly known as autoprothrombin IIa). In the presence of calcium and phospholipids, **activated protein C** (APC) subsequently inactivates the membrane-bound factors FVa and FVIIIa by limited proteolysis, thereby switching-off the coagulation cascade (Fig. 1.1, red arrows). (For reviews see (Esmon, 1995; Sadler et al., 1993; Walker and Fay, 1992)).

In addition to its protein C–cofactor activity, the thrombin-TM complex activates the procarboxypeptidase **thrombin-activatable fibrinolysis inhibitor** (TAFI; section 1.5.3.), resulting in the suppression of fibrinolysis (Bajzar et al., 1995; Bajzar et al., 1998; Broze and Higuchi, 1996; Nesheim et al., 1997) (indicated with blue arrows in Fig. 1.1). Thus, the combined effects of protein C and plasma procarboxypeptidase activation, along with the direct

inactivation of single chain u-PA (Molinari et al., 1992), protect the newly formed clot from premature lysis (Nesheim et al., 1997).

Protein C (EC 3.4.21.69) is expressed primarily in the liver as a single-chain precursor, which is cleaved into a light (residues Ala1–Leu155) and a heavy chain (Asp158–Pro419) held together by the single disulfide bridge Cys141–Cys277{122} (Foster and Davie, 1984; Stenflo and Fernlund, 1982). The zymogen is converted to the active proteinase (APC) upon thrombin cleavage of the Arg169{15}–Leu170{16} peptide bond (Fig. 1.11). In the absence of calcium, free thrombin catalyzes protein C activation at a low rate because aspartate residues at both P3 and P3' positions of the activation segment (Fig. 1.11) prevent access to the negatively charged active site cleft of thrombin (Bode et al., 1989; Bode et al., 1992) (Fig. 1.12b) and impair catalysis. At plasma Ca^{2+} concentrations, no protein C cleavage occurs unless the TM cofactor is bound to thrombin. The three-dimensional crystal structure of Gla-less activated protein C has been resolved at 2.8 Å resolution (Mather et al., 1996), and corroborated that the basic domain architecture corresponds closely to those of the coagulation factors VIIa, IXa and Xa (Fig. 1.20).

Thrombomodulin is a type I transmembrane glycoprotein that consists of a long N-terminal extracellular region followed by a highly conserved membrane-spanning domain (residues Gly498 to Leu521) and by a short cytoplasmic tail (residues Arg522 to Leu557) (Dittman and Majerus, 1990; Suzuki et al., 1987; Wen et al., 1987). The extracellular region comprises a lectin-like domain (Petersen, 1988; Villoutreix and Dahlbäck, 1998) (residues Ala1 to approximately Ala155 in the human protein) followed by a hydrophobic, alanine-rich domain with no clear sequence homology to other proteins, a string of six EGF-like repeats (residues 225 to Asp463), and a short serine/threonine-rich, *O*-glycosylated peptide (Ser464–Ser497). TM not only performs major regulatory functions in coagulation and fibrinolysis, but is also essential for embryonic development (Healy et al., 1995; Rosenberg, 1995; Weiler-Guettler et al., 1998). This is in keeping with reported effects on cell proliferation, which are independent of its anticoagulant activity (Zhang et al., 1998).

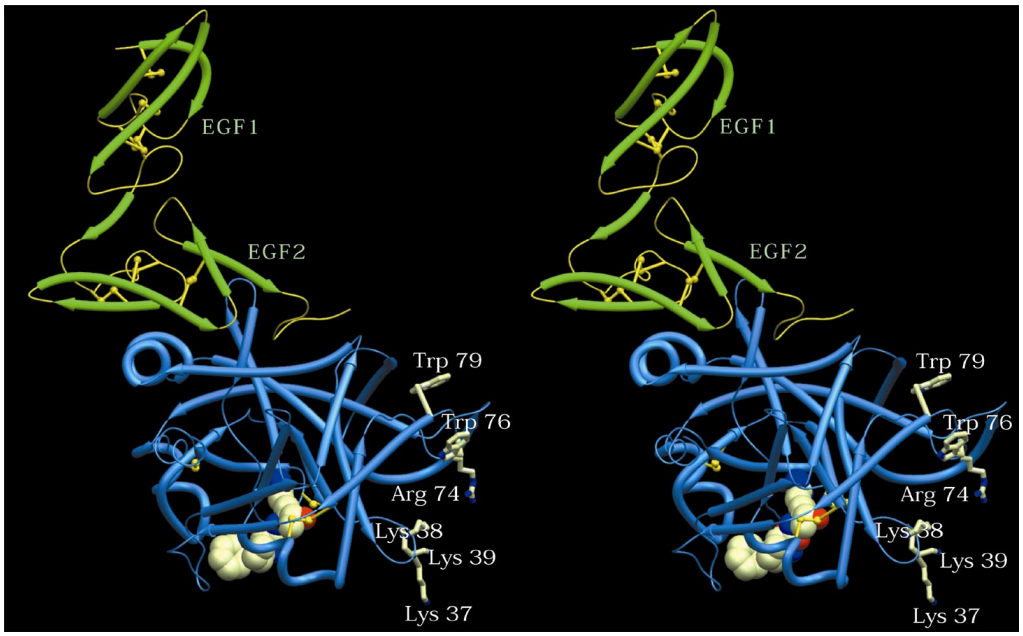

Fig. 1.20: Crystal structure of Gla-less activated protein C. EGF-like domains are shown in green, the catalytic domain is in blue. Domain EGF1 diverges from other EGF-like repeats due to the presence of an extra disulfide-bridged loop. A deep groove is found in a location analogous to the exosite I in thrombin (1.2.5.) and might represent a binding site for substrates / cofactors ((Mather et al., 1996); see also chapter 4).

Different hypothesis have been proposed to explain the TM-induced switch in thrombin specificity. Mutagenesis studies (Gibbs et al., 1995; Le Bonniec and Esmon, 1991; Le Bonniec et al., 1991; Rezaie and Esmon, 1994); discussed in detail in chapter 4) as well as experiments with fluorescence (Ye et al., 1991) or spin label probes (Musci et al., 1988) suggested allosteric changes in the environment of the thrombin active site upon TM-binding. However, calorimetric and enzyme kinetic experiments (Sadler, 1997; Vindigni et al., 1997) showed that TM binding is coupled only to those allosteric changes in the thrombin active site resulting from Na^+ saturation of the sodium binding site (Di Cera et al., 1997); section 1.2.5.). The activity of free thrombin, even if saturated by Na^+, is not adequate to meet the physiological requirements for activation of protein C and TAFI. Alternatively, it has been suggested that TM might influence the conformation of the bound PC substrate (Vindigni et al., 1997).

Models of thrombin-TME456, protein C and a docking model of their ternary complex have been recently proposed, suggesting that an additional binding site for protein C is present in thrombomodulin (Knobe et al., 1999). To elucidate the mechanism by which TM enhances the activation of protein C by thrombin, we have solved the crystal structure of TME456-bound to human α-

thrombin. This crystal structure is presented in chapter 4, along with a mechanism of protein C and TAFI activation.

1.2.10. Factor XI, Factor XII and the Contact Phase of Coagulation

Three additional serine proteinases and a non-enzymatic cofactor are involved in the **contact phase** of coagulation. The proteolytic components are **factor XI** or **plasma thromboplastin antecedent** (FXI, EC 3.4.21.27), **factor XII** (also termed **Hageman factor**) (FXII, EC 3.4.21.38), and **prekallikrein**, which is also known as **kininogenin** and as **Fletcher factor** (EC 3.4.21.34). The cofactor is **high molecular weight kininogen** (HMWK, or **Williams-Fitzgerald-Flaujeac factor**). FXI is a 160-kDa homodimeric plasma glycoprotein composed of two identical polypeptides connected by a disulfide bond (Fig. 1.2). Both the FXI monomer (Asakai et al., 1987; Fujikawa et al., 1986) and prekallikrein (Chung et al., 1986) consist of four tandem repeats termed A1, A2, A3 and A4 or **Apple domains**, followed by the actual serine proteinase catalytic domain (Fig. 1.2). Factor XII possesses a more complicated domain organization than other proteinases involved in thrombosis and hemostasis and consists of a linear array of a fibronectin type II, an EGF-like, a fibronectin type I (or **finger** domain), a second EGF-like repeat, followed by a kringle domain and the catalytic domain (Cool and MacGillivray, 1987), see also Fig. 1.2).

Binding of HMWK and factor XII to acidic surfaces or foreign materials (e.g., kaolin, glass) allows conversion of prekallikrein to kallikrein, which in turns activates FXII to factor XIIa. The latter can then hydrolyze additional prekallikrein to kallikrein, establishing a reciprocal activation cascade. FXI is then activated by FXIIa, by cleavage at a single site in each monomer (Arg369–Ile370), giving rise to **activated FXI** (FXIa) (Thompson et al., 1977). In the presence of calcium, activated factor XI triggers the **middle phase** of the intrinsic pathway of coagulation by activating factor IX (Fig. 1.1). Plasma FXI circulates in complex with its cofactor HMWK, from which the potent vasoactive and proinflammatory nonapeptide **bradikinin** is released upon conversion to a lower molecular form.

The physiological relevance of this mechanism for blood clotting *in vivo* is controversial, since deficiency of FXII, HMWK, or prekallikrein is not associated

with bleeding. In contrast, FXI is important in normal hemostasis because individuals deficient in FXI suffer a variable bleeding diathesis that may be particularly severe after surgery (Ragni et al., 1985). An alternative mechanism of FXI activation has been postulated, involving thrombin cleavage of FXI (Gailani and Broze, 1991; Naito and Fujikawa, 1991). Indeed, more recent experiments conducted *in vitro* using ultrasensitive assays for serine proteinases have granted conclusive evidence that factor XI activation is performed exclusively by thrombin (Butenas et al., 1997); activated platelets provide a physiologically relevant surface for the thrombin-mediated activation (Baglia and Walsh, 1998). In support of this mechanism, binding sites for both kringle 2 (Baglia and Walsh, 1998) and the catalytic domain (Baglia and Walsh, 1996) of prothrombin have been described in the Apple 1 domain of FXI.

Current evidence indicates that the proteins involved in the contact phase are actually antithrombotic, profibrinolytic, antiadhesive and proinflammatory factors, which contribute to the constitutive anticoagulant environment of the intravascular compartment (Bradford et al., 1997; Colman and Schmaier, 1997; Kluft et al., 1987; Lin et al., 1997; Schmaier, 1997). A role for FXIIa in fibrinolysis seems to result from its significant plasminogen activator activity (Braat et al., 1999), explaining the late onset of thrombotic phenotypes in combined t-PA–deficient and u-PA–deficient mice (Bugge et al., 1995; Carmeliet and Collen, 1996).

1.3. The Soluble Cofactors

1.3.1. Factors Va and VIIIa Are Cofactors of the Serine Proteinases Xa and IXa

Although free factor Xa is able to activate prothrombin (section 1.2.5.), at physiological concentrations it requires binding to **activated factor V** (FVa) and to a phospholipid surface for procoagulant activity. This calcium-dependent complex of factor Va, factor Xa (1.2.6.) and the phospholipid membrane (usually referred to as **prothrombinase complex**) enhances the rate of thrombin generation by five orders of magnitude when compared to FXa alone (Nesheim et al., 1979; Rosing et al., 1980). FXa, in turn, is generated from its zymogen either by a similar membrane-bound complex, the **intrinsic Xase complex**, which consists of activated factor IX (FIXa, section 1.2.7.) and the nonenzymatic

cofactor **activated factor VIII** (FVIIIa) (Fay et al., 1986), or by the tissue factor – factor VIIa complex (compare Fig. 1.1 and section 1.2.8.).

The functional similarities between the intrinsic Xase and prothrombinase complexes are underscored by remarkable sequence homologies. Not only possess both serine proteinases IXa and Xa closely related three-dimensional structures (compare Figs 1.15 and 1.17), but also the two cofactor precursors V and VIII share the same A1-A2-B-A3-C1-C2 multidomain architecture (Jenny et al., 1987; Kane and Davie, 1986; Toole et al., 1984) (Fig. 1.21). The non-homologous B domains are dispensable for procoagulant activity *in vitro* and are released during activation *in vivo* as the result of a few cleavages performed by trace amounts of α-thrombin (by far the best activator of both cofactors) or at a much slower rate by factor Xa, in the absence of thrombin (Foster et al., 1983; Kane and Davie, 1988). The proteolytic cleavage of factors V and VIII by thrombin and factor Xa thus provides potent positive feedback activation of the system. In the case of FV, these cleavages generate a heterodimeric, calcium-stabilized structure composed of a **heavy chain** (A1-A2, M_r ~104 kDa) and a **light chain** (A3-C1-C2, two glycoforms of different membrane affinity with M_r ~71 or 74 kDa) (Esmon, 1979; Kane and Davie, 1988; Rosing et al., 1993), whereas in FVIIIa an additional cleavage between domains A1 and A2 results in a heterotrimeric structure (Fay et al., 1986; Fay et al., 1991) (Fig. 1.21).

1.3.2. The A Domains Are Homologous to Several Metal-Binding Proteins

The A domains of coagulation factors V and VIII are approximately 40% identical to the triplicated domains of the major copper-binding protein in plasma, **ceruloplasmin** (Church et al., 1984; Kane and Davie, 1986). Each A domain possesses internal pseudo-twofold symmetry, with individual subdomains (designated D1 to D6 in both coagulation factors) revealing a β-barrel motif termed **cupredoxin fold** (Murphy et al., 1997). This motif has been observed in a large number of phylogenetically distant **blue copper–binding proteins** (Messerschmidt and Huber, 1990; Murphy et al., 1997; Ryden, 1988). The amino acid residues involved in Cu^{2+} binding define three different types of binding sites, which can be distinguished by spectroscopic analysis. In type I binding sites, the 'blue' copper is liganded by four residues: sequentially His, Cys, His and

Met, and give proteins such as **azurin** their characteristic blue color (intense optical absorbance at 600 nm). Type II copper ions are coordinated by three histidines (with no visible absorbance), while type III ions are associated with absorbance at 330 nm. Both factor V (Mann et al., 1984) and factor FVIII (Bihoreau et al., 1994) contain one mole copper ion/mol protein; at least for factor VIII this copper ion is in the reduced form (Cu^{+}), and is essential for proper folding (Tagliavacca et al., 1997).

The sequence homology with ceruloplasmin and related metal-binding proteins has been exploited to develop models of the A1-A3 domains of both FVa (Pellequer et al., 1998; Villoutreix and Dahlbäck, 1998) and FVIIIa (Pan et al., 1995; Pemberton et al., 1997).

1.3.3. The C Domains Are Homologous to a Fungal Lectin, Discoidin

The C domains of coagulation factors V and VIII (about 160 residues each) are homologous with discoidin I, a lectin with high affinity for galactose from the slime mould *Dictyostelium discoideum* (Poole et al., 1981; Vehar et al., 1984). Single or tandem copies of **discoidin domains** have so far been identified in several –mainly mammalian– proteins implicated in cell adhesion and/or developmental processes (recently reviewed by (Baumgartner et al., 1998), see also chapter 2). As in factors V and VIII, two consecutive discoidin-like repeats are found in **neuropilins** (receptors for axon guidance involved in the formation of certain neuronal circuits) and in **milk fat-globule membrane protein**, a protein identified in milk fat globule (Stubbs et al., 1990). Single copies of discoidin domains have been reported in the extracellular region of some **transmembrane tyrosine kinase receptors** (Johnson et al., 1993), which have been recently identified as orphan receptors for collagen (Vogel et al., 1997), and in the product of a gene (*XLRS1*), mutations of which lead to the degenerative disease **X-linked retinoschisis** (Sauer et al., 1997).

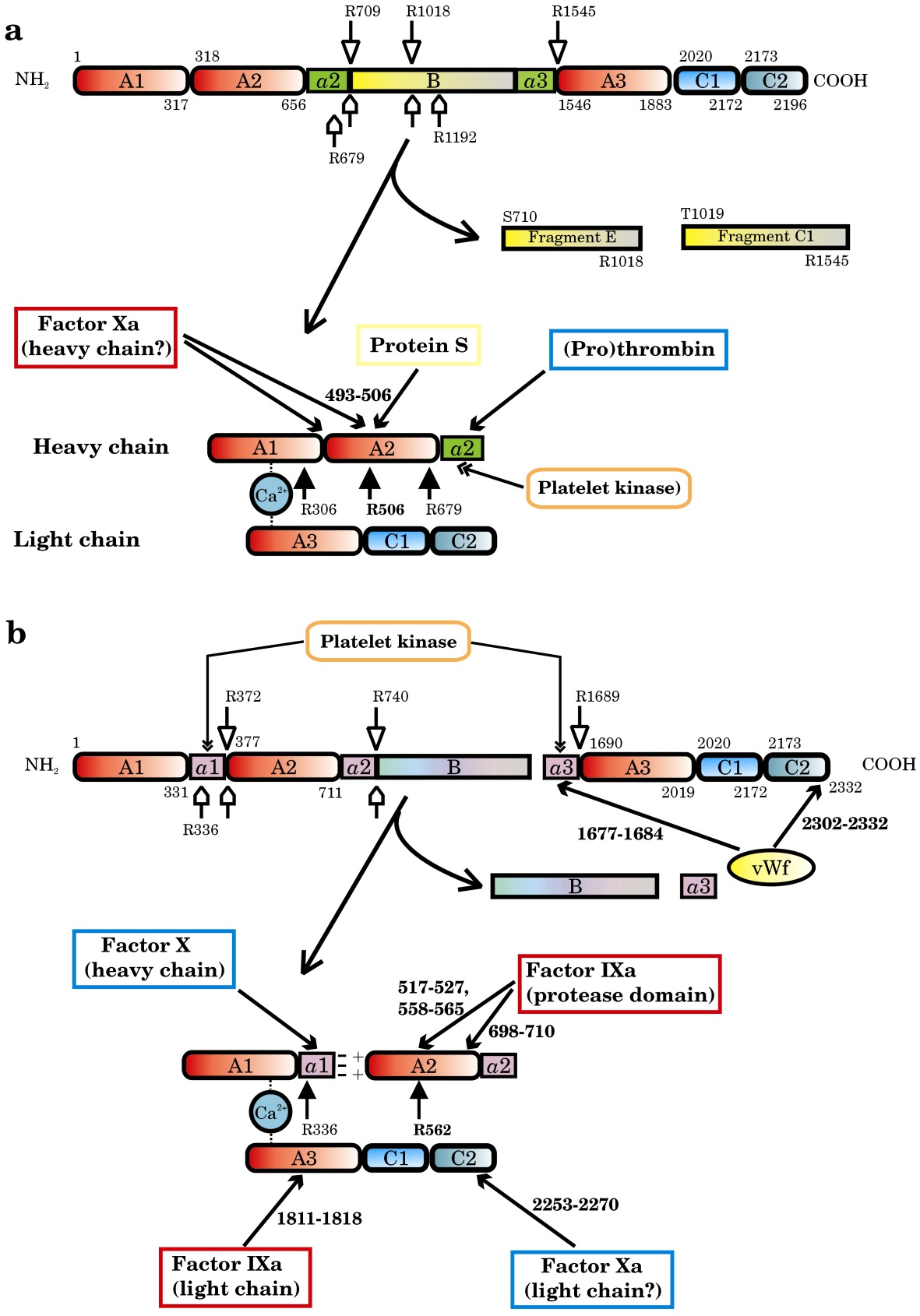

Legend

- Thrombin (factor Xa) cleavage
- sTF/FVIIa cleavage
- APC cleavage
- Phosphorylation

Fig. 1.21 (previous page): Domain organization and activation of factors V and VIII. Identified binding sites for substrates / cofactors are indicated. Notice that the cleavages performed by the sTF/FVIIa complex (Arg679, Arg1192) generate a molecule with a truncated heavy chain and an extended light chain (Safa et al., 1999). Cleavage of factor Va at Arg506 (bold in the figure) is not required for inactivation of the cofactor, but results in a more rapid cleavage at Arg306, a proteolytic event related to complete inactivation of factor Va (Heeb et al., 1995; Kalafatis et al., 1995; Kalafatis et al., 1994). APC resistance due to the mutation Arg506Gln (Aparicio and Dahlbäck, 1996; Bertina et al., 1994) is by far the most prevalent genetic cause of venous thrombosis. In addition to the proteolytic inactivation by protein C, the A2 subunit of factor VIIIa dissociates spontaneously, with complete loss of activity (Fay and Smudzin, 1992).

Previous investigations have shown that the C-terminal C2 domain of FV (FVa-C2) specifically binds to phosphatidyl-L-serine (P_LS) containing membranes (Ortel et al., 1992; Ortel et al., 1998). The homologous discoidin domain of FVIII has also been implicated in P_LS binding (Bardelle et al., 1993). Membrane interactions in both factor Va and factor VIIIa proceeds via stereoselective recognition of the *O*-phospho-L-serine polar head group (Comfurius et al., 1994; Gilbert and Drinkwater, 1993), targeting both trace cofactors to specific membrane environments on the surface of activated platelets (compare section 1.1. and chapter 2). The structure of FVa-C2 and its implications for membrane binding and prothrombinase assembly are presented in chapter 2.

1.3.4. Factor V Is Found Both in Plasma and in Platelets

Human factor V is a 330-kDa single-chain glycoprotein that is activated by thrombin cleavage at positions Arg709, Arg1018, Arg1545 within the B domain (Fig. 1.21). These cleavages generate the factor Va heavy (A1-A2) and light chain (A3-C1-C2) subunits, and releases the B domain as two activation fragments: fragment E (residues Ser710-Arg1018) and fragment C1 (Thr1019-Arg1545) (Jenny et al., 1987; Kane et al., 1987; Suzuki et al., 1982). Both heavy and light chains of factor Va remain noncovalently attached in an interaction mediated by a buried Ca^{2+} ion (apparent K_d ~ 50 μM), but which also involves hydrophobic interactions between the subunits (Laue et al., 1989). Recently, it has been reported that the TF-FVIIa complex generates a FVa variant with a truncated heavy chain (ending at Arg679) and an extended light chain (starting with Asn1193). This form could be further cleaved by thrombin to release the normal light chain, albeit at a significant slower rate than native factor V. Since the

modified form is as sensitive for inactivation by activated protein C (1.2.9.) as FVa, the extrinsic Xase complex appears to play an additional regulatory role, by producing a form of factor V that can be destroyed by APC without the requirement for full activation of the cofactor precursor (Safa et al., 1999).

The factor V activation pathway is initiated by exosite I-mediated binding of thrombin to a site in the heavy chain region of FV that facilitates the initial cleavage at Arg709 to generate the A1-A2 heavy chain of FVa (Dharmawardana et al., 1999) (see also section 1.2.5. and chapter 2). It has been early suggested on the basis of sequence homology that thrombin may bind to the heavy chain and fragment C1 of factor V *via* exosite I (Hortin, 1990; Pittman et al., 1994); direct interactions with the heavy chain have been experimentally demonstrated using active site-immobilized thrombin (Dharmawardana and Bock, 1998). Exosite I-dependent binding of thrombin to the FV heavy chain may direct the initial recognition of factor V as substrate and regulate the specificity of the cleavage reactions in the proteolytic processing pathway (Dharmawardana and Bock, 1998; Dharmawardana et al., 1999).

The cofactor role in the generation of FXa by the prothrombinase complex is the major physiological activity of factor Va. However, the precursor form factor V and protein S (1.3.6.) act synergistically with activated protein C in the degradation of factor VIIIa (Shen and Dahlbäck, 1994), implying an anticoagulant role for FV. The C-terminal part of the B-domain (in particular residues 1477-1545) is essential for this function (Thorelli et al., 1998). Therefore, cleavage by thrombin at Arg1545 (compare Fig. 1.21) results in loss of APC cofactor activity. Since this cleavage is the lowest reaction in the activation pathway of human FV (Keller et al., 1995; Suzuki et al., 1982), it is conceivable that intermediate activation forms retain anticoagulant activity.

1.3.5. Factor VIII Circulates in Complex With von Willebrand Factor

Sequencing of factor VIII cDNA predicted a mature secreted protein consisting of 2,332 amino acid residues with a calculated M_r of 265 kDa; with *N*-linked carbohydrate chains, the molecular mass of FVIII increases to 330 kDa (Vehar et al., 1984). Analysis of the sequence showed the repeating domain structure of A1-A2-B-A3-C1-C2 (compare Fig. 1.21). The A domains are bordered by short spacers (*a*1, *a*2, and *a*3) that are rich in aspartate and glutamate residues; the

overall structure of FVIII can be thus summarized as A1-*a*1-A2-*a*2-B-*a*3-A3-C1-C2. FVIII is highly sensitive to proteolysis before and after secretion. As a result, only a small fraction of circulating FVIII is in the single-chain form; the majority consists of **heavy chains** of variable lengths (A1 and A2 domains extended by variable lengths of B domain, M_r 90–220 kDa), linked noncovalently to the **light chain** (A3-C1-C2; M_r 80 kDa) (Vehar et al., 1984). Both chains are associated *via* bound metal ions, including copper ions (Tagliavacca et al., 1997).

Activation of factor VIII requires proteolytic cleavages after Arg372, Arg740 and Arg1689, which removes the B-chain segment as well as the acidic *a*3 peptide. In the resulting heterotrimer, domain A2 is noncovalently associated with the metal-ion linked A1/A3-C1-C2 dimer *via* electrostatic interactions between the acidic C-terminal tail of domain A1 and a basic region in A2 ((Fay, 1988; O'Brien et al., 1997); see Fig. 1.21). Expression of active recombinant FVIII constructs lacking almost the entire length of the B domain (factor VIII des(797–1652)) has confirmed that this region is not required for coagulant activity (Eaton et al., 1991).

In contrast to the freely circulating factor V, FVIII circulates in plasma in tight ($K_d \approx$ 0.2 nM) noncovalent association with the giant multimeric protein **von Willebrand factor** (vWf), which functions as a carrier for FVIII both during its secretion and in the general circulation. This association prevents both FVIII degradation (Koedam et al., 1988) and its untimely binding to phospholipid surfaces (Andersson and Brown, 1981); for recent reviews see (Matsushita et al., 1994; Sadler, 1998; Vlot et al., 1998). The vWf-binding site seems to be formed by two regions of the factor VIII light chain; the C2 domain and the acidic peptide N-terminal of the A3 domain (*a*3) (Leyte et al., 1989; Saenko et al., 1994). The light chain of factor VIII contains also a binding site for **low density lipoprotein receptor-related protein** (also known as **α2-macroglobulin receptor**), which mediates its transport to the intracellular degradation pathway (Lenting et al., 1999). This finding would explains the beneficial effect of vWf on the *in vivo* survival of FVIII. vWf is also present inside platelets, in endothelial cells and in the subendothelial matrix of the vessel wall. Besides its critical role in FVIII transport, it mediates initial adhesion of platelets to exposed subendothelium at sites of vascular injury, by binding both to the damaged vessel

wall (primarily through collagen) and to platelet **glycoprotein Ib** (GP Ib) (section 1.4.2.).

Like factors V and VIII, von Willebrand factor contains several repeated domains (Fig. 1.22a). It circulates in multimeric forms composed of up to 80 monomers (M_r 500 – 20,000 kDa) that are linked by disulfide bonds to make the largest protein found in plasma (Ruggeri and Ware, 1993; Ruggeri and Zimmerman, 1980; Sadler, 1998). The structures of recombinant fragments comprising the A1 (residues 475 to 709 of the mature sequence) (Emsley et al., 1998) and A3 domains (residues Cys923–Cys1109) (Huizinga et al., 1997) have recently been reported. Both domains possess a **dinucleotide–binding** or **Rossmann fold**, similar to that observed in the **inserted** (I-type) **domains** of several integrins (1.4.2.). The A1 domain possesses a major binding site for platelet glycoprotein (GP) Ibα (Andrews et al., 1989; Fujimura et al., 1986); see also section 1.4.2.), but its exposure seems to rely on interactions between domains A1 and A3 (Obert et al., 1999).

Although the exact mechanism by which FVIIIa functions is not known, it is likely that FVIIIa increases the catalytic efficiency of bound FIXa (section 1.2.7.) through both cofactor-enzyme and cofactor-substrate interactions, which in turn accelerate the reaction rate by optimizing the enzyme-substrate interaction. Two separate FIXa binding sites have been mapped to residues 1811–1818 of the A3 domain (Lenting et al., 1996) and to residues 517–527 and 558–565 of the A2 subunit (Fay and Koshibu, 1998) (Fig. 1.21). The former binding site appears to dominate the interprotein affinity, since the isolated light chain of FVIII exhibits a similar affinity for FIXa (K_d ~ 15 nM; (Lenting et al., 1994) as the intact factor VIIIa (K_d ~ 2 nM; (Duffy et al., 1992). On the other hand, binding of the A2 domain modulates the active site of the cognate factor IXa (Fay and Koshibu, 1998). It is tempting to speculate that this modulation involves rearrangements in the active site of factor IXa, in particular of the Tyr99 and/or Glu219 side chains (section 1.2.7.). The *a*1 peptide contains a substrate (FX) binding site (Lapan and Fay, 1997) within the acidic patch formed by residues 349–372. This peptide was shown to bind the serine proteinase moiety of factor X *via* a salt-bridge linkage(s) (Lapan and Fay, 1998).

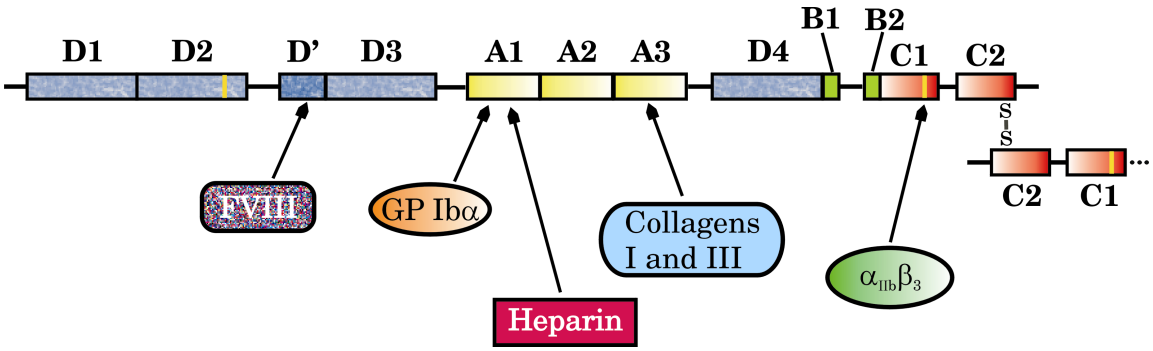
D1
D2
D'
D3
A1
A2
A3
D4
B1
B2
C1
C2
S-S
C2
C1
FVIII
GP Ibα
Collagens I and III
Heparin
$\alpha_{IIb}\beta_3$

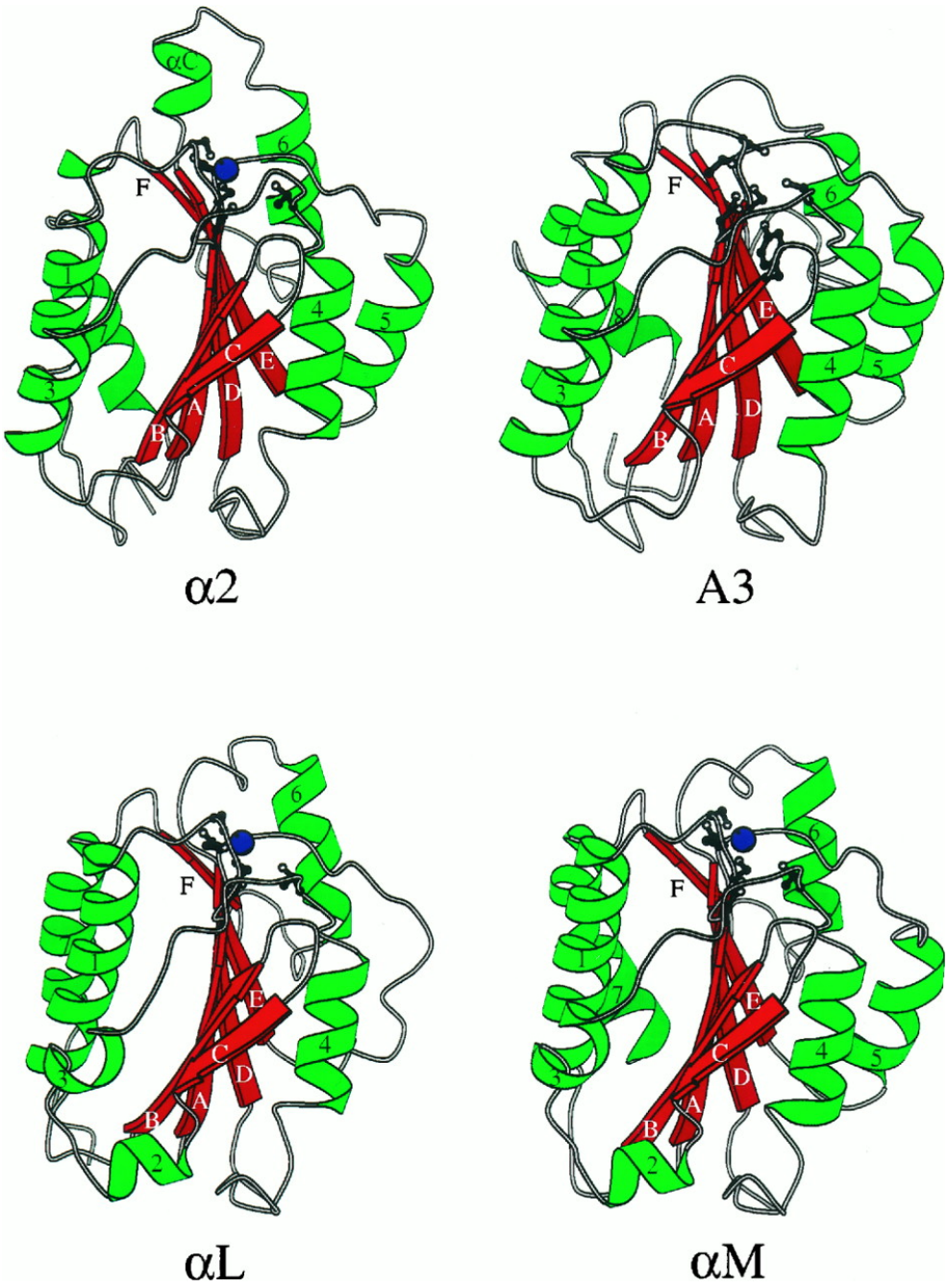
αC
F
A
B
C
D
E
α2
A3
αL
αM

Fig. 1.22 (previous page): Schematic domain organization of von Willebrand factor. (**a**) Structure of the vWf precursor (Shelton-Inloes et al., 1986; Verweij et al., 1986; Wagner and Marder, 1983), emphasizing binding sites for several cofactors. Processing of vWf monomers into larger multimers starts in the endoplasmic reticulum with the formation of intermolecular disulfide linkages (indicated), followed by multimerization and propeptide cleavage in the Golgi apparatus and secretory granules. Both domains D2 and C1 harbor a cell-attachment site characterized by the Arg-Gly-Asp sequence (indicated with yellow lines, see also section 1.4.2.). (**b**) Crystal structure of the vWf A3 domain, compared to related domains in several integrin **I domains** (from reference (Emsley et al., 1997)). The basic structure is a **dinucleotide-binding** or **Rossmann fold** – a central hydrophobic parallel β-sheet surrounded by amphipatic α-helices.

1.3.6. Protein S Is the Cofactor for Inactivation of FVa and FVIIIa by Activated Protein C

Protein S is a vitamin K-dependent protein that contains several modules; the N-terminal Gla domain (section 1.2.1.) is followed by a **thrombin-sensitive module** (the disulfide loop Cys47 to Cys72), four EGF-like domains, and a C-terminal domain with homology to **sex-hormone-binding globulins** (Dahlbäck, 1991; Lundwall et al., 1986). Up to 60% of protein S circulates in plasma in a noncovalent complex with **C4b-binding protein**, a major negative regulator of the complement cascade. It has been suggested that this association constitutes an important link between coagulation and inflammatory processes (Dahlbäck, 1991). The physiological importance of protein S as an anticoagulant is demonstrated by the association between protein S deficiency and thrombosis ((Dahlbäck, 1991); see also appendix A4).

Several effects of protein S binding contribute to the enhancement in APC activity. The cofactor increases the phospholipid affinity of the proteinase (Walker, 1981), and relocates its active site above the membrane surface to optimize factor Va cleavages (Yegneswaran et al., 1999; Yegneswaran et al., 1997); the slow peptide bond cleavage at Arg306 is specifically accelerated by protein S (Rosing et al., 1995) (compare also section 1.3.4. and Fig. 1.21). Additionally, protein S acts as a direct inhibitor of the prothrombinase complex, presumably by direct binding to both factor Va (Heeb et al., 1993) and Xa (Heeb et al., 1994). Protein S also directly inhibits prothrombinase assembly by competing for prothrombinase binding sites on membrane surfaces (Mitchell et al., 1988; van 't Veer et al., 1999; van Wijnen et al., 1996). A specific factor V binding site has been recently proposed on the C-terminal sex-hormone-binding

globulin domain of protein S, which appears to be important for the stimulation of FVIIIa degradation by APC (Nyberg et al., 1998) (see also section 1.3.4.).

Both protein S and its homologous Gas6 (see 1.2.1.) have been identified as ligands for the Axl subfamily of tyrosine kinase receptors, providing yet another link between coagulation and cellular responses required for tissue repair and growth (Godowski et al., 1995; Stitt et al., 1995).

1.4. Other Integral Membrane Proteins

Platelets interact with a whole array of plasma and extracellular matrix proteins, and possess also receptors for several small organic molecules (Fig. 1.23). Although a detailed analysis of these transmembrane receptors is out of the scope of the present work, the major platelet proteins involved in clot formation will be briefly introduced in the next two sections.

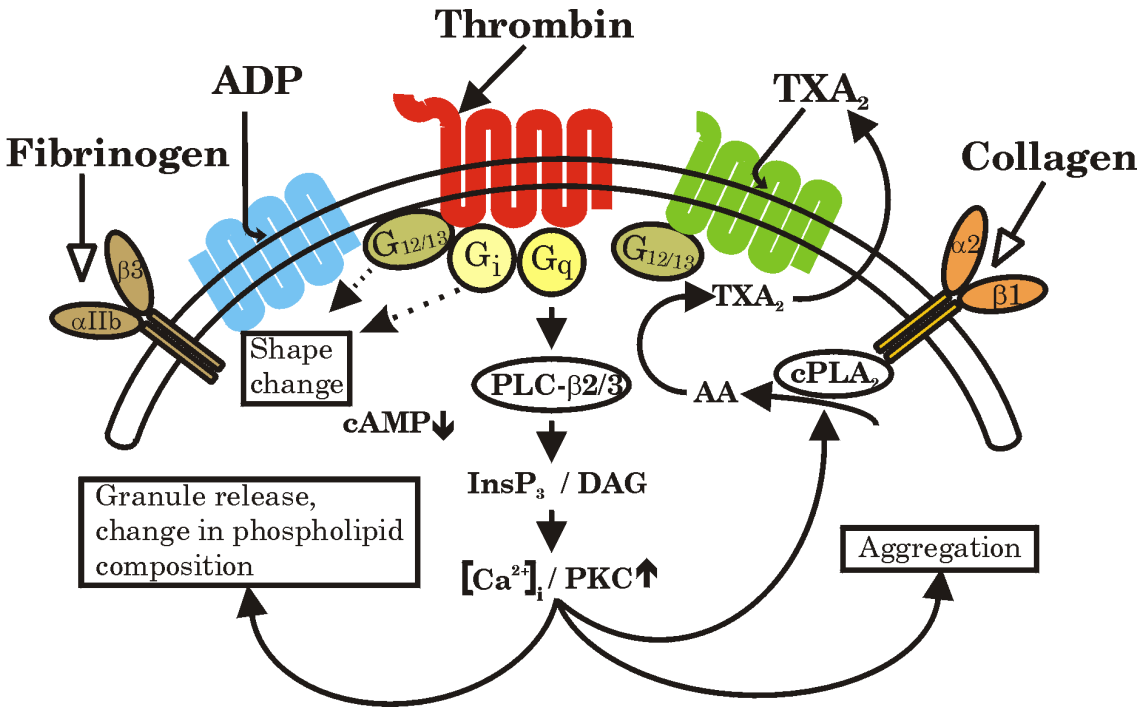

Fig. 1.23: Schematic representation of major events elicited upon platelet activation. Agonist binding leads to stimulation of **phospholipase C** (PLC) through a G-protein-coupled mechanism. Hydrolysis of phospholipids is mediated by the cytosolic **phospholipase A_2** ($cPLA_2$) to yield **arachidonic acid** (AA). Subsequently, the polyunsaturated fatty acid is metabolized to the eicosanoid, **thromboxane A_2** (TXA_2). $InsP_3$: inositol 1,4,5-triphosphate; DAG: diacylglycerol; PKC: protein kinase C. The central role of G_q in the initiation of platelet activation (Offermanns et al., 1997) is emphasized in this cartoon; see text for further details.

1.4.1. G-Protein–Coupled Protease-Activated Receptors

The activation of platelets by thrombin is mediated primarily by transmembrane **protease–activated receptors** (PARs; also known as **thrombin receptors**) (Vu et al., 1991), which belong to the widespread family of **rhodopsin–like** seven transmembrane proteins, and are characterized by the presence of seven α-helices folded into a bundle that spans the membrane (for reviews see (Bourne, 1997; Strader et al., 1995)). Until now, four different protease-activated receptors (PAR1 to PAR4) have been identified and characterized (Coughlin, 1999). PARs are activated when thrombin -or factor Xa and TF/FVIIa, in the case of PAR2 (Camerer et al., 2000)- binds to and cleaves the N-terminal receptor peptide to unmask a new amino terminus. This newly formed N-terminus inserts as a tethered ligand in the main body of the receptor, resulting in receptor activation. This mechanism is thus somehow analogous to the activation of zymogens of serine proteinases (1.2.4.1.). Accordingly, PARs can also be activated by small synthetic peptides corresponding to their tethered ligand sequences (e.g., the peptide SFLLRN that corresponds to the new N-terminus of PAR1).

In contrast to G-protein-coupled receptors for several small ligands (which are activated when agonists bind to the transmembrane region of the receptor), the specificity of PARs for their respective peptide agonists is determined by their extracellular loops, in particular by the N-terminal peptide and the second extracellular loop (e_2) (Gerszten et al., 1994). As for other macromolecular thrombin substrates, PAR1 recognition and cleavage seems to rely on interactions between an acidic, hirudin-like peptide located C-terminal to the receptor cleavage site and thrombin exosite I (Mathews et al., 1994).

Receptor activation requires switching interhelical constraints that stabilize the inactive state to a new set of contacts in the activated state, allowing binding of the cognate trimeric G-protein on the inside of the cell membrane. The free energy needed to drive this conversion is provided by agonist binding. Specific, conserved interhelical contacts between receptor α-helices 3, 6 and 7 seem to be important in stabilizing the off-state of the receptor, and could be broken or rearranged during receptor activation (Lu and Hulme, 2000). G proteins act then as transmembrane signaling systems coupled to GTP

hydrolysis, and generation of a second messenger molecule (e.g., cAMP, DAG). A general mechanism has been proposed to explain the transmission of the activating message from transmembrane receptors to the GDP-binding pocket of the α-subunit of G proteins (Iiri et al., 1998). Although the high-resolution structures of seven transmembrane receptors are unknown, general models for the Cα backbone have been published (Baldwin et al., 1997; Herzyk and Hubbard, 1998), based on analysis aided by the low resolution electron crystallographic structure of rhodopsin (Unger et al., 1997).

On the basis of sequence and functional homologies, G-protein α-subunits can be classified into four families: $G\alpha_s$, $G\alpha_{i/o}$, $G\alpha_q$ and $G\alpha_{12}$ (Simon et al., 1991). Although the receptors for platelet activators couple to several trimeric G proteins (e.g., G_i, G_q, G_{12}, and G_{13}), $G_{\alpha q}$ seems to be essential for the signaling processes used for different activators (Offermanns et al., 1997). The main down-stream events are believed to involve activation of β-isoforms of **phospholipase C** (PLC). PLC cleaves phosphatidyl-inositol 4,5-biphosphate to give inositol 1,4,5-triphosphate ($InsP_3$) and diacylglycerol (DAG), which in turn leads to the activation of **protein kinase C** (PKC). At the end of this cascade, granules are released and platelets aggregate. On the other hand, G proteins G_i, G_{12} and G_{13} might be involved in the induction of platelet shape change (see Fig. 1.23).

Recent investigations indicate the existence of a two-receptor system for platelet activation (Kahn et al., 1998). Two similar receptors (PAR3 and PAR4) contribute to platelet activation in mice, while PAR1 and PAR4 are the major human platelet thrombin receptors. A “high affinity” thrombin receptor (PAR1 in humans, PAR3 in mice) is necessary for responses to low concentrations of thrombin, while a second “low-affinity” receptor that lacks the hirudin-like acidic sequence responsible for binding to thrombin’s exosite I (PAR4), mediates responses at higher concentrations of thrombin (Coughlin, 1999). Recently, a role for PAR3 in mice as a cofactor in PAR4 activation has been inferred from experiments carried out in a heterologous system (Nakanishi-Matsui et al., 2000). However, the mouse system does not seem to have a direct analogy in human platelets.

In addition to the activation effect of the newly formed N-terminus, the cleaved N-terminal peptide of PAR1 (residues Met1 to Arg41) is a strong platelet

agonist (Furman et al., 1998), but the mechanism of activation remains to be fully elucidated.

1.4.2. Integrins and Other Platelet Receptors

The **integrins** are a large family of α/β noncovalent heterodimers that are expressed by virtually all cell types. Integrins mediate cell adhesion to the extracellular matrix (ECM), and also act as important signaling receptors (for reviews see (Giancotti and Ruoslahti, 1999; Hynes, 1992; Ruoslahti and Engvall, 1997; Schwartz et al., 1995; Shattil et al., 1998)). The extracellular domains of α- and β-subunits interact with each other to form a complex binding site for a wide variety of ligands. Integrins recognize short specific sequences present in ECM proteins; the most common and best characterized of these sequences is the Arg-Gly-Asp (RGD) motif. Integrins α and β subunits consist of a single transmembrane domain, a large extracellular domain of several hundred amino acid residues, and typically, a short cytoplasmic tail of about 20-70 residues devoid of enzymatic features (Bennett, 1996; Giancotti and Ruoslahti, 1999; Hynes, 1992). Hence, integrins can only transduce signals by associating with adapter proteins that connect the integrin with the cytoskeleton, cytoplasmic kinases, and transmembrane growth factor receptors. (For a recent review see (Giancotti and Ruoslahti, 1999)).

Several integrins play crucial roles during platelet activation and clot formation. The most prevalent protein on the platelet surface (50,000 to 80,000 copies) is the calcium-dependent integrin $\alpha_{IIb}\beta_3$ (also known as **glycoprotein IIb–IIIa** (GP IIb–IIIa) and as CD41-CD61; Fig. 1.24) (Pytela et al., 1986). The α_{IIb} subunit consists of an extracellular heavy chain (M_r ~125 kDa) and a transmembrane light chain of about 23 kDa (Poncz et al., 1987), while the β_3 subunit is a single, highly disulfide-bonded, transmembrane protein (for reviews see (Bennett, 1996; Calvete, 1994; Calvete, 1999; Phillips et al., 1991). GP IIb-IIIa mediates platelet-platelet and platelet-subendothelial matrix interactions by binding its ligands: fibrinogen (section 1.5.1.), von Willebrand factor (1.3.5.), thrombospondin, and the ECM proteins **fibronectin** and **vitronectin** (Phillips et al., 1988; Plow and Ginsberg, 1989), fibrinogen being the principal ligand of $\alpha_{IIb}\beta_3$ (Gardner and Hynes, 1985). The interaction between fibrinogen and $\alpha_{IIb}\beta_3$

involves several regions of the ligand, including the adhesion motif RGD, two copies of which are found in each α-chain of fibrinogen.

Although $\alpha_{IIb}\beta_3$ is present in the plasma membrane of resting platelets, it is inaccessible to soluble ligands. Platelet agonists activate the integrin (the **inside-out signaling**) by inducing structural changes in the complex and/or its microenvironment, which eventually allow the binding of soluble fibrinogen and von Willebrand factor. Ligand binding results in clustering of the $\alpha_{IIb}\beta_3$ complex in patches of the platelet surface and promotes platelet aggregation, presumably *via* cross-linking of adjacent platelets. This process is followed by **outside-in $\alpha_{IIb}\beta_3$ signaling**, which results in calcium mobilization, tyrosine phosphorylation of multiple proteins (included β_3 itself), increased cytoskeletal reorganization and further activation of $\alpha_{IIb}\beta_3$ (reviewed by (Shattil and Brugge, 1991)).

The phosphorylation state of the cytoplasmic region of the β_3 subunit is a major factor in the exposure of the extracellular ligand-binding sites on $\alpha_{IIb}\beta_3$ (van Willigen et al., 1996). In particular, phosphorylation of tyrosine residues Tyr747 and Tyr759 (Fig. 1.24a) seems to be essential for outside-in signaling, probably by mediating β_3 ability to interact with other signaling and cytoskeletal proteins (Law et al., 1999; Law et al., 1996). **Calpain** cleavage behind these two tyrosine residues could regulate bi-directional signaling across the plasma membrane (Du et al., 1995), in line with the postulated regulation of cytoskeletal signaling complexes by calpain in vWf-stimulated platelets (Yuan et al., 1997). On the other hand, the cytoplasmic domain of the α-subunit appears to independently modulate ligand binding affinity (O'Toole et al., 1991).

The three-dimensional solution structure of the myristoylated peptide comprising the intracellular part of α_{IIb} (residues Lys989 to Glu1008) has been recently determined in solution (Vinogradova et al., 2000). Comparison with the structure of a similar peptide that incorporates two point mutations leading to constitutive fibrinogen-binding (P998A/P999A) suggested a conformation-switch mechanism for regulating $\alpha_{IIb}\beta_3$ activation. In addition to its adhesive properties, a role for the integrin in prothrombin activation has been recently reported, pointing to another possible regulatory role (Byzova and Plow, 1997).

Platelets also express the unique adhesion receptor complex **glycoprotein Ib–IX–V** (GP Ib–IX–V), which contains four polypeptides assembled in a 2:2:2:1

stoichiometry (Lopez, 1994) (Fig. 1.24c). Glycoprotein Ib-IX is a heterotrimeric complex consisting of two disulfide linked subunits, GP Ibα and GP Ibβ; GP IX and GP V associate noncovalently with this complex. All four subunits of the GP Ib-IX-V receptor complex belong to a phylogenetically widespread family defined by the presence of a motif containing tandemly repeated leucine-rich sequences, known as **leucine-rich repeat** (LRR) motifs (Lopez and Dong, 1997; Ware, 1998). GP Ibα contains eight tandem leucine-rich repeats (Lopez et al., 1987; Titani et al., 1987), each GP Ibβ (Lopez et al., 1988) and GP IX (Hickey et al., 1990) contain one copy, and GP V presents fifteen tandem repeats (Hickey et al., 1993; Lanza et al., 1993). GP Ibα is a highly glycosylated protein (Fig. 1.24c), in which approximately half of the molecular mass of the extracellular domain is from carbohydrate (Korrel et al., 1984).

Fig. 1.24 (next page): Major adherent receptors on the platelet surface. The overall domain organization of (**a**) $\alpha_{IIb}\beta_3$, (**b**) $\alpha_2\beta_1$, and (**c**) GP Ib-X-V is presented. Major ligands are indicated, as well as phosphorylated residues, glycosylation sites, and several proteolytic cleavage sites. The major GP Ibα fragment is referred to as **glycocalicin**. The highly glycosylated macroglycopeptide mucin core of GP Ib creates an scaffold that locates the thrombin / vWf-binding site 45 nm away from the platelet plasma membrane (Fox et al., 1988). **Calreticulin** is a highly conserved intracellular protein, which binds to the cytoplasmic domains of integrin α-subunits and modulates both integrin adhesive functions and integrin-initiated signaling (Coppolino et al., 1997). ABP, **actin-binding protein** (also termed **filamin**). 14-3-3 proteins bind to oncogene and proto-oncogene products, including c-Raf-1. The structure of free ζ 14-3-3 protein (Liu et al., 1995) and of its complex with a phosphoserine-containing peptide derived from its binding site in Raf (Muslin et al., 1996) have been resolved by X-ray crystallography. The structure of the α_2 collagen-binding I domain (Emsley et al., 1997) is shown in Fig. 1.22b.

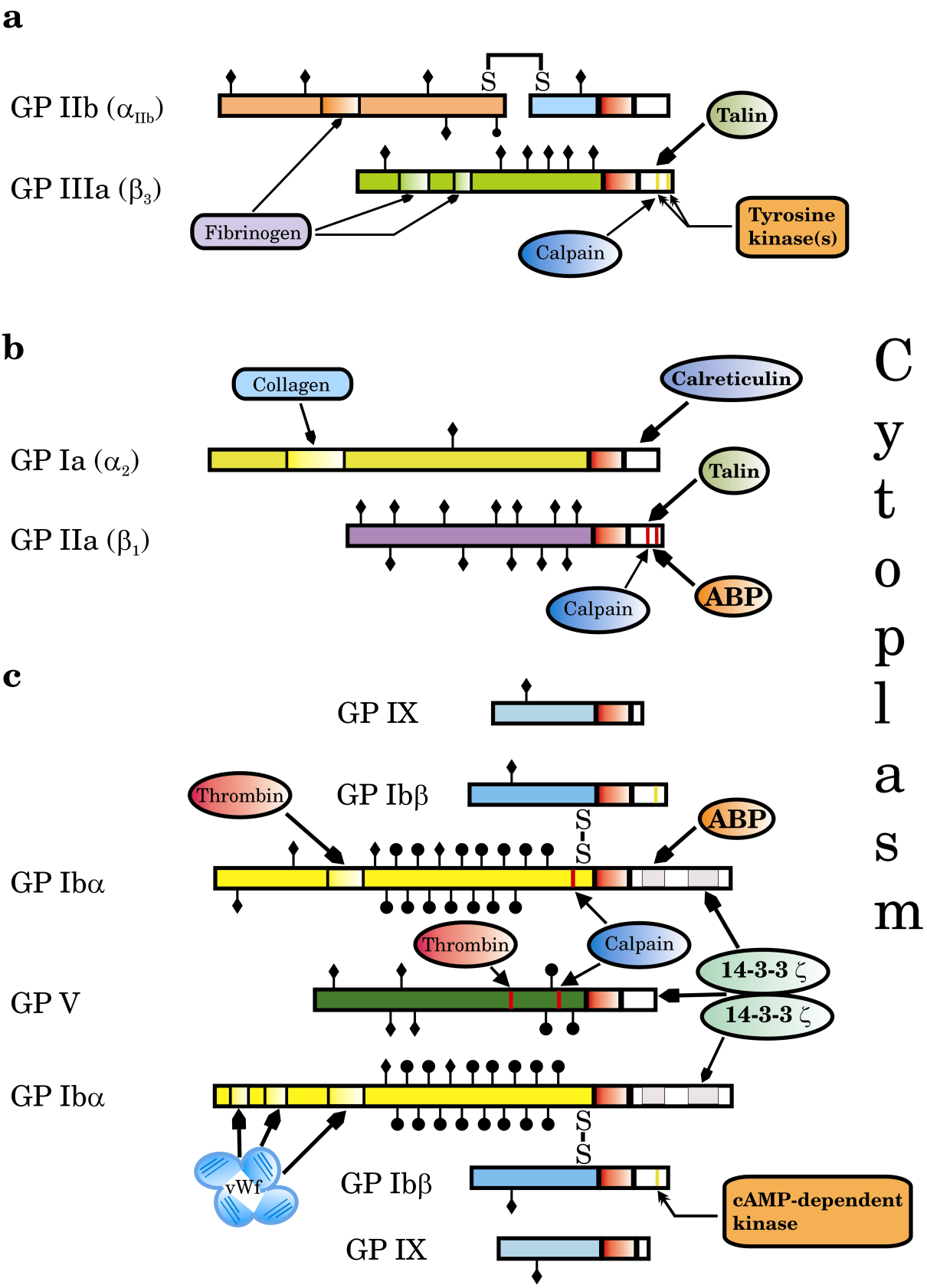
a
GP IIb (α_{IIb})
GP IIIa (β_3)
S
S
Talin
Fibrinogen
Calpain
Tyrosine kinase(s)
b
Collagen
Calreticulin
GP Ia (α_2)
GP IIa (β_1)
Talin
Calpain
ABP
c
GP IX
Thrombin
GP Ibβ
S-S
ABP
GP Ibα
Thrombin
Calpain
14-3-3 ζ
GP V
14-3-3 ζ
GP Ibα
S-S
vWf
GP Ibβ
cAMP-dependent kinase
GP IX
Cytoplasm
Legend
Binding
Proteolytic cleavage
Phosphorylation
Transmembrane domain
N-glycosylation
O-glycosylation

The receptor GP Ib-IX-V mediates platelet adhesion to sites of blood vessel injury by binding von Willebrand factor in the subendothelium, and facilitates thrombin-mediated platelet activation by providing a high affinity binding site for this agonist. GP Ibα is the only subunit of the receptor shown to possesses binding sites for thrombin (De Marco et al., 1994) and von Willebrand factor (Gralnick et al., 1994); the GP Ibα extracellular domain is necessary and sufficient for interacting with vWf under high shear stress (Marchese et al., 1999). The thrombin and vWf binding site(s) has been mapped to residues Phe199-Val295 within the N-terminal domain of GP Ibα; in particular to the highly acidic segment Asp272 to Glu282, comprising three sulfated tyrosine residues (Marchese et al., 1995). The vWf-binding site may also include residues Gly233–Met239, since mutations Gly233Val (Miller et al., 1991) and Met239Val (Russell and Roth, 1993) enhance the affinity of GP Ib for circulating vWf. GP V contributes to the formation of the thrombin binding site, and constitutes one of the primary proteolytic targets of thrombin on the platelet surface (Berndt and Phillips, 1981). However, expression of GP V is not needed for formation of a functional vWf-binding site. Instead, this subunit appears to act as a negative modulator of platelet activation (Ramakrishnan et al., 1999).

Thrombin binding to GP Ib appears to be mediated by electrostatic interactions with anion-binding exosite II, protecting the enzyme from antithrombin inhibition (De Cristofaro et al., 2000); see also 1.5.5.). This binding site on GP Ibα has been assigned to the high-affinity thrombin binding site on the platelet surface, but the physiological role of GP Ibα binding to thrombin is still a matter of controversy (Hayes and Tracy, 1999). In particular, platelet activation follows thrombin interaction with PAR1 and not with GP Ib (Liu et al., 1997). The results of De Cristofaro and co-workers suggest that GP Ibα binding to exosite II of proteolytically active thrombin may modulate platelet activation (*via* hydrolysis of PAR1 or PAR4) or fibrinogen cleavage (De Cristofaro et al., 2000). Another physiological role of this thrombin receptor may be the regulation of the α-thrombin concentration in circulation. On the other hand, GP Ibα binding to von Willebrand factor plays a key role in interplatelet cohesion, necessary to complement the function of activated $\alpha_{IIb}\beta_3$ at high shearing flow conditions (Goto et al., 1998).

Adhesion of platelets to **collagen** involves first the reversible recognition of collagen-bound von Willebrand factor by the platelet receptor complex GP Ib-IX-V, followed by direct interaction between collagen and the platelet integrin receptor $\alpha_2\beta_1$ (also known as GP Ia–IIa, CD49B-CD29, and as very late antigen-2) (Fig. 1.24b) (Barnes et al., 1998; Moroi and Jung, 1997; Santoro and Zutter, 1995). Platelet activation then follows from the recognition of GPP* (P*: hydroxyproline) collagen sequences by another collagen receptor, termed **GP VI** (Barnes et al., 1998). GP VI induces most of the signals involved in platelet activation, including phospholipase Cγ2 activation by a tyrosine kinase-dependent pathway (Ichinohe et al., 1995; Santoro and Zutter, 1995). $\alpha_2\beta_1$ can be converted to its activated (collagen-responsive) form by a mechanism similar to that responsible for activation of $\alpha_{IIb}\beta_3$ (Jung and Moroi, 2000). The structural basis of collagen recognition by integrin $\alpha_2\beta_1$ has been recently elucidated by R. Liddington and co-workers (Emsley et al., 2000). Three loops on the upper surface of the I-domain (residues Asp159-Met349 of the α-subunit, compare Fig. 1.22b) coordinate a Mg^{2+} ion and also engage collagen, with a glutamate side chain of the latter completing the metal coordination sphere. Comparison between the unliganded ("closed") and the collagen-bound ("open") conformation suggests a pathway of signal transduction upon ligand binding.

1.4.3. Endothelial Protein C Receptor

Endothelial cells of large vessels have been shown to express an integral membrane protein that binds both zymogen protein C and APC with high affinity (Fukudome and Esmon, 1994). The physiological function of this **endothelial protein C receptor** (EPCR) is not yet fully understood. Work done by Esmon and co-workers indicate that EPCR functions as an important regulator of the protein C anticoagulant pathway by binding protein C and enhancing activation by the thrombin-TM complex (Fukudome et al., 1998; Stearns-Kurosawa et al., 1996); this effect is enhanced in the presence of phosphatidylcholine vesicles (Xu et al., 1999). Furthermore, binding of activated protein C to EPCR does not prevent inactivation by serpins (1.5.5.). These results suggest that EPCR does not sterically block the active site cleft of APC, but modulates enzyme specificity in a manner resembling the effect of thrombomodulin on thrombin's specificity.

EPCR (221 residues) is type I transmembrane protein homologous to the antigen presenting major histocompatibility complex (MHC) class I/CD1 molecules (Fukudome and Esmon, 1994). The extracellular part of EPCR consists of two domains, which are similar to the α1 and α2 domains of MHC class I molecules, whereas the α3 domain of MHC is replaced in EPCR by a transmembrane region followed by a short cytoplasmic tail. A soluble form of EPCR (sEPCR, residues 1–194), probably released from the cell surface by the action of a metalloproteinase (Xu et al., 2000), blocks phospholipid interaction of activated protein C and alters the active site of the proteinase (Liaw et al., 2000). A three-dimensional model of this soluble region has been recently reported (Villoutreix et al., 1999), exploiting the high sequence similarity with mouse CD1 (Zeng et al., 1997).

1.5. Other Soluble Proteins

1.5.1. Fibrinogen, Fibrin and Blood Clot Formation

The rate of conversion of the primary substrate of thrombin, **fibrinogen** (also termed factor I) to the insoluble **fibrin** is a key factor in hemostasis. Fibrinogen is a high molecular weight molecule ($M_r \approx$ 340 kDa), made up of three pairs of disulfide-linked polypeptide chains denoted as Aα, Bβ, and γ (Doolittle, 1984; Herrick et al., 1999) (Fig. 1.25). Fibrinogen plays central roles both in the formation of the blood clot and in cell adhesion (Doolittle, 1984; Hynes, 1992). The fibrinogen molecule folds into three distinct domains, two distal globular entities (the **D domains**, M_r ~67 kDa, formed by the C-terminal domains of the β and γ subunits), each linked to a single central **E domain** of about 33 kDa (containing the N-termini of all three chains) by a triple stranded array of the polypeptide chains believed to exist in the form of α-helical 'coiled coils'. Electron microscopy studies confirm this trinodular structure (Rao et al., 1991). Thrombin cleavages at α-Arg16 and β-Arg14 and subsequent release of the **fibrinopeptides** A and B (see Fig. 1.11 for cleavage sites) exposes a site in the E domain after which adjacent fibrin monomers, $(\alpha,\beta,\gamma)_2$, associate spontaneously to form regular arrays. Thrombin exhibits a remarkable specificity by cleaving only two out of the 181 Arg/Lys-Xxx peptide bonds in the fibrinogen molecule (Blombäck et al., 1967). The molecular basis for thrombin recognition and

cleavage of fibrinopeptide A has been established (Martin et al., 1992; Stubbs et al., 1992); see also Fig. 1.26).

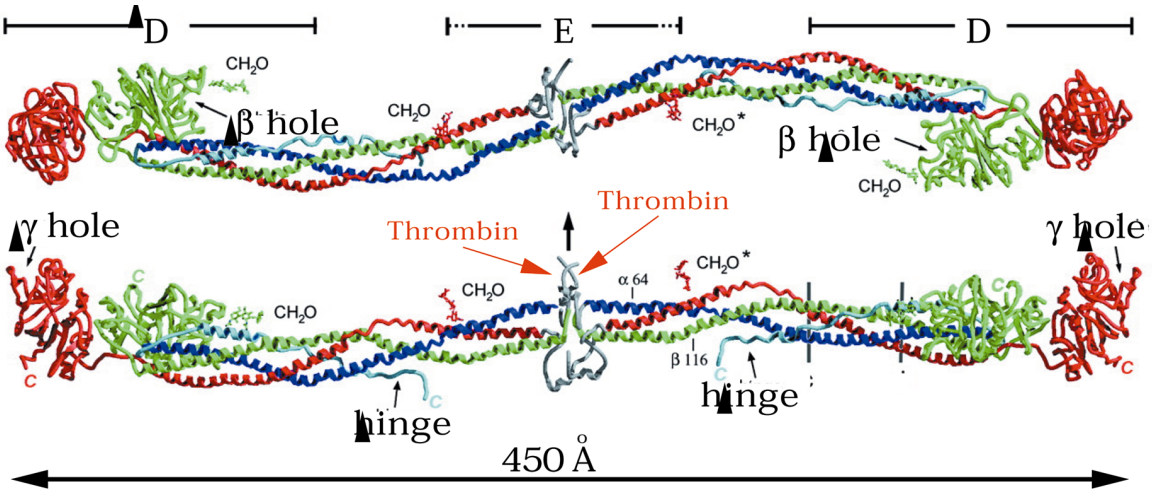

Fig. 1.25: Overall structure of the fibrinogen molecule. The globular C-terminus of the γ-chain contains a fibrin polymerization surface; residues Gln398 on one molecule (the amine acceptor) and Lys406 from another molecule (the amine donor) are cross-linked in a very rapid reaction catalyzed by factor XIIIa (1.5.2.). Potential recognition sites for the platelet receptor $\alpha_{IIb}\beta_3$ (section 1.4.2.) include residues γ400-411, as well as the 'classical' RGD-motifs at positions α95-α97 and α572-α574. The globular domain of the γ-chain also contains the PAR recognition site and a calcium-binding site (residues γ315-γ329). Modified from reference (Brown et al., 2000).

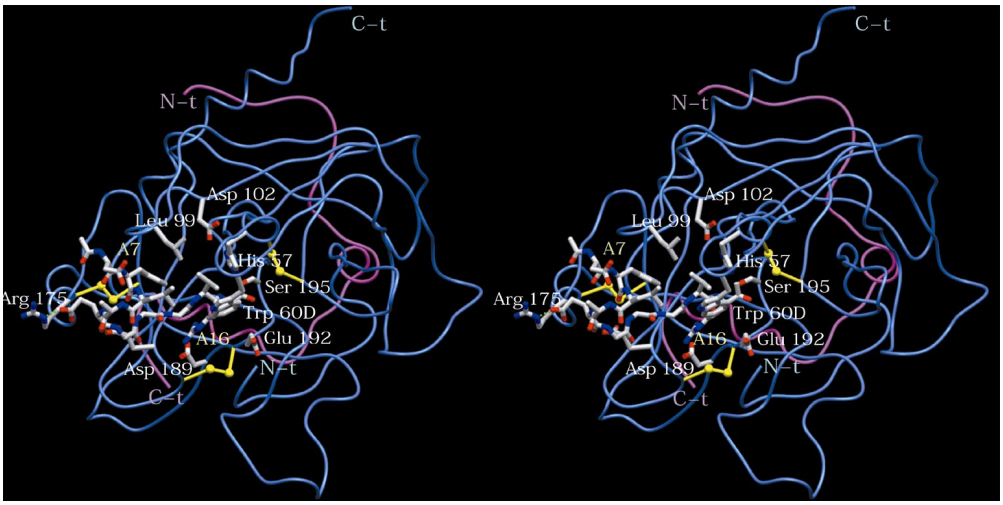

Fig. 1.26: Crystal structure of bovine thrombin bound to fibrinogen residues A7-A16. The light chain of thrombin is shown as a pink ribbon, the heavy chain is in blue. Active site residues of thrombin are given color-coded with all their non-hydrogen atoms, along with other residues that are important for specificity (e.g., Asp189, Glu192). The covalently bound chloromethylated decapeptide is also shown with all non-hydrogen atoms.

Determination of the three-dimensional structures of both fragment D and of the fibrin fragment comprising two covalently bound D domains (Everse et al.,

1998; Spraggon et al., 1997)), as well as of the C-terminal fragment of the γ chain (Yee et al., 1997) has provided insights into the molecular basis of the polymerization process (recently reviewed by (Doolittle et al., 1998)). More recently, low resolution structures of the essentially intact molecule have been reported (at≈ 4 Å (Brown et al., 2000) and at 5.2 Å (Yang et al., 2000) resolution, respectively).

1.5.2. The Transglutaminase Factor XIIIa Stabilizes the Fibrin Clot

Although fibrin monomers associate spontaneously upon release of the fibrinopeptides A and B, the thus formed clot lacks mechanical strength, and is therefore called a **soft clot**. Clot stabilization is achieved by the last enzyme to be activated in the coagulation cascade, a calcium-dependent **transglutaminase** known as **factor XIIIa** (EC 2.3.2.13) and as **fibrinoligase** (endo-γ-glutamine:ε-lysine transferase), which catalyzes the cross-linking of neighboring fibrin molecules (Greenberg et al., 1991; Takahashi et al., 1986). Factor XIIIa also links fibrin to the serpins (1.5.5.) α_2-antiplasmin (Reed et al., 1992; Sakata and Aoki, 1980; Sakata and Aoki, 1982) and PAI-2 (Ritchie et al., 1999), thus preventing premature degradation of the fibrin clot by plasmin. Furthermore, FXIIIa cross-links fibrin to extracellular matrix proteins such as fibronectin, collagen and thrombospondin, which facilitates wound healing (Barry and Mosher, 1988).

The plasma FXIII molecule is a tetrameric zymogen (A_2B_2) of two A and two glycosylated B chains, while monocytes and platelet FXIII exists as an intracellular dimer composed of two A chains which are identical to the plasma subunits (Greenberg et al., 1991; Muszbek et al., 1999; Takahashi et al., 1986). The B subunits are formed by 10 tandem repeats of approximately 60 residues known as **GP-I structures**, **short consensus repeats** (**SCR**) or **Sushi domains**. The B chains appear to stabilize and/or protect the catalytic A chains from degradation.

Cellular FXIII has been crystallized in two different crystal forms, and its structure has been solved at 2.8 (Yee et al., 1994) and 2.1 Å resolution (Weiss et al., 1998), respectively (see Fig. 1.27). The structural work revealed the presence of a catalytic triad (formed by residues His373, Cys314 and Asp396) that is reminiscent of that observed in papain-like **cysteine proteinases** (Yee et al.,

1994). It is therefore proposed that covalent ligation of the free amino group of one lysine residue to a nearby carboxyamide group of a glutamine residue to form the γ-glutaminyl-ε-lysyl-isopeptide bond proceeds by a mechanism that is the reverse of the peptidase mechanism ((Pedersen et al., 1994; Yee et al., 1994); see also section 1.2.4. and Fig. 1.10).

The activation peptide of each A subunit crosses the dimer interface and occludes the active site region of the other subunit (Fig. 1.27), explaining at least partially the zymogen character of the crystallized material. Thrombin activates FXIII by cleaving the N-terminal activation peptide (residues Ser1-Arg37) in a Ca^{2+}-dependent reaction. Interestingly, experimental data indicates that the N-terminal peptide remains bound to the catalytic core in FXIIIa (Muszbek et al., 1993; Polgar et al., 1990; Yee et al., 1995). Exposure of the active-site Cys314 requires a calcium-dependent conformational change in the thrombin-cleaved A chain. It is further suggested that cross-linking of macromolecular substrates requires displacement of one or both of the β-barrel domains (Pedersen et al., 1994; Yee et al., 1994). Calcium ions are also essential for the catalytic mechanism of the transglutaminase (Greenberg et al., 1991), and a calcium-binding site has been identified in the crystal structures (Fig. 1.27). The presence of two non-proline *cis* peptide bonds in the catalytic domain of FXIIIa (Arg310-Tyr311 and Gln425-Phe426) near the catalytic Cys314 and the dimer interface, respectively, have seeded the speculation that *cis*/*trans* isomerization of these peptide bonds triggers conformational rearrangements allowing exposure of the active site (Weiss et al., 1998).

Fig. 1.27 (next page): Structure of factor XIII. The molecule is viewed down the pseudo two-fold axis relating both monomers. In one of the molecules, the N-terminal activation peptide is in violet, domains I (β-sandwich), II (core), III (barrel 1), and IV (barrel 2) are colored, respectively, in red, yellow, green and blue. Domains III and IV are both of the fibronectin type III. The second dimer is colored Grey. Residues Glu485 and Glu490 have been recently identified as calcium ligands that regulate catalysis (Lai et al., 1999) and are explicitly shown.

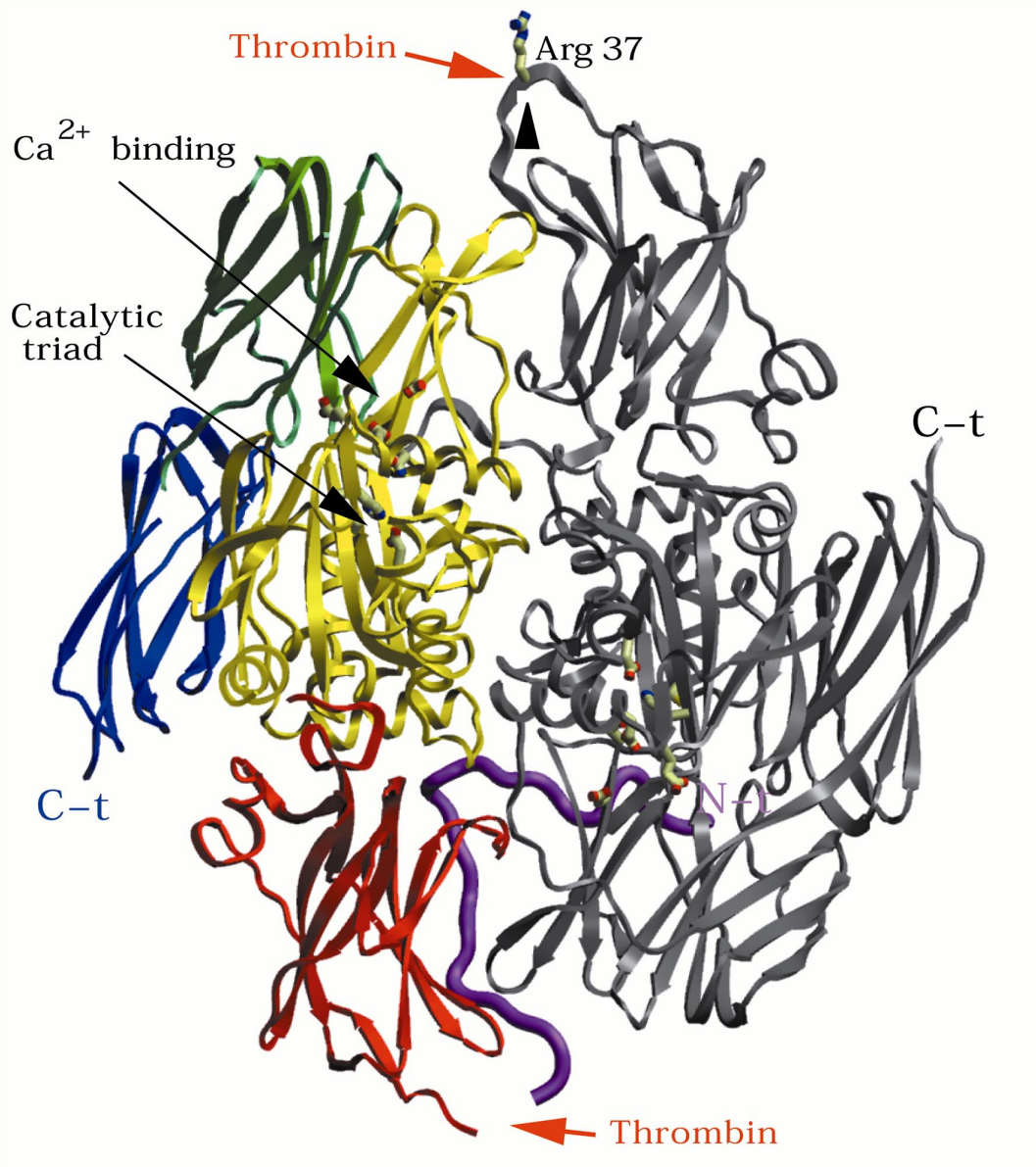

1.5.3. Plasma Carboxypeptidase B and the Inhibition of Fibrinolysis

The observation that thrombin activation retarded clot lysis provoked investigations that lead to the discovery of a plasma pro-carboxypeptidase known as **thrombin-activatable fibrinolysis inhibitor** (TAFI) (Bajzar et al., 1995). Surprisingly, it turned out that the enzyme (activated TAFI or TAFIa) had been previously isolated as a plasminogen-bound plasma carboxypeptidase (Eaton et al., 1991) also known as **c**arboxy**p**eptidase **u**nstable (CPU) (Wang et al., 1994). TAFI is the precursor of an enzyme with carboxypeptidase B-like specificity (TAFIa), which removes C-terminal lysine and arginine residues from partially degraded fibrin. Removal of these anchoring points for the essential fibrinolytic enzymes plasmin (or its precursor plasminogen) and its activators t-PA and u-PA

suppresses the ability of fibrin to assist in efficient plasminogen activation and delays clot lysis (Nesheim, 1998; Nesheim et al., 1997).

TAFI belongs to the carboxypeptidase A subfamily of carboxypeptidases (Rawlings and Barrett, 1994). Although the three-dimensional structure of TAFI has not been determined, its high degree of similarity with several procarboxypeptidases of known structure (Aloy et al., 1998; Coll et al., 1991) allows the development of an accurate model (see chapter 4).

1.5.4. Tissue Factor Pathway Inhibitor

Tissue factor pathway inhibitor (TFPI) is a multivalent plasma proteinase inhibitor that directly inhibits factor Xa and, in a FXa-dependent fashion, produces feed-back inhibition of the extrinsic Xase complex (FVIIa-TF) (Broze, 1995; Broze, 1995). The protein circulates in plasma at low concentrations (~2 nM). TFPI was formerly known as **lipoprotein-associated coagulation inhibitor** (LACI), since much of the inhibitor circulates associated with plasma lipoproteins. Platelets carry about 10% of the total blood TFPI and release the inhibitor after stimulation by thrombin or other agonists (compare sections 1.1. and 1.4.). Recent investigations indicate that TFPI mediates the internalization and degradation of factor Xa (Ho et al., 1996) and the transfer of factor VIIa/TF to **caveolae** (Sevinsky et al., 1996).

TFPI consists of an acidic N-terminal peptide which is followed by three tandem **Kunitz-type** domains, and by a basic C-terminal tail (Wun et al., 1988). (For a review on Kunitz-type domains see reference (Bode and Huber, 1992)). The first Kunitz-type domain of TFPI is responsible for factor VIIa inhibition and the second inhibits factor Xa, resulting in a quaternary inhibitory complex of Xa-TFPI-VIIa-TF. The function of the third domain has still to be worked out. Positively charged residues in this domain and the basic C-terminal tail, mediate binding to **heparin** and are required for localization of TFPI to the endothelium (Wesselschmidt et al., 1993). A recent structural analysis (Zhang et al., 1999) reveals binding to the tissue factor-factor VIIa complex by a mutant of **bovine pancreatic trypsin inhibitor** (BPTI) (Bode et al., 1976; Huber et al., 1974), that incorporates some of the TFPI-specific residues of the first Kunitz domain. Additionally, the crystal structure of the second Kunitz domain has been solved at 1.7 Å resolution (Burgering et al., 1997). As expected, the overall three-

dimensional structure is similar to that of the prototypical Kunitz-type inhibitor, BPTI (see also section 3.6.).

1.5.5. Serpins Inhibition of Serine Proteinases: A 'Suicide' Substrate Mechanism

The proteolytic activity of thrombin and other serine proteinases involved in such processes as coagulation, fibrinolysis, complement activation, inflammation and tumor metastasis is controlled *in vivo* by endogenous serum inhibitors known as **serpins** (Huber and Carrell, 1989; Potempa et al., 1994; Travis and Salvesen, 1983). Serpins are rather large (~400 amino acid residues, M_r ~50 kDa) single-domain proteins that possess seemingly flexible C-terminal **reactive-site loops** able to adopt multiple conformations. Serpins inhibit their cognate proteinases by forming tight stoichiometric complexes between the serpin P1-P1' reactive center and the active site of the proteinase (Olson and Shore, 1982; Tollefsen et al., 1982). Complex formation is enhanced in several cases by negatively charged **glycosaminoglycans**, especially by heparin, which is believed to clamp serpins and proteinases together, thus accelerating complex formation. The final complex exists either as a tetrahedral intermediate (Matheson et al., 1991) or as an acyl enzyme in which the P1 residue is covalently bound to Ser195 of the enzyme after hydrolysis of the P1-P1' scissile bond (Lawrence et al., 1995; Potempa et al., 1994; Wilczynska et al., 1995). Cleavage of the reactive loop by the target proteinase elicits a large conformational change in the serpin known as the **S→R** (stressed → relaxed) **transition**, and in which the loop, with the proteinase covalently linked, is inserted into the center of β-sheet A ((Lawrence et al., 1995); the mechanism of serpin inhibition is summarized in Fig. 1.28a). Concomitantly, the bound proteinase is translocated by more than 70 Å from one end of the serpin to the other (Stratikos and Gettins, 1999; Stratikos and Gettins, 1997).

Free α-thrombin is rapidly inhibited by the serpins **antithrombin** (AT; formerly known as antithrombin III), **heparin cofactor II** and **protease nexin 1**. (For reviews see references (Stubbs and Bode, 1994; Stubbs and Bode, 1993)). Antithrombin circulates in a quiescent form in which its reactive C-terminal loop is not fully exposed and thus cannot bind target proteinases. Binding (through a so called **cation site** on its A and D helices) (Fig. 1.28b) to heparin-like molecules

attached to the cells that line blood vessels immobilizes antithrombin and promotes small structural rearrangements stabilizing the S-conformation. In this way, the rate of antithrombin-proteinase reactions is enhanced several thousand-fold (Bjork and Olson, 1997; Streusand et al., 1995). Proteinases that bind to heparin-immobilized antithrombin cleave the exposed loop and reverse the conformational changes at the heparin-binding site, with a consequent release of the proteinase-antithrombin complex into the circulation. *In vivo,* antithrombin is rapidly converted into a range of six-stranded locked "L-forms", which are similar in conformation to the cleaved (R-)molecule. Recent results indicate that both the R- and L-forms possess potent antiangiogenic and antitumor activities (O'Reilly et al., 1999). The three-dimensional crystal structure of antithrombin has been determined independently at medium resolution by the groups of R. W. Carrell (Carrell et al., 1994) and W. Hol (Schreuder et al., 1994) (Fig. 1.28b).

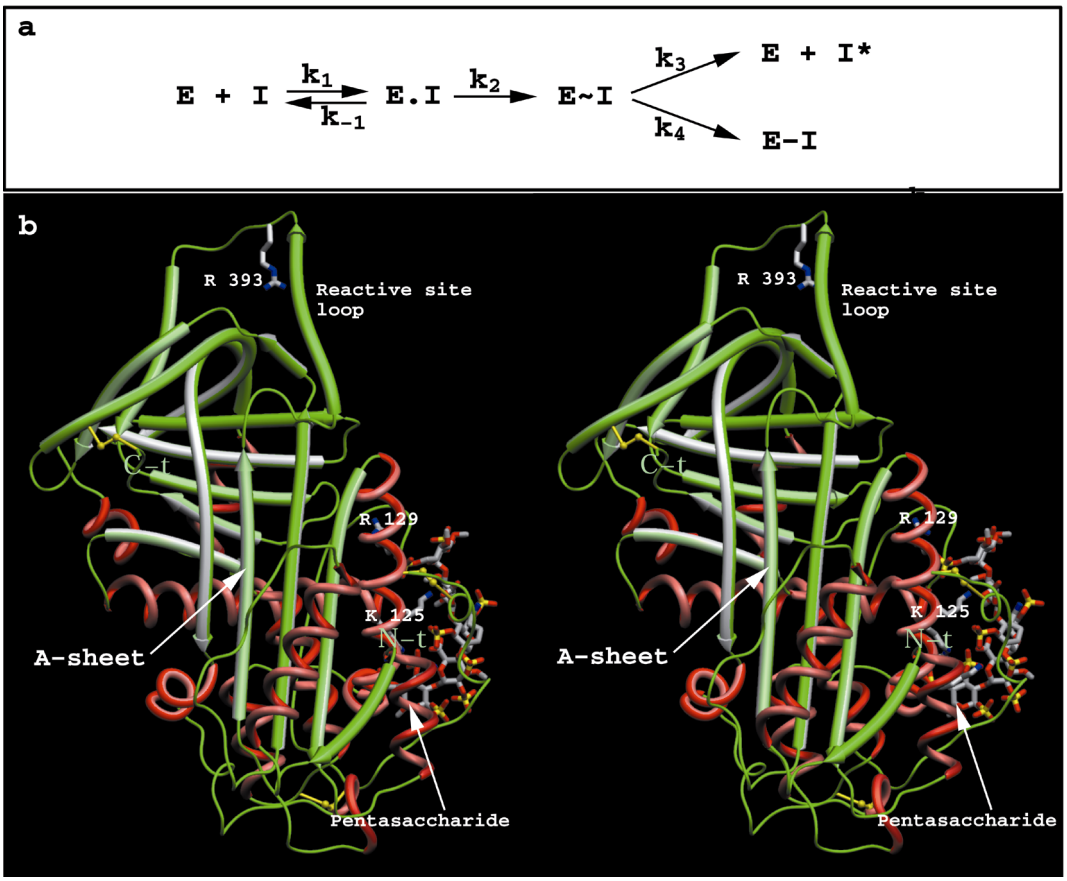

Fig. 1.28 (previous page): Serpins are 'suicide' inhibitors of serine proteinases. (**a**) Scheme of the general mechanism of inhibition. E, serine proteinase; I, serpin; E.I non-covalent (Michaelis) complex; E~I, acyl enzyme intermediate; E-I, stabilized form of the acyl enzyme; I*, scissile bond hydrolyzed serpin. (**b**) Three-dimensional structure of antithrombin bound to a core pentasaccharide present in heparin (Jin et al., 1997). The P1 residue (Arg393) and some side chains of the heparin-binding site are shown with all its non-hydrogen atoms; crystal contacts seem to force the P1 side chain to adopt a nonproductive conformation. The reactive site loop of AT assumes a variety of conformations ranging from fully inserted as an extra strand into the A sheet in cleaved and latent (inactive) serpins, to an exposed loop with partial helical or β-strand character. For an atlas of serpin conformations see reference (Whisstock et al., 1998).

Finally, we mention that the serpin initially identified as an inhibitor of activated protein C (**protein C inhibitor**; PCI) seems to play an important role in the down-regulation of the protein C pathway by binding to TM-bound thrombin and thus inhibiting thrombin-TM mediated protein C activation ((Elisen et al., 1998; Rezaie et al., 1995); see also chapter 4).

Chapter 2

Structural Basis for the Membrane Binding Ability of Coagulation Factor V:

Crystal Structures of Human Factor V C2 Domain

2.1. The C2 Domains of Factors Va and VIIIa Mediate Cofactor Binding to Phospholipid Membranes

Binding of coagulation factors Va and VIIIa to the cell surface is the first step in a series of still poorly understood protein-protein and protein-membrane rearrangements (Koppaka et al., 1997) that allow binding of their cognate proteinases factor Xa and factor IXa and thereby localization of the fully active prothrombinase / intrinsic Xase complexes on cellular membranes (see sections 1.1., 1.3.4., and 1.3.5.). The C2 domains of both factor Va (Kalafatis et al., 1994; Ortel et al., 1992; Ortel et al., 1994) and VIIIa (Foster et al., 1990; Saenko et al., 1994; Shima et al., 1993) bind to phosphatidyl-L-serine (P_LS) containing membranes, a process essential for generation of procoagulant activity (for a recent review see (Zwaal et al., 1998)). An additional but presumably less selective membrane-binding site(s) has been mapped to the A3 domain of FVa (Cutsforth et al., 1996; Kalafatis et al., 1994). More recently, the finding that the heavy chain of factor Va associates with neutral lipid membranes (Koppaka et al., 1997) pointed to a more complex view of the cofactor interactions with membrane surfaces.

In contrast to the Ca^{2+}-dependent membrane binding of the coagulation proteinases factor Xa and factor IXa (section 1.2.1.), their cofactors Va and VIIIa do not require calcium ions for membrane association (Krishnaswamy and Mann, 1988; Nesheim et al., 1988; Pusey et al., 1982; van de Waart et al., 1983). In view of their overall homology, the very low plasma concentrations of FV (~10 μg/ml) and especially of FVIII (~0.1-0.2 μg/ml) pose a tremendous challenge to their non-competitive association with cellular membranes.

The low abundance, heterogeneity and complex multidomain structure of the protein cofactors V and VIII have so far hampered structural investigations. Recently, homology models of the A- (Pan et al., 1995; Pemberton et al., 1997; Villoutreix and Dahlbäck, 1998) and C-domains (Pellequer et al., 1998; Villoutreix et al., 1998) of FV and FVIII have been proposed based upon the structures of **nitrite reductase** (Godden et al., 1991) and ceruloplasmin (Zaitseva et al., 1996), and of the N-terminal non-catalytic domain of the fungal enzyme galactose oxidase (N-GOase) (Ito et al., 1991; Ito et al., 1994), respectively. Here we present the first three-dimensional structures of a domain

from coagulation factor V, and discuss the implications of the structural findings for the mechanism of membrane association.

2.2. Structure determination

2.2.1. Purification and Crystallization

The C2 domain of human coagulation factor V (FVa-C2, residues Gly2037 to Tyr2196 of the mature protein, preceded by an N-terminal (artificial) sequence of Ala-Gln-Trp-Tyr-Gln) was produced using a baculovirus-driven insect cell system, and purified to homogeneity from conditioned media using cation-exchange chromatography on Mono S (Ortel et al., 1998). Purification was done by Mary-Ann Quinn-Allen, Duke University. After dialysis against 5 mM 3-morpholino-propane sulphonic acid, pH 8.0, the sample was concentrated to about 6 mg/ml and crystallized by the hanging-drop vapor-diffusion method. Two different crystal forms have been obtained, containing one and two molecules *per* asymmetric unit (in the following referred to as XTAL1 and XTAL2, respectively). Crystals of the monomeric crystal form (XTAL1) were grown at 6°C from 0.1 M Tris, 1.0-1.4 M ammonium sulfate, pH 10.2. The dimeric crystal form was obtained in two unrelated crystallization conditions. The form used for initial structure determination (XTAL2-NAT) grows at 20°C from 0.1 M potassium phosphate, 0.7 M ammonium sulfate, pH 9.5-10.0, after several cycles of micro- and macroseeding (work done by Dr. S. Macedo-Ribeiro). After solution of both crystal forms, we succeeded in obtaining the same dimeric crystal form in a completely different, more physiological condition (0.1 M MES, 0.2 M ammonium sulfate, 15% PEG 4,000). This form will be in following termed XTAL2-PEG.

2.2.2. Search for Heavy Atom Derivatives

Analysis of the cell constants of both crystal forms indicated the presence of one, respectively two FVa-C2 molecules in crystal forms XTAL1 / XTAL2. Because of the presence of a single free cysteine in this domain (Cys2113 in the mature human protein) (Xue et al., 1993), we looked for a mercury derivative of the monomeric crystal form. Considering the preference of the C2 domain for phospholipid membranes, the hydrophobic mercury compound **phenylmercury** (PheHg) was selected. Crystals were soaked for 6 hours in mother liquor

containing 5 mM PheHg, and a complete data set was collected (XTAL1-PheHg). An initial search for the position of the bound metal was done by visual inspection of the Harker sections, the position of the single bound Hg atom (x_{Hg} = 0.590, y_{Hg} = 0.452, z_{Hg} = 0.250) was confirmed with SHELX (Sheldrick, 1984) and with RSPS (Knight, 1989). This mercury atom refined to an occupancy of 80% and a B-factor of 25.77 using VECREF (Collaborative Computational Project No. 4, 1994).

Since previous systematic attempts to identify heavy atom derivatives had failed, we decided to solve the structure of FVA-C2 by **multiple-wavelengths anomalous diffraction** (MAD) techniques using this mercury derivative. For MAD data collection, crystals derivatized with PheHg were quickly transferred to the cryo buffer (25-30% (v/v) glycerol, 1.4 M ammonium sulfate). Because these crystals were extremely fragile, they were plunged into liquid nitrogen and then transferred to a cold nitrogen stream at 100 K.

2.2.3. Data Collection

MAD data were collected from a single phenylmercury crystal (XTAL1-PheHg) on the MPG beamline BW6 at DESY (Hamburg, Germany). Data were collected in 0.5° rotation frames using a MAR-CCD detector. A preliminary X-ray fluorescence spectrum near the LIII edge of mercury was used to select the monochromator settings at the LIII absorption edge (λ_1=1.0047 Å, f''), and at the inflection point (λ_2=1.010 Å, maximal Δf'). Bijvoet pairs to 1.9 Å resolution were collected in two continuous sweeps of 90° (separated by 180°) for each wavelength, in order to optimize the measurement of the Bijvoet differences. Additionally, a complete data set was collected at a remote wavelength (λ_0=1.05 Å). The diffraction images were evaluated, merged and scaled with the programs DENZO / SCALEPACK (Otwinowski and Minor, 1993) and reduced with programs from the CCP4 program suite (Collaborative Computational Project No. 4, 1994).

X-ray diffraction data for all other crystals were collected "in house" using a MAR image plate system (MAR Research, Germany) installed on a RIGAKU rotating anode generator. Data were evaluated with MOSFLM (Leslie, 1991), scaled with SCALA (Evans, 1993) and reduced with programs from the CCP4

suite (Collaborative Computational Project No. 4, 1994). Data collection statistics are depicted in Table 2.1.

Table 2.1. Summary of Data Collection, Processing and Phasing Statistics

Crystal	**XTAL1-PheHg**			**XTAL1-NAT**	**XTAL2-NAT**	**XTAL1-OPS**
Data	λ_0	λ_1	λ_2			
Wavelength (Å)	1.0500	1.0047	1.0100	1.5418	1.5418	1.5418
Resolution (Å)	13.61–1.90	15.73–1.90	13.72–1.90	26.73–1.87	24.60–2.40	24.65–1.80
Space group	$P2_12_12_1$	$P2_12_12_1$	$P2_12_12_1$	$P2_12_12_1$	$P2_12_12$	$P2_12_12_1$
Unit Cell						
a (Å)	46.43	46.46	46.40	46.89	86.52	46.21
b (Å)	51.83	51.78	51.61	53.33	70.54	54.08
c (Å)	68.15	67.95	68.25	68.52	60.58	69.19
R_{merge}[§],%						
Overall (outer shell)	4.7 (22.5)	4.4 (11.8)	5.4 (14.1)	6.1 (28.7)	9.4 (39.9)	5.4 (45.7)
Total reflections	24,655	24,143	24,843	80,514	131,486	91,159
Unique reflections	12,417	13,028	13,373	13,815	14,635	15,612
Completeness, %						
Overall (outer shell)	98.5 (98.7)	96.6 (97.7)	99.6 (99.4)	94.0 (86.8)	96.8 (90.7)	94.3 (88.5)
R_{Cullis}[+]						
Isomorphous						
(centric/acentric)	0.656/0.613	0.565/0.558				
Anomalous	0.719	0.516	0.817			
Phasing power[++]						
Isomorphous						
(centric/acentric)	0.962/1.664	1.046/1.666				
Anomalous	2.104	3.452	1.876			
FOM[&]	0.599/0.875					

[§]R_{merge} : $\sum\sum |\langle I(h)\rangle - I(h)| / \sum\sum I(h)_j$, where $I(h)_j$ is the mean intensity of the j^{th} source and $\langle I(h)\rangle$ is the intensity of reflection h over all measurements of I(h);

[+]R_{Cullis} : $\sum ||E| / \sum |F_\lambda - F_{\lambda 0}||$, where E is the lack of closure;

[++]Phasing power = $\langle |FH(calc)| / |E| \rangle$, where FH(calc) is the calculated anomalous/isomorphous difference and E is the lack of closure;

[&]FOM: figure of merit as defined in SHARP ((de la Fortelle and Bricogne, 1997)).

2.2.4. Phasing and Refinement

Data sets collected at wavelengths λ_1 and λ_2 were scaled to data measured at λ_0 using the program SCALEIT from the CCP4 program suite (Collaborative Computational Project No. 4, 1994). The position of the mercury site was confirmed with RSPS (Knight, 1989) from a Patterson map calculated using data

with the highest anomalous differences (λ_1) as coefficients. The maximum-likelihood program SHARP (de la Fortelle and Bricogne, 1997) was used for heavy atom refinement and phasing, and solvent flattening was carried out with SOLOMON (Abrahams, 1997; Abrahams and Leslie, 1996) as implemented in SHARP, considering a solvent content of 44%. Although the combined effects of mercury derivatization and shock-freezing gave rise to high mosaicity, a straightforwardly interpretable density was obtained after phasing with SHARP. Inspection of this map contoured at 5σ clearly showed the mercury atom in the proximity of the single free cysteine (Cys76), with the (poorly defined) phenyl moiety interacting with the side chains Trp31 and Met83. Protein and solvent regions could easily be distinguished in the initial experimental map at 2.5 Å resolution. Its quality was high enough for building an almost complete protein model with MAIN (Turk, 1992), with the only exception of a few residues within two solvent exposed loops.

Rigid body and positional refinement with XPLOR (Brünger, 1993), using the parameters derived by Engh and Huber (Engh and Huber, 1991) and the λ_0 data set from 8.0-2.5 Å resolution yielded an initial R_{factor} of 38.9% (R_{free} 43.0%). In the 2.5 Å map calculated after the first refinement cycle with combined model and experimental (SHARP) phases (SIGMAA, (Read, 1986), additional residues at the surface loops became visible. The structure refinement was then continued with a combination of X-PLOR and REFMAC (Collaborative Computational Project No. 4, 1994). Finally, individual but constrained B-factors were refined and waters were included in the model. This model was then used for refinement against a native data set (XTAL1-NAT). Additionally, a data collected from a crystal soaked in 20 mM *O*-phospho-L-serine (XTAL1-OPS) has been solved using the XTAL1-NAT model.

The dimeric crystal form (XTAL2-NAT) was solved by Patterson search techniques using the previously refined model. Initial phases for crystal form XTAL2-NAT were obtained after molecular replacement with AMoRe (Navaza, 1994) using a truncated model from XTAL1-NAT. The best solutions corresponded to a correlation coefficient of 68.3% and an initial R-factor of 38.7%, respectively. The appropriately placed model was subjected to rigid body and positional refinement with X-PLOR, initially applying strong NCS restraints.

The two independent molecules in the asymmetric unit reveal only minor differences compared with the monomeric crystal form, as indicated by average root-mean-square deviations (r.m.s.d.) of only 0.28 Å for 145 Cα atoms not deviating more than 1 Å. Table 2.2 summarizes the refinement statistics for all the models. They all possess excellent stereochemistry, as revealed by analysis with PROCHECK (Laskowski et al., 1993). The only residues in disallowed regions (Leu63, Gln145) are well defined in the electron densities and are associated with strong structural constraints.

Table 2.2. Refinement Statistics of Crystal Used for Structure Determination

Data set	XTAL1-PheHg	XTAL1-NAT	XTAL2-NAT	XTAL1-OPS
Refinement				
R factor, % (outer shell)	19.5 (30.1)	20.1 (32.3)	20.5 (29.0)	20.4 (35.2)
R_{free}, % (outer shell)	25.8 (35.4)	24.2 (28.0)	25.7 (32.3)	27.5 (42.5)
Resolution range	8.00–1.90	8.00–1.87	8.00–2.40	8.00–1.80
Number of reflections (1σ cut-off)	12,266	13,591	14,119	15,541
Number of atoms				
All non-hydrogen atoms	1,454	1,403	2,708	1,428
Non-hydrogen protein atoms	1,312	1,312	2,616	1,361
Solvent	136	91	92	67
PheHg	7	–	–	–
Average B-factors (Å^2)				
All atoms	24.9	29.0	28.2	32.6
Main chain	22.5	26.5	27.4	30.7
Side chain	24.9	29.8	28.3	33.3
Solvent	35.0	41.4	37.6	43.9
PheHg	34.2	–	–	–
r.m.s.d. for bonded B's (Å^2)	2.16	2.46	1.97	2.44
r.m.s.d. bonds (Å)	0.008	0.007	0.006	0.008
r.m.s.d. angles (°)	1.81	1.79	1.39	1.78
Ramachandran				
Allowed (%)	84.2	88.2	82.7	84.7
Additionally allowed (%)	13.7	10.3	14.4	13.2
Generously allowed (%)	1.4 (Leu63, Glu98)	0.7 (Leu63)	1.4 (Leu79, Ser106)	0.7 (Leu63)
Disallowed (%)	0.7 (Gln145)	0.7 (Gln145)	1.4 (Leu63, Gln145)	1.4 (Leu79, Gln145)

2.3. The Crystal Structure of FVa-C2

The conservation of the overall structure of FVa-C2 in spite of different crystallization conditions (section 2.2.) is highlighted by an average root-mean-square difference of only 0.28 Å for 145 equivalent Cα atoms between both crystal forms. In this section we will refer to the structure of XTAL1-NAT, unless otherwise stated. Differences between crystal forms and their functional implications will be discussed in the following sections.

The main structural feature of FVa-C2 is an eight-stranded antiparallel β-barrel approximately 25 Å in length, divided into two β-sheets packed against each other. The front sheet (according to the orientation shown in Fig. 2.1a) is composed of strands S1, S2, S7, S4 and S5, whereas the back sheet includes strands S6, S3 and S8. Both sheets are twisted and oriented at an angle of about 45° relatively to each other. The barrel displays a strongly distorted "jelly roll" or "Swiss roll" motif, characterized by pairs of β-strands (S2–S3 and S6–S7, in this case) which are wrapped around the barrel core to form a more complicated structure. The "right" edge of the β-barrel is covered by the amino terminal segment (Leu5 to Lys15), which is organized in a multiple-turn structure before entering the first regular strand (S1). (A sequential numbering starting with the first cysteine –Cys2038 in mature human FV– will be used in this work, refer to Fig. 2.2 for the sequence of the mature human cofactor). This segment is stabilized in an extended structure by hydrophobic interactions to the underlying strand S2, as well as *via* several remarkable polar side chain - main chain contacts with the buried side chains of Arg37 and Glu152. At the opposite edge of the β-barrel, strands S5 from the front and S6 from the back sheet are positioned in such a way that polar side chains of one strand hydrogen-bond to main chain atoms from the neighboring strand, closing the gap between the two sheets together with a chain of well-ordered water molecules.

In the dimeric crystal form of FVa-C2, both molecules are quasi-symmetrically packed through the free edges of their β-strands S6, building a six-stranded antiparallel β-sheet. However, dimer formation does not result in any noticeable structural rearrangements compared to the monomeric crystal form, as indicated by the low r.m.s. deviations. The single disulfide bridge Cys1-

Cys156 clamps the N- and C-terminal peptides together (Fig. 2.1), thus contributing to structural stabilization.

Most of the segments connecting sequential β-strands also contain short hydrogen-bonded antiparallel β-structures, denoted S1'-S4' and β_1-β_5. (The overall complex topology of FVa-C2 is schematically shown in Fig. 2.1b.). Two short segments of 3_{10}-helical structure (Ile12–Lys15, preceding strand S1 and Glu32–Arg37, following strand S2') are located in close proximity. Strands β3, β2 and β5 on 'top' of the molecule (as seen in Fig. 2.1a) generate a flat surface that is completed to the 'left' by a long extension connecting strands S4 and S5. The bottom of the barrel is formed by the hydrogen-bonded segments β_1 and β_4. These strands also make up the roof of a pronounced groove encircled by two prominent β-hairpin structures (residues Ser21–Trp31 and Gly75–Tyr84) and a neighboring loop (Asn39–Asn45), which project away over 12 Å from the bottom of the barrel (Fig. 2.1). The structures of the three protruding 'spikes' are intimately associated with each other and with those of the three neighboring loops (Ala49–Gln56, Asn116–His122 and Thr142–Thr148) through a multitude of hydrogen-bonded interactions involving both main chain and polar side chain atoms. These three essentially hydrophobic spikes are circularly arranged at the bottom of the barrel, creating a groove that is lined by both hydrophobic (Trp31, Met83) and polar (Gln48, Ser78) side chains (Fig. 2.1a). We refer to this structure as the 'open form' of FVa-C2.

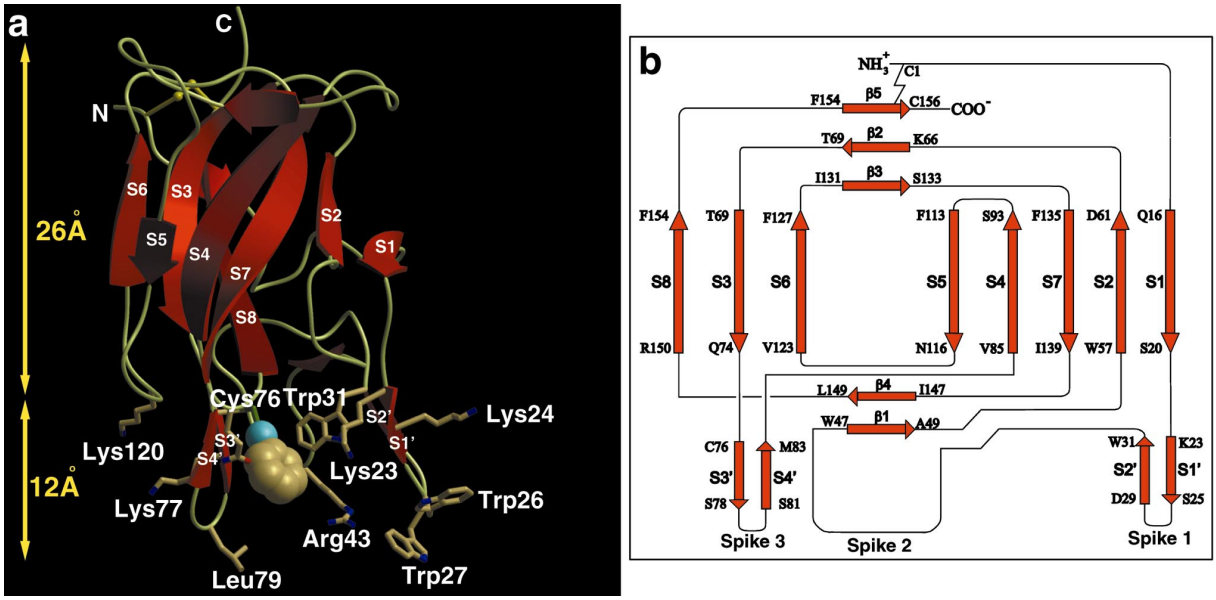

Fig. 2.1 (previous page): The C2 domain of human factor Va forms a β-barrel with a complex folding topology. (**a**) Ribbon plot of the 'open' crystal form of FVa-C2, highlighting the major secondary structure elements and the spike-like loops at its bottom. The phenyl mercury molecule (space-filling model) used for structure determination is shown covalently attached to Cys76. (**b**) Topology diagram illustrating the arrangement of the secondary-structure elements in FVa-C2. The short N-terminal β-strand Thr3–Leu5 and the internally hydrogen-bonded stretches in the loop connecting strands S4 and S5 have been omitted for the sake of simplicity.

This peculiar arrangement of hydrogen-bonded β-strands is supported by a densely packed hydrophobic core. FVa-C2 is a very basic protein domain, with 7 arginine, 17 lysine and 2 histidine side chains outbalancing 13 aspartate and/or glutamate residues. Interestingly, most of the arginine side chains are engaged in major intra-domain interactions. The role of Arg37 in stabilization of the N-terminal loop has already been mentioned. Both Arg43 and Arg150 are involved in important inter-loop contacts. A strong hydrogen-bonded salt bridge between residues Asp61 and Arg134 clamps the jelly roll strands β_B and β_G together, whereas Arg103 and Asp110 associate to support the exposed, otherwise rather flexible loop Arg103–Lys111. Finally, the side chain of Arg137 is sandwiched between the indole moieties of Trp57 and Trp99, covering the front sheet of the barrel. In contrast, several of the lysine side chains are flexible, as reflected by their truncated electron densities. These lysine side chains are distributed over the surface of the protein, and together with the guanidinium groups of the exposed arginine residues they generate extended patches of positive electrostatic potential (see below).

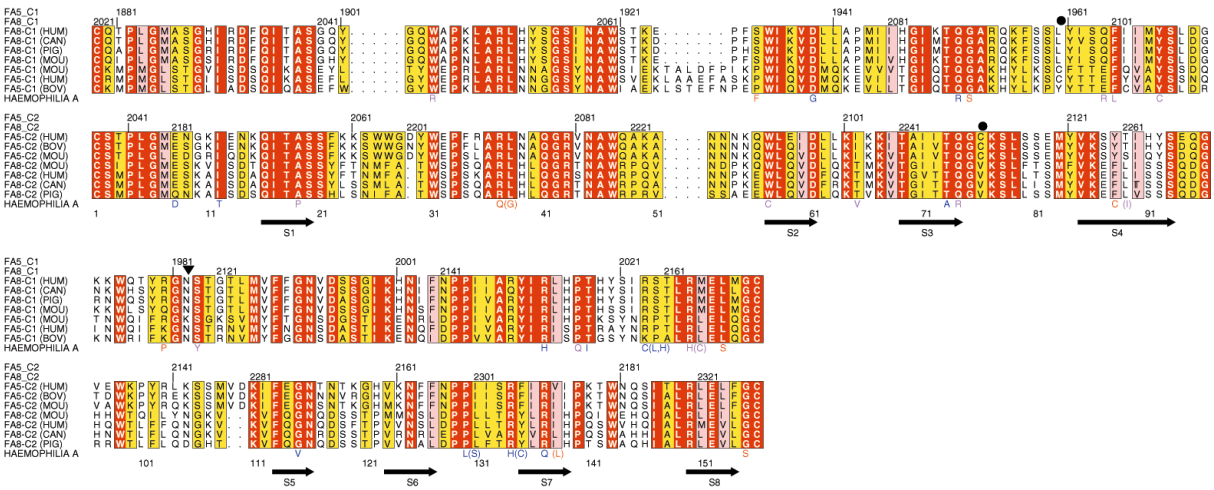

Fig. 2.2 (previous page): Sequence alignment of the C1 and C2 domains of human coagulation factors. Numbers for the full-length human cofactors are given above the alignment, the FVa-C2 numbering used in this paper is indicated below. Red, strictly conserved residues within C1 or C2 domains; pink: substitutions within the hydrophobic core; yellow, other conservative substitutions. Glycosylation sites (closed triangles) and free cysteines (closed circles) are indicated. Missense mutations deposited in the hemophilia A data base (URL:http://europium.mrc.rpms.ac.uk) are given in red (severe cases), pink (moderate) or blue (mild). Notice that most mutations affect conserved residues.

2.4. Structural Homology With the N-Terminal Domain of Galactose Oxidase

The crystal structures of FVa-C2 confirms that the overall fold of this domain is similar to the N-terminal domain of galactose oxidase (N-GOase) from the fungus *Dactylium dendroides* (Ito et al., 1991; Ito et al., 1994), as previously predicted (Baumgartner et al., 1998; Pellequer et al., 1998; Villoutreix et al., 1998) (Fig. 2.3a). A least-squares superposition of both structures reveals that 102 Cα atoms of FVa-C2 and N-GOase occupy topologically equivalent positions with a r.m.s.d. of 1.4 Å. Particularly striking is the high similarity observed within stretch Gln56–Cys76 of FVa-C2 (His53–Arg73 of N-GOase). This overall structural homology contrasts with the low degree of sequence conservation, since only 15 of the topologically equivalent amino acid residues are common to both modules (Fig. 2.3b). Several side chains of these topologically equivalent residues superimpose remarkably well. This is true not only for internal residues (such as Trp47 (Trp39 in N-GOase)), but also for some exposed side chains. (Notice the conservation of the hydrogen-bonded salt-bridge Asp61–Arg134 (Asp58–Arg122), Fig. 2.3a). While the distantly related N-GOase belongs to the minor subfamily of **microbial discoidin domains** (Baumgartner et al., 1998), FVa-C2 represents the first member of the **eukaryotic subfamily** for which high resolution crystal structures are available. Although the predictions made on the basis of homology models (Pellequer et al., 1998; Villoutreix et al., 1998) are essentially correct, the precise polypeptide fold, charge distribution, and in particular the shape of major loops diverge markedly in both structures and are therefore not predictable.

The conformations of the N- and C-terminal peptides FVa-C2 are constrained by the connecting disulfide bridge, which is absent in N-GOase. As a result, the N-terminal segments from both domains are not superimposable in

spite of their sequence homology (compare Figs 2.3a, 2.3b). Further, the extended loops at the bottom of both β-barrels differ in conformation and size. In both cases, residues from these extended loops contribute to the formation of the only noticeable cavity found in the structures (Figs 2.1a, 2.3a). In the N-GOase discoidin domain the shallow pocket formed by the exposed spikes has been shown to specifically bind *D*-galactose, probably regulating attachment of the enzyme to the cell wall (Ito et al., 1994).

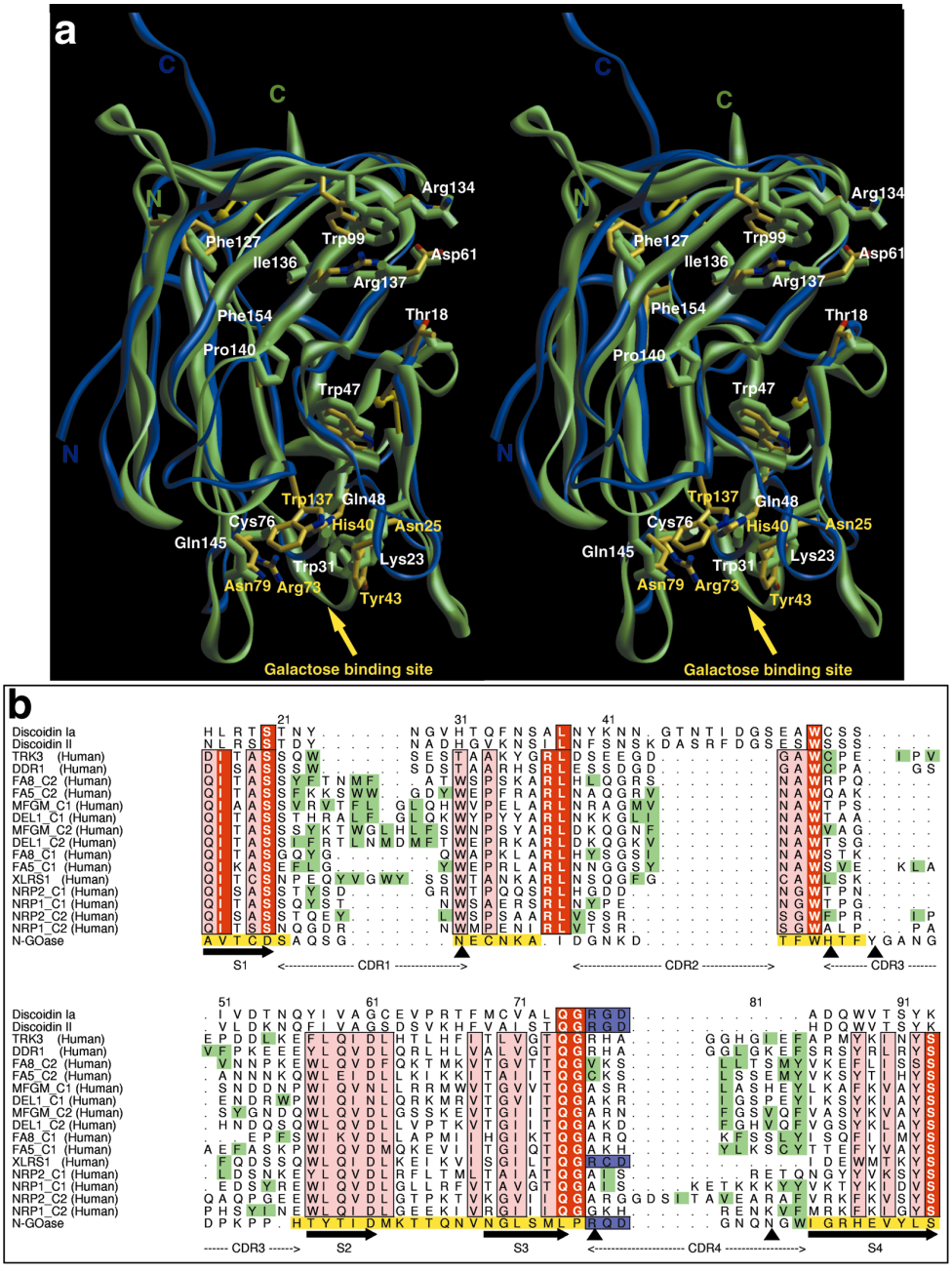

Fig. 2.3: Sequence homology within the discoidin family. (**a**) Superposition of the crystal structures of FVa-C2 (green, open form) and N-GOase (blue). Side chains of several conserved residues in FVa-C2 (green) and in N-GOase (color coded as in Fig. 2.1a) are displayed explicitly. FVa-C2 side chains are labeled in white, N-GOase side chains involved in D-galactose binding in yellow. Noteworthy is the overall conservation of the β-barrel, contrasting with the extremely different loop structures. (**b**) Structure-based sequence alignment of several representative discoidin domains (see also section 1.3.3.). Numbers refer to the FVa-C2 sequence. The highly variable loops have been termed CDR1 to CDR4, in analogy to the immunoglobulin nomenclature. Stretches of topologically equivalent residues between FVa-C2 and N-GOase are shadowed yellow; residues involved in galactose binding are indicated with closed triangles. The cell adhesion motif RGD (section 1.4.1.) in the discoidins and related motifs are shadowed blue. Hydrophobic/aromatic residues within the CDRs (shadowed green) are likely candidates for membrane insertion or ligand binding.

2.5. Conformational Flexibility of the First 'Spike' of FVa–C2

As stated before, in the dimeric crystal form of FVa-C2, both molecules are quasi-symmetrically packed *via* the free edges of their S6 strands. The structures of these crystallographically independent molecules are extremely similar (with a root-mean-square deviation of only 0.38 Å for all Cα atoms). Deviations larger than 1 Å are limited to the flexible Leu104-Val109 loop protruding from the upper flat surface, but there are virtually no differences in the rest of the molecule. In the spike region, however, both "dimeric" molecules differ significantly from the monomeric form.

The first and third spikes are tilted towards the interior of the groove, with spike 1 additionally deformed due to a strong twist around Gly28 (Fig. 2.4a). This concerted tilting-twisting movement not only results in main chain atom shifts of up to 7 Å, but also leads to a 90° rotation and a 12 Å displacement of the Trp27 indole moiety into the groove previously described. However, this tryptophan side chain still leaves a small entrance to the shallow inter-spike groove, in particular to the important Gln48 carboxamide group (see below). The indole side chain of Trp26 moves in concert with Trp27 and packs against it. As a result, a hydrogen-bonded salt bridge is formed between the carboxylate of Asp29 and the guanidinium group of Arg43, and the Trp26 indole approaches the opposing Leu79. The side chains of Trp26, Trp27 and Leu79 form thus a contiguous hydrophobic ridge (Fig. 2.4b), which to a large extent covers the

groove present in the open form (Figs 2.1a, 2.4c). For this reason, the molecular form of FVa-C2 observed in the dimeric crystals will be termed the "closed form".

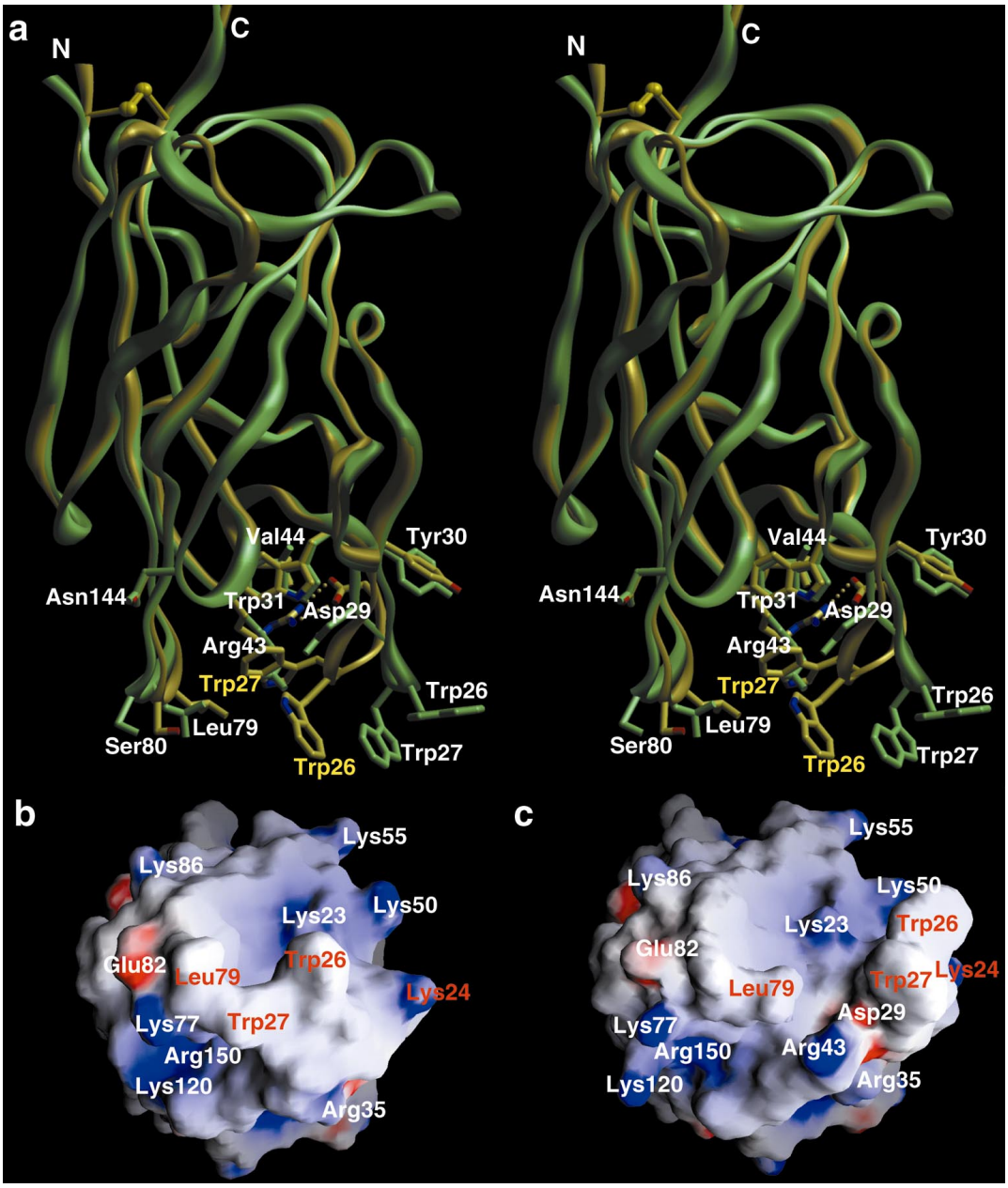

Fig. 2.4: Conformational flexibility in the spike region. (**a**) Stereo view of the superimposed FVa-C2 structures in the reference orientation. The open crystal form is shown in green. The closed form is displayed in yellow, with several side chains color-coded (carbon, yellow; oxygen, red; nitrogen, blue). **b**, **c,** GRASP (Nicholls et al., 1993) surface representations of the FVa-C2 electrostatic potential contoured from -15 (intense red) to 15 k_BT/e (intense blue) in the closed (**b**) and in the open (**c**) crystal form. The view is from the membrane side, that is perpendicular to the reference orientation.

2.6. Experimental Evidence Suggests That the Closed Form Is Favored in Solution

On the basis of the present crystal structures we suggest that the open form of FVa-C2 corresponds to the membrane bound molecular form, while the closed form represents the major form circulating in plasma. This assignment is supported by both structural features and biochemical evidence. The markedly smaller (370 compared to 520 $Å^2$) hydrophobic surface exposed by residues Trp26, Trp27 and Leu79 indicates that the closed form may be favored in aqueous solution. Residues of the first spike refine to temperature factors similar to the core structure in the closed crystal form, whereas their corresponding B-values in the open crystal forms are up to 20 $Å^2$ higher than the average temperature factor. The energetically unfavorable character of the first spike in the open form is also suggested by the high energy conformation of Trp27 (Θ=-112°, Ψ=+54°), and by the lack of electron density for residues Leu79/Ser80 in both XTAL1-NAT and XTAL1-PheHg. Considering that the latter was measured at 100 K, dynamic and not static disorder is the likely reason for this observation.

Two additional observations suggest that the closed form represents the structure of FVa-C2 favored in solution. First, both free thiol groups of the FVa light chain (Cys1960 and Cys2113 in the mature human protein, compare Fig. 2.2) are only very slowly modified by the specific reagent dithiobis-(nitrobezoic acid) under native conditions, and one of them reacts only partially even in the presence of denaturing reagents (Krishnaswamy and Mann, 1988). Considering that the C1 domain lacks the residues that form the first spike in C2 (Fig. 2.2), the free cysteine within this domain would be more accessible to bulk solvent. It is thus plausible that Cys2113 (Cys76 within C2) is shielded in solution by the Ser21–Trp31 peptide.

Further, antibodies specific for the N-terminal region of FVa-C2 seem to recognize the exposed residues Asp29 and/or Glu32 (Kim et al., 2000). Taking into account that residues at the tip of the first spike (Trp26, Trp27) protrude up to 12 Å from the end of the barrel in the open form (Figs 2.1a, 2.4a) and that epitope binding sites usually have a rather flat conformation (Braden and Poljak, 1995), it seems likely that these antibodies recognize the closed form of the C2 domain. The fact that the same closed conformation is observed in crystals

grown under different conditions also indicates that it is a relatively stable molecule conformation, which therefore favors crystal growth.

2.7. Putative Stereospecific P_LS–Binding Sites Are Enclosed By the C2 Spikes

Inspection of the inter-spike region revealed determinants that may account for the experimentally observed stereospecific discrimination of *O*-phospho-L-serine over other phospholipid polar heads (Comfurius et al., 1994). More relevant, the interior of the groove between the major spikes in the open crystal form is decorated with hydrophobic residues as well as several polar side chains that are ideally arranged for interactions with head groups of the procoagulant lipid phosphatidyl-L-serine. Spikes 1 and 2 enclose the most obvious of these putative binding sites (depicted schematically in Fig. 2.5a). Within this 'P_LS-specificity pocket', the serine carboxylate of P_LS could accept hydrogen bonds from the carboxamide nitrogen of Gln48 and the hydroxyl group of Ser78, whereas its amino group is within hydrogen-bonding distance to the Gln48 side-chain oxygen. The ε-amino group of Lys23 would compensate the negative charge of the P_LS phosphate group. The strict conservation of these residues within the FVa-C2 domains of the three species sequenced so far (Fig. 2.2) substantiates the predicted interactions. Highly directional interactions inside this pocket would be strengthened by the hydrophobic environment made by the adjacent fatty-acid tails and hydrophobic residues (Trp27, Trp31, Leu79, Met83). Another specific P_LS binding site can be localized between the second and the third spike lined by the side chains of Gln41, Asn45 and Arg150 and the carbonyls of Gly42 and Lys77. This second, strongly basic and freely accessible binding site (Fig. 2.4b), this second binding site may constitute a preferred anchoring point for acidic lipids.

Binding of a phenylmercury molecule inside this groove in XTAL1-PheHg (Fig. 2.1a) is also in line with its ligand-binding capability. We notice that most residues proposed to interact with the polar head group of P_LS have counterparts in the galactose binding pocket of N-GOase (Fig. 2.3b). Some more putative sites can be identified, as depicted in Fig. 2.5b.

Although the exact locations of the bound phospholipid molecules are speculative, these binding sites provide the most likely explanation for the

stereospecific discrimination of *O*-phospho-L-serine over the D-form (Comfurius et al., 1994), since the stereoisomer would not be able to satisfy all these interactions. This is in line with the 25-fold increase in the apparent K_d for FVa on replacing P_LS- for P_DS-containing membranes (Comfurius et al., 1994), and also explains the preference of P_LS over other acidic phospholipids (Gerads et al., 1990), as well as the importance of both the carboxyl (Gerads et al., 1990) and the amino groups (Rosing et al., 1988) of P_LS for formation of a fully active prothrombinase complex.

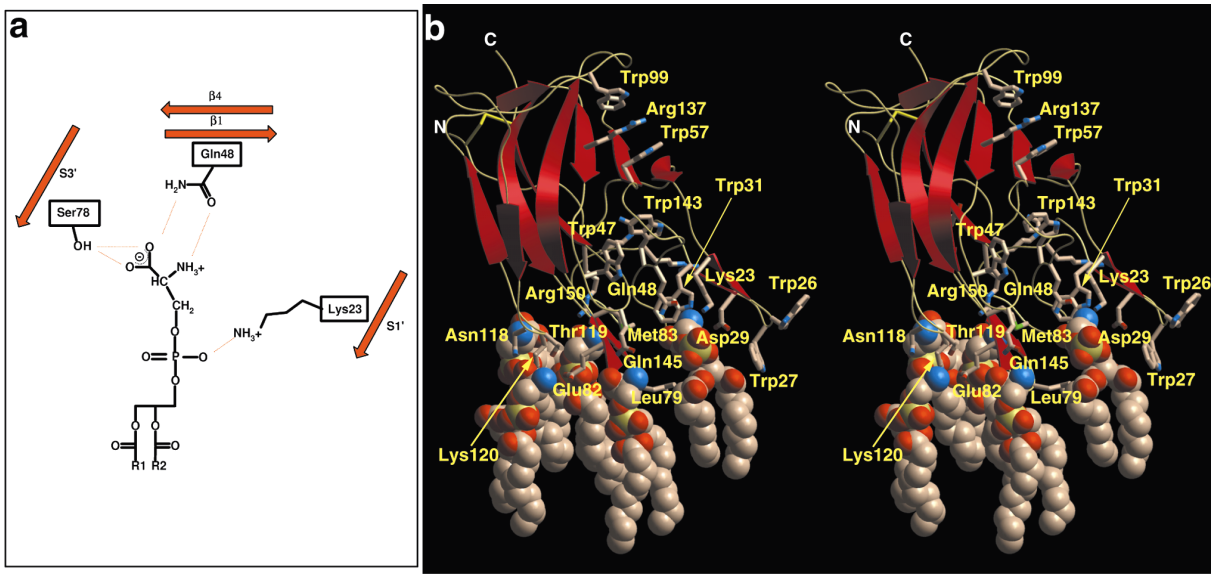

Fig. 2.5: Structural basis of the stereospecific recognition of P_LS by FVa-C2. (**a**) Predicted hydrogen bond interactions (dashed red lines) inside the major P_LS-binding site. (**b**) Stereo view of the 'open', membrane-competent form of FVa-C2 with five P_LS molecules bound to the proposed anchoring points in the spikes region. Relevant side chains are labeled; bound phospholipid molecules are shown as space-filling models.

2.8. Implications for Membrane Association

The structural features of FVa-C2 discussed in the previous sections, the very positive electrostatic potential created at the bottom of the barrel by the unbalanced charges of several lysine and arginine side chains (Figs 2.4b, 2.4c), as well as the relevance of the homologous loops in discoidin I and N-GOase for membrane attachment, strongly suggest that the groove enclosed by the three spikes in the open crystal form of FVa-C2 represents a major binding site for acidic phospholipid-rich membranes. The results of previous investigations concerning the cofactor interactions with P_LS-rich phospholipid membranes also lend extraordinary support to this hypothesis.

(1) Deletion of the C2 domain results in the loss of FVa procoagulant activity, concomitantly with the lack of P_LS-binding ability, while FVa-C2 alone binds to P_LS-containing vesicles ((Ortel et al., 1992) and W. Kane, personal communication). This implies the presence of a major P_LS-binding site(s) which is located entirely within this domain.

(2) Substitution of residues C-terminal to Ile112 or Ala51 by the corresponding FVIII peptides (compare Fig. 2.2) leads to a ~50% decrease in P_LS-binding activity. Replacement of the whole domain by FVIIIa-C2 results in a chimera which binds only ~10-20% P_LS (Ortel et al., 1994). The major role of the amino-terminal region Cys1-Lys50 of FVa-C2 in membrane binding suggested by these results is also supported by antibody mapping, since

(3) Binding of the inhibitor antibody H1 and of the murine monoclonal antibody HV-1 to FVa-C2 requires the presence of the amino-terminal peptide Cys1-Lys50 (Ortel et al., 1994). Both antibodies had been previously shown to interfere with FVa P_LS-specific binding, therefore neutralizing its procoagulant activity (Ortel et al., 1992). In light of the current three-dimensional structures of FVa-C2, both latter points implicate the first two spikes as the major determinants for membrane insertion. The recent investigation of FVa-C2 by alanine scanning mutagenesis establishes the first spike as the major epitope within this region, since the (D29A, E32A) double mutant is no longer recognized by HV-1, but is otherwise biologically indistinguishable from the native protein (Kim et al., 2000).

(4) Membrane interactions of neighboring loops are indicated by studies conducted with isolated glycoforms of natural FVa. Although the increase in K_d for the form glycosylated at Asn144 (Asn2181 in the mature human protein) fluctuates between a modest 3- to 6-fold for bovine FVa (Koppaka et al., 1997) and a 45-fold for human FVa (Rosing et al., 1993) when compared with the non-glycosylated form, these results certainly localize this barrel end in close proximity to the cell surface. Interestingly, both glycoforms of FVa seem to undergo different conformational rearrangements upon membrane binding (Koppaka et al., 1997), but are functionally indistinguishable once assembled at the phospholipid surface (Rosing et al., 1993).

(5) Finally, and although the results are not limited to a definite domain, it is worth mentioning that charge reversal of ~15% of lysine side chains within the light chain of FVa by modification with citraconic anhydride results in an almost complete loss of membrane binding ability (Pusey and Nelsestuen, 1984).

2.9. A Kinetic Mechanism for Factor Va Membrane Binding

Altogether, a mechanism for the stereospecific recognition and co-operative association with P_LS-rich membranes emerges from the current structures and available biochemical data. (1) Factor Va, with the C2 domain in its closed form (Fig. 2.4b), approaches acidic membrane sites guided by favorable protein-membrane electrostatic interactions. (2) One or two P_LS molecules bind to anchoring points (such as Arg150 and/or Gln48) in the small sized groove of the closed form, triggering the widening of the groove and conversion to the open form (Fig. 2.4c). (3) A P_LS molecule fully occupies the thus opened specificity pocket (Fig. 2.5). Simultaneously, (4) the hydrophobic and now unfolded spikes perforate the polar membrane surface, with the side chains of Trp26, Trp27 and Leu79 immersing in the apolar membrane core. (5) The bottom of the barrel contacts the negatively charged phosphate head groups of the membrane, allowing favorable ionic interactions of basic residues (Lys23, Lys24, Lys50, Lys77, Lys120) located in the spikes and neighboring loops (see Figs 2.1a and 2.4).

Because the spikes and neighboring loops are highly interconnected, and several contiguous P_LS molecules would be necessary for membrane association, spike unfolding and membrane insertion would be highly co-operative, assuring that FVa-C2 binds only to cell membranes with P_LS concentrations exceeding a critical threshold value. This feature would selectively target factor Va to procoagulant, P_LS-rich surfaces. The co-operative nature of this process presumably precludes binding of isolated P_LS head group mimics to FVa-C2. Soaking experiments with phospholipid head group-mimics (*O*-phospho-L-serine and L-α-glycerophosphorylserine) showed stabilization at the apex of spike 3 in crystals of the open form, but no clear electron density for the putative head groups that elicited this stabilization. In this regard, it is noteworthy that the phenyl moiety of PheHg is poorly defined in the electron density in XTAL1-PheHg (Fig. 2.1a), despite covalent attachment to Cys76 Sγ.

It is not predictable to which extent the indole moieties of Trp26 and Trp27 penetrate into the apolar membrane core. As first noted in integral membrane proteins, aromatic residues tend to be localized near the membrane-aqueous phase interface (Weiss et al., 1991). The preferential location of Trp side chains within the protein-lipid interface with little penetration into the hydrocarbon core has also been suggested from biochemical investigations (Yau et al., 1998). Assuming similar interactions of FVa-C2 with the lipid bilayer as those seen in the annexin V structure (see below), it is conceivable that Trp26 and/or Trp27 wrap around the bound P_LS molecule(s) and exclude it from bulk water. On the other hand, insertion of Leu79 into the membrane would appear even more likely, but its alanine mutant shows similar levels of membrane affinity and procoagulant activity in the preliminary characterization (Kim et al., 2000).

2.10. Comparison With Other Peripheral Membrane Proteins

The interactions of peripheral membrane proteins with the lipid bilayer are rather poorly understood to date. The proposed membrane immersion of the hydrophobic C2 spikes into the apolar membrane core resembles that postulated for γ-carboxyglutamic acid (Gla)-rich domains of vitamin K-dependent coagulation factors ((Stenflo, 1999); see also section 1.2.1.). However, while the structurally unrelated Gla domains are probably in a membrane-competent form at plasma calcium concentrations of about 1.4 mM (Figs 1.4 and 1.5), a critical but low number of P_LS molecules is necessary to promote the subtle calcium-independent conformational changes necessary for FVa binding (Krishnaswamy and Mann, 1988).

The role of the indole side chains of Trp26/Trp27 has a remarkable parallel in the anticoagulant protein **annexin V** (Huber et al., 1990). Annexins are a ubiquitously family of structurally related peripheral membrane proteins that share the common property of Ca^{2+}-dependent binding to PS-containing membranes. Several biological roles have been proposed for these proteins. It is believed that annexins are in general sense membrane organizers, which influence binding of other peripheral membrane proteins by modifying the membrane properties. Particularly relevant is the ability of annexin to interfere with the binding of coagulation factors to procoagulant membranes (Andree et

al., 1992), which explains its strong anticoagulant activity (Funakoshi et al., 1987; Kondo et al., 1987; Reutelingsperger et al., 1988).

In annexin V, the unique tryptophan side chain has been implicated in membrane binding (Meers, 1990; Meers and Mealy, 1993). This tryptophan interacts with the phosphoglycerol backbone of phospholipid head group mimics in the crystal structures of reported complexes (Swairjo et al., 1995). Related, but less dramatic movements to the ones observed for Trp26/Trp27 in FVa-C2 have also been documented for this tryptophan residue, which is buried in the calcium-depleted form but becomes exposed upon calcium binding (Berendes et al., 1993; Concha et al., 1993).

There is also a remarkable structural resemblance between the spikes of FVa-C2 and three exposed loops of the otherwise unrelated C_2 domain of synaptotagmin I (Sutton et al., 1995), a protein that belongs to a family of peripheral membrane proteins ubiquitously involved in membrane trafficking and signal transduction (for a recent review see (Nalefski and Falke, 1996)). These loops have been implicated both in calcium co-ordination and in membrane interactions (Shao et al., 1996; Sutton et al., 1995; Sutton and Sprang, 1998; Verdaguer et al., 1999). Several exposed hydrophobic residues at the apex of two of the loops from synaptotagmin I superimpose perfectly with two FVa-C2 spikes (not shown).

2.11. Comparison With the Structure of FVIIIa-C2: Implications for Modeling Other Mammalian Discoidin Domains

Shortly after determination of the crystal structure of FVa-C2, the crystal structure of the homologous domain from factor VIIIa was solved at 1.5 Å (Pratt et al., 1999). As expected from the high degree of sequence homology (compare Fig. 2.2), both structures can be perfectly superimposed, with an r.m.s.d. of only 0.58 Å for 149 Cα atoms. Differences are limited to the first spike (residues 25–28) and loop 104–109, and arise from deletion of one and two residues, respectively, in FVIIIa-C2. Moreover, most of the side chains of both modules occupy very close positions.

The amino acid sequences of all factor V / factor VIII discoidin (C1 and C2) domains are highly homologous, with ~25% of all residues strictly conserved and

another ~33% replaced by residues of similar character (Fig. 2.2). These values increase to ~38 to 48% when only the four domains of the human cofactors are compared. Therefore, the structures of FVa-C2 and FVIIIa-C2 represent accurate templates for modeling other discoidin domains of coagulation factors. These models provide structural basis for understanding several point mutations identified in hemophilia A patients, as most of the reported mutations affect strictly conserved residues (Appendix A5). Moreover, the current structures may also be useful for modeling the three-dimensional structures of several members of this ever growing family.

To illustrate the potential of the here presented structure, and in an attempt to predict the overall spatial arrangement of the domains comprising factor Va / factor VIIIa, we have modeled the three-dimensional structure of human FVa-C1. The replacement of the side chains and the regularization of the structure was done with MAIN (Turk, 1992), with only a few manual interventions to avoid steric clashes. The four residue insertion Leu51A-Ala51B-Ala51C-Glu51D (residues 1925-1928 of the mature protein) was modeled based on the β-hairpin conformation adopted by residues Leu79–Glu82 in the open form of FVa-C2. The obtained model of FVa-C1 was energy-minimized with XPLOR and is represented as a ribbon plot in Fig. 2.6.

As expected, the β-barrel structure is conserved and provides a fixed scaffold for the exposed loops at its bottom. The five-residue deletion within the first spike, the four-residue insertion Leu51A-Glu51D, as well as several notable substitutions (e.g., Ser78His, Asn144Tyr; Fig. 2.2) account for the formation of a groove which is differently shaped as the one seen in the open conformation of FVa-C2, in agreement with the C1 domain lacking P_LS-binding activity (Ortel et al., 1992). However, clustering of several exposed hydrophobic / aromatic side chains in this region (e.g., Phe22, Leu23, Leu51A, Tyr79, Leu80) strongly suggests that C1 might also contribute to membrane binding.

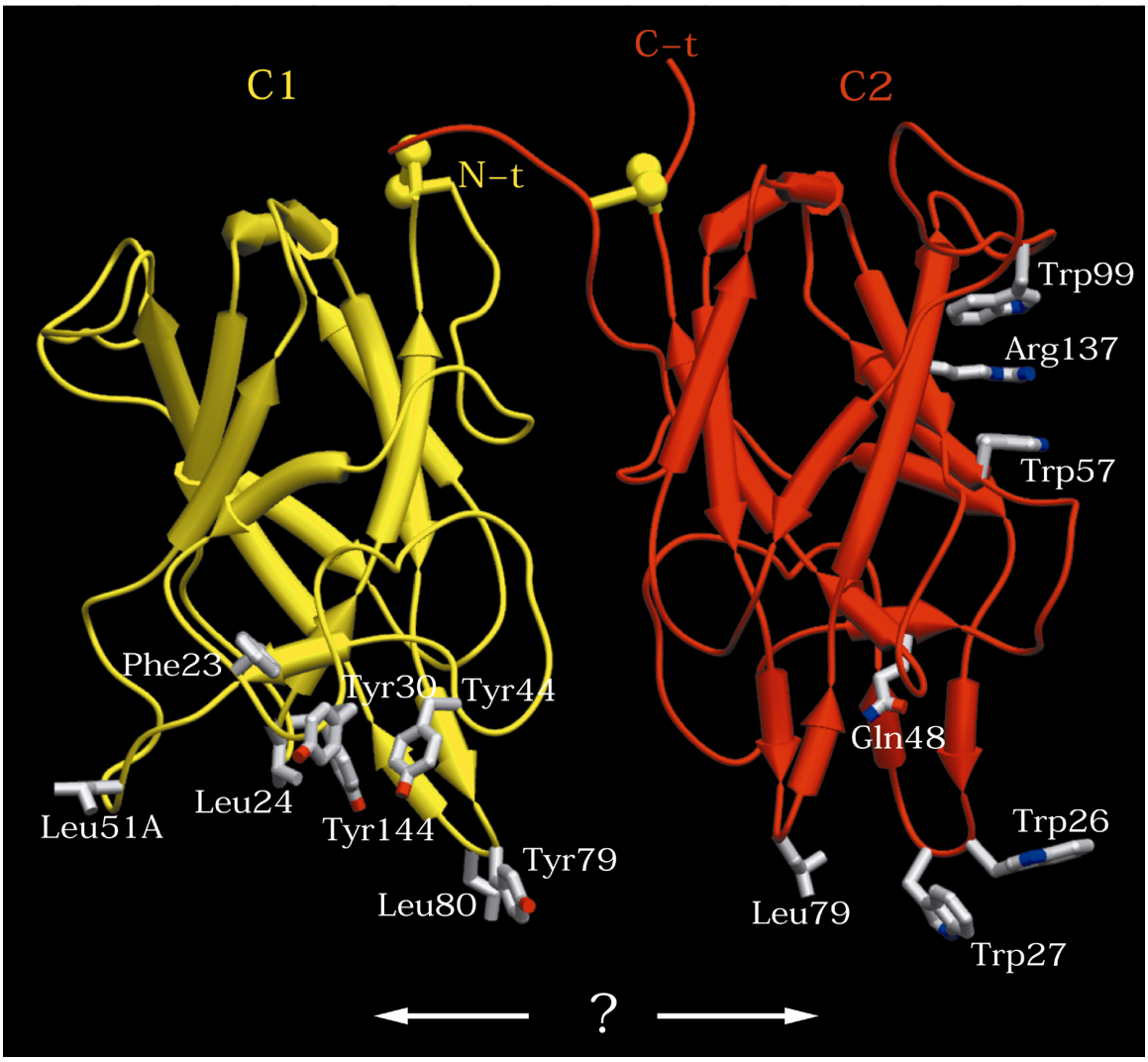

Fig. 2.6: Putative arrangement of human FVa-C1 and -C2 domains on the membrane surface. Disulfide bridges are shown as yellow ball-and-stick models. Notice the presence of aromatic and hydrophobic residues at the apex of the 'spikes' in FVa-C1, suggesting their involvement in interactions with particularly hydrophobic membrane patches. It is likely that the presence of binding sites on neighboring domains supports synergistic protein-protein and protein-membrane interactions that target factor Va to the membrane surface of activated platelets. Arrows indicate a possible "sliding" of both domains after the initial interaction with the membrane surface, allowing more extended surface patches to come in contact with the phospholipid membrane. (Notice the position of the Trp57-Arg137-Trp99 triplet).

The C1-C2 domains are connected by a four-residue, well conserved linker (Glu-Val-Asn-Gly in the human protein), which is flanked by the disulfide bridges Cys1-Cys156 linking the chain termini of both domains. The rigidity imposed by these disulfide bonds implies that the N- and C-terminal regions from both domains will be close to each other. There is, however, a high degree of conformational flexibility around the five peptide bonds linking both domains,

and this would allow for extremely different arrangements of both discoidin-like domains, ranging from an almost parallel "side-by-side" arrangement (as shown in Fig. 2.6) to a "head-to-to-head" orientation, in which the flat upper regions of the two domains associate to generate an extended dimer.

2.12. Conclusions

The three-dimensional structure of the membrane-binding C2 domain of factor V (FVa-C2) has been determined by a three-wavelength anomalous diffraction experiment using a mercury-derivatized crystal. The protein model has been refined against a native data set at 1.87 Å resolution (XTAL1-NAT) as well as against a data set collected from a crystal soaked in an *O*-phospho-L-serine solution (XTAL1-OPS) at 1.80 Å. A second crystal form (XTAL2-NAT) has been solved by Patterson search techniques using the previously refined model for XTAL1-NAT, and refined to 2.40 Å resolution. The conserved β-barrel framework provides a scaffold for three protruding loops, one of which adopts markedly different conformations in the two crystal forms. A mechanism of calcium-independent, stereospecific binding of factors Va and VIIIa to phospholipid membranes is suggested, based on (a) immersion of hydrophobic residues at the apices of these loops in the apolar membrane core, (b) specific interactions with phosphatidylserine head groups in the groove enclosed by these loops, and (c) favorable electrostatic contacts of basic side chains with negatively charged membrane phosphate groups.

Chapter 3

Thrombin Inhibition:

Crystal Structure of the Thrombin–Triabin Complex

3.1. Triabin Is a Thrombin Inhibitor With a Unique Inhibitory Profile

Considering the critical roles played by thrombin in the regulation of coagulation and fibrinolysis (see Fig. 1.1 and sections 1.2.5. and 1.2.9.), thrombin inhibitors are best candidates for therapeutic applications, and their development continues to be an area of intensive research (Fenton et al., 1993; Fenton et al., 1991; Lombardi et al., 1999). Most thrombin inhibitors characterized to date not only block the physiologically relevant activities of the proteinase (e.g., fibrinogen cleavage, platelet activation), but interfere also with thrombin's amidolytic activity. (For reviews see (Lombardi et al., 1999; Stubbs and Bode, 1994). This is not only true for small synthetic thrombin inhibitors, but also for all proteinaceous inhibitors previously characterized by X-ray crystallography (see section 3.6.).

To avoid blood clotting during feeding and digestion, hematophageous animals secrete proteinase inhibitors directed towards several blood coagulation factors of their prey, most notably towards thrombin. (For reviews see (Markwardt, 1994; Stubbs and Bode, 1994). Of the several specific thrombin inhibitors from blood-sucking animals known to date, the structures of **hirudin** (Grütter et al., 1990; Rydel et al., 1990), **rhodniin** (van de Locht et al., 1995), and **ornithodorin** (van de Locht et al., 1996) have been crystallographically studied in their complexes with thrombin and are particularly illustrative of the diversity of structural motifs that allow interactions with the proteinase.

A common feature of these non-homologous inhibitors is their two-domain structure, with the N-terminal domain binding directly to or adjacent to thrombin's active site, and the C-terminal domain (or peptide) interacting with its anion-binding exosite I (1.2.5.). Consequently, the corresponding thrombin complexes lack any proteolytic activity, both towards small chromogenic substrates as well as towards macromolecular protein substrates.

In marked contrast triabin, a protein isolated from the saliva of the triatomine bug *Triatoma pallidipennis* by the group of Prof. Schleuning at the Research Laboratories of Schering AG (Berlin, Germany), reduces thrombin's hydrolytic activity towards chromogenic substrates only slightly. (A modest 35% inhibition is achieved with up to 67-fold molar excess of triabin). In spite of the

retained amidolytic activity, triabin effectively abolishes thrombin-catalyzed hydrolysis of fibrinogen (1.5.1.) with an apparent K_i of about 3 pM (Noeske-Jungblut et al., 1995). However, a small but definite fibrinogen-clotting activity remains even after equimolar (non-covalent) complex formation ((Glusa et al., 1997; Noeske-Jungblut et al., 1995), and C. Noeske-Jungblut, unpublished). Furthermore, triabin inhibits thrombin-induced platelet aggregation (section 1.4.1.) in a dose-dependent manner, and prolongs the thrombin-clotting time. Triabin also inhibits the thrombomodulin-mediated activation of protein C by thrombin (section 1.2.9. and chapter 4). These observations led to the assumption that triabin binds to thrombin at a surface site(s) located more distantly from the active site, most probably to its anion-binding exosite I or to both exosites (compare Figs 1.12b, 1.14), and provoked a detailed structural investigation.

3.2. Structure Determination

3.2.1 Protein Purification, Crystallization and Data Collection

Recombinant triabin was over-expressed in insect cells using a baculovirus-driven expression system, and purified using a two-step procedure that involves (i) ion-exchange chromatography on DE52 cellulose followed by (ii) affinity chromatography on a thrombin-Sepharose column (Noeske-Jungblut et al., 1995). This work was performed by Dr. Christiane Noeske-Jungblut at the Research Laboratories of Schering AG (Berlin, Germany). Initial crystallization trials were independently conducted with triabin complexes formed with either human or bovine α-thrombin, and in the two cases both the free and the D-**P**he-**P**ro-**A**rg **c**hloromethyl **k**etone (PPACK)-inhibited enzymes were tried. The thrombin-triabin complexes were formed by incubating equimolar amounts of both proteins for 30 minutes on ice. Complexes were dialyzed against 10 mM sodium acetate (pH 5.5), 25 mM NaCl, concentrated in Centricon 30 tubes (Amicon, USA), and used for sitting-drop vapor-diffusion crystallization without further purification. Several conditions were found where small crystals of the complexes between triabin and the active-site free enzymes appeared after a few days (Fig. 3.1a), sometimes forming bizarre aggregates (Fig. 3.1b), but none of them diffracted below 4.0 Å. No crystals of the PPACK-inhibited complexes were obtained in this

initial screening. Therefore, both (PPACK-free) thrombin-inhibitor complexes were purified before pursuing further crystallization trials.

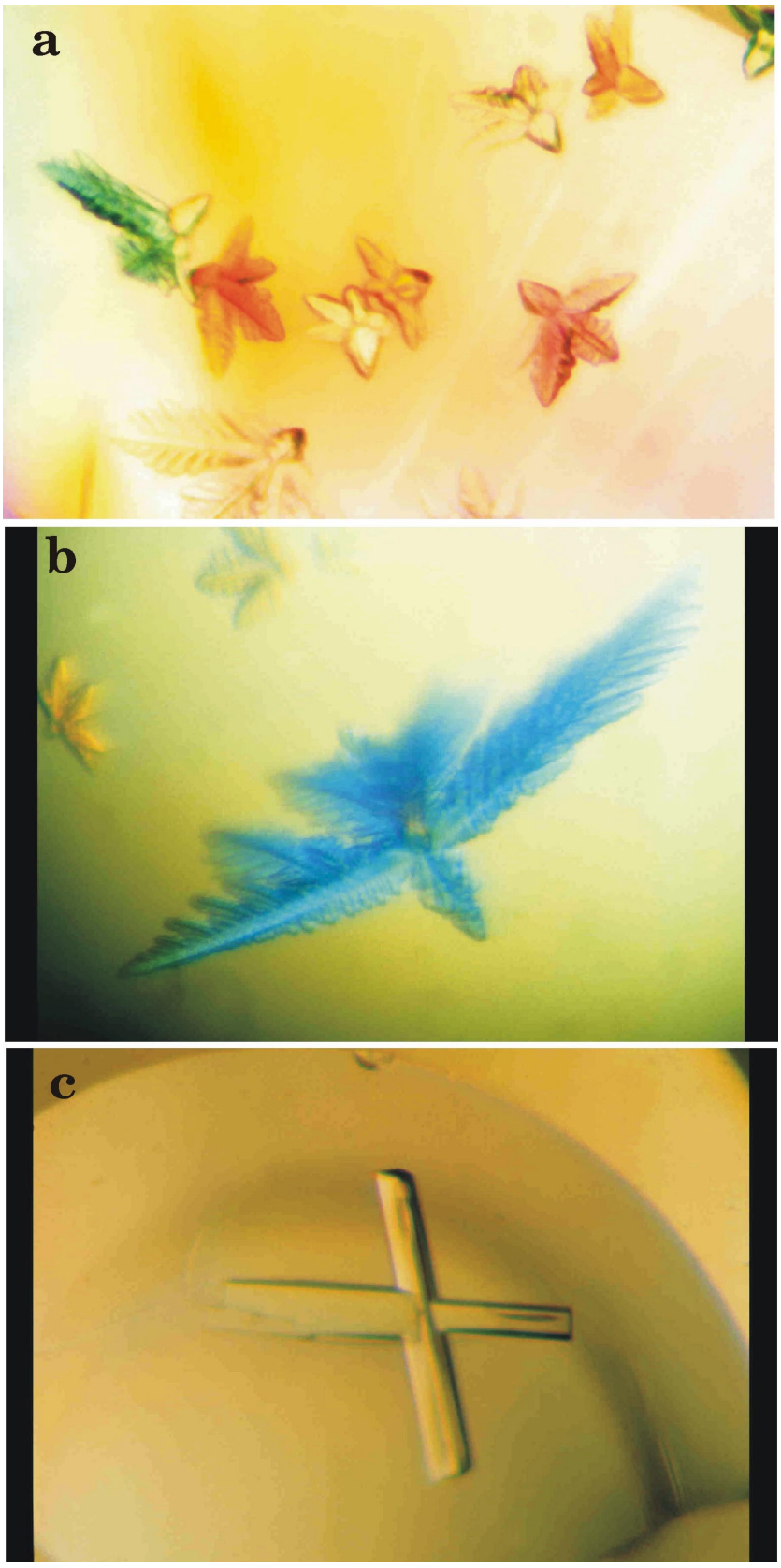

Fig. 3.1 (previous page): Crystals of thrombin-triabin complexes. (**a**) and (**b**) Crystals of the human α-thrombin-triabin complex, grown using the non-purified complex. (**c**) Crystals of the bovine α-thrombin-triabin complex, grown after purification by anion-exchange chromatography. Crystallization solution: 100 mM Na acetate pH 4.6, 200 mM $(NH_4)_2SO_4$, 16% PEG 4,000.

For anion-exchange chromatography, the thrombin-triabin complexes were dialyzed against 20 mM Tris-HCl (pH 8.0) (buffer A) and applied to a 7.5 mm x 7.5 cm DEAE-5PW column (TosoHaas, Germany). A shallow salt-gradient (from 0 to 250 mM NaCl in buffer A over 60 minutes) allowed separation of several (three to six) fractions of thrombin-triabin (Fig. 3.2) that migrated differently in native gels (not shown), suggesting differences in sugar composition and/or minor proteolytic cleavages. The major fractions were used for further crystallization trials.

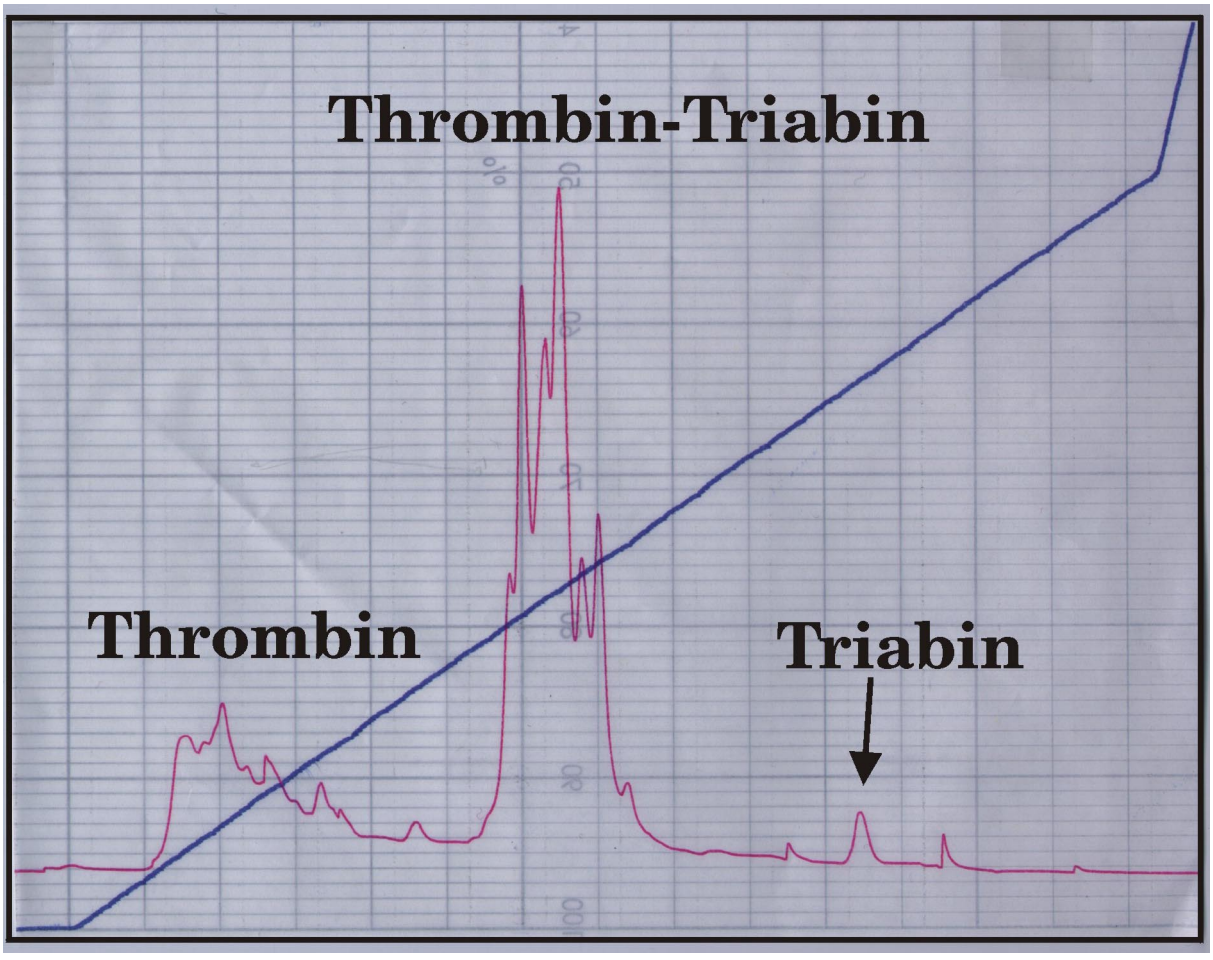

Fig. 3.2: Purification of the bovine thrombin-triabin complex. Samples of the thrombin-triabin complexes were applied to the DEAE-5PW column and eluted with a shallow salt gradient (blue line). Absorbance was monitored at 222 nm (red curve).

Crystals of the bovine thrombin-triabin complex appropriate for structural analysis grew within a week at 20°C in sitting drops containing 50 mM Na acetate pH 4.6, 100 mM $(NH_4)_2SO_4$, 0.01% NaN_3 and 8% PEG 4,000 that were equilibrated against a reservoir solution containing 16% PEG 4,000. Crystals used for data collection reached maximal dimensions of 0.7 mm x 0.15 mm x 0.1 mm (Fig. 3.1c). Diffraction data to 2.6 Å were collected from two crystals at 7° C on a 300 mm MAR image plate system (MAR Research, Germany) using monochromatized CuKα radiation produced by a conventional rotating anode. These data were evaluated with programs from the MOSFLM package (Leslie, 1991), and merged and scaled using programs of the CCP4 program suite (Collaborative Computational Project No. 4, 1994). The crystals belong to the orthorhombic space group $P2_12_12_1$ and contain one complex molecule per asymmetric unit (solvent content: approximately 54%, Matthews coefficient 2.69 $Å^3$/Da). (See Table 3.1 for a summary of crystallographic data).

3.2.2. Phasing and Refinement

Searches for the orientation and position of the thrombin molecule in the crystals were performed with the program suite AMoRe (Navaza, 1994), using diffraction data from 10.0 to 3.5 Å and the coordinates of bovine α-thrombin as observed in its complex with rhodniin (van de Locht et al., 1995) (see section 3.6.). In the search model, residues Thr1U to Asp1A and Leu14L to Arg15 of the A-chain and most of the residues forming the autolysis (149-)loop (Glu146 to Glu149E) were excluded. Rotational search yielded two possible solutions with correlation factors of 0.211; only one of them gave rise to a favorable translation solution. This solution exhibited a correlation value of 0.555 and an R factor of 38.2% (values for the next highest peak: c = 0.131, R = 52.5%). A 3.0 Å-Fourier map calculated after appropriate positioning of the thrombin molecule in the crystal cell allowed building of the autolysis loop and of the omitted parts of the thrombin A-chain. Additionally, some stretches of continuous electron density were visible near the fibrinogen-recognition exosite of thrombin, and allowed modeling of three polyalanine strands with MAIN (Turk, 1992). The complex was crystallographically refined with X-PLOR (Brünger, 1987; Brünger, 1993) using the target parameters of Engh and Huber (Engh and Huber, 1991). This procedure was cyclically repeated several times, until side chains were identified

so that the correct amino acid residues could be built in. After the whole inhibitor polypeptide chain (except segments Gly46I to Lys48I and Asn74I to Lys75I; the suffix 'I' serves to distinguish triabin from thrombin residues), was fitted to the density map, water molecules were added at stereochemically reasonable positions at 1σ and 2σ peaks in the ($2F_{obs} - F_{calc}$) density and ($F_{obs} - F_{calc}$) difference density maps. Finally, individual but highly restrained B-values were refined.

Table 3.1: Summary of Data Collection and Refinement Statistics.

Parameter	Value
Crystal data	
Space group	$P2_12_12_1$
Cell constants	a= 44.84 Å, b= 67.23 Å, c= 183.49 Å
Temperature	279 K
Limiting resolution	2.60 Å
Significant measurements	79,890
R_{merge}*, %	9.9
Independent reflections	16,392
Completeness, %	
Overall	93.2
Outermost shell, 2.67–2.60	81.0
Refinement	
Non-hydrogen protein atoms	4,304
Solvent molecules	172
Reflections used for refinement	14,627
Resolution range, Å	10.0–2.6
R_{factor}†, %	18.4
R_{free}¶, %	27.5
r.m.s.d.	
Bond lengths, Å	0.008
Main chain bond angles, °	1.49
Side chain bond angles, °	25.92

*R_{merge} : $\sum_h \sum_i (|I(h_i) - \langle I(h)\rangle|) / \sum_h \sum_i I(h_i)$, where $I(h_i)$ is the intensity of the *h*th reflection as determined by the *i*th measurement and $\langle I(h)\rangle$ the average value.

†R_{factor} : $\sum(|F_{obs}| - |F_{calc}|) / \sum |F_{obs}|$, where $|F_{obs}|$ is the observed and $|F_{calc}|$ is the calculated structure factor amplitude of reflection *hkl*.

¶R_{free} : R_{factor} calculated for a randomly selected test set comprising 5% of all reflections, that were excluded for refinement.

The final model comprises residues Phe1M to Arg15 of the A-chain, all 259 residues of the B-chain, segments Ala1I to Ser45I, Gly49I to Asp73I and Asn76I

to Cys142I of triabin, and 172 water molecules. A discrepancy with the previously reported protein sequence (Phe127I instead of Leu) was found and verified at the Research Laboratories of Schering AG by sequencing both strands of the gene. Weak electron density near Asn60G Nε2 and Asn22I Nε2, accounting for the carbohydrate moieties of the single α-thrombin sugar chain and of the inhibitor, respectively, was left uninterpreted. All main chain dihedral angles of non-glycine residues fall into "allowed" regions of the Ramachandran plot, with 85.6% of them in the most favored conformations. A summary of the crystal and refinement data is presented in Table 3.1.

3.3. Overall Structure of the Bovine Thrombin-Triabin Complex

Crystals contain a single thrombin-triabin complex *per* asymmetric unit, but both moieties make also important contacts with molecules of symmetry-related complexes (Fig. 3.3a). Each thrombin molecule interacts through the C-terminal segment of its A-chain (residues Glu14C^S to Arg15^S; side chains of the symmetry-related thrombin light chain are denoted by an 'S') with unprimed subsites of a neighboring thrombin molecule in a substrate-like manner ((Bode and Huber, 1992); see also section 1.2.4.). The Arg15^S side chain occupies the S1 pocket, making a strong hydrogen-bonded salt-bridge with Asp189 at the bottom of the specificity pocket. Its free C-terminal carbonyl accepts hydrogen bonds from the main chain nitrogen atoms of Gly193 and Ser195, on the one side (the oxyanion hole, see 1.2.4.) and from the catalytic His57 Nε2, on the other (Fig. 3.3b). Further, the P3-residue Glu14L^S binds through two hydrogen bonds to Gly216, and the Ile14K^S side chain slots into the aryl- (S4) binding site. Additional interactions between acidic side chains of the thrombin 'substrate' light chain (Glu14H^S, P7, and Glu14C^S, P12) and positively charged heavy chain residues of the 'enzyme' (Arg175 and Arg173, respectively) might help complex formation and/or strengthen the binding (Fig. 3.3b).

This inter-thrombin interaction results in extended chains of assembled thrombin molecules that make the crystal "scaffold". A similar situation has been previously observed in crystals of free factor Xa (Padmanabhan et al., 1993). We notice that the conformation of the bound peptide strongly differs from the one adopted by fibrinopeptide A (Fig. 1.26).

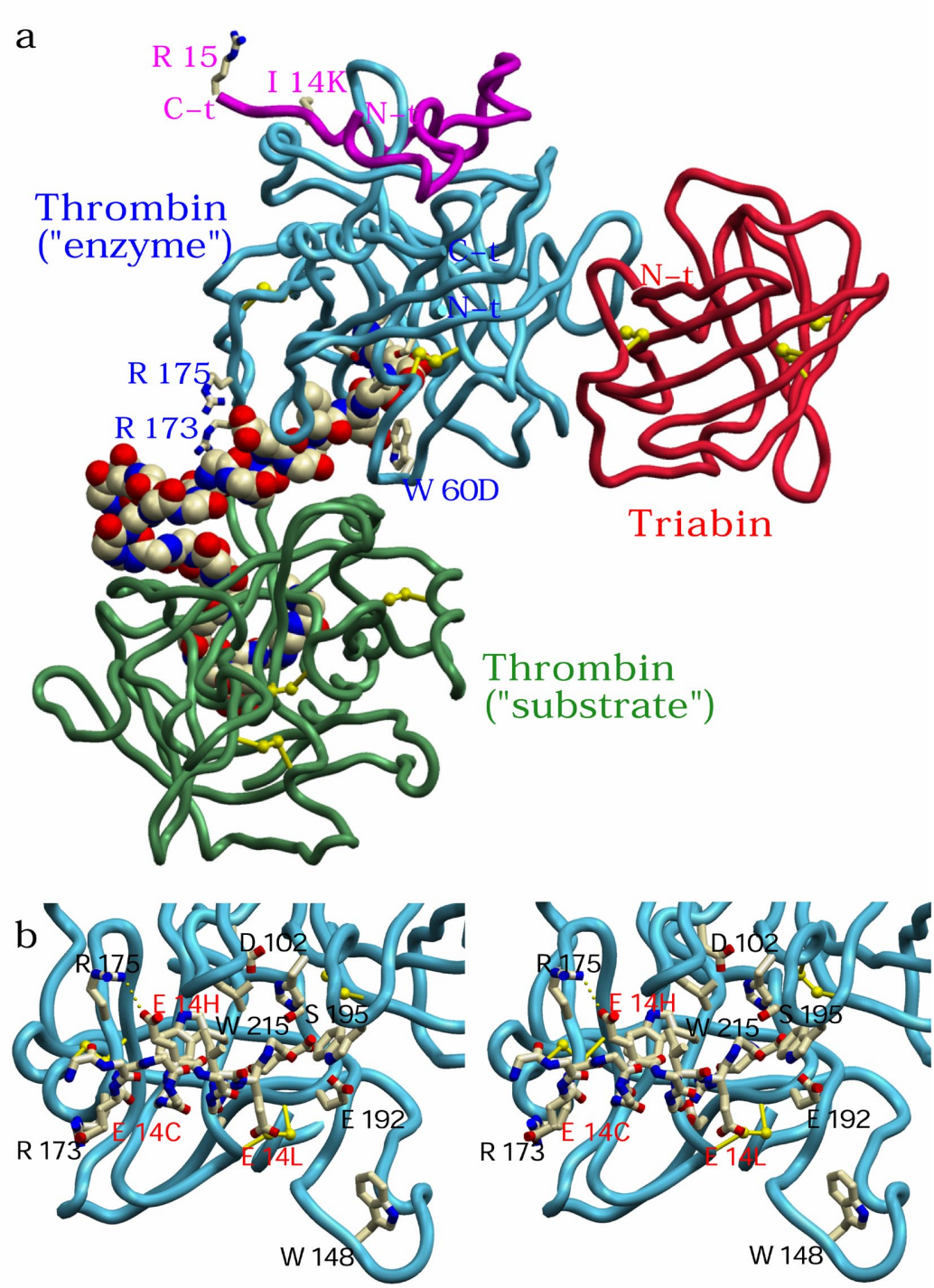

Fig. 3.3: Crystal contacts in the structure of thrombin–triabin mimic a thrombin–substrate complex. (**a**) Structure of the thrombin-triabin complex, showing a neighboring thrombin molecule bound to the active site of the triabin-bound proteinase. The complex forming the asymmetric unit is shown as blue (thrombin heavy chain), pink (thrombin light chain) and red (triabin) ribbons. The neighboring thrombin molecule is depicted as a green ribbon (heavy chain) or as van der Waals spheres (Cα trace of the light chain). Some important contact side chains are given in full length. (**b**) Detail of the thrombin (enzyme)–thrombin ('substrate') interaction interface. Notice that favorable thrombin-thrombin contacts extend to residue Glu14C (P12) of the 'substrate' light chain.

Each triabin molecule is in direct contact with two thrombin molecules through two very different surface patches. The first of these intermolecular contacts (described in detail in section 3.5.) comprises 90 non-hydrogen atom-atom contacts below 4.0 Å, which are made upon removal of 940 $Å^2$ molecular surfaces from bulk water. The second interaction surface comprises 61 such contacts and buries areas of 445 $Å^2$ in each molecule. Due to the larger number of contacts and the superior shape and charge complementarity within the first intermolecular interface (Fig. 3.4a), and because of the correspondence with previous experimental data (e.g., protection of trypsin cleavage at Arg73–Asn74, inhibition of TM-mediated protein C activation) (Noeske-Jungblut et al., 1995), we are confident that the binary complex shown in Fig. 3.4b is the one relevant in solution.

In the triabin complex, the thrombin moiety differs only slightly from other reported thrombin structures, whether active-site inhibited (e.g., PPACK-thrombin, (Bode et al., 1989) or bound to the unrelated inhibitors hirudin (Rydel et al., 1990), rhodniin (van de Locht et al., 1995), and ornithodorin (van de Locht et al., 1996) (see section 3.6.). The observation that complex formation with triabin does not result in gross conformational changes of the thrombin active site explains the marginal 35% decrease in amidolytic activity upon complex formation (Noeske-Jungblut et al., 1995).

Fig. 3.4 (next page): Triabin is an exosite I–binding inhibitor. (**a**) "Opened-book" view of the thrombin and inhibitor moieties. Notice the overall complementarity of electrostatic surface potentials, as calculated with the program GRASP (Nicholls et al., 1993). Blue, positive; red, negative potential areas. (**b**) Ribbon plot of the complex formed between bovine α-thrombin (light chain - pink, heavy chain - blue) and triabin (red). The proteinase is shown in its 'standard' orientation, i.e. with the active-site cleft facing the viewer and binding peptide substrates running from left to right. Side chains of the catalytic triad residues of thrombin are explicitly shown, as well as several residues of the thrombin-triabin interface. Notice in particular the salt-bridge formed between Arg77A (thrombin) and Asp135I (triabin).

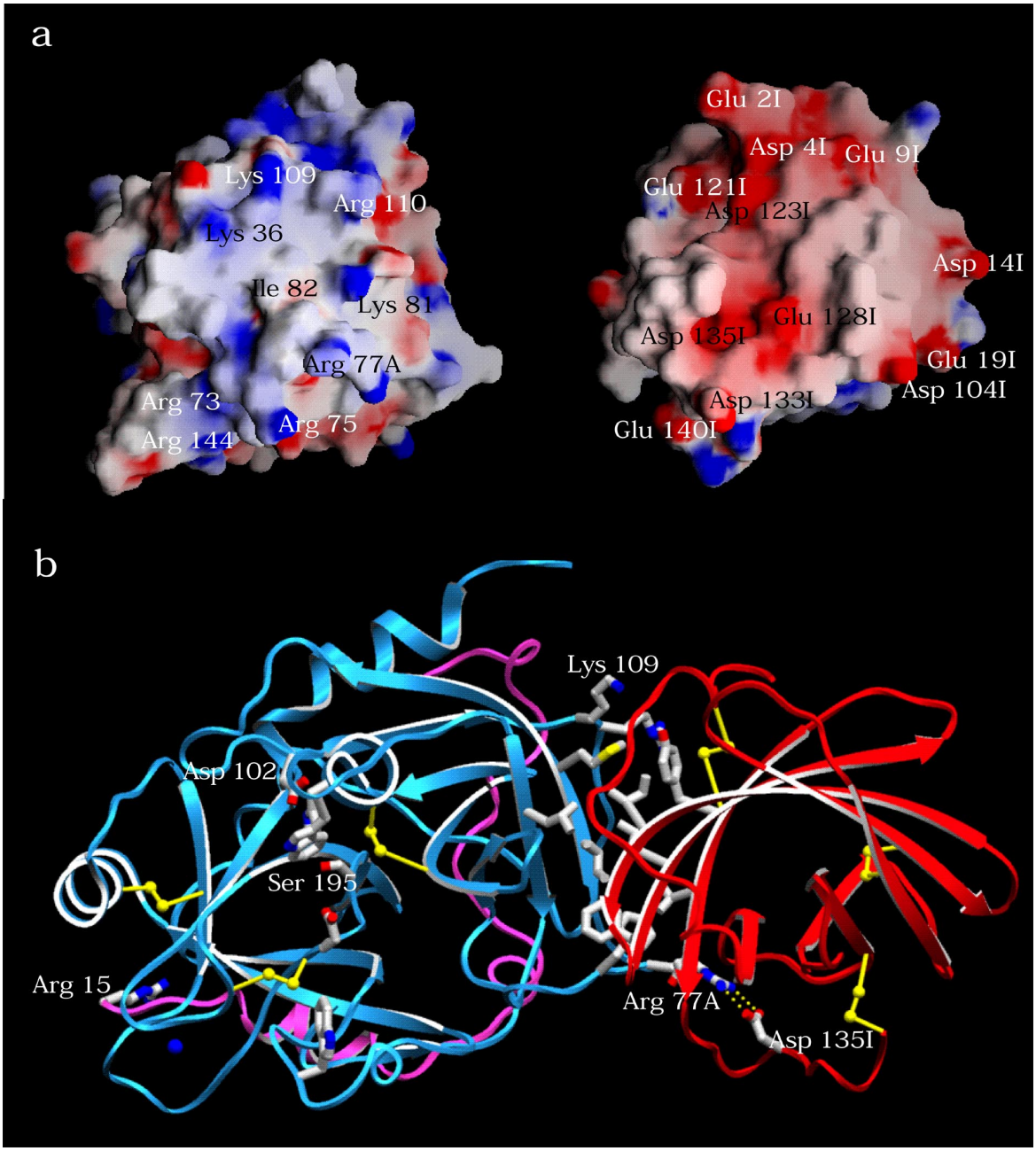

3.4. Triabin Structure

Triabin is a single domain molecule of approximate dimensions 32 Å x 30 Å x 25 Å. Its main structural feature is an eight-stranded β-sheet, which is smoothly rolled and annealed at both edges forming a slightly flattened and conical barrel with the overall appearance of a calyx (Fig. 3.5). This sheet is characterized by a **shear number** (the residue offset upon surrounding the barrel) of 12 (Fig. 3.6). The first (β_A) and the last strand (β_H) are aligned with each other at an angle of about 30°, allowing formation of a single pair of hydrogen bonds between Tyr26I (strand β_A) and Glu128I (strand β_H). This contrasts with the extended hydrogen-bonding network formed between all other pairs of neighboring strands within

the β-sheet, which are cross-linked through 5-10 hydrogen bonds (see Fig. 3.6 for a schematic representation of triabin's secondary structure).

The first four N-terminal strands are adjacently arranged in the order β_A-β_C-β_B-β_D, thus with an unusual up-up-down-down or 2x, -1, 2x topology. They are connected by relatively long loops, two of which (β_B/β_C and β_D/β_E; loops are identified by the strands they connect) are partially disordered. The β_A/β_B and the β_C/β_D loops project into the wider "back" opening of the conical barrel (Fig. 3.5b), acting together with the side chains of residues His29I, Tyr58I, Lys60I and Phe61I like a lid of the calyx.

The five C-terminal strands β_D to β_H are arranged in a regular up-and-down manner; the last four of them (β_E to β_H) are connected by short, well-defined β-hairpin loops. The barrel interior is densely packed with hydrophobic (mainly aromatic) side chains donated from all eight strands (Fig. 3.5). It also includes disulfide bridge Cys69I–Cys84I, which cross-connects the neighboring strands β_D and β_E. The interior of the barrel is crossed by a polar cluster, which is fully embedded in the hydrophobic core and clamps opposite barrel strands tightly together. Central to this cluster is the Glu55I (strand β_C) carboxylate, which asymmetrically opposes the guanidinium group of Arg111I (strand β_G), forming a forked 1N-2O hydrogen bond. The Glu55I carboxylate group is further flanked by the carboxamide group of Gln40I (strand β_B) and by the imidazole ring of His29I (strand β_A), forming Nε-Oε hydrogen bonds to either side (Fig. 3.5).

Fig. 3.5 (next page): Triabin is a single-domain protein with the overall appearance of a calyx. Two approximately perpendicular stereo views of triabin. Several aromatic side chains, as well as the polar residues involved in the buried salt-bridge cluster are shown with all non-hydrogen atoms. The eight β-strands are labeled. Disulfide bridges are shown as yellow ball-and-stick models. See text for details.

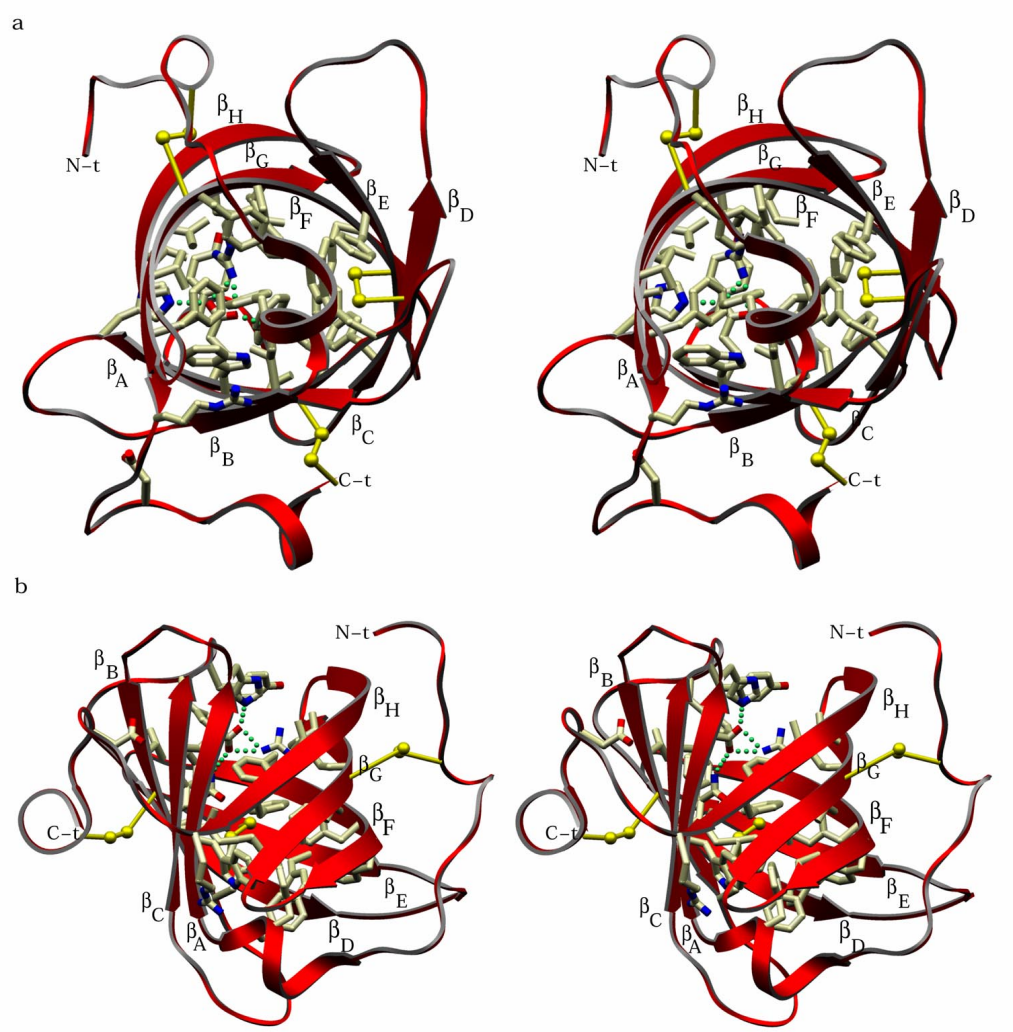

The extended N-terminal segment Ala1I–Phe21I crosses the barrel side on top of β-strands β_F, β_G and β_H and is covalently linked to strand β_G *via* disulfide bridge Cys6I–Cys110I. It terminates in a short mixed 3_{10}-α-helix (h1), which acts like a lid at the "front" barrel opening (Fig. 3.5). Similarly, the C-terminal peptide of triabin (Thr130I to Cys142I) is located on the outer barrel surface and covers the N-terminal strands β_A, β_C and β_B. The short C-terminal helix h2 is covalently clamped to strand β_B through disulfide bridge Cys39I–Cys142I (Figs 3.5, 3.6). Thus, all six cysteine residues of triabin are disulfide-paired according to the connectivity pattern [1-5, 2-6, 3-4] and link together sequentially distant parts of the polypeptide chain.

Fig. 3.6 (next page): Schematic representation of the polypeptide chain arrangement of triabin. Acidic, basic and cysteine residues are emphasized with red, blue and yellow circles, respectively. Disulfide bridges are shown explicitly, and inter main chain hydrogen bonds are represented as dotted lines. Residues involved in interactions with thrombin are shadowed in dark gray if in contact with Tyr76 and/or Arg77A, and in light gray otherwise.

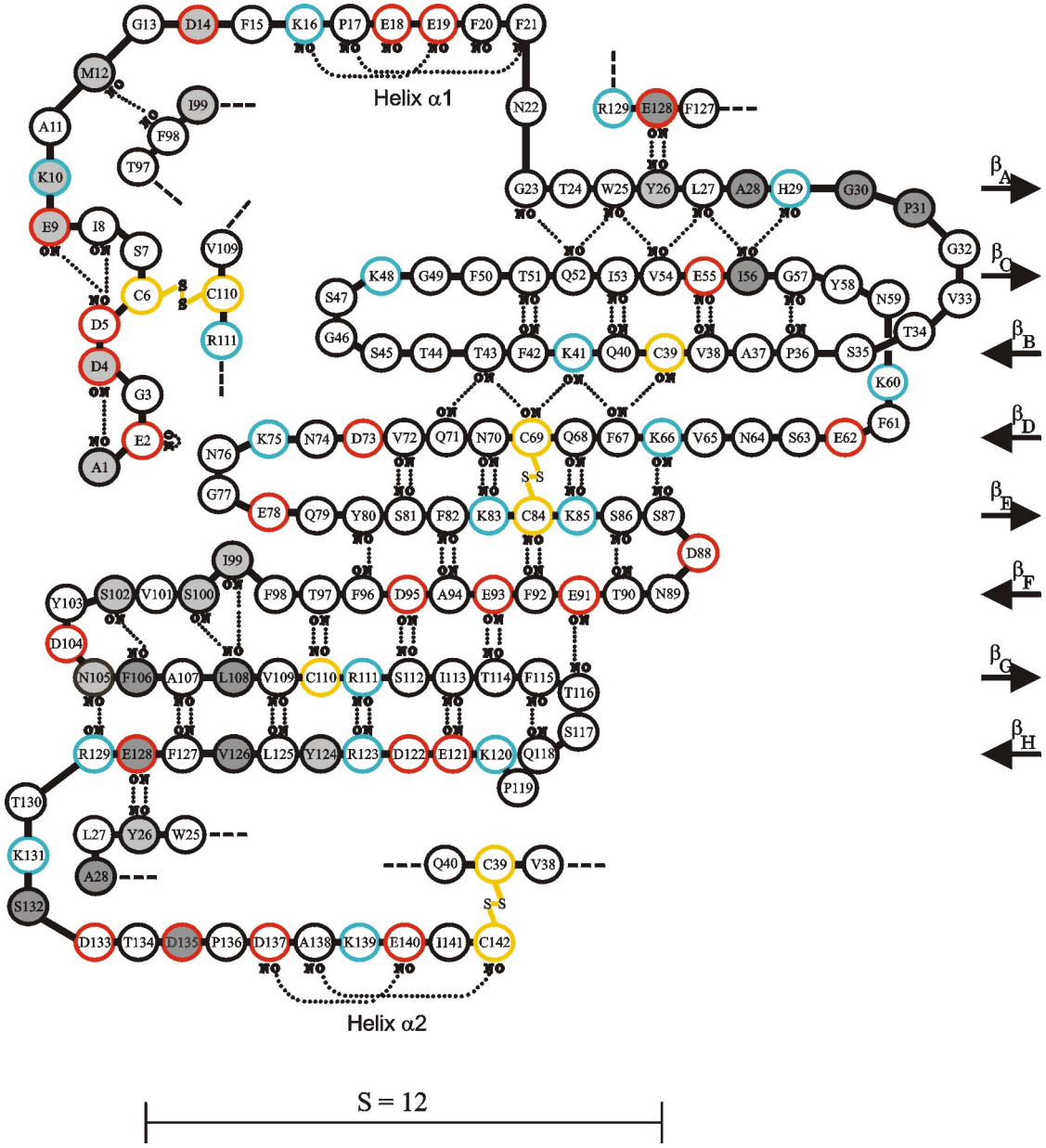

3.5. Thrombin-Triabin Interaction Interface

Thrombin contacts the triabin molecule exclusively *via* the "distal" part of its positively charged anion-binding exosite I (Fig. 3.7). Both contacting surfaces are slightly convex and are surrounded by side pockets filled with a number of ordered solvent molecules, eight of which (interpreted as water molecules) directly cross-connect polar groups from both proteins. A total of 20 triabin residues (shadowed in Fig. 3.6) and 13 thrombin residues participate in (mostly side chain to side chain) direct contacts below 4.0 Å. On the thrombin side, polypeptide segments Thr74 to Met84, Lys36 to Gln38, as well as the side chains of Leu65, Lys109, and Arg110 are in direct contact with the inhibitor.

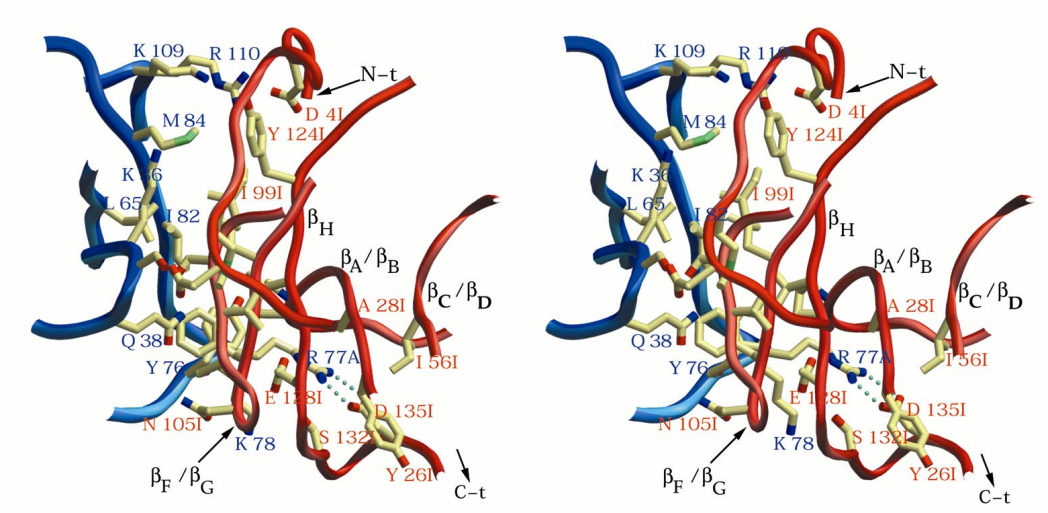

Fig. 3.7: Closed-up stereo view of the interaction interface between bovine thrombin and triabin. The contacting segments of thrombin (blue) and triabin (red) are shown as α-carbon traces, and only the most important side chains are given with all atoms. Water molecules are omitted for the sake of simplicity. Orientation is similar to that seen in Fig. 3.2 (with thrombin in the standard orientation).

It has been long known from experiments with native and proteolytically cleaved thrombin species that an intact exosite I is essential for a number of thrombin functions such as fibrinogen clotting (1.5.1.), thrombomodulin-dependent protein C cleavage (1.2.9.) and platelet activation (1.4.1.). (See also (Bode et al., 1992; Stubbs and Bode, 1993), and references therein). The results of mutagenesis studies suggest that the exosite residues Arg73, Tyr76, Asn78, Lys81, Lys109 and Lys110 are particularly critical for fibrinogen recognition and cleavage, while Gln38, Arg75 and Tyr76 are essential for thrombin-thrombomodulin interactions (Hall et al., 1999; Tsiang et al., 1995; Wu et al., 1991). According to crystal structures of thrombin in complex with PAR1 peptides (Mathews et al., 1994), the N-terminal extracellular segment of the thrombin receptor seems to insert into the anion-binding exosite I at least up to residues Tyr76, Ile82 and Lys36. All these interaction sites might not be identical, but clearly overlap and include thrombin residues that are also in direct contact with triabin. Thus, triabin competes for identical exosite I residues with several macromolecular substrates and cofactors, explaining its inhibitory effect on fibrinogen cleavage, platelet stimulation, and TM-mediated protein C activation (Noeske-Jungblut et al., 1995). Contacting residues of thrombin's exosite I are well conserved in all mammalian thrombin species sequenced so far

(Banfield and MacGillivray, 1992); similar interactions are thus anticipated between triabin and human thrombin.

Considering the predominance of negatively over positively charged residues in triabin (12 glutamate and 11 aspartate residues oppose 12 lysine and 3 arginine residues, see Fig. 3.6) a large number of direct ion pairs had been anticipated, in particular participation of triabin residues harbored in segments with successive acidic residues. Surprisingly also in view of the overall complementarity of electrostatic potentials (compare Fig. 3.4a), most of the contacts in thrombin-triabin are made through hydrophobic side chains. The only important salt-bridge interactions are formed between Arg77A (thrombin) and the acidic side chains of Asp135I and Glu128I in triabin (see below). Besides this ion pair cluster, the oppositely charged residues of triabin and thrombin, respectively, will assist in binding through the complementarity of their overall electrostatic potentials. Most glutamate and aspartate residues flanking Asp135I (Glu121I, Asp122I, Asp133I, Asp137I and Glu140I; see Fig. 3.6) are directed away from the thrombin surface, however.

The larger "northern" region of the thrombin-triabin interface is essentially made by hydrophobic side chains such as Ile99I, Leu108I, Val126I and Phe106I (triabin), and the aliphatic side chains of Leu65 and Met84 (thrombin). Towards the periphery of this interface also a few polar residues form intermolecular contacts. For instance, the carboxylate of Glu9I (triabin) contacts the ammonium groups of Lys36 and Lys109. This northern interface region is separated by a water-filled notch and the Tyr76 side chain from a smaller and much more polar southern region, which is dominated by an intermolecular ion pair/hydrogen bond cluster. Here, the almost extended side chain of Arg77A (thrombin) fits into a rather hydrophobic triabin pocket, where its guanidinium group opposes the carboxylate group of Asp135I and forms symmetrical charged 2N-2O hydrogen bonds. These hydrogen-bonded salt bridges are fully shielded from the bulk solvent and thus presumably quite strong. Aside of this Arg77A guanidinium group, the carboxylate of Glu128I is suitably placed to make an additional charged Nε-Oε hydrogen bond, which, in contrast to the Arg77A–Asp135I bonds, is flanked by ordered solvent molecules and thus most probably not of comparable strength. Placed on top of the Arg77A

side chain and aside the carboxylate group of Glu128I, the Tyr76 side chain of thrombin is directed towards a water-filled pocket extending from the bulk water into the thrombin-inhibitor interface (Fig. 3.7). This Tyr76 phenol ring packs further against the hydrophobic chains of triabin residues Phe106I and Val126I (see Fig. 3.7). The side chains of Tyr76 and Arg77A together account for almost half of all atom-atom contacts below 4.0 Å made by the thrombin component.

3.6. Comparison With Other Proteinaceous Thrombin Inhibitors

As stated above (section 3.1.), thrombin is a common, and probably obligatory target for blood-sucking animals. The most prevalent thrombin inhibitors possess a characteristic two-domain architecture, in which the N-terminal domain occupies or blocks the active site cleft of the proteinase, while a markedly acidic C-terminal domain (or peptide) binds the basic fibrinogen-recognition exosite. This mode of inhibition was first identified in **hirudin** (Fig. 3.8a; Grütter et al., 1990; Rydel et al., 1990), a small ($M_r \approx 8$ kDa) polypeptide isolated from the leech *Hirudo medicinalis* (Markwardt, 1994; Walsmann and Markwardt, 1985). **Rhodniin**, a Kazal-type inhibitor isolated from the assassin bug *Rhodnius prolixus* (Fig. 3.8b; van de Locht et al., 1995), and the Kunitz-type inhibitor **ornithodorin** purified from the soft tick *Ornithodorus moubata* (Fig. 3.8c; van de Locht et al., 1996),) are double-headed inhibitors that contact both the active site and exosite I. (For a detailed discussion of protease-inhibitor families see reference (Bode and Huber, 1992)).

Fig. 3.8 (next page): Thrombin inhibition is achieved by proteins that possess unrelated folds. Ribbon plots of the thrombin complexes with the inhibitors hirudin, (**a**) (Grütter et al., 1990; Rydel et al., 1990); ornithodorin, (**b**) (van de Locht et al., 1996); rhodniin, (**c**) (van de Locht et al., 1995); and triabin, (**d**) ((Fuentes-Prior et al., 1997), this work). In contrast to triabin, hirudin, rhodniin and ornithodorin block both the active site and exosite I of thrombin. Notice also the preponderance of hydrophobic interactions in other thrombin-inhibitor complexes.

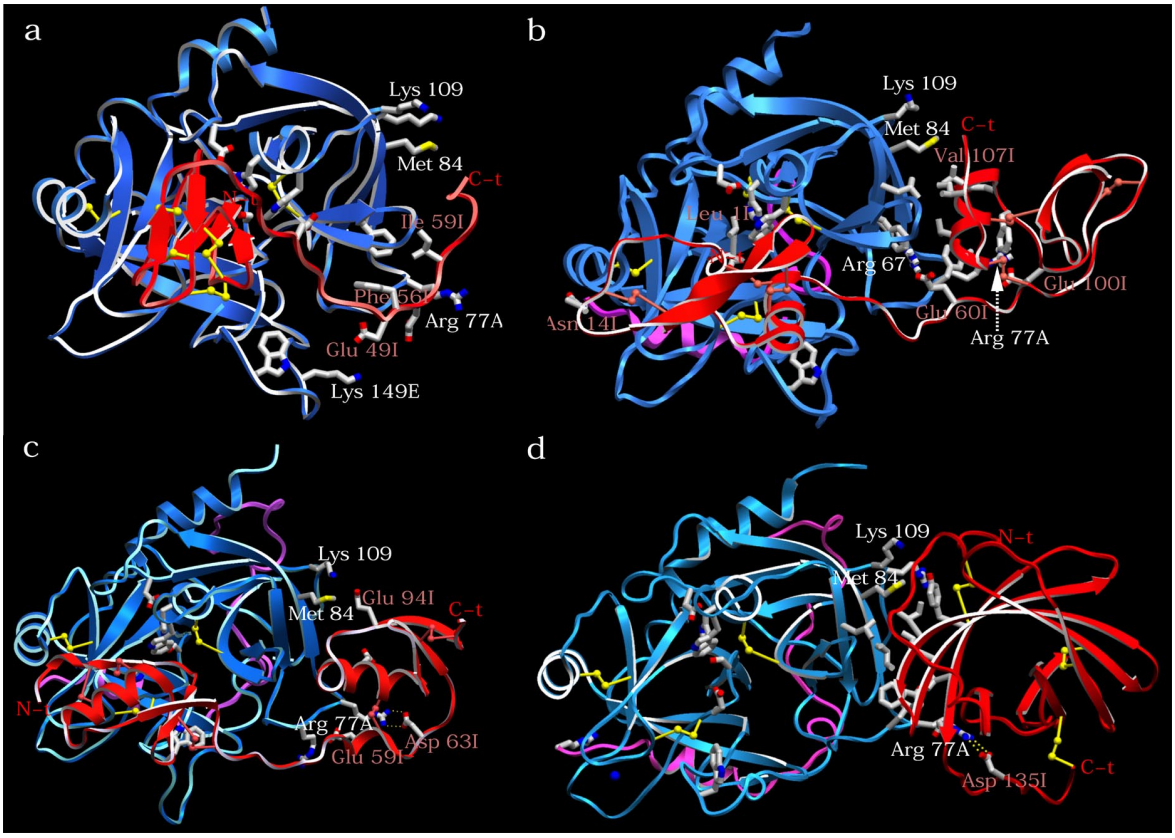

In marked contrast with these thrombin-specific protein inhibitors, triabin occupies exclusively the exosite I of thrombin, thus leaving the active site of the liganded enzyme free to act on small peptidic molecules. In the thrombin-triabin complex, thrombin utilizes similar surface regions as it does in the interactions with the second domains of the thrombin inhibitors rhodniin (van de Locht et al., 1995) and ornithodorin (van de Locht et al., 1996), which exhibit, however, quite different folds belonging to the Kazal- and the Kunitz inhibitor family, respectively (compare Figs 3.8b - 3.8d). Due to its much larger size (142 residues, compared with 48 and 58), however, triabin binds across a surface almost doubling that of rhodniin and ornithodorin, allowing several additional interactions (section 3.5., Figs 3.7, 3.8).

The low ratio of direct ion pairs at the thrombin-triabin interface is reminiscent of the exosite I interactions with the C-terminal tail/domains of hirudin (Grütter et al., 1990; Rydel et al., 1990) rhodniin (van de Locht et al., 1995), and ornithodorin (van de Locht et al., 1996), where also the majority of the oppositely charged residues are found to interact *via* their overall electrostatic potentials. The better adaptation of triabin to the architecture of thrombin's exosite I explains its nearly 500 times higher activity in platelet activation

assays, compared to the C-terminal hirudin tail, **hirugen** (Noeske-Jungblut et al., 1995).

3.7. Triabin Is a Distant Member of the Lipocalin Family

A search in the Swiss Prot data base conducted after elucidating the primary structure of triabin did not reveal any significant sequence homology with other proteins of known three-dimensional structure (Noeske-Jungblut et al., 1995). After determination of the three-dimensional crystal structure of triabin in its thrombin complex, we performed a systematic computer search against all protein structures deposited with the Protein Data Bank (Bernstein et al., 1977) using the program GDF3D (Lessel and Schomburg, 1994). Search parameters limited the maximal distance of matching Cα atoms to 1.8 Å for polypeptide stretches containing at least 6 residues. This search revealed a striking similarity between triabin and several structurally related but otherwise non-homologous transport proteins, such as **bilin binding protein** (BBP) from the insect *Pieris brassicae* (Huber et al., 1987), and the mammalian **retinol binding proteins** (RBP) (Newcomer et al., 1984; Zanotti et al., 1993).

The term **lipocalin** has been coined by D. Flower (Flower, 1996; Flower et al., 1993) to design this family of medium-sized proteins comprising an eight-stranded calyx-shaped β-barrel, which in all structurally characterized cases encloses an internal cavity suitable for binding small, usually hydrophobic molecules. Other typical representatives of this widespread family for which three-dimensional structures have been reported are the bovine **odorant-binding protein** (OBP) (Bianchet et al., 1996; Tegoni et al., 1996), rat **epididymal retinoic acid-binding protein** (E-RABP) (Newcomer, 1993), a pheromone-carrying protein isolated from the urine of mice and termed **major urinary protein** (MUP) (Bocskei et al., 1992) and the camouflage protein **insecticyanin** (Holden et al., 1987). Table 3.2 lists the structurally characterized lipocalins, and compares them to triabin. Ribbon plots of several lipocalins are presented in Fig. 3.9, highlighting the bound ligand.

Table 3.2: Comparison of Triabin With Other Members of the Lipocalin Family

Protein / Resolution (Å)	**Organism**	**Ligand**	**PDB Code**	**Residues / r.m.s.d. (Å)**	**Reference**
Bilin binding protein / 2.0	*Pieris brassicae*	Biliverdin IXγ	1BBP	66 / 1.18	(Huber et al., 1987)
Retinol binding protein / 2.5	*Homo sapiens* (plasma)	– / Retinol	1BRQ/ 1BRP	70 / 1.16	(Zanotti et al., 1993)
Retinol binding protein / 1.65	*Sus scrofa* (plasma)	Retinol	1AQB	70 / 1.13	(Zanotti et al., 1998)
Retinol binding protein / 1.9 (1.7)	*Bos taurus* (plasma)	Retinol	1HBP/ 1HBQ	70 / 1.15	(Zanotti et al., 1993)
E-RABP / 2.1	*Rattus norvegicus* (epididymis)	Retinoic acid	1EPB	66 / 1.15	(Newcomer, 1993)
Odorant binding protein / 2.0	*Bos taurus* (nasal mucosa)	Unidentified	1OBP	50 / 1.15	(Tegoni et al., 1996)
Odorant binding protein / 2.2	*Bos taurus* (nasal epithelium)	2-amino-4-butyl-5-propylselenazole	1PBO	51 / 1.24	(Bianchet et al., 1996)
Odorant binding protein / 2.25	*Sus scrofa* (nasal mucosa)	–	1A3Y	49 / 1.22	(Spinelli et al., 1998)
Major urinary protein / 2.4	*Mus musculus* (urine)	2-(sec-butyl) thiazoline	1MUP	57 / 1.13	(Bocskei et al., 1992)
Insecticyanin / 2.6	*Manduca sexta*	Biliverdin (γ isomer)	n.d.	– / –	(Holden et al., 1987)
β-Lactoglobulin / 2.5	*Bos taurus* (milk)	Palmitate	1B0O	60 / 1.12	(Wu et al., 1999)
β-Lactoglobulin / 1.8	*Bos taurus* (milk)	–	1BEB	60 / 1.24	(Brownlow et al., 1997)
Allergen Bos d 2 / 1.8	*Bos taurus* (recombinant)	None (Indan?)	1BJ7	41 / 1.34	(Rouvinen et al., 1999)
NGAL / n.a. (NMR)	*Homo sapiens* (recombinant)	None	1NGL	45 / 1.24	(Coles et al., 1999)
Nitrophorin 1 / 2.0	*Rhodnius prolixus* (recombinant)	Heme + histamine	1NP1	87 / 1.24	(Weichsel et al., 1998)
Nitrophorin 4 / 1.5	*Rhodnius prolixus* (recombinant)	Heme + NH_3	1NP4	85 / 1.24	(Andersen et al., 1998)
Nitrophorin 1 / 2.0	*Rhodnius prolixus* (recombinant)	Heme + NH_4	2NP1	84 / 1.22	(Weichsel et al., 1998)
Nitrophorin 1 / 2.3	*Rhodnius prolixus* (recombinant)	Heme + cyanid	3NP1	87 / 1.25	(Weichsel et al., 1998)
Nitrophorin 1 / 2.3	*Rhodnius prolixus* (recombinant)	Heme + NO	4NP1	85 / 1.24	(Ding et al., 1999)

E-RABP, epididymal retinoic acid binding protein; NGAL, neutrophil gelatinase associated lipocalin

Fig. 3.9 (next page): Comparison of triabin with other members of the lipocalin family. The three-dimensional structures of triabin (**a**); nitrophorin 1, (**b**); retinol-binding protein (**c**), bilin-binding protein, (**d**); the murine major urinary protein (**e**); and the horse allergen (**f**) are presented at the same magnification. The corresponding ligands are labeled. Notice also the pair of conserved residues in strands β_A (a tryptophan residue) and β_H (a positively charged residue, usually arginine).

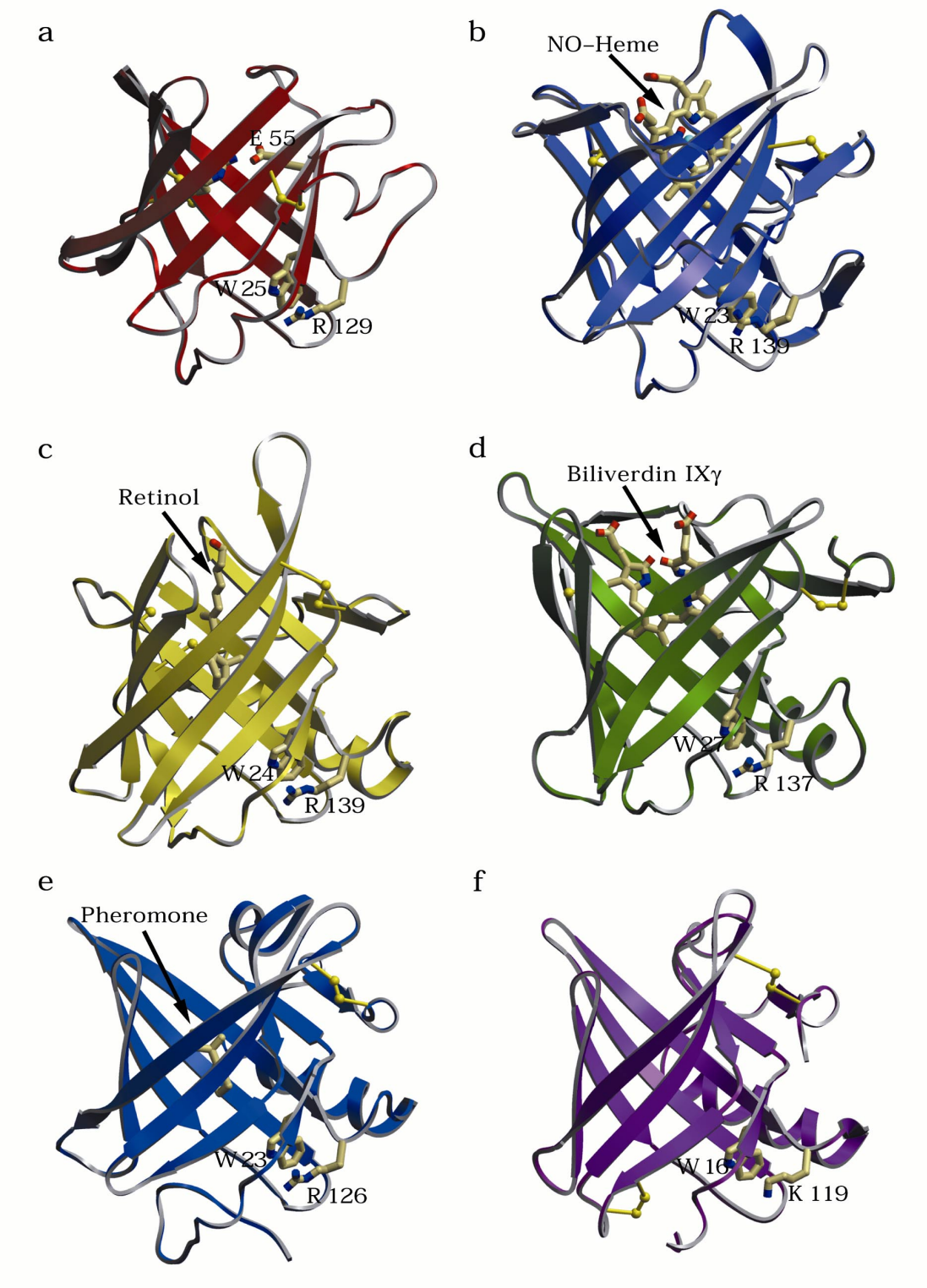

In contrast to triabin, however, the eight β-strands of all these "classical" lipocalins are arranged in an "up-and-down" manner, thus with adjacent strands aligned antiparallel to one another. In spite of this structural divergence, about half of all Cα atoms of triabin occupy positions within 2.0 Å distance of equivalent Cα atoms of lipocalins, with r.m.s. deviations of about 1.2 Å (Table 3.2). This structural similarity is evident in Fig. 3.10, showing a superposition of

the Cα traces of triabin and bilin-binding protein. All eight triabin β-strands (neglecting strand directions) and most of the N-terminal segment superimpose astonishingly well. Strands β_B and β_C, although interchanged, also have very similar curvatures, as emphasized by the fact that eleven Cα atoms of these strands can be superimposed (Figs 3.10 and 3.11).

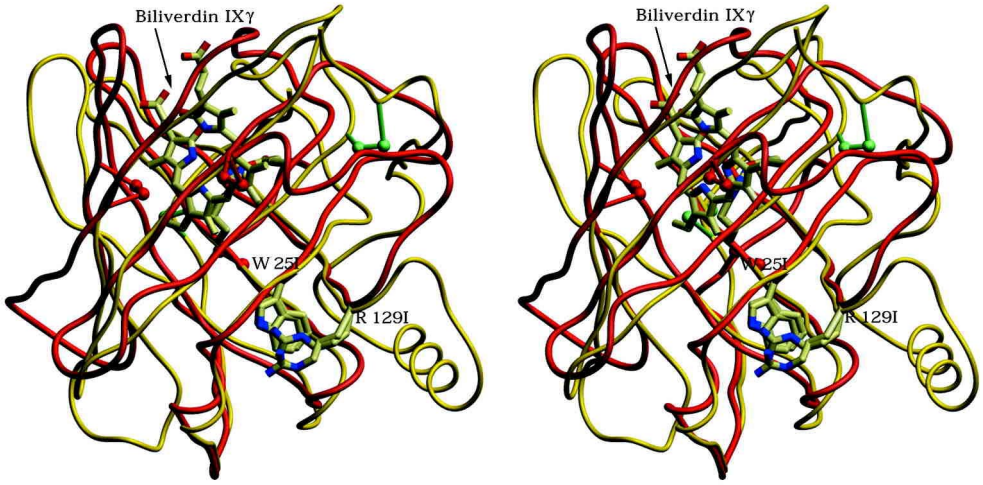

Fig. 3.10: Triabin and the bilin-binding protein are structurally related. Stereo view of the structures of triabin (red) and of the bilin-binding protein (yellow, disulfide bridges in green). The bound pigment (biliverdin IXγ, color-coded) is presented to indicate the cavity in the ligand binding lipocalins. Notice the close superposition of the side chains of equivalent residues Trp25I (Trp27 in the bilin-binding protein) and Arg129I (Arg137).

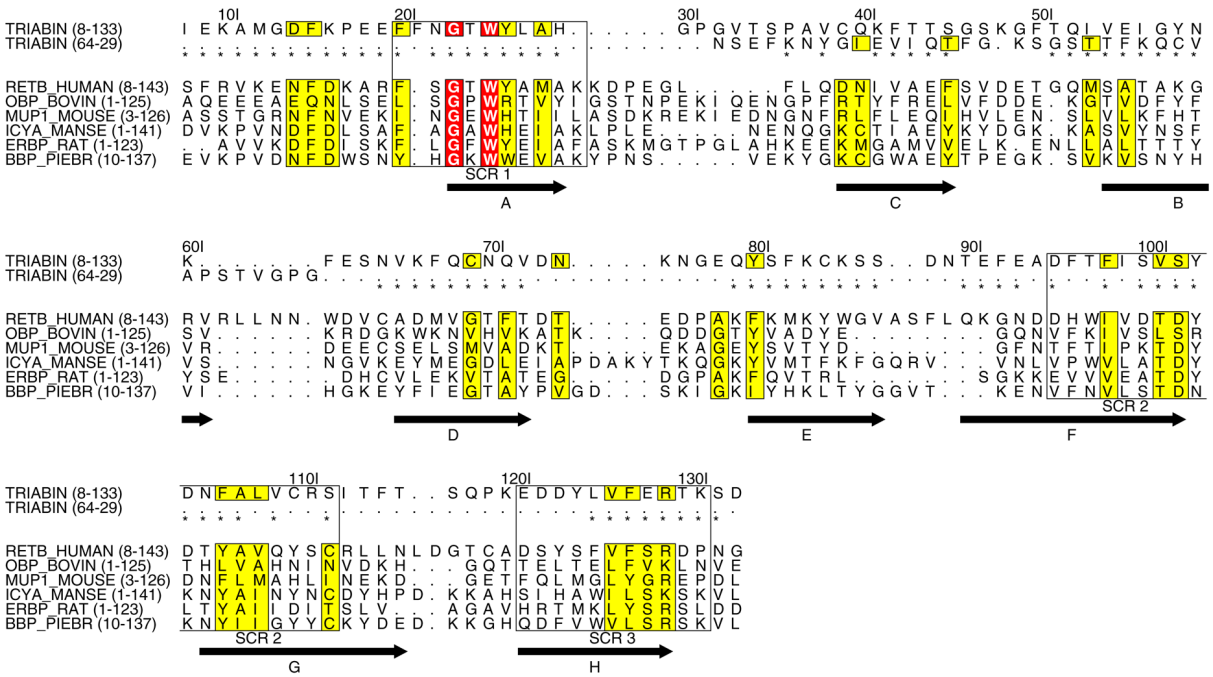

Fig. 3.11 (previous page): Structure-based alignment of the amino acid sequences of triabin and of several lipocalins of known three-dimensional structure: retinol binding protein (RETB_HUMAN; Newcomer et al., 1984; Zanotti et al., 1993), odorant binding protein (OBP_BOVIN; Bianchet et al., 1996; Tegoni et al., 1996), major urinary protein (MUP1_MOUSE; Bocskei et al., 1992), insecticyanin (ICYA_MANSE; Holden et al., 1987), retinoic acid binding protein (ERBP_RAT; Newcomer, 1993) and bilin binding protein (BBP_PIER; Huber et al., 1987). The three major structurally conserved regions (SCRs 1–3) are indicated. Numbers refer to the triabin sequence. Topologically equivalent residues between triabin and retinol binding protein are indicated by asterisks. Note that they correspond to the 'reversed' sequence for residues 29I to 64I. The aligned sequences were formatted with ALSCRIPT (Barton, 1993).

The similarity between triabin and the "classical" lipocalins is not restricted to the overall appearance of the barrel, but extends also to single residues such as the Asp14I-Phe15I pair positioned at the entrance to helix h1, and the adjacent Phe20I. Both phenylalanine side chains are part of the "front" barrel lid (see Fig. 3.5). Strand β_A, as in all other crystallographically studied lipocalins, starts with a strictly conserved **Gly**-Xaa-**Trp** motif, followed by an aromatic residue. The first residue in this motif exhibits a high energy main chain conformation (Θ=+67°, Ψ=–151° in triabin), usually confined to glycine residues, while the indole side chain of Trp25I is packed in the interior of the barrel, with its indole ring shielded from bulk water by the side chain of a positively charged residue (usually arginine, compare Figs 3.10 and 3.11). Furthermore, the last four barrel strands β_E to β_H of triabin also share several common sequence motifs with the lipocalins (Fig. 3.11).

In summary, the closest similarities are observed for three regions that had previously been found to be particularly conserved in lipocalins, and had therefore been termed **structurally conserved regions** (SCRs) (Flower, 1996; Flower et al., 1993). These regions comprise helix h1 and strand β_A (SCR1), most of strands β_F and β_G (SCR2), while SCR3 comprises essentially strand β_H (Fig. 3.11).

As expected, the loops connecting the β-strands show greater differences. The large β_A/β_B loop forms half of the wall surrounding the entrance to the internal cavities in the "classical" lipocalins, and is accordingly most variable among them (compare Fig. 3.11). In triabin, the β_G/β_H loop folds over the "back" opening of the barrel, forming together with the side chains of His29I (β_A/β_B loop),

and Tyr58I, Lys60I and Phe61I (β_C/β_D loop), a lid covering triabin's internal core. The equivalent barrel side in the ligand-binding lipocalins is open and represents the entrance to the internal binding cavities (Figs 3.9 and 3.10). Also the C-terminal segment of triabin deviates strongly from the standard lipocalin fold. Lack of a 3½ turn α-helix, as well as of an additional C-terminal β-strand present in most lipocalins, essentially accounts for the lower molecular weight of triabin (142 residues) compared with the classical lipocalins (from 160 to more than 190 residues, compare Table 3.2). In lipocalins such as bilin-binding protein the long C-terminal helix covers the outer face of strands β_F-β_G-β_H, while the corresponding surface of triabin is a major part of the site of interaction with thrombin (Fig. 3.7). In spite of the considerable topological similarity, the sequence identity between triabin and lipocalins such as the bilin- or retinol-binding proteins is rather low. As shown in Fig. 3.10 and Table 3.2, about 20% of all amino acid residues occupying topologically equivalent strand positions are identical in triabin-BBP or triabin-RBP pairs. This value is only slightly lower than the residue identity between the two transport proteins, but still too low to be statistically significant on its own.

In summary, triabin notably differs from the ligand-binding lipocalins (for which three-dimensional information is available) by the topological interchange of strands β_B and β_C (what is compulsorily connected with a different organization of the adjacent β_A/β_B and β_C/β_D loops), the lack of an internal cavity, and a much shorter C-terminal segment. Such a strand interchange, accompanied by the filling out of the internal cavity and shortening and remodeling of the long C-terminal segment during evolution, is conceivable (see below).

The barrel surface which is placed roughly opposite to the cavity entrance in transport lipocalins has been suggested to represent the receptor binding site and/or a macromolecular interaction site in some lipocalins (Flower et al., 1993). Thus, triabin might represent the first member of a new lipocalin sub-class, for which this protein recognition site is known in atomic detail. Whether the counterparts of this thrombin-recognition surface in other lipocalins are, at least partially, involved in receptor binding or in other macromolecular interactions, is an attractive hypothesis that could be tested by structural and/or site-directed mutagenesis investigations of the corresponding proteins.

3.8. A Putative Evolutionary Mechanism Converting a Small-Ligand Binding Protein Into a Thrombin Inhibitor

Hematophageous animals employ various mechanisms to interfere with the blood coagulation system of their hosts. Isolation and sequencing of several antihemostatic lipocalins from blood-sucking insects (Table 3.3), and in particular two recent structural investigations lend extraordinary support to the hypothesis that triabin's topological similarity with the lipocalins is more than casual. Indeed, the combination of sequence conservation and functional reciprocity strongly suggests that triabin has evolved from a common lipocalin ancestor by divergent evolution.

The assassin bug *Rhodnius prolixus* possesses several isoforms of a unique group of **n**itric **o**xide (NO)-carriers termed **nitrophorins** (NPs) (Ribeiro et al., 1993). Three major activities ascribed to this heme-containing protein assist in blood feeding (Table 3.3). First, nitrophorins store NO in the insect saliva over large periods of time. Binding is reversible, and at the higher pH of their victim's blood, NO is released and acts as a potent vasodilator by stimulating soluble **guanylate cyclase** to produce cyclic GMP. (For recent reviews on the NO/cGMP signaling pathway see (Denninger and Marletta, 1999; Koesling and Friebe, 1999)). The now ligand-free lipocalin binds tightly to another second messenger released by mast cells in response to tissue damage, **histamine**. Histamine signals the endothelial cells of the capillary walls to allow platelets and cells of the immune system to pass from the blood into the damaged tissue, resulting in local inflammation and the onset of wound healing. (For a recent review see (Mannaioni et al., 1997)). Histamine sequestering by nitrophorins reduces thus the anti-inflammatory response of the bug's victims. Finally, one of the nitrophorin isoforms (NP2, also known as **prolixin S**) functions as an anti-clotting factor in a mechanism that does not require heme (Ribeiro et al., 1995; Sun et al., 1996), but appears to rely on the tight binding to the calcium-bound Gla domain of factor IX / IXa (Isawa et al., 2000; Zhang et al., 1998) (compare section 1.2.1.). The group of W. Montfort has made a detailed structural characterization of the most abundant nitrophorin, NP1 (Ribeiro and Walker, 1994), including structures of the cyanogen (CN)- and histamine-bound protein (Andersen et al., 1998; Weichsel et al., 1998) (see also Fig. 3.9b).

In the tick *Rhipicephalus appendiculatus*, three closely related **h**istamine-**b**inding **p**roteins (HBP1-3) have been identified. The high resolution crystal structure of HPB2 revealed also in this case a lipocalin-like fold, although with several unique features like an extended N-terminal peptide that is hydrogen-bonded to strands β_F and β_G (Paesen et al., 1999). Despite the conserved fold and the presence of a common ligand (histamine, but there are two histamine-binding sites in HBP2), these novel histamine binding proteins and the nitrophorins lack any sequence homology.

Another antihemostatic protein isolated from the saliva of *T. pallidipennis* is a potent inhibitor of the collagen-induced platelet aggregation termed **pallidipin** (Noeske-Jungblut et al., 1994). Pallidipin displays a fairly high degree (about 45%) of sequence similarity with triabin (Fig. 3.12). Interestingly, other inhibitors of platelet aggregation have recently been identified in *R. prolixus*, but seem to act as ADP scavengers and do not interact with collagen receptors such as $\alpha_2\beta_1$ (GP Ia-IIa) or GP VI (Francischetti et al., 2000) (see also section 1.4.2.). These inhibitors have been termed RPAIs (from ***R***. ***p****rolixus* **a**ggregation **i**nhibitors) and possess a slightly higher similarity to triabin than the 'own' pallidipin from *T. pallidipennis* (Fig. 3.12).

Table 3.3: Salivary Antihemostatic Lipocalins

Protein	Insect	M_r (kDa)	Amino acids	Activity	References
Triabin	*Triatoma pallidipennis*	21.0	142	Thrombin inhibition	(Fuentes-Prior et al., 1997; Noeske-Jungblut et al., 1995)
Pallidipin	*T. pallidipennis*	19.0	170–171	Inhibition of collagen-mediated platelet aggregation	(Noeske-Jungblut et al., 1994)
Nitrophorins 1-4	*Rhodnius prolixus*	~20.0	179–184	NO transport (vasodilator); histamine binding (anti-inflammatory)	(Champagne et al., 1995; Ribeiro et al., 1993)
Nitrophorin 2 (Prolixin-S)	*R. prolixus*	19.7	179	Inhibition of intrinsic Xase complex.	(Ribeiro et al., 1995; Sun et al., 1996)
RPAI 1, 2a, 2b	*R. prolixus*	19.0	155–157	Inhibition of ADP-mediated platelet aggregation.	(Francischetti et al., 2000)
HBP 1-3	*Rhipiceppalus appendiculatus*	20.0–25.0	171–176	Histamine binding (reduced inflammation and immune response).	(Paesen et al., 1999)
Moubatin	*Ornithodorus moubata*	17.5	156	Inhibition of collagen-induced platelet aggregation.	(Keller et al., 1993; Waxman and Connolly, 1993)

In contrast with triabin, all other antihemostatic lipocalins possess an extended C-terminus, similar to that of other transport lipocalins. Sequence comparisons also suggest that pallidipin and the RPAIs conserve the "classical"

up-and-down organization of β-strands β_A-β_D. For instance, with the exception of the (partially surface exposed) His29I, the residues involved in the internal hydrogen-bonding network in triabin are not conserved in other cases (Fig. 3.12).

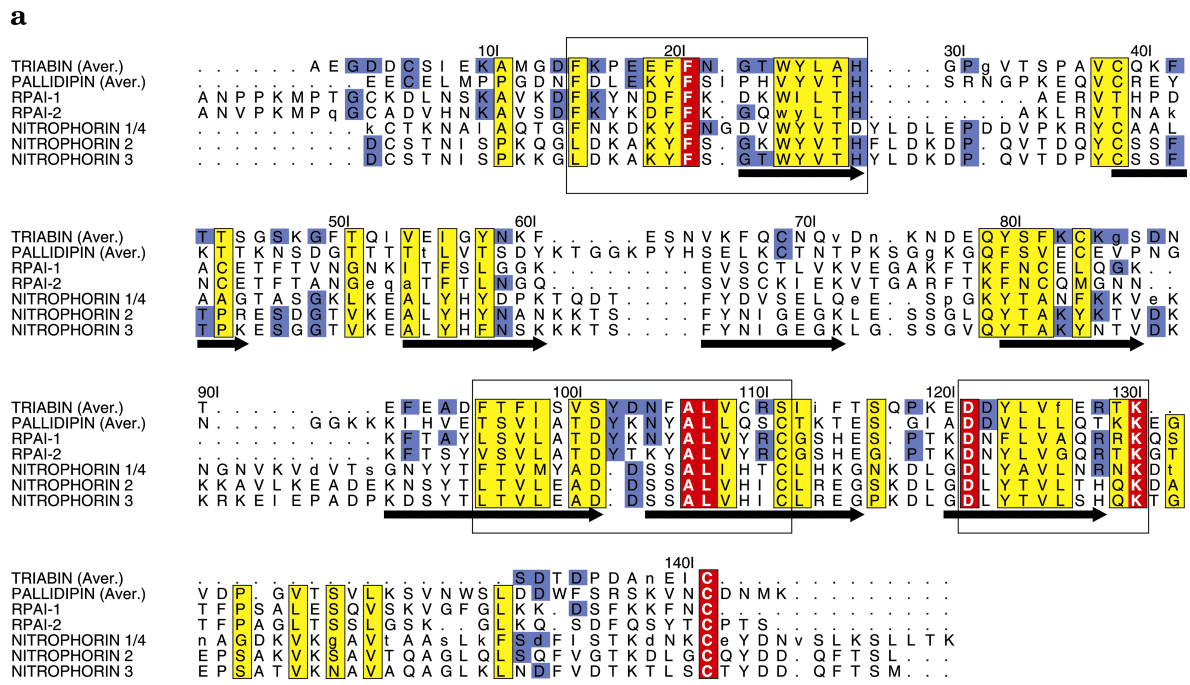

Fig. 3.12: Sequence alignment of several lipocalin-like antihemostatic proteins. "Average" protein sequences are given for the *Triatoma pallidipennis* inhibitors triabin (four variants) and pallidipin (two variants), for nitrophorins 1 and 4, as well as for *Rhodnius prolixus* aggregation inhibitors RPAI-2a and -2b (lower case letters indicate variation within the particular protein). The sequences of nitrophorin 2 (prolixin S), nitrophorin 3 and RPAI-1 are also included in this alignment. The structural conserved regions are boxed.

Considering the extreme low sequence homology between the histamine-binding proteins from *R. prolixus* (nitrophorins) and *Rhipicephalus appendiculatus* (Paesen et al., 1999), which is typical of the lipocalin family (Flower et al., 1993) (Fig. 3.11), the relatively high degree of sequence conservation between triabin, pallidipin, RPAIs and nitrophorins (compare Figs 3.11 and 3.12) strongly suggests that these proteins have only recently diverged from a common ancestor. We propose that these inhibitors might be grouped together as a subfamily within the lipocalin family. However, the still low sequence homology within this subfamily does not allow to discriminate between two alternative evolutionary mechanisms: either sequential or parallel evolution from the heme-carrying nitrophorins into an ADP-binding protein (RPAI) and an

integrin-binding protein (pallidipin), and finally into a thrombin inhibitor, triabin.

3.9. Conclusions

Triabin, a 142-residue protein isolated from the triatomine bug *Triatoma pallidipennis*, is a potent and selective thrombin inhibitor. Its stoichiometric complex with bovine α-thrombin was crystallized, and the crystal structure was solved by Patterson search methods and refined at 2.6 Å resolution to an R-value of 0.184. The structural analysis revealed that triabin is a compact single-domain molecule essentially consisting of an eight-stranded β-barrel. The eight strands β_A to β_H are arranged in the order β_A-β_C-β_B-β_D-β_E-β_F-β_G-β_H, thus with the first four strands exhibiting a unusual up-up-down-down topology. Except for the β_B-β_C inversion, the triabin fold exhibits the regular up-and-down topology of the transport proteins called lipocalins. In contrast to the typical ligand-binding lipocalins, however, the triabin barrel encloses a hydrophobic core intersected by a unique salt-bridge cluster.

Triabin interacts with thrombin exclusively *via* the fibrinogen-recognition exosite. Surprisingly, most of the interface interactions are hydrophobic. A prominent exception represents thrombin's Arg77A side chain, which extends into a hydrophobic triabin pocket forming partially buried salt bridges with Glu128 and Asp135 of the inhibitor. The fully accessible active site of thrombin in this complex is in agreement with its retained hydrolytic activity towards small chromogenic substrates. The faint, but measurable fibrinogen clotting activity of the triabin-thrombin complex in the presence of excess triabin might indicate that docking of fibrinogen to thrombin does not occur as a rigid body encounter, but exhibits some degree of flexibility. Impairment of thrombin's fibrinogen clotting activity or of its thrombomodulin-mediated protein C activation capacity upon triabin binding is explained by the occupation of overlapping interaction sites of fibrinogen, thrombomodulin and triabin on thrombin.

Chapter 4
Structural Basis for the Anticoagulant Activity of Thrombomodulin-Bound Thrombin:
Crystal Structure of the Human α-Thrombin-TME456 Complex

4.1. Three Consecutive EGF-Like Domains of Thrombomodulin Confers Protein C Cofactor Activity to Bound Thrombin

The delicate balance between procoagulant and anticoagulant states depends critically upon the diverse proteolytic activities of the serine proteinase α-thrombin (section 1.2.5.; Bode et al., 1989; Bode et al., 1992; Stubbs and Bode, 1993) (see also Fig. 1.1). Free α-thrombin is the primary promoter of blood clotting through limited proteolysis of fibrinogen (1.5.1.), platelet receptors (1.4.1.) and factors V and VIII (1.3.4., 1.3.5.). Upon binding to the endothelial receptor thrombomodulin (TM, section 1.2.9.), the procoagulant activities of thrombin are drastically impaired, and it becomes anticoagulant by activating protein C (1.2.9.) and antifibrinolytic by activating the procarboxypeptidase TAFI (1.5.3.).

Thrombomodulin has been the subject of several independent biochemical and mutagenesis studies, which have established the functional roles played by individual domains. The N-terminal lectin domain (residues Ala1 to Ala155) has been proposed to regulate constitutive internalization (Conway et al., 1997). The serine/threonine-rich peptide Ser464–Ser497 acts as a spacer to correctly position the thrombin-binding site above the membrane (Tsiang et al., 1992). The cytoplasmic tail contains potential sites for threonine and tyrosine phosphorylation (Dittman et al., 1988), and a single cysteine that may mediate multimerization of the molecule (Conway et al., 1994). However, no functional role has been ascribed to this region. The TME56 tandem alone binds thrombin tightly but has no cofactor activity and acts as a competitive inhibitor for protein C activation (K_i = 8.6 ± 1.4 nM) (Kurosawa et al., 1988). (The six EGF domains of thrombomodulin will be termed TME1 to –6 in this work). Deletion mutants lacking 6, 16, and 38 residues from the C-terminus of TME6 possess only 9.4, 1.4, and 1.1% residual activator activity, respectively (Honda et al., 1995). The smallest soluble TM fragment retaining full PC cofactor activity is the structure formed by the three C-terminal EGF-like repeats, TME456 (Stearns et al., 1989; Zushi et al., 1989). TME456 also stimulates the inactivation of TM-bound thrombin by the protein C inhibitor, PCI (Rezaie et al., 1995). The thrombin-

catalyzed activation of TAFI requires the additional presence of TME3 (Kokame et al., 1998).

4.2. Structure Determination

4.2.1. Preparation of Proteins

The Val345–Cys462 fragment of human TM (with residues Arg456 and His457 mutated to Gly and Gln and the N-terminus extended by a Phe-Pro dipeptide) was expressed in CHO cells. This truncated form thus contain the three C-terminal EGF-like repeats of TM, along with the residues of the linker between TME3 and TME4. After anion-exchange chromatography (Clarke et al., 1993), the minor glycoform *N*-glycosylated at Asn364 was further purified on a C4 column using an acetonitrile gradient in 0.1% TFA. This fraction was treated with recombinant N-glycosidase F (Boehringer Mannheim, Germany) and the carbohydrate-free Asp364 analogue (in following also termed TME456) was purified by RP-HPLC and lyophilized as the TFA-salt. This work was done by Galina Rumennik and Rene Pagila under the supervision of Dr. David R. Light, Berlex Biosciences (Richmond, CA). Human α-thrombin was purified from frozen plasma according to standard procedures and irreversibly inhibited with an excess of L-Glu-Gly-Arg chloromethyl ketone (EGR-CMK) (Bachem, Germany) for one hour at room temperature.

4.2.2. Complex Formation, Crystallization and Data Collection

Lyophilized TME456 was dissolved in 10 mM Na-Hepes (pH 7.5), 20 mM NaCl, 2 mM $CaCl_2$ and added to the thrombin solution. Formation of the stoichiometric complex was confirmed by native gel electrophoresis. The complex was crystallized by vapor-diffusion techniques from solutions of 0.1 M sodium acetate (pH 4.6), 1.8 M sodium formate, 2 mM calcium chloride. The cubic shaped crystals grow to maximal dimensions of 0.2x0.2x0.2 mm^3, belong to the space group R3 (cell constants: a=b=214.40 Å, c=131.41 Å) and contain four molecules in the asymmetric unit. A single crystal was transferred to a solution of mother liquor containing 22.5% (v/v) glycerol, cooled down in a nitrogen stream and measured using synchrotron radiation (λ=1.105 Å) at the beam line BW6 (DESY, Hamburg). Diffraction data (99.7% complete to 2.28 Å resolution) were evaluated with MOSFLM (Leslie, 1991) and scaled and reduced with programs supported

by the Collaborative Computational Project No. 4 (Collaborative Computational Project No. 4, 1994), yielding 99,777 independent reflections in the 43.80-2.30 Å resolution range, with an R_{merge} of 6.4% (16.9% in the 2.42–2.30 Å shell).

4.2.3. Phasing and Refinement

A truncated model of α-thrombin derived from the thrombin-PPACK structure (Bode et al., 1989) and X-ray data from 15.0 to 3.5 Å were used for Patterson search with AMoRe (Navaza, 1994), yielding four independent solutions with a final correlation factor of 43.9% and an R-factor of 42.4% (values for the next best solution: 29.1% and 47.0%). The appropriately placed thrombin models were used for the generation of the initial phases. The straightforward interpretable density allowed completion of the thrombin model with MAIN (URL:http://www-bmb.ijs.si/doc) (Turk, 1992) (including the bound ERG-CMK moiety), and revealed strong additional density accounting for the bound TME5 fragment. Model building was followed by refinement using X-PLOR (Brünger, 1987; Brünger, 1993). This procedure was repeated several times until the whole TME456 sequence had been fitted to the density. The structure has been refined with X-PLOR to an R-factor of 19.6% (R_{free} 24.0%) using 98,582 independent reflections in the 10.0-2.3 Å resolution range. The polypeptide chain is defined except for residues Ile14K–Arg15 and Thr147–Lys149E (thrombin) as well as the N-terminus and residues Gly449(Pro450)–Ile454 in TME456. All non-glycine residues fall into most favored (85.5%) or additionally allowed (14.5%) regions of the Ramachandran plot.

4.3. Overall Structure of the Thrombin-TME456 Complex

Crystals contain four independent complexes of L-Glu-Gly-Arg chloromethyl ketone (EGR-CMK) inhibited thrombin and TME456 per asymmetric unit. Three of this complexes are related by a local rotation axis, while the fourth is loosely attached to this trimer (Fig. 4.1). In spite of the different crystal environments, all four crystallographically independent complexes exhibit almost identical structures, which are thus unaffected by crystal contacts. The following descriptions apply thus to all four complexes. Each consists of an ellipsoidal α-thrombin molecule and an angular Y-shaped TME456 fragment (Figs 4.1 and 4.2). The lower edge of the elongated 'left arm' of the Y, formed by domains

TME5 and TME6, binds to thrombin's anion-binding exosite I, in agreement with previous evidence from mutagenesis (Hall et al., 1999; Tsiang et al., 1995; Wu et al., 1991) and other biochemical studies (Lougheed et al., 1995; Tsiang et al., 1990). Occupancy of this region by TME56 prevents binding of procoagulant substrates (e.g., fibrinogen, PARs), explaining their impaired cleavage by TM-bound thrombin. Contrary to expectations, however, TME4 and much of TME6 protrude from the thrombin surface stretching into the bulk solvent (Fig. 4.2).

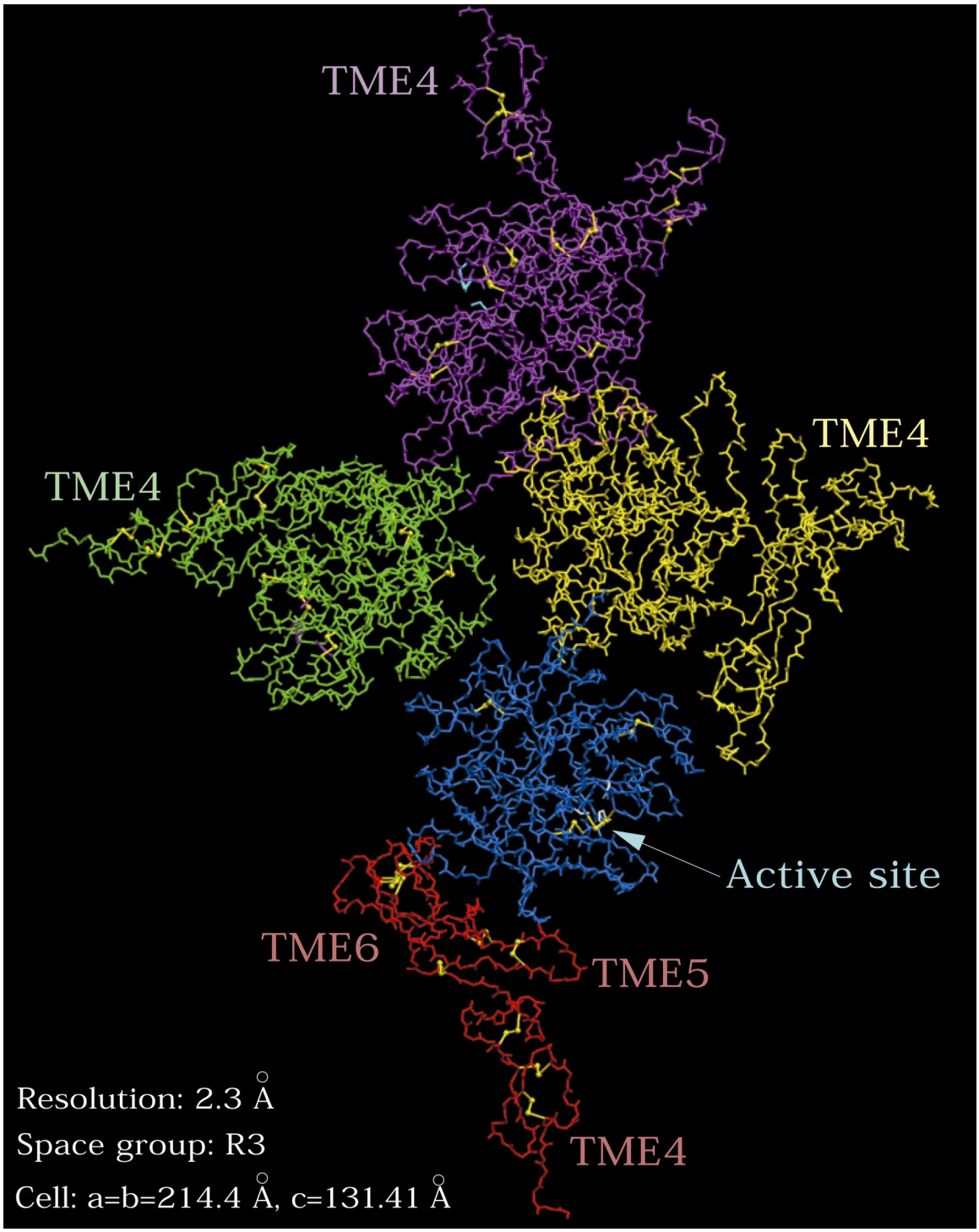

Fig. 4.1 (previous page): Crystal structure of the thrombin-TME456 complex. Notice that the N-terminal domain TME4 protrude in all cases from the main body of the macromolecular complex.

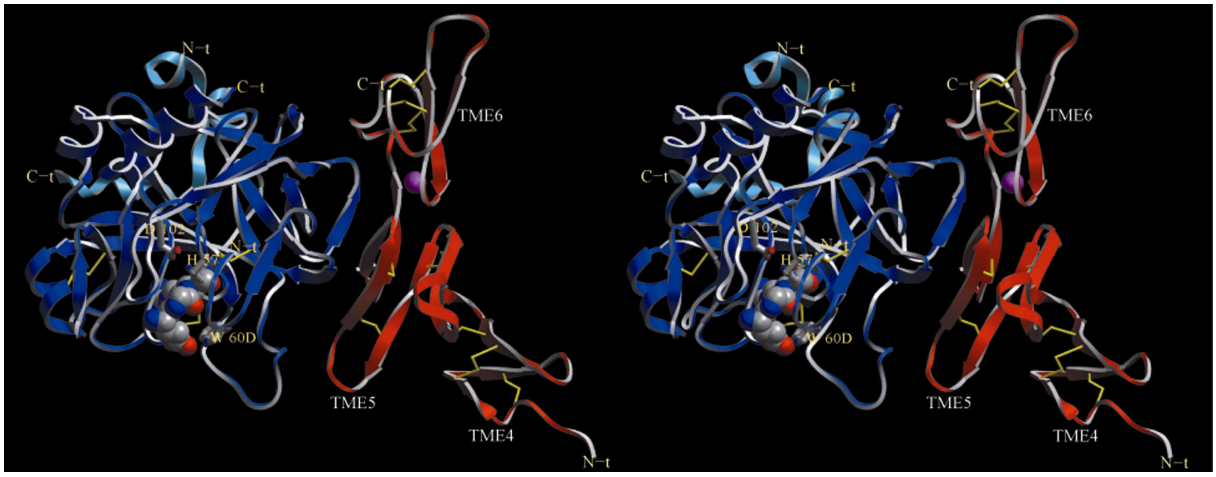

Fig. 4.2: Overall structure of the human thrombin-TME456 complex. Ribbon model of the complex between α-thrombin (light and heavy chains are colored light and dark blue, respectively) and TME456 (red). The irreversible inhibitor L-Glu-Gly-Arg chloromethyl ketone (EGR-CMK) mimics the protein C activation peptide and is shown as a space-filling model with atoms color-coded (carbon, gray; nitrogen, blue; oxygen, red). The disulfide linkages are shown in yellow. N- and C-termini of all three chains are labeled. The side chains of active site residues His57 and Asp102 as well as Trp60D are explicitly shown. The buried calcium ion (TME6) is shown as a pink sphere.

4.4. Absence of Allosteric Effects in Thrombin

The current dogma regarding the mechanism of activation of protein C asserts that thrombomodulin binding induces conformational rearrangements in the active site of thrombin to accommodate a non-optimal substrate such as the activation peptide of protein C (Fig. 1.11). In addition to the general evidence indicating allosteric modulation of thrombin upon binding to either exosite (section 1.2.5.1.), there is specific experimental data concerning the modulation of thrombin upon thrombomodulin binding.

(1) The thrombin mutant Glu39→Lys retains similar P1, P2 and P3 specificities against peptide substrates but altered P3' and/or P4' specificities (Le Bonniec et al., 1991). However, protein C activation by free E39K thrombin is enhanced only 2.2-fold, and the rate for TM-mediated activation is unchanged. Nevertheless, authors concluded from the kinetics of peptide cleavage that TM

may function in part by alleviating the electrostatic repulsion between Asp18 (P3') in PC and thrombin's Glu39.

(2) Substitution Glu192→Gln in thrombin has been claimed to mimic the catalytic switch induced by thrombomodulin (Le Bonniec and Esmon, 1991). Indeed, compared to thrombin the E192Q mutant activates protein C 22 times more rapidly and also cleaves the Glu9 (P7) – Lys20 (P5') peptide from the activation site 19 times faster. Furthermore, the Kunitz–type inhibitor BPTI becomes a potent inhibitor of the mutant form ($K_i \approx 10^{-8}$ M), while wild-type thrombin is poorly inhibited by BPTI (Rezaie et al., 1998). The crystal structure of the (E192Q)thrombin-BPTI complex revealed that binding of the inhibitor is accompanied by a drastic rearrangement in thrombin's 60-loop, with all Cα atoms deviating from the thrombin-PPACK structure (maximal deviation: 8 Å for the Cα atom of Trp60D) (van de Locht et al., 1997). Concomitant displacements of neighboring 37-, 99- and 149-loops were also observed. On the other hand, the Glu192→Gln mutation does not influence fibrinopeptide A release and only increases the rate of fibrinopeptide B release 2.7-fold (Le Bonniec and Esmon, 1991). Authors concluded that TM may function in part by altering the conformation of Glu192 and alleviating the inhibitory interactions with aspartates at positions P3 and P3'.

(3) Substitution of Glu217 by alanine results in a thrombin form that substantially shifts thrombin's specificity in favor of the anticoagulant substrate, protein C (Gibbs et al., 1995). However, this change in specificity does not result from an improvement in protein C activator activity, but from a poor processing of fibrinogen. Along the same line, the Glu217→Lys mutant shifted the specificity thrombin by over 130-fold to favor activation of protein C over fibrinogen cleavage (Tsiang et al., 1996).

(4) An investigation performed using fluorosulfonyl spin-label inhibitors provided evidence for multiple conformations in the active center of thrombin induced upon complex formation with thrombomodulin (Musci et al., 1988). Also fluorescence probes bound to active site residues Ser195 or His57 show spectral changes upon thrombomodulin binding, which are saturable and reach a maximum at 1:1 stoichiometry (Ye et al., 1991).

Also along these lines,

(5) Thrombin inactivation rates by the serpin PAI-1 (1.5.5.) are improved 50-fold and 31-fold by mutants E39K and E192Q, respectively. The inactivation rate of the double mutant was improved 628-fold over wild-type thrombin, indicating that repulsive interactions and/or lack of productive electrostatic interactions between and Glu39 and Glu192 of thrombin are responsible for the slow reaction of thrombin with this serpin (Rezaie, 1998).

In contrast to the general expectations, in the TM456-thrombin complex the main chain of thrombin departs only slightly from the over one-hundred reported thrombin structures. This point is illustrated in Fig. 4.3 by comparing thrombin in the TM complex with bovine thrombin bound to the exosite I inhibitor triabin (Figs 3.3a and 4.3a; Fuentes-Prior et al., 1997) or with the prototypical D-Phe-Pro-Arg chloromethyl ketone (PPACK)-inhibited thrombin structure (Fig. 4.3b; Bode et al., 1989; Bode et al., 1992). In both cases, the maximal root-mean-square deviations are below 0.60 Å for more than 280 Cα pairs. This high degree of structural conservation applies also to the active-site residues of thrombin and the surrounding acidic residues Glu217, Glu192 and Glu39, which have identified as possible candidates to explain the thrombomodulin-mediated conversion of thrombin to an anticoagulant proteinase (see above). Displacements are restricted to the prominent 60-loop, whose exposed Tyr60A-Trp60D bulge pulls up to 1.7 Å away from the active site compared to PPACK-thrombin (up to 2.6 Å in case of the triabin complex) (Fig. 4.3). The nearby 37- and 96-loops diverge even less, while the 149-loop is disordered in TM-bound thrombin, as frequently observed.

These small conformational differences are comparable to those reported in other thrombin structures in complex with various active-site or exosite I-binding inhibitors, and result mainly from crystal packing. It is particularly relevant that the structural changes in the active site of thrombin are of similar magnitude as those observed upon occupancy of exosite I by inhibitors such as triabin (chapter 3; Fuentes-Prior et al., 1997) or the C-terminal tail of hirudin, hirugen (Skrzypczak-Jankun et al., 1991). The virtually unaltered active-site conformation of thrombin-TM indicates that allosteric modification of the thrombin active site is not the main mechanism by which thrombomodulin enhances activation of protein C.

It can be argued that irreversible (covalent) binding of the chloromethyl ketone moiety to thrombin's active site residues His57 and Ser195 stabilizes thrombin in a conformation that is not responsive to thrombomodulin-induced rearrangements. In support of this criticism, calorimetric investigations had shown indeed that the peptidyl chloromethyl ketones invariably increase the melting temperature of serine proteinases by as much as 28.5 K, and cause both proteinase subdomains to merge into a single cooperative unit (Novokhatny et al., 1993). However, the recently determined crystal structure of "free" (chloromethyl ketone-inhibited) factor VIIa has shown that cofactor binding elicits conformational changes in both the serine proteinase moiety (factor VIIa) and in the CMK-moiety (Pike et al., 1999), highlighting the high degree of plasticity conserved by the active-site modified proteinase; compare also section 1.2.8. and Fig. 1.19).

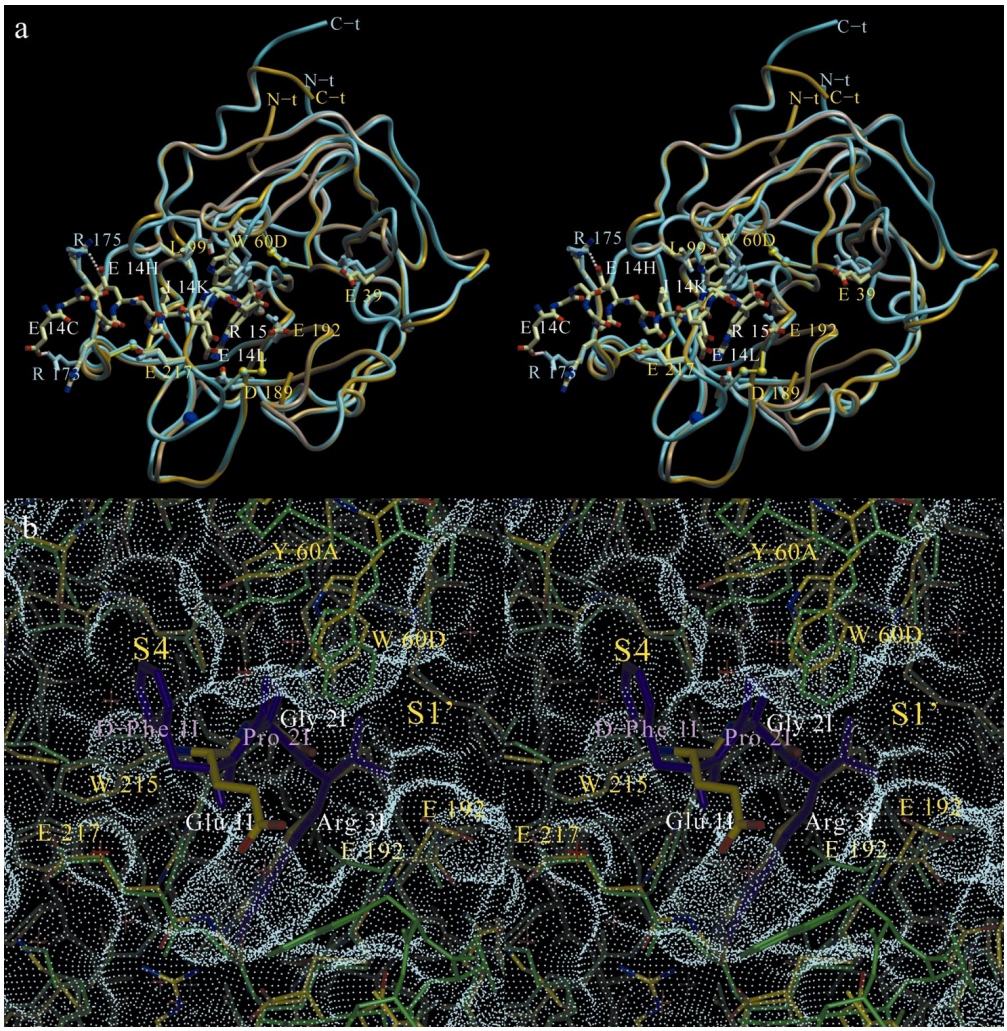

Fig. 4.3 (previous page): Thrombomodulin is not an allosteric modulator of thrombin. (**a**) Stereo view of TM-bound thrombin (yellow, side chains color-coded: carbon, yellow; nitrogen, blue; oxygen, red; Na^+ ion depicted as a blue sphere), overlaid with triabin-bound thrombin (light blue). The light chain of a neighboring thrombin molecule binds in a substrate-like manner in the active site of thrombin-triabin (compare Fig. 3.1) and is shown color-coded, as well as the EGR-moiety. (**b**) Close-up of the active site region (color-coded; Connolly surface shown as blue dots), overlaid on the structure of PPACK-thrombin (green). The chloromethyl ketone moieties (EGR-CMK, color-coded; PPACK purple) are represented.

An additional line of evidence contradicts the putative role of thrombomodulin as modulator of the thrombin active site. TM56 is the only TM fragment that interacts with thrombin (Figs 4.1, 4.2). However, it is well known that this fragment alone does not increase protein C activation by bound thrombin (Kurosawa et al., 1988), as would have been expected in case of an allosteric mechanism. TME4, the domain actually conferring protein C specificity (Zushi et al., 1991; Zushi et al., 1989), protrudes away from the proteinase, and thus cannot modulate the active site region of thrombin. Accordingly, peptide substrates are cleaved with similar kinetics by thrombin bound to thrombomodulin or hirugen (Vindigni et al., 1997). Alterations in the thrombin active site that were detected upon TM-binding ((Musci et al., 1988; Ye et al., 1991), see above) may therefore reflect changes in the electrostatic environment of the proteinase and / or small structural rearrangements.

4.5. Structure of the TME456 Fragment

4.5.1. Overall Arrangement of EGF-Like Repeats

The fundamental change in thrombin specificity appears to reside in the unique three-dimensional arrangement of EGF-like repeats observed in TME456. A rod-like arrangement of the three EGF-like repeats in TME456 was anticipated (Knobe et al., 1999), based on the observation of linear arrangements of two cb-EGF domains in the extracellular matrix protein **fibrillin-1** (Downing et al., 1996), as well as in a triplet of the remotely related **laminin-type** EGF domains (Stetefeld et al., 1996). Contrary to these expectations, TME4 is anchored nearly perpendicular to the linear TME56 tandem (Figs 4.1, 4.2, and 4.4). This compact nonlinear arrangement of TME456 was suggested previously to account for a small nodule observed by electron microscopy studies of soluble TM, while a

second larger nodule was attributed to the N-terminal lectin domain (Weisel et al., 1996).

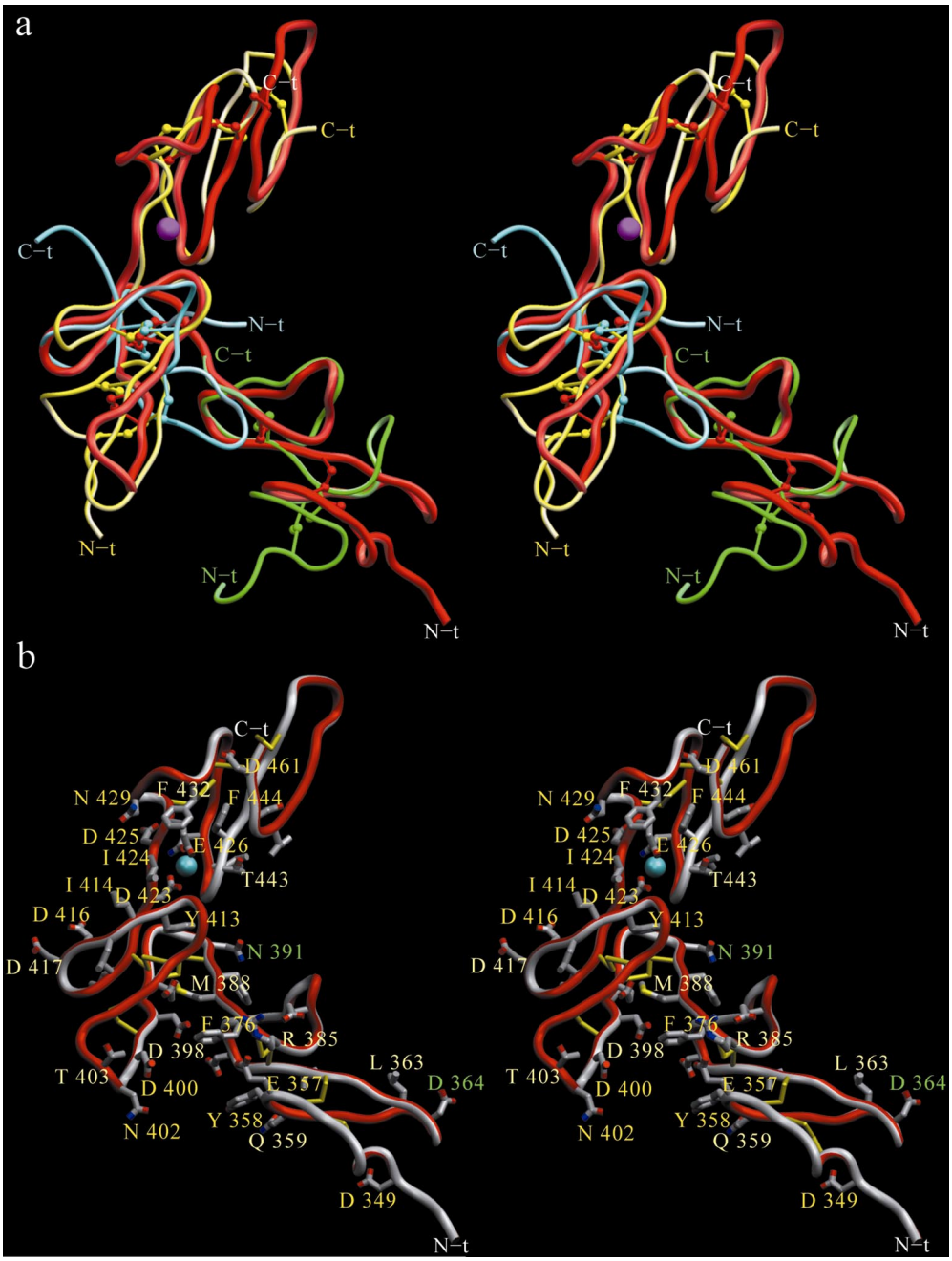

Fig. 4.4: TME456 exhibits a novel arrangement of EGF-like repeats. (**a**) Ribbon plot of TME456 (red) overlaid with the lowest energy solution structures of isolated TME4 (green) (Meininger et al., 1995), TME5 (Sampoli Benitez et al., 1997) (light blue) and the pair of EGF-like repeats of fibrillin-1 (Downing et al., 1996) (yellow). Disulfide bridges and the N- and C-termini of each structure are indicated. Notice the differences between the structures of EGF domains TME4 and TME5 within TME456 and the corresponding conformations of the isolated domains in solution. (**b**) Ribbon plot, highlighting side chains of residues critical for cofactor activity. Side chains *N*-glycosylated in the native protein, Asn364 (here Asp, after PNGase treatment) and Asn391 are also shown (labeled green).

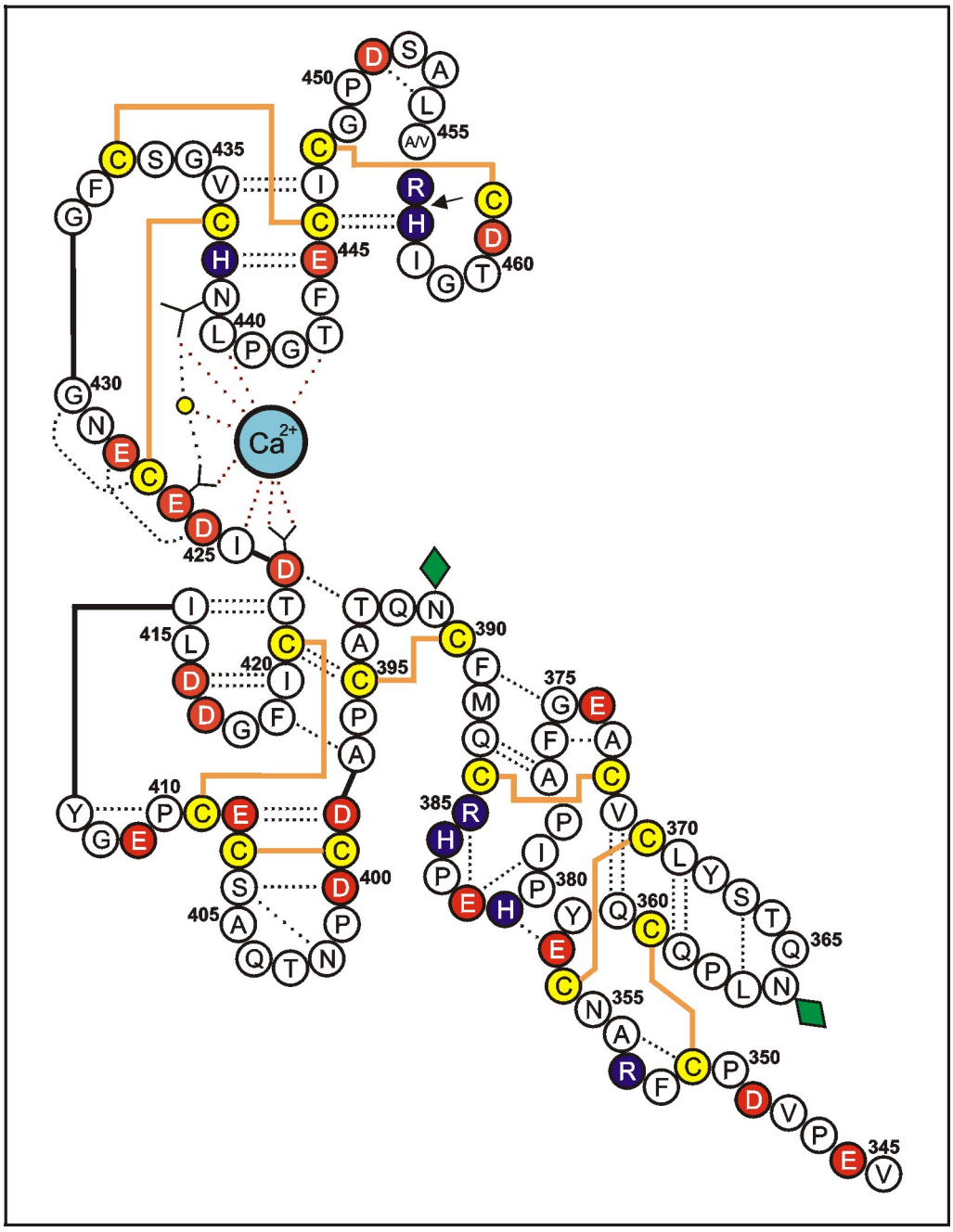

Fig. 4.5: Sequence and secondary structure of the human TME456 fragment. Acidic residues are shadowed red, basic residues blue. Protein–protein hydrogen bonds are indicated with black dotted lines, those made with the bound calcium ion with red dotted lines. Disulfide bridges are indicated with solid orange lines, glycosylation sites with green diamonds. The trypsin cleavage site Arg456–His457 (shown with an arrow) has been replaced in the form used in this study by the Gly–Gln sequence conserved in TM from other species to prevent proteolysis. Notice that domains TME4 and TME5 are separated by an unusually short three-residue linker.

Overall, TME4 and TME6 fold similarly to other EGF-like domains (Campbell and Bork, 1993) and consist of a flat major and a twisted minor β-sheet with the usual [1-3, 2-4, 5-6] disulfide pairing (section 1.2.2.). However,

they differ considerably in detail (see below). The three EGF-like repeats assemble through the interactions of two dissimilar interdomain surfaces resulting in the Y-shaped TME456 (Figs 4.2 and 4.4). The short connecting segment between TME4 and TME5 (Gln387-Phe389) is clamped to TME4 *via* hydrogen bonds and to TME5 through major hydrophobic contacts. In particular, Met388 slots into a central hydrophobic groove of TME5 spanned by the disulfide bridges [1-2] (Cys390-Cys395) and [5-6] (Cys409-Cys421), to anchor TME4 to TME5 and direct TME4 away from the thrombin surface (Fig. 4.4b). Oxidation of Met388 (Glaser et al., 1992) and all insertions, deletions as well as most amino acid substitutions in this segment (with exception of Met388→Leu) (Clarke et al., 1993) drastically reduce anticoagulant activity, underlining the importance of the proper orientation between TME4 and the TME5-TME6 tandem. Adjacent side chains of Pro410 and Phe376 reinforce this hydrophobic anchoring.

At the TME5-TME6 interface, the conserved internal side chain of Tyr413 (TME5) contacts the β2-β3 loop of TME6 (Fig. 4.4b). Highlighting this essential structural role, the Tyr413Ala mutant lacks cofactor activity (Nagashima et al., 1993). A similar role is played in fibrillin-1 by Tyr2157 (Downing et al., 1996), but the bending of TME5 allows additional interdomain contacts in TME456 (e.g., Asn391-Pro441). These contacts may further protect the bound Ca^{2+} ion in TME6 from bulk solvent, explaining its markedly low K_d (Light et al., 1999).

4.5.2. Structure of TME4

The TM polypeptide chain enters TME4 through a coiled strand (β1), folds back to form the major sheet (strands β2 and β3), and turns back again before running through the more irregular minor sheet (Figs 4.4 and 4.5). Several proline residues in the segment Pro378-His384 allow sharp turns of the main chain, so that the C-terminal segment connecting to TME5 is placed antiparallel to β4, resulting in a three-stranded minor sheet. Both sheets are aligned almost antiparallel to each other, locating the N- and C-termini of TME4 on opposite poles of the domain (Fig. 4.4). In the context of TME456, the shape of TME4 is thus more rod-like than in the compact NMR structure of the isolated TME4 fragment (Meininger et al., 1995), due to a more extended major sheet (Fig. 4.4a). We note that the structure of the C-loop peptide (Val371-Phe389) in solution corresponds closely to its structure within TME456, in agreement with the

previous proposal that this highly structured peptide constitutes a nucleation site for folding (Adler et al., 1995).

4.5.2. An Atypical EGF-Like Domain: TME5

The central TME5 domain diverges strongly from archetypal EGF-structures because of its unusual [1-2, 3-4, 5-6] disulfide pairing, as found by chemical (White et al., 1996) and NMR analysis (Sampoli Benitez et al., 1997) of the isolated TME5 fragment. Its extended major sheet (strands β2 and β3 and the connecting loop β2/β3) projects into thrombin's active site groove (Fig. 4.2), while the short strand β1 is shifted towards the C-terminal domain pole and runs through the β1/β2 loop circularized by the unusual [1-2] (Cys390–Cys395) disulfide (Figs 4.4a and 4.5; compare with the standard disulfide pairing, Figs 1.6 and 1.7). Strands β2 and β3 shift relative to one another bringing Cys399 and Cys407 in position to form the second novel disulfide ([3-4]). Thus, both the major (β2-β3) and the minor (β4-β5) sheets are more twisted than in other EGF-like structures. Strand β5 is hydrogen-bonded to β1, forming a three-stranded sheet. In contrast to the compact NMR structure of isolated TME5, the integrated TME5 domain is more elongated (compare Fig. 4.4a) and its extended major sheet (β2-β3) projects towards thrombin's active site groove (Fig. 4.2). Although this projection is well defined by electron density, the NMR structure suggests that it may exhibit flexibility (Fig. 4.4a; Sampoli Benitez et al., 1997). Due to a shortened and shifted β1 strand, both the N- and C-termini of TME5 emerge from the domain in close proximity. As a consequence, TME4 joins the TME5 domain near the TME5-6 junction, and is therefore also close to TME6 (Figs 4.2, 4.4).

Surprisingly, TME5 shows structural similarity to two otherwise unrelated proteins. The N-terminal subdomain of TME5 can be superimposed on residues the **f**olli**s**tatin- (FS) like domain present in the anti-adhesive secreted glycoprotein **BM-40** (also known as **SPARC** or **osteonectin**) (Hohenester et al., 1997), while the C-terminal subdomain displays similarity with an insect cytokine peptide, **plasmatocyte-spreading peptide 1** from *Pseudoplusia includens* (Volkman et al., 1999). The resemblance between the human FS domain of BM-40 and EGF module of factor IXa had been previously noted, but the significance of this finding is obscure.

4.5.4. TME6 and Calcium Binding

TME6 follows the classical scheme of EGF-like repeats in that its chain runs through a coiled strand β1 before building up the major sheet (β2-β3). However, the short stretch that corresponds to the minor sheet (residues Gly449–Ala455, disordered in all four TME456 molecules) precedes an additional strand that aligns antiparallel to β3 (Figs 4.4, 4.5). Cardinal to the overall domain folding is a calcium ion with octahedral co-ordination predicted by mutagenesis (Nagashima et al., 1993) and calcium-binding studies (Light et al., 1999). This calcium ion is held by the carboxylate groups of Asp423 and Glu426, the carboxamide oxygen of Asn439, the carbonyl oxygens of Ile424, Leu440 and Thr443, and a water molecule (Fig. 4.5). These ligands are the same observed in cb-EGF domains of coagulation factors (Figs 1.6 and 1.7), and are also conserved in fibrillin-1. There are, however, slight differences in the precise metal-protein interactions.

4.6. The Thrombin–Thrombomodulin Interface

Several lines of evidence had indicated interactions between TM and the anion-binding exosite I of thrombin (Hall et al., 1999; Hofsteenge et al., 1988; Hofsteenge et al., 1986; Wu et al., 1991). In agreement with the biochemical evidence, an interface of ~900 $Å^2$ is buried between TME56 and exosite I. Electrostatic interactions of the oppositely charged moieties (Figs 4.6a and 4.6b) certainly guide formation of the tight thrombin-TM complex ($K_d \sim 10^{-9}$ M) (Clarke et al., 1993; Jakubowski et al., 1986). However, the direct intermolecular contacts are largely hydrophobic in nature (Figs 4.6c and 4.6d). Besides several intermolecular hydrogen bonds, there is only a single direct (solvent exposed) salt bridge between thrombin and TM (Lys110 Nζ-Asp461 Oδ2). This constitutes yet another example indicating that complementarity of electrostatic potentials at protein–protein interfaces is not accompanied by concomitant formation of direct salt bridges (McCoy et al., 1997).

Basic residues of thrombin either form solvent-mediated hydrogen bonds with uncharged groups on TM (e.g., Arg67, Arg75 and Lys81) or extend freely into the bulk solvent (Lys36, Arg73 and Lys109). However, the side chains of some basic residues could rotate to easily reach negatively charged TM groups. Substitution of basic residues on thrombin by either glutamic acid (R73E, R75E)

(Wu et al., 1991) or alanine (e.g., R75A, K81A) (Hall et al., 1999; Tsiang et al., 1995) greatly impairs protein C activation by decreasing TM binding. These findings reinforce the important contribution of the overall positive surface potential of exosite I for complex formation.

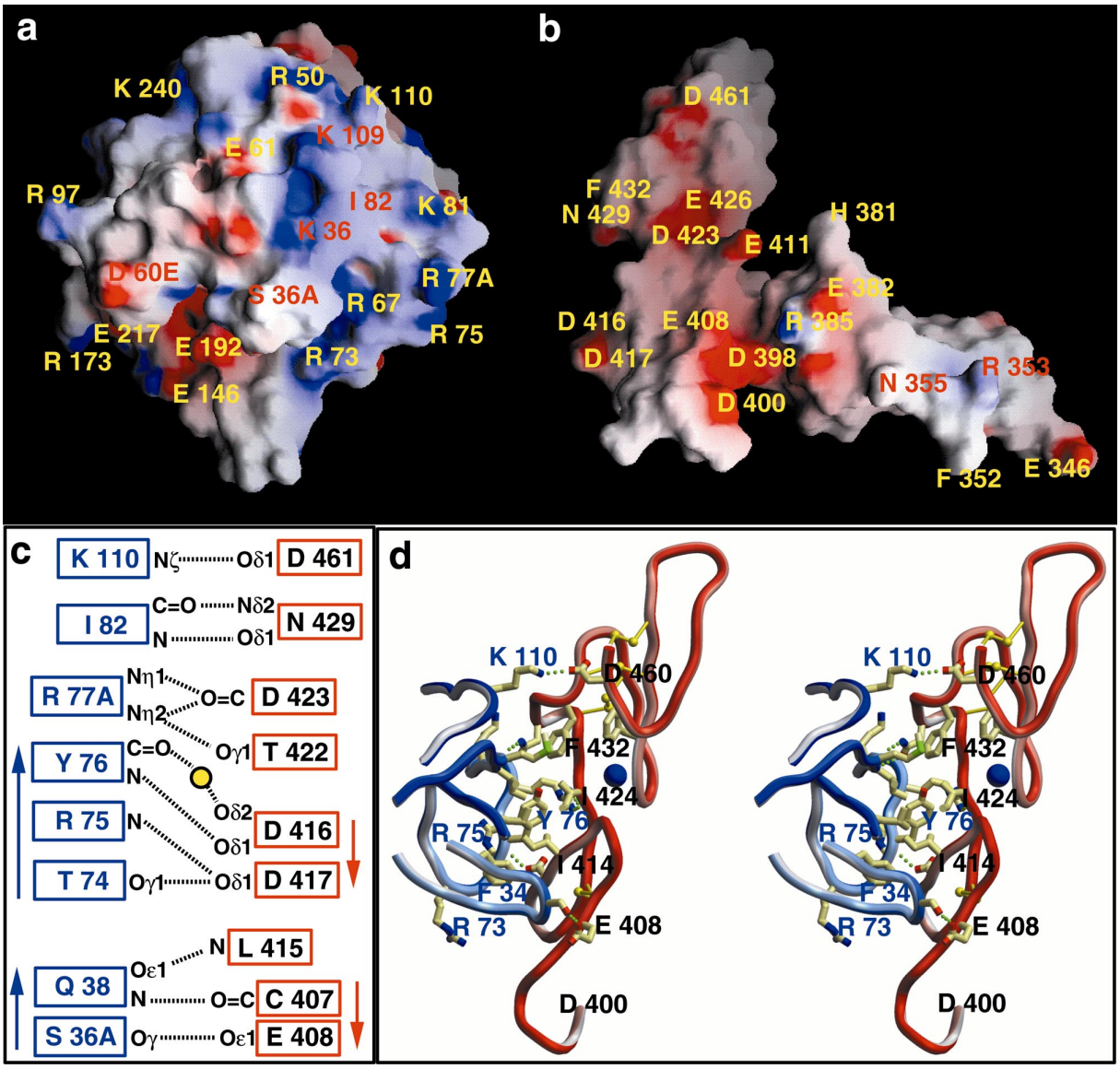

Fig. 4.6: The thrombin–thrombomodulin interaction interface is dominated by hydrophobic contacts. GRASP (Nicholls et al., 1993) electrostatic surface potentials of α-thrombin (**a**) and TME456 (**b**). Both moieties have been slightly rotated around the y-axis to present their interaction interfaces to the viewer. Notice the overall complementarity of electrostatic potentials. **(c)** Major hydrogen-bonding interactions (dotted lines) between thrombin and TM. (**d**) Detail of the interaction interface, highlighting its primary hydrophobic character. Selected hydrogen bonds are indicated as green spheres. Notice that a single, solvent-exposed salt-bridge forms between thrombin and TM (Lys110 Nζ-Asp461 Oδ2). For clarity, only residues Asp400-Cys462 of TM and the thrombin loops of the contact interface are shown.

The region of TME5 that contacts α-thrombin encompasses segments Ser406–Glu408 and Ile414–Asp417, which run antiparallel to thrombin segments Ser36A–Pro37 and Thr74–Tyr76, respectively (Figs 4.6c and d). The interface is completed by the TME5-6 connecting peptide and the coiled strand β1 of TME6 (residues Ile424–Phe432), which fold around the thrombin side chains of Tyr76 and Arg77A and nestle into the adjacent Asn78–Met84 groove (Fig. 4.6d). The side chain of Ile414 plays a central role in this intermolecular interaction. This alkyl group fits in a hydrophobic surface depression on thrombin formed by the side chains of Phe34, Tyr76 and Ile82; the hydrophobic patch is completed by the side chains of Leu65 (thrombin) and Ile424 (TM) (Fig. 4.6d). Alanine mutations at Ile414 and Ile424 lead to drastically reduced thrombin affinities and cofactor activities (Nagashima et al., 1993) and emphasize the importance of both hydrophobic residues. The bound calcium ion stabilizes the TME56 junction into a shape complementary to thrombin's exosite I and increases the affinity of soluble TM fragments by two orders of magnitude (Light et al., 1999). This feature explains the greatly reduced activity of alanine replacements for calcium ligands Asp423, Glu426 and Asn439 (Nagashima et al., 1993).

The crystal structure of thrombin complexed with the reduced nonadecapeptide Glu408–Glu426 from TME5 has been reported (Mathews et al., 1994). This peptide sandwiches between the exosite I regions of two α-thrombin molecules in the reported structure. The main chain path followed by this peptide while contacting one of the two thrombin molecules corresponds closely to the conformation of residues Cys407–Asp425 in the current thrombin–TME456 complex. However, most peptide residues are shifted by one compared to the corresponding segment in the thrombin–TME456 structure, with unsatisfactory consequences. For instance, in the peptide structure the side chain of Tyr413 contacts thrombin (instead of the above mentioned Ile414), and Cys409 and Cys421 are not in position to form a disulfide bond.

4.7. An Extended Exosite on TME45 Facing Thrombin

There is a notorious asymmetry in the electrostatic surface potential of TME456. The thrombin-binding surfaces of TME5 and TME6 possess a strong negative potential, in contrast to the less negative character of the molecular surfaces facing away from the proteinase (Fig. 4.6b). The "outer" TME4 surface is

noticeable hydrophobic (Leu363, Leu369, Pro380). It harbors the fully glycosylated side chain of Asn364 (Edano et al., 1998), while the partly glycosylated Asn391 emerges from the disulfide-closed loop β1-β2 of TME5 and extends into the narrow outer groove between TME4 and TME5 (Fig. 4.4b). Carbohydrate moieties attached to these asparagine side chains are not required for either thrombin binding or cofactor activity (Edano et al., 1998), also shown by the expression of active recombinant TM in *E. coli* (Adler et al., 1995; Lin et al., 1994; Nagashima et al., 1993). No residues relevant to thrombomodulin function map to this surface (Fig. 4.4b).

In contrast, the TME4 surface extending towards the active site groove carries a number of polar and charged side chains, (Arg385, His384, Glu382, Glu357, Asn355 and, more distal, Glu346 and Asp349), as well as several exposed aromatic residues (Phe352, Tyr358, Phe376) (Fig. 4.4b). The side chains of residues Asp398, Asn402, Thr403, Gln404 and Glu408 of the projecting β2/β3 loop of TME5 point towards thrombin's active site groove. Most of these residues have been identified as indispensable for cofactor activity through extensive mutagenesis studies (Adler et al., 1995; Nagashima et al., 1993) or replacement of disulfide loops (Lentz et al., 1993) (compare Fig. 4.4b). This clustering of functionally critical residues along an extended solvent exposed region of TME45 strongly suggests their involvement in substrate binding. We postulate that this surface represents the primary interacting region of the anticoagulant substrate, protein C.

4.8. A Docking Mechanism of Substrate Activation

4.8.1. Generation of a Model for the Activation Complex Protein C–(Meizo)thrombin–TM456

To explore this possibility in more detail, we docked a protein C model based on the crystal structure of Gla-less APC (Mather et al., 1996) to the thrombin-TME456 structure. For developing the protein C model and docking it to the thrombin TME456 complex, we took advantage of the conformation of the thrombin (enzyme) – thrombin ("substrate") complex observed in crystals of the thrombin-triabin complex (see chapter 3, Fig. 3.1).

First, the coordinates of the EGF2-catalytic domain tandem of APC (PDB code 1AUT; Mather et al., 1996) were superimposed on the "substrate" thrombin

molecule of the thrombin-triabin-thrombin complex (Fig. 3.3; Fuentes-Prior et al., 1997). We notice that the similarity between the activation peptide segments of prothrombin and protein C (compare Fig. 1.11) suggests that they could adopt similar conformations. Therefore, we used the conformation adopted by the twelve C-terminal residues of thrombin's light chain bound to the active site of thrombin-triabin to model the unprimed residues of PC's activation peptide (Asp4 (P12) to Arg15 (P1)). This allows the activation peptide of protein C to satisfy important specificity requirements of thrombin. For instance, Arg15, Pro14 and Val12 perfectly fill the S1-, S2- and S4 subsites of the proteinase, and residues Glu9 (P7) and Asp4 (P12) could form salt-bridges with thrombin residues Arg175 and Arg173, respectively (see Fig. 4.3a).

Keeping this peptide fixed, the N-terminal Leu16(P1')-Ile17-Asp18-Gly19(P4') segment of the APC heavy chain was removed from its internal anchoring site and loosely arranged in a canonical conformation (Bode and Huber, 1992), allowing for the Arg15-Leu16 peptide bond to be formed. This EGF2-PC-thrombin complex was minimized with XPLOR. Next, the current crystal structure of thrombin-TM456 was superimposed on the "enzyme" moiety of the PC-thrombin complex. Finally, the co-ordinates of the (bovine) fragment 2-thrombin complex (Martin et al., 1997) (PDB code 1AOH) were overlaid on the ternary complex to generate the highly homologous human fragment 2 model. Additionally, we completed the protein C model with a Gla domain model derived from the crystal structure of the FVIIa Gla domain (compare Fig. 1.4). The final model is presented in Fig. 4.7. In the following, we discuss its major implications for the mechanism of PC activation by thrombin-TM.

Fig. 4.7 (next page): Hypothetical structure of the activation complex thrombin-TM-PC. Stereo view of the predicted ternary complex, highlighting some functionally critical residues. The arrow indicates the postulated rotation of the TME3-4 linker towards the 60-loop of PC. The transmembrane peptide of TM and the Gla-domains of both meizothrombin and PC would be appropriately inserted into the cell membrane (which runs approximately parallel to the top of the figure). Calcium ions are shown as light blue spheres, the Na^+ ion in thrombin is dark blue.

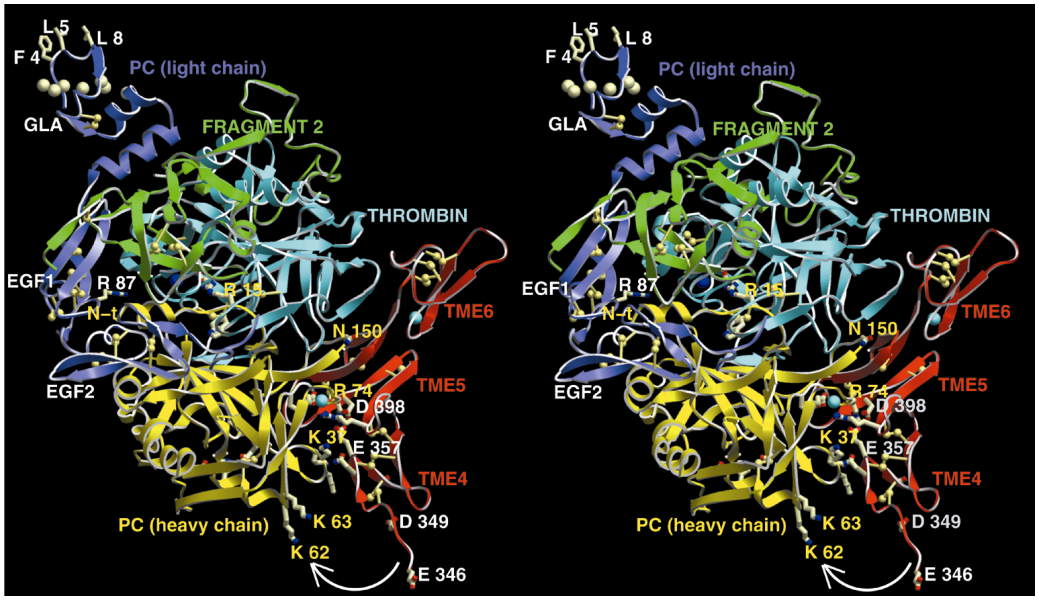

4.8.2. Manifold Interactions Between Thrombin and Protein C Validate the Model

A very satisfying aspect of the current model (Figs 4.7, 4.8) is the prediction of a multitude of interactions well beyond those initially assumed in order to generate the model. Many of these interactions may be rationalized as important to form the activation complex under physiological conditions. Without additional assumptions, the docking experiment anticipates important interactions between the activation peptide and the basic linker connecting the EGF domains of protein C, as well as between PC and thrombin. For instance, the hydrogen-bonding potential of the prominent carboxylate of Glu192 (thrombin) is satisfied by the carboxylamide of Gln118 (PC) and Nζ of Lys20 (PC). The guanidinium group of Arg23 (PC) hydrogen bonds the thrombin carbonyls of Cys58 and Leu59. The cluster of basic residues of human PC formed by Lys20 (Lys174), Arg23 (Arg177) and Arg22 (Arg178) appears to be required for TM-stimulated activation by thrombin under physiological Ca^{2+} concentrations, as shown with a protein C variant in which all three residues were replaced with glutamate (Grinnell et al., 1994). Our model indicates that thrombin, rather than thrombomodulin, forms the contact site of this cluster. Several hydrophobic side chains of protein C (e.g., Pro14, Leu16, Leu137, Phe157, Trp207), form together with the aliphatic parts of Lys20 and Lys159 a shallow hydrophobic surface depression that accommodates thrombin's Trp60D, explaining the important role of this side chain in protein C activation (Hall et al., 1999).

An intact Gla-EGF region is required for protein C binding to the thrombin-TM complex (Hogg et al., 1992). In our model, the EGF2 domain of the protein C makes favorable contacts with the kringle 2 domain of meizothrombin (Fig. 4.7; Martin et al., 1997), while the EGF1 domain is slightly shifted from the conformation seen in APC crystals (Mather et al., 1996), and binds in the groove between kringle 2 and the intermediate helix of (meizo)thrombin. Further, the N-terminus of the activation peptide is placed in the junction between both EGF-like domains of protein C allowing basic/polar residues of PC (e.g., Arg87, Gln90, Arg91) to compensate for the negative potential created by carboxylates at the N-terminus of the activation peptide (e.g., Glu4 (P12), Asp7 (P9)).

The 149-loops of both APC (Mather et al., 1996) and TM-bound thrombin are found disordered in the crystal structures, suggesting that they are reasonably flexible. The basic 149-loop of PC (e.g., Lys149, Arg149D) would experience strong electrostatic repulsion from exosite I. This electrostatic clash, combined with unfavorable interactions at positions P3 and/or P3' of the PC activation peptide, are likely to impede formation of the thrombin-TM complex under physiological conditions. Occupancy of thrombin's exosite I by TME56 would force the 149-loop of PC to adopt a conformation quite different from that modeled in the APC structure (Fig. 1.20; Mather et al., 1996). Clashes between the flexible 149-loops of both thrombin and PC (and/or with the TME5 loop Pro401–Ala405) were relieved in our model by rearrangements of both loops.

The Asn150Gln protein C mutant, which lacks the carbohydrate moiety attached to this asparagine in the wild-type protein, has a rate of activation three-fold higher than wild type (Grinnell et al., 1991). This observation suggests that the 149-loop of protein C contacts the thrombin-TM complex. In our model, the carbohydrate moiety would emerge between domains TME5 and TME6 (Fig. 4.7). Also along these lines, a recent loop-swapping study indicates that the lower potency of human protein C compared to the bovine protein is related to the presence of a four residues longer 149-loop (Shen et al., 1999). The 149-loop of thrombin is apparently less important for activity, because the deletion mutant des(Ala149A-Lys149E)-thrombin shows a three-fold increase in protein C activation rate (Dang et al., 1997).

4.8.3. TME45 Presents the Substrate Protein C to the Active Site of Thrombin

Most relevant for the mechanism of protein C activation by thrombin-TM, our model anticipates manifold interactions between the neighboring 37- and 70-loops of PC and TM45 (Figs 4.7, 4.8). The highly conserved Lys37-Lys38-Lys39 triplet important for thrombin-TM catalyzed activation of PC (Gerlitz and Grinnell, 1996) projects towards TME4 and directly contacts Glu382. The calcium-binding (70-80) loop of protein C interacts with the β1/β2 loop of TME4 and the β2-β3 extension of TME5; the critical side chain of Arg74 (Vincenot et al., 1995) is clamped between the carboxylates of Asp398 and Glu357 (Fig. 4.9). Evidence supporting the relevance of this electrostatic "grip" includes (a) thrombomodulin mutants Asp398→Ala and Glu357→Ala (Nagashima et al., 1993) or Glu357→Gln (Adler et al., 1995) are inactive, while the Glu357→Asp mutant retains half of the wild-type cofactor activity (Adler et al., 1995), and (b) the Arg74→Gln variant of protein C (protein C Marseille) yields fully active APC when activated artificially, but resists activation by the thrombin-TM complex (Vincenot et al., 1995).

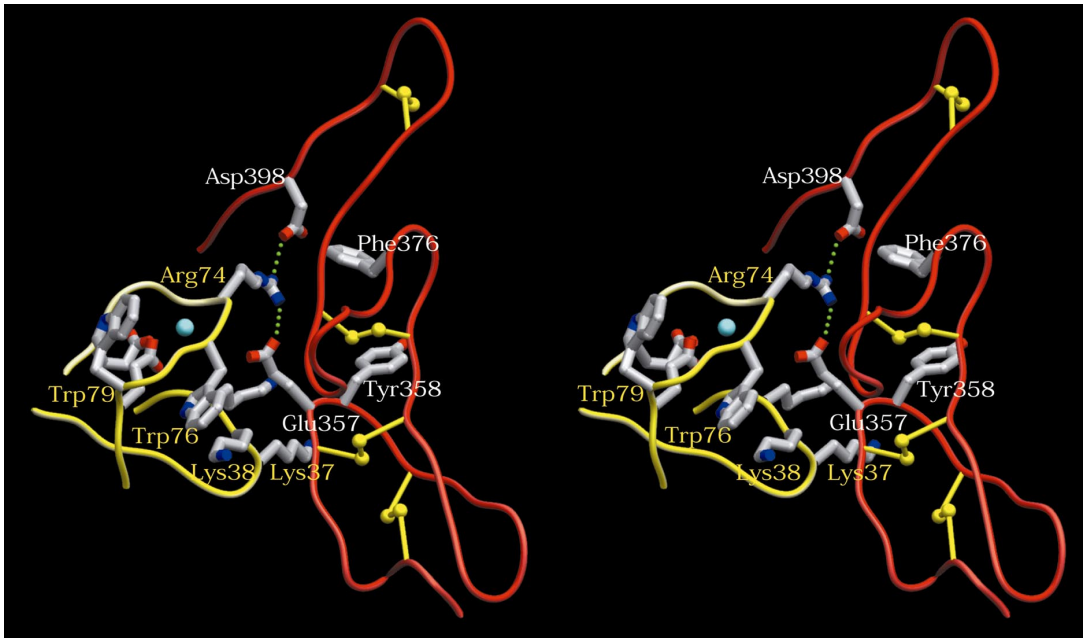

Fig. 4.8: Close-up of the predicted protein C – TME45 interaction interface. Only some of the relevant side chains are shown. Notice the hydrogen-bonded salt bridges that clamp the side chain of Arg74 (thrombin).

Further, the guanidinium group of Arg74 (protein C) is sandwiched between the critical pair of aromatic side chains of Tyr358 and Phe376 (Lentz et al., 1993; Nagashima et al., 1993) (Fig. 4.9), contacting a solvent molecule of high electron density. This density has been tentatively interpreted as a sodium ion, in accordance with the composition of the crystallization solution. However, it is conceivable that under physiological conditions this position is occupied by calcium. In fact, a Ca^{2+} bridge between TM and protein C has been proposed earlier (Kurosawa et al., 1987; Zushi et al., 1991), but its relevance for formation of the ternary complex has been questioned (Olsen et al., 1992). Our model also predicts direct contacts between TME4 side chains and protein C residues that co-ordinate calcium (Arg385–Glu80). Such interactions might explain the unique calcium-dependence of PC activation catalyzed by thrombin bound to chondroitin sulfate-free thrombomodulin variants (Kurosawa et al., 1987; Zushi et al., 1991). In this regard, substitution of Glu80 (PC) by a lysine eliminates this calcium-dependence (Rezaie et al., 1994).

Finally, the acidic TME3-4 linker may move towards the bound substrate, as suggested by the NMR structure of the isolated TME4 domain (Fig. 4.4a; Meininger et al., 1995), allowing residues Lys62 and/or Lys63 to interact with the side chain of Asp349, critical for thrombin-TM catalyzed PC activation (Nagashima et al., 1993; Zushi et al., 1991). The importance of the Lys62/Lys63 pair is indicated by the 10-fold lower activation rate of the PC double mutant (K62S, K63D) by thrombin-TM (Knobe et al., 1999). This loop displacement would also bring the highly acidic TME3 domain (e.g., Asp338, Asp341, Glu343) close to the bound substrate and further stabilize the ternary thrombin-TM-PC complex. These residues can be individually replaced by alanine without major decrease of cofactor activity (Nagashima et al., 1993). However, their combined contribution to complex formation has still to be addressed.

The manifold, mainly electrostatic interactions described above would allow TME45 to align the substrate PC presenting its scissile peptide bond Arg15–Ile16 to the thrombin active site residues with an optimal conformation for cleavage.

4.9. Activation on the Cell Membrane Surface

Under physiological conditions activation of protein C seems to be largely confined to the endothelial cell surface (Esmon, 1995; Sadler, 1997). However, membrane binding is not needed for enhancement of the catalytic efficiency of the thrombin-TM complex, as indicated by the conserved anticoagulant and profibrinolytic activities of both natural (Takahashi et al., 1995) and recombinant (Bajzar et al., 1998; Parkinson et al., 1992; Zushi et al., 1989) soluble TM variants. In the cell environment, protein C activation critically depends on TM correctly positioning thrombin's active site over the cell surface, to interact with the activation peptide of PC (Tsiang et al., 1992). *In vitro* studies show that TM is also a receptor for meizothrombin, the intermediate form of thrombin activation which is membrane-bound *via* its N-terminal Gla-domain (see section 1.2.5.). TM-bound meizothrombin has almost the same PC cofactor activity as α-thrombin itself (Doyle and Mann, 1990), but a six-fold higher activity in the presence of negatively charged phospholipids (Cote et al., 1997). Clearly, protein C activation would require the exquisitely fine-tuned arrangement of thrombin's active site and PC's activation peptide. In elegant mutagenesis studies, E. Sadler and co-workers have shown that the Ser/Thr-rich peptide of TM that connects TME6 with the transmembrane peptide plays and essential spacer role (Tsiang et al., 1992). On the other hand, the N-terminal regions of both protein C and meizothrombin are responsible for arranging enzyme and substrate at the correct distance above the cell membrane. In particular, the flexible linker peptides between kringles 1 and 2 (in meizothrombin) (section 1.2.5.) and between both EGF domains of protein C (1.2.9.) seems to be appropriately "designed" to allow the correct assembly of all three components on the cell membrane.

Kringle K2 occupies the heparin-binding exosite of thrombin (Martin et al., 1997), see also Fig. 1.13b), leaving a groove between the kringle domain and the intermediate helix of (meizo)thrombin, in which the first EGF domain of PC can bind, if slightly rotated outward from its (presumably artificial) conformation in APC (Mather et al., 1996). The EFG2 domain of PC is rigidly attached to the catalytic domain (see sections 1.2.2. and 1.2.9., and Fig. 1.20) and makes in our thrombin-TM-PC model favorable contacts with K2 (Fig. 4.7). The Gla-domain of protein C in turn leans against the sodium loop, the 186-loop and the C-terminus

of the A-chain of (meizo)thrombin, allowing numerous interactions between thrombin and the protein C light chain and in agreement with biochemical data (Hogg et al., 1992). The N-terminal hydrophobic Gla-loop (residues Phe4, Leu5 and Leu8; see Fig. 4.7) projecting beyond the thrombin surface can be immersed into a nearby phospholipid membrane. With full-length TM, the membrane is also positioned perfectly to accommodate the transmembrane anchor of TM. A chondroitin sulfate moiety, when present on the *O*-linked domain could reach exosite II of the same thrombin molecule, in accordance with the biochemical data (Ye et al., 1993). Our model predicts a distance of ~50 Å between the scissile bond Arg15-Leu16 of PC and the plane of the cell surface, a value slightly lower than the distance of 66±5 Å measured using labeled phospholipids (Lu et al., 1989), but in nice agreement with the distance that would be spanned by the putative α-helix forming the Ser/Thr-rich peptide (Tsiang et al., 1992).

Another interesting feature of this arrangement is the restriction of the possible orientations of the Gla-F1 tandem relative to the F2 domain and therefore to the catalytic domain of thrombin. It is apparent that the combination of flexible and rigid domain-domain associations result in a very fine tuning of enzymatic activity (Gaboriaud et al., 1998). Both kringle domains are most probably arranged approximately antiparallel to each other (compare Figs 1.13 and 1.14), allowing also the Gla-domain of meizothrombin to insert into the phospholipid membrane.

4.10. Other Physiological Implications

4.10.1. Activation of TAFI

It is conceivable that the exosite formed by domains TME4 and TME5 plays also an essential role for recognition of TAFI. In contrast with the activation peptide of protein C, most residues of TAFI's activation peptide (Val-(P4), Pro-(P2), Arg-(P1), Ala-(P1')) closely match specificity requirements of thrombin. TAFI would dock in the thrombin groove in a similar manner as PC, since both substrates compete with each other for thrombin-TM (Kokame et al., 1998). This assumption is also justified by the notable sequence similarity of the unprimed sites of both substrates and thrombin's light chain (Fig. 1.11). It is noteworthy that the activation peptides of all procarboxypeptidases studied so far possess a α-helical structure (Coll et al., 1991), further supporting our modeling procedure

(compare Fig. 4.7). Interactions with the TME5 projecting loop β2/β3 and with TME4 might be important but not sufficient to orient the substrate properly, as indicated by the lack of enhancement of TAFI activation by TME456 (Hall et al., 1999). The TAFI surface that would face TME45 in the activation complex is not particularly basic, although some alkaline side chains (Lys54, Arg101; carboxypeptidase numbering) would be appropriately positioned to contact acidic residues of the TM45 exosite. To strengthen binding of the substrate, the acidic TME3-4 linker and the TME3 domain might fold along a more extended TAFI substrate to guide it into an optimal alignment for cleavage. The TAFI surface opposite the activation segment contains several basic residues. A cluster formed by the basic side chains of Lys234, Arg272, Lys287 and Arg284 in the mature carboxypeptidase is a likely candidate for docking domains TME3 and/or TME4. The unique triplet of basic residues Lys48A-Lys49A-Lys50A in the prodomain might also contribute to interactions with acidic patches on TME34.

4.10.2. Inactivation by the Serpin Protein C Inhibitor

Electrostatic interactions might be also essential for guiding the serpin PCI towards the active site of TM-bound thrombin, explaining the 60-fold increase in inhibition rate by TME456, compared to free thrombin (Rezaie et al., 1995). In this context, a highly basic region formed by the N-terminal peptide of PCI (residues His5–Arg16, α_1-antitrypsin numbering) together with the H helix and the following loop (residues Arg273–Arg281) would face the polar/acidic exosite of TME45. This surface patch of PCI has been implicated in heparin-mediated protein C inhibition (Kuhn et al., 1990). We postulate that a similar mechanism accounts for the stimulation of thrombin-TM inhibition by PCI, but based on protein-protein electrostatic interactions. However, accommodation of the bulky phenylalanine residue at positions P2 and P4 in the reactive loop of PCI would require displacements of thrombin's 60-loop greater than those observed in the current crystal structure, and presumably similar to the ones observed in the crystal structure of E192Q thrombin bound to the non-physiological inhibitor BPTI (van de Locht et al., 1997).

4.11. Conclusions

Thrombomodulin (TM), a transmembrane thrombin receptor containing six contiguous epidermal growth factor domains (TME1 to TME6), profoundly alters

the substrate specificity of thrombin from a pro- to an anticoagulant proteinase. We have determined the 2.3 Å crystal structure of human α-thrombin bound to TME456, the smallest TM fragment required for full protein C cofactor activity. The angular Y-shaped TM fragment binds to thrombin's anion-binding exosite I, preventing binding of procoagulant substrates (e.g., fibrinogen, PARs). Contrary to expectations, however, thrombomodulin binding does not seem to induce major allosteric structural rearrangements at the thrombin active site. A second surprising feature of the structural investigation is that TME4 points away from bound TME5 precluding its interaction with thrombin. Therefore, TME4 cannot modulate the enzymatic activity of the proteinase. Instead, the overall structure suggests that TME45 bind substrates (protein C, TAFI) in such a manner that their activation cleavage sites are presented optimally to the unaltered thrombin active site. Thus, bound thrombomodulin creates an additional "exosite" to position substrates but does not act through allosteric modulation of thrombin.

The current structure emphasizes the crucial role of secondary enzyme-substrate interactions for processing macromolecular substrates. Procoagulant substrates with non-optimal cleavage sites are efficiently activated upon binding to thrombin's exosite I. Occupancy of exosite I by the two C-terminal EGF-like domains of thrombomodulin (TME56) blocks procoagulant activities by preventing binding of fibrinogen, PARs, and factors V and VIII. In the presence of calcium, also protein C has a non-optimal cleavage site (Fig. 1.11), and secondary contacts between its light chain and thrombin (Hogg et al., 1992) are insufficient to overcome electrostatic repulsion by the active site region of the proteinase. Thrombomodulin overcomes this repulsion by promoting association of the scissile peptide bond of protein C / TAFI with the catalytic machinery of thrombin in a stereochemical conformation optimal for cleavage, manifested in the strong enhancement of k_{cat} and relatively small but favorable effects on K_M (Clarke et al., 1993; Jakubowski et al., 1986). In this respect, TM resembles the bacterial plasminogen activator staphylokinase, which also functions by presenting the non-optimal cleavage segment of plasminogen to the active site of plasmin (Parry et al., 1998). It is tempting to speculate that also the clotting factors Va and VIIIa bring the activating proteinase (FXa, FIXa) and the zymogen (prothrombin, FX) together in a mode optimal for activation.

Appendix A1: Results of Investigations with Knockout Mice

Protein	Description of knockout	References
Factor VII	FVII(-/-) embryos developed normally. FVII(-/-) mice succumbed perinatally because of fatal hemorrhaging from normal blood vessels.	(Rosen et al., 1997)
Factor IX (catalytic domain)	Tail bleeding time of FIX(-/-) mice markedly prolonged compare with those of normal and carrier female litter mates. Aside from the factor IX defect, the carrier female and hemizygous male mice had no liver pathology, were fertile and transmitted the FIX mutation in the expected Mendelian frequency. Murine model of hemophilia B.	(Kundu et al., 1998)
Protein C	PC(-/-) pups at E17.5 and at birth appeared to develop normally macroscopically, but possessed obvious sign of bleeding and thrombosis and did not survive > 24 h after delivery.	(Jalbert et al., 1998)
Factor V	About one-half of FV(-/-) embryos died by E10.5, associated with gross and microscopic abnormalities of the yolk sac vessels. Remaining FV(-/-) embryos progressed normally to term, but died from massive hemorrhage within 2 h of birth.	(Cui et al., 1996)
Factor VIII	Model of hemophilia A.	(Bi et al., 1995)
von Willebrand factor	vWf(-/-) mice appeared normally at birth, were viable and fertile. However, mutant mice exhibited defects in hemostasis with a highly prolonged bleeding time and spontaneous bleeding events. Model of von Willebrand disease.	(Denis et al., 1998)
Fibrinogen (Aα chain)	No evidence of fetal loss of Aα(-/-) mice. Aα(-/-) mice were born normal in appearance. All the components of fibrinogen (Aα, Bβ, γ) were undetectable in plasma and overt bleeding events developed shortly after birth. Most newborns ultimately control the loss of blood. Pregnancy uniformly results in fatal uterine bleeding around the tenth day of gestation.	(Suh et al., 1995)
Tissue Factor	Abnormal circulation from yolk sac to embryo beyond E8.5, leading to embryo wasting and death *in utero* between E8.5 and E10.5. TF(-/-) embryos morphologically distinct from their TF(+/+) and TF(+/-) littermates after E9.5 in that they were pale, nearly bloodless, and growth retarded. Initial failure in TF(-/-) embryos appeared to be hemorrhaging, leading to the leakage of embryonic red cells from both extraembryonic and embryonic vessels. Approximately 15% of the TF(-/-) embryos survived beyond E10.5, but none completed gestation. Vitelline vessels from null mice were deficient in smooth-muscle α-actin-expressing mesenchymal cells.	(Bugge et al., 1996; Carmeliet et al., 1996; Toomey et al., 1996)
TFPI (Kunitz 1)	Sixty percent of TFPI-K1(-/-) embryos died between E9.5 and E11.5 with signs of yolk sac hemorrhage. Hemorrhage, particularly in the CNS and tail evident during later gestation. Unregulated TF-FVIIa activity and consequent consumptive coagulopathy underlies bleeding diathesis in these older embryos. None of the TFPI-K1(-/-) mice survived to the neonatal period.	(Huang et al., 1997)
TFPI + **TF**	TF(-/-)/TFPI(-/-) embryos uniformly completed embryonic development.	(Chan et al., 1999)
TXA_2 receptor (**TP**)	TP(-/-) mice reproduced and survived in expected (Mendelian) numbers. Bleeding times were prolonged in TP(-/-) mice and their platelets did not aggregate after addition of TXA_2 agonists.	(Thomas et al., 1998)
GP V	Deficiency in GP V did not affect viability at birth. GP V (-/-) platelets were normal in size and expressed normal amounts of functional GP Ib-IX complex. GP V (-/-) platelets were hypersensitive to thrombin.	(Ramakrishnan et al., 1999)
PAR1	Profound effect on fetal development (only 7% of homozygous PAR1(-/-) offspring). About 50% of PAR1(-/-) embryos died at E9-E10. Remaining embryos showed transient growth retardation, but recovered normal size by the end of gestation. PAR1-deficiency had no detectable effect in adult PAR1(-/-) mice.	(Connolly et al., 1996; Darrow et al., 1996)
PAR3	PAR3(-/-) mice developed normally and showed no spontaneous bleeding. Thrombin responses in platelets from PAR3(-/-) mice were delayed but not absent.	(Kahn et al., 1998)
Prothrombin	More than one-half of FII(-/-) embryos died between E9.5 and E11.5. Surviving embryos had characteristic defects in yolk sac vasculature and varying degrees of tissue necrosis. Most of remaining FII(-/-) embryos died by E15.5, but those surviving to E18.5 appeared normal. At least one-quarter of FII(-/-) mice survived to term, but developed fatal hemorrhagic events and died within a few days of birth.	(Sun et al., 1998; Xue et al., 1998)
Thrombomodulin	TM(-/-) embryos died before E9.5. Overall retardation in growth and development of TM(-/-) embryos first evident on E8.5. However, no specific pathologic abnormalities were observed. Point mutation Glu387Pro generated mice that developed to term, in spite of the severely reduced capacity to generate APC or inhibit thrombin.	(Healy et al., 1995; Weiler-Guettler et al., 1998)

E, embryonic day; TFPI, Tissue factor pathway inhibitor; CNS, central nervous system.

Appendix A2: Posttranslational Modifications of Major Human Coagulation Factors

Protein	Residues	Modification	Function	References
Prothrombin	**E**6, **E**7, **E**14, **E**16, **E**19, **E**20, **E**25, **E**26, **E**29, **E**32 (Gla)	γ-Carboxylation	Calcium binding / Membrane binding	(Walz et al., 1977)
	S?	Phosphorylation	Regulation of blood coagulation?	(Abe et al., 1991)
	N78, **N**100 (K1), **N**373{60G} (catalytic domain)	*N*-Glycosylation	Expression? Solubility?	(Walz et al., 1977)
Factor VII	**E**6, **E**7, **E**14, **E**16, **E**19, **E**20, **E**25, **E**26, **E**29, **E**35 (Gla)	γ-Carboxylation	Calcium binding / Membrane binding	(Thim et al., 1988)
	S52, **S**60 (EGF1)	*O*-Glycosylation (Fucosylation)	Calcium binding affinity?	(Bjoern et al., 1991; Harris and Spellman, 1993; Hase et al., 1988; Kao et al., 1999)
	N145 (activation peptide), **N**322{175} (catalytic domain)	*N*-Glycosylation	Solubility?	(Thim et al., 1988)
Tissue factor	**N**11 (1st Fn-III), **N**124, **N**137 (2nd Fn-III)	*N*-Glycosylation	?	(Paborsky and Harris, 1990)
Factor X	**E**6, **E**7, **E**14, **E**16, **E**19, **E**20, **E**25, **E**26, **E**29, **E**32, **E**39 (Gla)	γ-Carboxylation	Calcium binding / Membrane binding	(McMullen et al., 1983)
	D63 (EGF1)	β-Hydroxylation	?	(McMullen et al., 1983)
	N181, **N**191 (activation peptide)	*N*-Glycosylation	Stiff conformation required for activation?	(Inoue and Morita, 1993)
	T159, **T**171 (activation peptide)	*O*-Glycosylation	Stiff conformation required for activation?	(Inoue and Morita, 1993)
Factor IX	**E**7, **E**8, **E**15, **E**17, **E**20, **E**21, **E**26, **E**27, **E**30, **E**33, **E**36, **E**40 (Gla)	γ-Carboxylation	Calcium binding / Membrane binding	(Fryklund et al., 1976)
	D64 (EGF1)	β-Hydroxylation	?	(McMullen et al., 1983)
	N157, **N**167 (activation peptide)	*N*-Glycosylation	Stiff conformation required for activation?	(Di Scipio et al., 1978)
	S53, **S**61 (EGF1)	*O*-Glycosylation (Fucosylation)	Calcium binding affinity?	(Harris et al., 1993; Hase et al., 1988; Nishimura et al., 1992)
	T159, **T**169 (activation peptide)	*O*-Glycosylation (partial)	Stiff conformation required for activation?	(Agarwala et al., 1994)
Factor V	**N**23?, **N**27?, **N**211?, **N**269? (A1), **N**354?, **N**432?, **N**440?, N526? (A2), **N**1531? (*a*3), **N**1675? (A3), **N**1982 (C1)[a]	*N*-Glycosylation	Secretion, Inactivation by APC	(Fernandez et al., 1997; Pittman et al., 1994)
	N2181	*N*-Glycosylation	Membrane binding, prothrombinase assembly	(Hoekema et al., 1997; Kim et al., 1999)
	*a*2 (**S**690? + ?)	Phosphorylation	Extracellular distribution? / Down-regulation of activity?	(Kalafatis et al., 1993; Rand et al., 1994)
	Y665?, **Y**696?, **Y**698? (A2), **Y**1494? (B) **Y**1510?, **Y**1515?, **Y**1565? (A3)	Sulfation	Interaction with factor Xa and / or (pro)thrombin	(Hortin, 1990)

Factor VIII	**N**41?, **N**239? (A1), **N**582 (A2), **N**1810? (A3), **N**2128? (C1)[b]	*N*-Glycosylation	Secretion	(Pittman et al., 1994)
	Y346 (*a*1), *a*3 (**S**1657?)	Phosphorylation	Down-regulation of activity?	(Kalafatis et al., 1993)
	Y346 (*a*1), **Y**1664 (*a*3)	Sulfation	Interaction with thrombin	(Pittman et al., 1994; Pittman et al., 1994)
	Y718, **Y**719, **Y**723 (*a*2)	Sulfation	Optimal interaction with factor IXa	(Pittman et al., 1994)
	Y1680	Sulfation	vWf binding	(Leyte et al., 1991)
TM	**N**29, **N**98 (lectin domain), **N**364 (EGF4), **N**391 (EGF5)	*N*-Glycosylation	Secretion?	(Edano et al., 1998)
	S474, **S**480, **T**482, **T**486, **T**488	*O*-Glycosylation	?	(Bourin et al., 1990; Parkinson et al., 1992)
	S472	Chondroitin sulfate + dermatan sulfate	Secondary thrombin binding site, protein C activation, antithrombin inhibition	(Edano et al., 1998; Parkinson et al., 1992)
Protein C	**E**6, **E**7, **E**14, **E**16, **E**19, **E**20, **E**25, **E**26, **E**29 (Gla)	γ-Carboxylation	Calcium binding / Membrane binding	(Foster and Davie, 1984)
	D71 (EGF1)	β-Hydroxylation	?	(Foster and Davie, 1984)
	N97 (EGF2)	*N*-Glycosylation	Secretion, Glycosylation at N329	(Grinnell et al., 1991)
	N248{93}, **N**313{150} (catalytic domain)	*N*-Glycosylation	Intracellular processing of the K-R cleavage site, affinity for thrombin-TM	(Grinnell et al., 1991)
	N329{166} (catalytic domain)	*N*-Glycosylation (except in β-protein C)	Secretion?	(Grinnell et al., 1991; Miletich and Broze, 1990)
Protein S	**E**6, **E**7, **E**14, **E**16, **E**19, **E**20, **E**25, **E**26, **E**29, **E**32, **E**36 (Gla)	γ-Carboxylation	Calcium binding / Membrane binding	(Dahlbäck, 1991)
	D95 (EGF1)	β-Hydroxylation	?	(Lundwall et al., 1986; Stenflo, 1999)
	N458, **N**468 (sex-hormone)	*N*-Glycosylation	Secretion?	(Lundwall et al., 1986; Stenflo, 1999)

[a]Fourteen additional asparagines in domain B could be N-glycosylated.

[b]Seventeen additional asparagines in domain B could be N-glycosylated.

Appendix A3: Sequence Alignment of the Serine Proteinase Moieties of Coagulation Factors

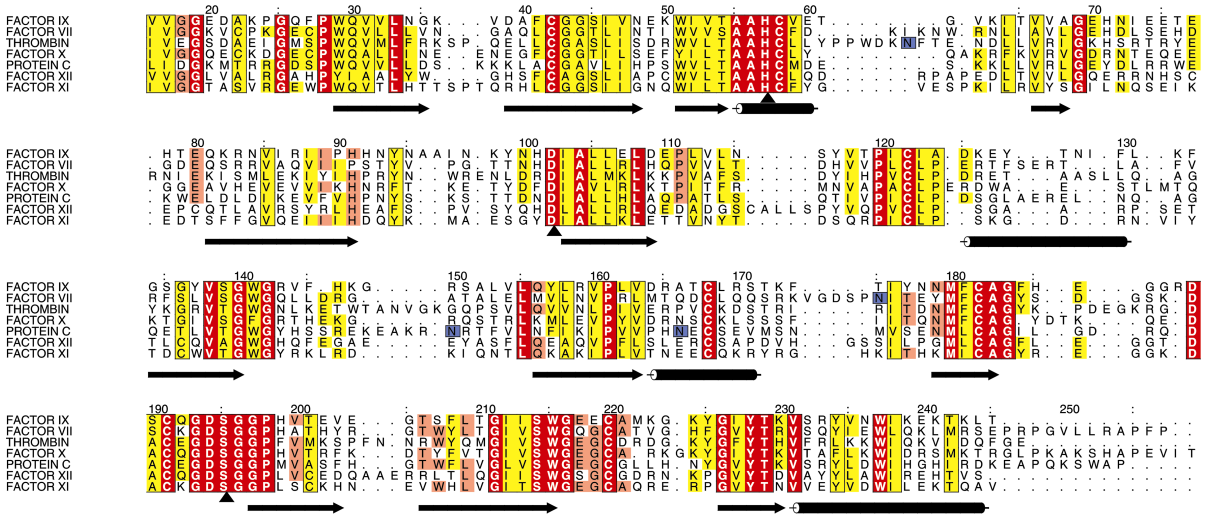

Residues have been aligned according to the chymotrypsin-based numbering system; catalytic triad residues are indicated with full arrows. The given secondary structure corresponds to thrombin (Bode et al., 1989; Bode et al., 1992), but is representative of the whole family. Conserved residues are white with red underground, conservative substitutions are shadowed yellow. Other residues conserved in at least half of the domains are shadowed pink, some additional similarities are shadowed yellow. Asparagine residues that are N-glycosylated in the natural proteins are shadowed blue (only partially in the case of protein C Asn166, compare appendix A2). The C-terminal residues of factor X (Ser-Ser-Pro-Leu-Lys) are not included in the alignment. Notice the unique insertion in thrombin's 60-loop.

Appendix A4: Some Clinical Implications of Coagulation Factors Deficiencies

Absence or deficiencies in the proteins involved in blood coagulation lead to imbalance of the hemostatic processes and thus either to bleeding episodes or to manifold arterial and venous occlusive disorders, which might result in life-threatening diseases such as myocardial infarction and thrombotic stroke (Miletich et al., 1993). In particular, imbalance of the thrombin activity can result in severe pathological states such as myocardial infarction, stroke or pulmonary embolism. Several variants of thrombin are known, with defective processing of physiological cofactors (see for instance (Bezeaud et al., 1988)).

Some polymorphisms in receptors expressed on the platelet surface (in particular α_{IIb} and β_3) are associated with functional disorders (Nurden, 1995). Inherited abnormalities in $\alpha_{IIb}\beta_3$ expression or function that impair platelet aggregation (see section 1.4.1.) result in the bleeding disorder **Glanzmann thrombosthenia** (Bennett, 1996), the most common inherited disease of platelets. Moreover, absence of functional GP Ib-IX-V complex causes the severe bleeding disorder known as **Bernard-Soulier syndrome** (Lopez et al., 1998).

Deficiencies in the procoagulant activity of the non-enzymatic cofactors V and VIII results in a number of pathologic disorders. Inherited factor V deficiency leads to abnormal bleeding in the rare autosomal recessive disease **parahemophilia** (Seeler, 1972; Tracy and Mann, 1987), whereas inheritance of the point mutation Arg506Gln that renders factor Va resistant to protein C inactivation is one important risk factor for thrombosis (Bertina et al., 1994). Allo- or autoantibodies directed against factor V are being repeatedly found in the clinical praxis (Ortel et al., 1994). Reduced or absent FVIIIa procoagulant activity is the cause of the common bleeding disorder, **hemophilia A** (or **classical hemophilia**). This X-linked, autosomal recessive disease affects 1 in 5,000 males with different degrees of severity (for reviews see (Antonarakis, 1995; Gitschier et al., 1991; Sadler and Davie, 1987)). Additionally, up to 15% of patients with severe hemophilia A develop inhibitor antibodies directed against FVIII (Gill, 1984). Inhibitory antibodies (inhibitors) to FVIII arise as alloantibodies in patients with hemophilia A transfused with FVIII or as autoantibodies in non-hemophiliacs (Hoyer and Scandella, 1994). Deficiencies in

the FVIII carrier molecule (vWf) lead to the most common inherited human bleeding disorder. Furthermore, multiple coagulation factor deficiencies (e.g., in both factor V and factor VIII or in factors VIII, IX and XI) have also been described (Soff and Levin, 1981; Soff et al., 1981). Deleterious mutations in the factor IX gene cause the X-linked clotting disorder **hemophilia B** that affects one in 30,000 males (Gerrard et al., 1993; Kurachi et al., 1993; Sadler and Davie, 1987). Mutations in the catalytic domain account for the largest number of cases of hemophilia B in humans. Deficits in factor XI are the cause of another bleeding disease, **hemophilia C** (Cawthern et al., 1998). Finally, deficiency of factor XIII results in inefficient wound healing, and women with this deficiency have a high risk of early abortions (Grundmann et al., 1986).

Deficits in the protein C anticoagulant pathway activated by the thrombin-TM complex are strongly associated with venous thrombosis (Esmon, 1997). Protein C deficiency is an autosomally inherited disorder that is associated with an increased risk of venous thrombosis. Patients homozygous for protein C deficiency suffer from life-threatening thrombotic complications immediately after birth. Numerous patients suffering from this disease have been screened for genetic abnormalities, and 160 different mutations have been identified (Reitsma et al., 1995; Reitsma et al., 1993). The critical anticoagulant role of its cofactor protein S is most dramatically revealed by the massive thrombotic complications suffered by infants homozygous for protein S deficiency (Mahasandana et al., 1990; Pegelow et al., 1992). Also thrombomodulin plays an important role in the pathogenesis of thrombin-induced thromboembolisms (Kumada et al., 1988), and mutations in the TM gene are proposed as risk factors for thrombosis (Doggen et al., 1998; Ohlin and Marlar, 1995; Ohlin et al., 1997).

Appendix A5: Mutations within the discoidin domains of FVIII from hemophilia A patients, grouped according to their locations on the three-dimensional structure.

Mutations (Number of patients)	FVIII:C/FVIII:Ag	Residue in FVa-C2	Solvent access. (%)
A) Mutations disrupting the structure of the membrane binding spikes and/or neighboring loops			
Trp2046→Arg (1)	n.d. / n.d.	Trp31 (conserved in all FV/FVIII discoidin domains)	2
Ser2069→Phe (1)	> 1 / n.d.	Gln56	2
Gln2087→Arg (1)	22 / n.d.	Gln74 (conserved in all FV/FVIII discoidin domains)	0
Gly 2088→Ser (1)	1 / 60-80	Gly75 (conserved in all FV/FVIII discoidin domains)	0
Pro2153→Gln (1)	3 / 6	Pro140 (conserved in all FV/FVIII discoidin domains)	0
Thr2154→Ile (1)	6 / n.d.	Lys141 (polar residues in all FV/FVIII discoidin domains)	20
Arg2159→Cys (15) Arg2159→His (1) Arg2159→Leu (2)	10-15 / 6-16 22 / 12 12-25 / 15	Ser146 (polar residues in all FV/FVIII discoidin domains)	17
Arg2163→Cys (2) Arg2163→His (6)	1 / <10 > 1-6 / n.d.	Arg150 (conserved in all FV/FVIII discoidin domains)	2
Arg2150→His (21)	< 1-9 / 6	Arg137 (conserved in all FV/FVIII discoidin domains)	7
Leu2166→Ser (1)	< 1 / n.d.	Leu153 (aliphatic side chain in all FV/FVIII discoidin domains)	0
Ala 2192→Pro (1)	1 / n.d.	Ala19 (conserved in all FV/FVIII discoidin domains)	0
Ser2204 (Deletion) (1)		Glu32	27
Pro2205 (Deletion) (3)	< 1 / n.d.	Pro33	0
Trp2229→Cys (4)	3-10 / n.d.	Trp57 (conserved in all FV/FVIII discoidin domains)	24
Thr2245→Ala (1)	7 / 10	Thr73 (conserved in all FV/FVIII discoidin domains)	0
Gln2246→Arg (2)	4.5 / <1	Gln74 (conserved in all FV/FVIII discoidin domains)	0
Arg2307→Leu (4) Arg2307→Gln (9)	< 1-2 / 4 < 1-10 / 6	Arg137 (conserved in all FV/FVIII discoidin domains)	7
B) Mutations disrupting the structurally conserved salt bridge Asp61-Arg134			
Asp2074→Gly (3)	5-9 / 10-15	Asp61 (conserved in all FV/FVIII discoidin domains)	3
Met2238→Val (5)	< 2 / n.d.	Lys66	10
Arg2304→Cys (2) Arg2304→His (1)	1 / <10 10 / n.d.	Arg134 (conserved in all FV/FVIII discoidin domains)	32
C) Mutations disrupting the β-strands S4 and S5			
Gln2100→Arg (1)	9 / 12	Ser87	1
Phe2101→Leu (2)	7-11 / 5	Tyr88 (aromatic in all FV/FVIII discoidin domains)	0
Phe2260→Cys (1) Phe2260→Ile (1)	<2 / n.d. 3 / n.d.	Tyr88 (aromatic in all FV/FVIII Ds domains)	0
Ile2262→Thr (1)	n.d. / n.d.	Ile90 (aliphatic in all FV/FVIII discoidin domains)	0
Gly2285→Val (1)	14 / 16	Gly115 (conserved in all FV/FVIII discoidin domains)	0

D) Mutations at the top of the barrel			
Tyr2105 → Cys (2)	8-14 / n.d.	Tyr92	10
Arg2116 → Pro (1)	<1 / n.d.	Arg103	33
Ser2119 → Tyr (2)	4-8 / 9	Ser106	108
Pro2300 → Leu (1) Pro2300 → Ser (1)	8 / n.d. 16 / n.d.	Pro130 (conserved in all FV/FVIII discoidin domains)	13
E) Mutations within the N-terminal loop or involved in its stabilization			
Glu2181 → Asp (1)	36 / n.d.	Glu8/Gln8 in all FV/FVIII-C2 domains)	20
Ile2185 → Thr (1)	23 / n.d.	Ile12 (conserved in all FV/FVIII discoidin domains)	0
Arg2209 → Gly (1) Arg2209 → Leu (1) Arg2209 → Gln (16) Arg2209 → Gln (1)	<1 / n.d. 3 / 3 <1 / 4 7 / 130	Arg37 (conserved in all FV/FVIII discoidin domains)	3
Gly2325 → Ser	n.d. / n.d.	Gly155 (conserved in all FV/FVIII discoidin domains)	0

A6: Programs and Data Bases Used

Structural comparisons were made after least-squares superposition with TURBO-Frodo (Roussel and Cambillau, 1989). Cavities were calculated with the program VOIDOO (Kleywegt and Jones, 1994) using a probe radius of 1.4 Å. Hydrogen bonds were calculated with the program HBPLUS (McDonald and Thornton, 1994), and residue accessibilities were determined with NACCESS (Hubbard et al., 1991). Plots of three-dimensional structures presented throughout this work have been prepared with SETOR (Evans, 1990), unless otherwise stated. Electrostatic calculations were performed with GRASP (Nicholls et al., 1993). Protein sequences were taken from the Swiss Prot Data Bank, DNA sequences from the EMBL Data Bank. Mutations identified in hemophilia patients were extracted from the hemophilia A data base (URL:http://europium.mrc.rpms.ac.uk, (Kemball-Cook and Tuddenham, 1997)).

A

Abe, K., Sakurada, K., Tanaka, M., Uehara, Y., Matsuno, K., Miyazaki, T., and Katoh, N. (1991). Phosphorylation of coagulation factor II by phospholipid/Ca^{2+}-dependent protein kinase (protein kinase C). Biochem. Biophys. Res. Commun. *176*, 1123-9.

Abrahams, J. P. (1997). Bias reduction in phase refinement by modified interference functions: introducing the γ correction. Acta Crystallogr. D *53*, 371-6.

Abrahams, J. P., and Leslie, A. G. W. (1996). Methods used in the structure determination of bovine mitochondrial F_1 ATPase. Acta Crystallogr. D *52*, 30-42.

Adler, M., Seto, M. H., Nitecki, D. E., Lin, J. H., Light, D. R., and Morser, J. (1995). The structure of a 19-residue fragment from the C-loop of the fourth epidermal growth factor-like domain of thrombomodulin. J. Biol. Chem. *270*, 23366-72.

Agarwala, K. L., Kawabata, S., Takao, T., Murata, H., Shimonishi, Y., Nishimura, H., and Iwanaga, S. (1994). Activation peptide of human factor IX has oligosaccharides *O*-glycosidically linked to threonine residues at 159 and 169. Biochemistry *33*, 5167-71.

Aloy, P., Catasus, L., Villegas, V., Reverter, D., Vendrell, J., and Aviles, F. X. (1998). Comparative analysis of the sequences and three-dimensional models of human procarboxypeptidases A1, A2 and B. Biol. Chem. *379*, 149-55.

Altieri, D. C. (1995). Xa receptor EPR-1. FASEB J. *9*, 860-5.

Ambrosini, G., Plescia, J., Chu, K. C., High, K. A., and Altieri, D. C. (1997). Activation-dependent exposure of the inter-EGF sequence Leu83-Leu88 in factor Xa mediates ligand binding to effector cell protease receptor-1. J. Biol. Chem. *272*, 8340-5.

Andersen, J. F., Weichsel, A., Balfour, C. A., Champagne, D. E., and Montfort, W. R. (1998). The crystal structure of nitrophorin 4 at 1.5 Å resolution: transport of nitric oxide by a lipocalin-based heme protein. Structure *6*, 1315-27.

Anderson, P. J. (1998). A dimeric form of prothrombin on membrane surfaces. Biochem. J. *336*, 631-8.

Andersson, L. O., and Brown, J. E. (1981). Interaction of factor VIII-von Willebrand factor with phospholipid vesicles. Biochem. J. *200*, 161-7.

Andree, H. A., Stuart, M. C., Hermens, W. T., Reutelingsperger, C. P., Hemker, H. C., Frederik, P. M., and Willems, G. M. (1992). Clustering of lipid-bound annexin V may explain its anticoagulant effect. J. Biol. Chem. *267*, 17907-12.

Andrews, R. K., Gorman, J. J., Booth, W. J., Corino, G. L., Castaldi, P. A., and Berndt, M. C. (1989). Cross-linking of a monomeric 39/34-kDa dispase fragment of von Willebrand factor (Leu-480/Val-481-Gly-718) to the N-terminal region of the α-chain of

membrane glycoprotein Ib on intact platelets with bis(sulfosuccinimidyl) suberate. Biochemistry *28*, 8326-36.

Antonarakis, S. E. (1995). Molecular genetics of coagulation factor VIII gene and hemophilia A. Thromb. Haemost. *74*, 322-8.

Aparicio, C., and Dahlbäck, B. (1996). Molecular mechanisms of activated protein C resistance. Properties of factor V isolated from an individual with homozygosity for the Arg506 to Gln mutation in the factor V gene. Biochem. J. *313*, 467-72.

Arni, R. K., Padmanabhan, K., Padmanabhan, K. P., Wu, T. P., and Tulinsky, A. (1994). Structure of the non-covalent complex of prothrombin kringle 2 with PPACK-thrombin. Chemistry & Physics of Lipids *67-68*, 59-66.

Arni, R. K., Padmanabhan, K., Padmanabhan, K. P., Wu, T. P., and Tulinsky, A. (1993). Structures of the noncovalent complexes of human and bovine prothrombin fragment 2 with human PPACK-thrombin. Biochemistry *32*, 4727-37.

Asakai, R., Davie, E. W., and Chung, D. W. (1987). Organization of the gene for human factor XI. Biochemistry *26*, 7221-8.

Ashton, A. W., Boehm, M. K., Johnson, D. J., Kemball-Cook, G., and Perkins, S. J. (1998). The solution structure of human coagulation factor VIIa in its complex with tissue factor is similar to free factor VIIa: a study of a heterodimeric receptor-ligand complex by X-ray and neutron scattering and computational modeling. Biochemistry *37*, 8208-17.

B

Baglia, F. A., and Walsh, P. N. (1996). A binding site for thrombin in the apple 1 domain of factor XI. J. Biol. Chem. *271*, 3652-8.

Baglia, F. A., and Walsh, P. N. (1998). Prothrombin is a cofactor for the binding of factor XI to the platelet surface and for platelet-mediated factor XI activation by thrombin. Biochemistry *37*, 2271-81.

Bajzar, L., Manuel, R., and Nesheim, M. E. (1995). Purification and characterization of TAFI, a thrombin-activable fibrinolysis inhibitor. J. Biol. Chem. *270*, 14477-84.

Bajzar, L., Nesheim, M., Morser, J., and Tracy, P. B. (1998). Both cellular and soluble forms of thrombomodulin inhibit fibrinolysis by potentiating the activation of thrombin-activable fibrinolysis inhibitor. J. Biol. Chem. *273*, 2792-8.

Baldwin, J. M., Schertler, G. F., and Unger, V. M. (1997). An α-carbon template for the transmembrane helices in the rhodopsin family of G-protein-coupled receptors. J. Mol. Biol. *272*, 144-64.

Banfield, D. K., and MacGillivray, R. T. (1992). Partial characterization of vertebrate prothrombin cDNAs: amplification and sequence analysis of the B chain of thrombin from nine different species. Proc. Natl Acad. Sci. USA *89*, 2779-83.

Banner, D. W. (1997). The factor VIIa/tissue factor complex. Thromb. Haemost. *78*, 512-5.

Banner, D. W., D'Arcy, A., Chene, C., Winkler, F. K., Guha, A., Konigsberg, W. H., Nemerson, Y., and Kirchhofer, D. (1996). The crystal structure of the complex of blood coagulation factor VIIa with soluble tissue factor. Nature *380*, 41-6.

Bardelle, C., Furie, B., Furie, B. C., and Gilbert, G. E. (1993). Membrane binding kinetics of factor VIII indicate a complex binding process. J. Biol. Chem. *268*, 8815-24.

Barnes, M. J., Knight, C. G., and Farndale, R. W. (1998). The collagen-platelet interaction. Curr. Opin. Hematol. *5*, 314-20.

Baron, M., Norman, D. G., Harvey, T. S., Handford, P. A., Mayhew, M., Tse, A. G., Brownlee, G. G., and Campbell, I. D. (1992). The three-dimensional structure of the first EGF-like module of human factor IX: comparison with EGF and TGF-al. Protein Sci. *1*, 81-90.

Barry, E. L., and Mosher, D. F. (1988). Factor XIII cross-linking of fibronectin at cellular matrix assembly sites. J. Biol. Chem. *263*, 10464-9.

Bar-Shavit, R., Benezra, M., Sabbah, V., Bode, W., and Vlodavsky, I. (1992). Thrombin as a multifunctional protein: induction of cell adhesion and proliferation. Am. J. Respiratory Cell Mol. Biol. *6*, 123-30.

Bar-Shavit, R., Kahn, A., Wilner, G. D., and Fenton, J. W. d. (1983). Monocyte chemotaxis: stimulation by specific exosite region in thrombin. Science *220*, 728-31.

Barton, G. J. (1993). ALSCRIPT: a tool to format multiple sequence alignments. Protein Eng. *6*, 37-40.

Basse, F., Stout, J. G., Sims, P. J., and Wiedmer, T. (1996). Isolation of an erythrocyte membrane protein that mediates Ca^{2+}-dependent transbilayer movement of phospholipid. J. Biol. Chem. *271*, 17205-10.

Baumgartner, S., Hofmann, K., Chiquetehrismann, R., and Bucher, P. (1998). The discoidin domain family revisited - new members from prokaryotes and a homology-based fold prediction. Protein Sci. *7*, 1626-31.

Bennett, J. S. (1996). Structural biology of glycoprotein IIb-IIIa. Trends Cardiovasc. Med. *6*, 31-6.

Berendes, R., Voges, D., Demange, P., Huber, R., and Burger, A. (1993). Structure-function analysis of the ion channel selectivity filter in human annexin V. Science *262*, 427-30.

Berndt, M. C., and Phillips, D. R. (1981). Interaction of thrombin with platelets: purification of the thrombin substrate. Ann. N. Y. Acad. Sci. *370*, 87-95.

Bernstein, F. C., Koetzle, T. F., Williams, G. J. B., Meyer, E. F., Brice, M. D., Rodgers, J. R., Kennard, O., Shimanouchi, T., and Tasumi, M. (1977). Protein data bank - Computer-based archival file for macromolecular structures. J. Mol. Biol. *112*, 535-42.

Bertina, R. M., Koeleman, B. P., Koster, T., Rosendaal, F. R., Dirven, R. J., de Ronde, H., van der Velden, P. A., and Reitsma, P. H. (1994). Mutation in blood coagulation factor V associated with resistance to activated protein C. Nature *369*, 64-7.

Betz, A., and Krishnaswamy, S. (1998). Regions remote from the site of cleavage determine macromolecular substrate recognition by the prothrombinase complex. J. Biol. Chem. *273*, 10709-18.

Bevers, E. M., Comfurius, P., Dekkers, D. W., and Zwaal, R. F. (1999). Lipid translocation across the plasma membrane of mammalian cells. Biochim. Biophys. Acta *1439*, 317-30.

Bevers, E. M., Rosing, J., and Zwaal, R. F. (1985). Development of procoagulant binding sites on the platelet surface. Adv. Exp. Med. Biol. *192*, 359-71.

Bezeaud, A., Elion, J., and Guillin, M. C. (1988). Functional characterization of thrombin Salakta: an abnormal thrombin derived from a human prothrombin variant. Blood *71*, 556-61.

Bi, L., Lawler, A. M., Antonarakis, S. E., High, K. A., Gearhart, J. D., and Kazazian, H. H., Jr. (1995). Targeted disruption of the mouse factor VIII gene produces a model of haemophilia A. Nature Gen. *10*, 119-21.

Bianchet, M. A., Bains, G., Pelosi, P., Pevsner, J., Snyder, S. H., Monaco, H. L., and Amzel, L. M. (1996). The three-dimensional structure of bovine odorant binding protein and its mechanism of odor recognition. Nature Struct. Biol. *3*, 934-9.

Bihoreau, N., Pin, S., de Kersabiec, A. M., Vidot, F., and Fontaine-Aupart, M. P. (1994). Copper-atom identification in the active and inactive forms of plasma-derived FVIII and recombinant FVIII-delta II. Eur. J. Biochem. *222*, 41-8.

Bjoern, S., Foster, D. C., Thim, L., Wiberg, F. C., Christensen, M., Komiyama, Y., Pedersen, A. H., and Kisiel, W. (1991). Human plasma and recombinant factor VII. Characterization of O-glycosylations at serine residues 52 and 60 and effects of site-directed mutagenesis of serine 52 to alanine. J. Biol. Chem. *266*, 11051-7.

Bjork, I., and Olson, S. T. (1997). Antithrombin. A bloody important serpin. Adv. Exp. Med. Biol. *425*, 17-33.

Blombäck, B., Blombäck, M., Hessel, B., and Iwanaga, S. (1967). Structure of N-terminal fragments of fibrinogen and specificity of thrombin. Nature *215*, 1445-8.

Blow, D. (2000). So do we understand how enzymes work?. Structure with Folding & Design *8*, R77-R81.

Bock, P. E. (1992). Active-site-selective labeling of blood coagulation proteinases with fluorescence probes by the use of thioester peptide chloromethyl ketones. II. Properties of thrombin derivatives as reporters of prothrombin fragment 2 binding and specificity of the labeling approach for other proteinases. J. Biol. Chem. *267*, 14974-81.

Bocskei, Z., Groom, C. R., Flower, D. R., Wright, C. E., Phillips, S. E., Cavaggioni, A., Findlay, J. B., and North, A. C. (1992). Pheromone binding to two rodent urinary proteins revealed by X-ray crystallography. Nature *360*, 186-8.

Bode, W., Brandstetter, H., Mather, T., and Stubbs, M. T. (1997). Comparative analysis of haemostatic proteinases: structural aspects of thrombin, factor Xa, factor IXa and protein C. Thromb. Haemost. *78*, 501-11.

Bode, W., and Huber, R. (1992). Natural protein proteinase inhibitors and their interaction with proteinases. Eur. J. Biochem. *204*, 433-51.

Bode, W., Mayr, I., Baumann, U., Huber, R., Stone, S. R., and Hofsteenge, J. (1989). The refined 1.9 Å crystal structure of human α-thrombin: interaction with D-Phe-Pro-Arg chloromethylketone and significance of the Tyr-Pro-Pro-Trp insertion segment. EMBO J. *8*, 3467-75.

Bode, W., Schwager, P., and Huber, R. (1976). Structural studies on the pancreatic trypsin inhibitor - trypsin complex and its free components: structure and function relationship in serine protease inhibition and catalysis. pp. 43-76. In: Ribbons DW, Brew K, ed. Proteolysis and physiological regulation. New York, Academic Press *11*.

Bode, W., Schwager, P., and Huber, R. (1978). The transition of bovine trypsinogen to a trypsin-like state upon strong ligand binding. The refined crystal structures of the bovine trypsinogen-pancreatic trypsin inhibitor complex and of its ternary complex with Ile-Val at 1.9 Å resolution. J. Mol. Biol. *118*, 99-112.

Bode, W., Turk, D., and Karshikov, A. (1992). The refined 1.9-Å X-ray crystal structure of D-Phe-Pro-Arg chloromethylketone-inhibited human α-thrombin: structure analysis, overall structure, electrostatic properties, detailed active-site geometry, and structure-function relationships. Protein Sci. *1*, 426-71.

Bouchard, B. A., Catcher, C. S., Thrash, B. R., Adida, C., and Tracy, P. B. (1997). Effector cell protease receptor-1, a platelet activation-dependent membrane protein, regulates prothrombinase-catalyzed thrombin generation. J. Biol. Chem. *272*, 9244-51.

Bourin, M. C., Lundgren-Akerlund, E., and Lindahl, U. (1990). Isolation and characterization of the glycosaminoglycan component of rabbit thrombomodulin proteoglycan. J. Biol. Chem. *265*, 15424-31.

Bourne, H. R. (1997). How receptors talk to trimeric G proteins. Curr. Opin. Cell Biol. *9*, 134-42.

Braat, E. A., Dooijewaard, G., and Rijken, D. C. (1999). Fibrinolytic properties of activated FXII. Eur. J. Biochem. *263*, 904-11.

Braden, B. C., and Poljak, R. J. (1995). Structural features of the reactions between antibodies and protein antigens. FASEB J. *9*, 9-16.

Bradford, H. N., Dela Cadena, R. A., Kunapuli, S. P., Dong, J. F., Lopez, J. A., and Colman, R. W. (1997). Human kininogens regulate thrombin binding to platelets through the glycoprotein Ib-IX-V complex. Blood *90*, 1508-15.

Brandstetter, H., Bauer, M., Huber, R., Lollar, P., and Bode, W. (1995). X-Ray structure of clotting factor IXa - Active site and module structure related to Xase activity and hemophilia B. Proc. Natl Acad. Sci. USA *92*, 9796-800.

Brandstetter, H., Künhe, A., Bode, W., Huber, R., von de Saal, W., Wirthensohn, K., and Engh, R. A. (1996). X-ray structure of active site-inhibited clotting factor Xa: Implications for drug design and substrate recognition. J. Biol. Chem. *271*, 29988-92.

Brown, J. H., Volkmann, N., Jun, G., Henschen-Edman, A. H., and Cohen, C. (2000). The crystal structure of modified bovine fibrinogen. Proc. Natl Acad. Sci. USA *97*, 85-90.

Brownlow, S., Morais Cabral, J. H., Cooper, R., Flower, D. R., Yewdall, S. J., Polikarpov, I., North, A. C., and Sawyer, L. (1997). Bovine β-lactoglobulin at 1.8 Å resolution - Still an enigmatic lipocalin. Structure *5*, 481-95.

Broze, G. J., Jr. (1995). Tissue factor pathway inhibitor and the current concept of blood coagulation. Blood Coagul. Fibrinolysis *6*, S7-13.

Broze, G. J., Jr. (1995). Tissue factor pathway inhibitor and the revised theory of coagulation. Annu. Rev. Med. *46*, 103-12.

Broze, G. J., Jr., and Higuchi, D. A. (1996). Coagulation-dependent inhibition of fibrinolysis: role of carboxypeptidase-U and the premature lysis of clots from hemophilic plasma. Blood *88*, 3815-23.

Broze, G. J., Jr., and Miletich, J. P. (1984). Human protein Z. J. Clin. Invest. *73*, 933-8.

Brünger, A., Kuryian, K., Karplus, M. (1987). Crystallografic R factor refinement by molecular dynamics. Science *235*, 458-460.

Brünger, G. J. (1993). XPLOR (version 3.1) A system for X-ray crystallography and NMR (New Haven, CT: Yale University Press).

Bugge, T. H., Flick, M. J., Daugherty, C. C., and Degen, J. L. (1995). Plasminogen deficiency causes severe thrombosis but is compatible with development and reproduction. Genes Devel. *9*, 794-807.

Bugge, T. H., Xiao, Q., Kombrinck, K. W., Flick, M. J., Holmback, K., Danton, M. J., Colbert, M. C., Witte, D. P., Fujikawa, K., Davie, E. W., and Degen, J. L. (1996). Fatal embryonic bleeding events in mice lacking tissue factor, the cell-associated initiator of blood coagulation. Proc. Natl Acad. Sci. USA *93*, 6258-63.

Burgering, M. J., Orbons, L. P., van der Doelen, A., Mulders, J., Theunissen, H. J., Grootenhuis, P. D., Bode, W., Huber, R., and Stubbs, M. T. (1997). The second Kunitz domain of human tissue factor pathway inhibitor: cloning, structure determination and interaction with factor Xa. J. Mol. Biol. *269*, 395-407.

Butenas, S., van 't Veer, C., and Mann, K. G. (1997). Evaluation of the initiation phase of blood coagulation using ultrasensitive assays for serine proteases. J. Biol. Chem. *272*, 21527-33.

Byeon, I. J., Kelley, R. F., and Llinas, M. (1991). Kringle-2 domain of the tissue-type plasminogen activator. 1H-NMR assignments and secondary structure. Eur. J. Biochem. *197*, 155-65.

Byeon, I. J., and Llinas, M. (1991). Solution structure of the tissue-type plasminogen activator kringle 2 domain complexed to 6-aminohexanoic acid, an antifibrinolytic drug. J. Mol. Biol. *222*, 1035-51.

Byzova, T. V., and Plow, E. F. (1997). Networking in the hemostatic system. Integrin αIIbβ3 binds prothrombin and influences its activation. J. Biol. Chem. *272*, 27183-8.

C

Calvete, J. J. (1994). Clues for understanding the structure and function of a prototypic human integrin: the platelet glycoprotein IIb/IIIa complex. Thromb. Haemost. *72*, 1-15.

Calvete, J. J. (1999). Platelet integrin GPIIb/IIIa: structure-function correlations. An update and lessons from other integrins. Proc. Soc. Exp. Biol. Med. *222*, 29-38.

Camerer, E., Huang, W., and Coughlin, S. R. (2000). Tissue factor- and factor X-dependent activation of protease-activated receptor 2 by factor VIIa. Proc. Natl Acad. Sci. USA *97*, 5255-60.

Camerer, E., Kolsto, A. B., and Prydz, H. (1996). Cell biology of tissue factor, the principal initiator of blood coagulation. Thromb. Res. *81*, 1-41.

Campbell, I. D., and Bork, P. (1993). Epidermal growth factor-like modules. Curr. Opin. Struct. Biol. *3*, 385-92.

Carlisle, T. L., Bock, P. E., and Jackson, C. M. (1990). Kinetic intermediates in prothrombin activation. Bovine prethrombin 1 conversion to thrombin by factor X. J. Biol. Chem. *265*, 22044-55.

Carmeliet, P., and Collen, D. (1996). Genetic analysis of the plasminogen and coagulation system in mice. Haemostasis *26*, 132-53.

Carmeliet, P., Mackman, N., Moons, L., Luther, T., Gressens, P., Van Vlaenderen, I., Demunck, H., Kasper, M., Breier, G., Evrard, P., et al. (1996). Role of tissue factor in embryonic blood vessel development. Nature *383*, 73-5.

Carrell, R. W., Stein, P. E., Fermi, G., and Wardell, M. R. (1994). Biological implications of a 3 Å structure of dimeric antithrombin. Structure *2*, 257-70.

Castillo, M. J., Kurachi, K., Nishino, N., Ohkubo, I., and Powers, J. C. (1983). Reactivity of bovine blood coagulation factor IXa β, factor Xa β, and factor XIa toward fluorogenic peptides containing the activation site sequences of bovine factor IX and factor X. Biochemistry *22*, 1021-9.

Cawthern, K. M., van 't Veer, C., Lock, J. B., DiLorenzo, M. E., Branda, R. F., and Mann, K. G. (1998). Blood coagulation in hemophilia A and hemophilia C. Blood *91*, 4581-92.

Celie, P. H., Lenting, P. J., and Mertens, K. (2000). Hydrophobic contact between the two epidermal growth factor-like domains of blood coagulation factor IX contributes to enzymatic activity. J. Biol. Chem. *275*, 229-34.

Champagne, D. E., Nussenzveig, R. H., and Ribeiro, J. M. C. (1995). Purification, partial characterization, and cloning of nitric oxide-carrying heme proteins (nitrophorins) from salivary glands of the blood-sucking insect *Rhodnius prolixus*. J. Biol. Chem. *270*, 8691-95.

Chan, J. C., Carmeliet, P., Moons, L., Rosen, E. D., Huang, Z. F., Broze, G. J., Jr., Collen, D., and Castellino, F. J. (1999). Factor VII deficiency rescues the intrauterine lethality in mice associated with a tissue factor pathway inhibitor deficit. J. Clin. Invest. *103*, 475-82.

Chang, Y., Mochalkin, I., McCance, S. G., Cheng, B., Tulinsky, A., and Castellino, F. J. (1998). Structure and ligand binding determinants of the recombinant kringle 5 domain of human plasminogen. Biochemistry *37*, 3258-71.

Chasan, R., Jin, Y., and Anderson, K. V. (1992). Activation of the *easter* zymogen is regulated by five other genes to define dorsal-ventral polarity in the *Drosophila* embryo. Development *115*, 607-16.

Cho, K., Tanaka, T., Cook, R. R., Kisiel, W., Fujikawa, K., Kurachi, K., and Powers, J. C. (1984). Active-site mapping of bovine and human blood coagulation serine proteases using synthetic peptide 4-nitroanilide and thio ester substrates. Biochemistry *23*, 644-50.

Christophe, O. D., Lenting, P. J., Kolkman, J. A., Brownlee, G. G., and Mertens, K. (1998). Blood coagulation factor IX residues Glu78 and Arg94 provide a link between both epidermal growth factor-like domains that is crucial in the interaction with factor VIII light chain. J. Biol. Chem. *273*, 222-7.

Chung, D. W., Fujikawa, K., McMullen, B. A., and Davie, E. W. (1986). Human plasma prekallikrein, a zymogen to a serine protease that contains four tandem repeats. Biochemistry *25*, 2410-7.

Church, W. R., Jernigan, R. L., Toole, J., Hewick, R. M., Knopf, J., Knutson, G. J., Nesheim, M. E., Mann, K. G., and Fass, D. N. (1984). Coagulation factors V and VIII and ceruloplasmin constitute a family of structurally related proteins. Proc. Natl Acad. Sci. USA *81*, 6934-7.

Cirino, G., Cicala, C., Bucci, M., Sorrentino, L., Ambrosini, G., DeDominicis, G., and Altieri, D. C. (1997). Factor Xa as an interface between coagulation and inflammation. Molecular mimicry of factor Xa association with effector cell protease receptor-1 induces acute inflammation in vivo. J. Clin. Invest. *99*, 2446-51.

Clarke, J. H., Light, D. R., Blasko, E., Parkinson, J. F., Nagashima, M., McLean, K., Vilander, L., Andrews, W. H., Morser, J., and Glaser, C. B. (1993). The short loop between epidermal growth factor-like domains 4 and 5 is critical for human thrombomodulin function. J. Biol. Chem. *268*, 6309-15.

Coles, M., Diercks, T., Muehlenweg, B., Bartsch, S., Zolzer, V., Tschesche, H., and Kessler, H. (1999). The solution structure and dynamics of human neutrophil gelatinase-associated lipocalin. J. Mol. Biol. *289*, 139-57.

Coll, M., Guasch, A., Aviles, F. X., and Huber, R. (1991). Three-dimensional structure of porcine procarboxypeptidase B: a structural basis of its inactivity. EMBO J. *10*, 1-9.

Collaborative Computational Project No. 4 (1994). The CCP4 suite: programs for protein crystallography. Acta Crystallogr. D *50*, 760-3.

Colman, R. W., and Schmaier, A. H. (1997). Contact system: a vascular biology modulator with anticoagulant, profibrinolytic, antiadhesive, and proinflammatory attributes. Blood *90*, 3819-43.

Colwell, N. S., Blinder, M. A., Tsiang, M., Gibbs, C. S., Bock, P. E., and Tollefsen, D. M. (1998). Allosteric effects of a monoclonal antibody against thrombin exosite II. Biochemistry *37*, 15057-65.

Comfurius, P., Smeets, E. F., Willems, G. M., Bevers, E. M., and Zwaal, R. F. A. (1994). Assembly of the prothrombinase complex on lipid vesicles depends on the stereochemical configuration of the polar headgroup of phosphatidylserine. Biochemistry *33*, 10319-24.

Concha, N. O., Head, J. F., Kaetzel, M. A., Dedman, J. R., and Seaton, B. A. (1993). Rat annexin V crystal structure: Ca^{2+}-induced conformational changes. Science *261*, 1321-24.

Connolly, A. J., Ishihara, H., Kahn, M. L., Farese, R. V., Jr., and Coughlin, S. R. (1996). Role of the thrombin receptor in development and evidence for a second receptor. Nature *381*, 516-9.

Conway, E. M., Nowakowski, B., and Steiner-Mosonyi, M. (1994). Thrombomodulin lacking the cytoplasmic domain efficiently internalizes thrombin *via* nonclathrin-coated, pit-mediated endocytosis. J. Cell. Physiol. *158*, 285-98.

Conway, E. M., Pollefeyt, S., Collen, D., and Steiner-Mosonyi, M. (1997). The amino terminal lectin-like domain of thrombomodulin is required for constitutive endocytosis. Blood *89*, 652-61.

Cool, D. E., and MacGillivray, R. T. (1987). Characterization of the human blood coagulation factor XII gene. Intron/exon gene organization and analysis of the 5'-flanking region. J. Biol. Chem. *262*, 13662-73.

Coombs, G. S., Rao, M. S., Olson, A. J., Dawson, P. E., and Madison, E. L. (1999). Revisiting catalysis by chymotrypsin family serine proteases using peptide substrates and inhibitors with unnatural main chains. J. Biol. Chem. *274*, 24074-9.

Coppolino, M. G., Woodside, M. J., Demaurex, N., Grinstein, S., St-Arnaud, R., and Dedhar, S. (1997). Calreticulin is essential for integrin-mediated calcium signalling and cell adhesion. Nature *386*, 843-7.

Côté, H. C., Bajzar, L., Stevens, W. K., Samis, J. A., Morser, J., MacGillivray, R. T., and Nesheim, M. E. (1997). Functional characterization of recombinant human meizothrombin and meizothrombin(desF1). Thrombomodulin-dependent activation of protein C and thrombin-activatable fibrinolysis inhibitor (TAFI), platelet aggregation, antithrombin-III inhibition. J. Biol. Chem. *272*, 6194-200.

Coughlin, S. R. (1999). How the protease thrombin talks to cells. Proc. Natl Acad. Sci. USA *96*, 11023-7.

Cox, M., Schaller, J., Boelens, R., Kaptein, R., Rickli, E., and Llinas, M. (1994). Kringle solution structures *via* NMR: two-dimensional 1H-NMR analysis of horse plasminogen kringle 4. Chemistry & Physics of Lipids *67-68*, 43-58.

Cui, J., O'Shea, K. S., Purkayastha, A., Saunders, T. L., and Ginsburg, D. (1996). Fatal haemorrhage and incomplete block to embryogenesis in mice lacking coagulation factor V. Nature *384*, 66-8.

Cutsforth, G. A., Koppaka, V., Krishnaswamy, S., Wu, J. R., Mann, K. G., and Lentz, B. R. (1996). Insights into the complex association of bovine factor Va with acidic-lipid-containing synthetic membranes. Biophys. J. *70*, 2938-49.

D

Dahlbäck, B. (1991). Protein S and C4b-binding protein: components involved in the regulation of the protein C anticoagulant system. Thromb. Haemost. *66*, 49-61.

Dang, Q. D., Guinto, E. R., and di Cera, E. (1997). Rational engineering of activity and specificity in a serine protease. Nature Biotech. *15*, 146-9.

Dang, Q. D., Sabetta, M., and Di Cera, E. (1997). Selective loss of fibrinogen clotting in a loop-less thrombin. J. Biol. Chem. *272*, 19649-51.

Darrow, A. L., Fung-Leung, W. P., Ye, R. D., Santulli, R. J., Cheung, W. M., Derian, C. K., Burns, C. L., Damiano, B. P., Zhou, L., Keenan, C. M., et al. (1996). Biological consequences of thrombin receptor deficiency in mice. Thromb. Haemost. *76*, 860-6.

Davie, E. W., Fujikawa, K., and Kisiel, W. (1991). The coagulation cascade: Initiation, maintenance and regulation. Biochemistry *30*, 10363-70.

Davie, E. W., and Ratnoff, O. D. (1964). Waterfall sequence for intrinsic blood clotting. Science *145*, 1310-2.

de Cristofaro, R., de Candia, E., Croce, G., Morosetti, R., and Landolfi, R. (1998). Binding of human α-thrombin to platelet GpIb: energetics and functional effects. Biochem. J. *332*, 643-50.

De Cristofaro, R., De Candia, E., Rutella, S., and Weitz, J. I. (2000). The Asp(272)-Glu(282) region of platelet glycoprotein Ib α interacts with the heparin-binding site of α-thrombin and protects the enzyme from the heparin-catalyzed inhibition by antithrombin III. J. Biol. Chem. *275*, 3887-95.

de la Fortelle, E., and Bricogne, G. (1997). Maximum-likelihood heavy-atom parameter refinement for the multiple isomorphous replacement and multiwavelength anomalous diffraction methods. In Methods Enzymol., C. W. Carter, Jr. and R. M. Sweet, eds. (New York: Academic Press), pp. 472-94.

De Marco, L., Mazzucato, M., Masotti, A., and Ruggeri, Z. M. (1994). Localization and characterization of an α-thrombin-binding site on platelet glycoprotein Ib α. J. Biol. Chem. *269*, 6478-84.

de Vos, A. M., Ultsch, M. H., Kelley, R. F., Padmanabhan, K., Tulinsky, A., Westbrook, M. L., and Kossiakoff, A. A. (1992). Crystal structure of the kringle 2 domain of tissue plasminogen activator at 2.4-Å resolution. Biochemistry *31*, 270-9.

Degen, S. J., and Sun, W. Y. (1998). The biology of prothrombin. Crit. Rev. Eukaryot. Gene Expression *8*, 203-24.

Deguchi, H., Takeya, H., Gabazza, E. C., Nishioka, J., and Suzuki, K. (1997). Prothrombin kringle 1 domain interacts with factor Va during the assembly of prothrombinase complex. Biochem. J. *321*, 729-35.

DeLotto, R., and Spierer, P. (1986). A gene required for the specification of dorsal-ventral pattern in *Drosophila* appears to encode a serine protease. Nature *323*, 688-692.

Denis, C., Methia, N., Frenette Paul, S., Rayburn, H., Ullman-Cullere, M., Hynes Richard, O., and Wagner Denisa, D. (1998). A mouse model of severe von Willebrand disease: Defects in hemostasis and thrombosis. Proc. Natl Acad. Sci. USA *95*, 9524-9.

Denninger, J. W., and Marletta, M. A. (1999). Guanylate cyclase and the .NO/cGMP signaling pathway. Biochim. Biophys. Acta *1411*, 334-50.

Dennis, M. S., Eigenbrot, C., Skelton, N. J., Ultsch, M. H., Santell, L., Dwyer, M. A., O'Connell, M. P., and Lazarus, R. A. (2000). Peptide exosite inhibitors of factor VIIa as anticoagulants. Nature *404*, 465-70.

Devaux, P. F. (1992). Protein involvement in transmembrane lipid asymmetry. Annu. Rev. Biophys. Biomolec. Struct. *21*, 417-39.

Devaux, P. F. (1991). Static and dynamic lipid asymmetry in cell membranes. Biochemistry *30*, 1163-73.

Dharmawardana, K. R., and Bock, P. E. (1998). Demonstration of exosite I-dependent interactions of thrombin with human factor V and factor Va involving the factor Va heavy chain: analysis by affinity chromatography employing a novel method for active-site-selective immobilization of serine proteinases. Biochemistry *37*, 13143-52.

Dharmawardana, K. R., Olson, S. T., and Bock, P. E. (1999). Role of regulatory exosite I in binding of thrombin to human factor V, factor Va, factor Va subunits, and activation fragments. J. Biol. Chem. *274*, 18635-43.

Di Cera, E., Dang, Q. D., and Ayala, Y. M. (1997). Molecular mechanisms of thrombin function. Cell. Mol. Life Sci. *53*, 701-30.

Di Cera, E., Guinto, E. R., Vindigni, A., Dang, Q. D., Ayala, Y. M., Wuyi, M., and Tulinsky, A. (1995). The Na^+ binding site of thrombin. J. Biol. Chem. *270*, 22089-92.

Di Scipio, R. G., Hermodson, M. A., and Davie, E. W. (1977). Activation of human factor X (Stuart factor) by a protease from Russell's viper venom. Biochemistry *16*, 5253-60.

Di Scipio, R. G., Kurachi, K., and Davie, E. W. (1978). Activation of human factor IX (Christmas factor). J. Clin. Invest. *61*, 1528-38.

Dickinson, C. D., Kelly, C. R., and Ruf, W. (1996). Identification of surface residues mediating tissue factor binding and catalytic function of the serine protease factor VIIa. Proc. Natl Acad. Sci. USA *93*, 14379-84.

Ding, X. D., Weichsel, A., Andersen, J. F., Shokhireva, T. K., Balfour, C., Pierik, A. J., Averill, B. A., Montfort, W. R., and Walker, F. A. (1999). Nitric oxide binding to the ferri- and ferroheme states of nitrophorin 1, a reversible NO-binding heme protein from the saliva of the blood-sucking insect, *Rhodnius prolixus*. J. Am. Chem. Soc. *121*, 128-38.

Dittman, W. A., Kumada, T., Sadler, J. E., and Majerus, P. W. (1988). The structure and function of mouse thrombomodulin. Phorbol myristate acetate stimulates degradation and synthesis of thrombomodulin without affecting mRNA levels in hemangioma cells. J. Biol. Chem. *263*, 15815-22.

Dittman, W. A., and Majerus, P. W. (1990). Structure and function of thrombomodulin: a natural anticoagulant. Blood *75*, 329-36.

Doggen, C. J., Kunz, G., Rosendaal, F. R., Lane, D. A., Vos, H. L., Stubbs, P. J., Manger Cats, V., and Ireland, H. (1998). A mutation in the thrombomodulin gene, 127G to A coding for Ala25Thr, and the risk of myocardial infarction in men. Thromb. Haemost. *80*, 743-8.

Dolis, D., Moreau, C., Zachowski, A., and Devaux, P. F. (1997). Aminophospholipid translocase and proteins involved in transmembrane phospholipid traffic. Biophys. Chem. *68*, 221-31.

Doolittle, R. F. (1984). Fibrinogen and fibrin. Annu. Rev. Biochem. *53*, 195-229.

Doolittle, R. F., Spraggon, G., and Everse, S. J. (1998). Three-dimensional structural studies on fragments of fibrinogen and fibrin. Curr. Opin. Struct. Biol. *8*, 792-8.

Downing, A. K., Knott, V., Werner, J. M., Cardy, C. M., Campbell, I. D., and Handford, P. A. (1996). Solution structure of a pair of calcium-binding epidermal growth factor-like domains: implications for the Marfan syndrome and other genetic disorders. Cell *85*, 597-605.

Doyle, M. F., and Mann, K. G. (1990). Multiple active forms of thrombin. IV. Relative activities of meizothrombins. J. Biol. Chem. *265*, 10693-701.

Du, X., Saido, T. C., Tsubuki, S., Indig, F. E., Williams, M. J., and Ginsberg, M. H. (1995). Calpain cleavage of the cytoplasmic domain of the integrin β3 subunit. J. Biol. Chem. *270*, 26146-51.

Duchosal, M. A., Rothermel, A. L., McConahey, P. J., Dixon, F. J., and Altieri, D. C. (1996). In vivo immunosuppression by targeting a novel protease receptor. Nature *380*, 352-6.

Duffy, E. J., Parker, E. T., Mutucumarana, V. P., Johnson, A. E., and Lollar, P. (1992). Binding of factor VIIIa and factor VIII to factor IXa on phospholipid vesicles. J. Biol. Chem. *267*, 17006-11.

E

Eaton, D. L., Malloy, B. E., Tsai, S. P., Henzel, W., and Drayna, D. (1991). Isolation, molecular cloning, and partial characterization of a novel carboxypeptidase B from human plasma. J. Biol. Chem. *266*, 21833-8.

Edano, T., Kumai, N., Mizoguchi, T., and Ohkuchi, M. (1998). The glycosylation sites and structural characteristics of oligosaccharides on recombinant human thrombomodulin. Intern. J. Biochem. Cell Biol. *30*, 77-88.

Elisen, M. G., von dem Borne, P. A., Bouma, B. N., and Meijers, J. C. (1998). Protein C inhibitor acts as a procoagulant by inhibiting the thrombomodulin-induced activation of protein C in human plasma. Blood *91*, 1542-7.

Emsley, J., Cruz, M., Handin, R., and Liddington, R. (1998). Crystal structure of the von Willebrand factor A1 domain and implications for the binding of platelet glycoprotein Ib. J. Biol. Chem. *273*, 10396-401.

Emsley, J., King, S. L., Bergelson, J. M., and Liddington, R. C. (1997). Crystal structure of the I domain from integrin α2β1. J. Biol. Chem. *272*, 28512-7.

Emsley, J., Knight, C. G., Farndale, R. W., Barnes, M. J., and Liddington, R. C. (2000). Structural basis of collagen recognition by integrin α2β1. Cell *101*, 47-56.

Engelmann, B., Kogl, C., Kulschar, R., and Schaipp, B. (1996). Transfer of phosphatidylcholine, phosphatidylethanolamine and sphingomyelin from low- and high-density lipoprotein to human platelets. Biochem. J. *315*, 781-9.

Engelmann, B., Schaipp, B., Dobner, P., Stoeckelhuber, M., Kogl, C., Siess, W., and Hermetter, A. (1998). Platelet agonists enhance the import of phosphatidylethanolamine into human platelets. J. Biol. Chem. *273*, 27800-8.

Engh, R., and Huber, R. (1991). Accurate bond and angle parameters for X-ray protein structure refinement. Acta Crystallogr. A *47*, 392-400.

Esmon, C. T. (1997). Defects in natural anticoagulant pathways as potential risk factors for myocardial infarction. Circulation *96*, 9-11.

Esmon, C. T. (1979). The subunit structure of thrombin-activated factor V. Isolation of activated factor V, separation of subunits, and reconstitution of biological activity. J. Biol. Chem. *254*, 964-73.

Esmon, C. T. (1995). Thrombomodulin as a model of molecular mechanisms that modulate protease specificity and function at the vessel surface. FASEB J. *9*, 946-55.

Esmon, C. T., Esmon, N. L., and Harris, K. W. (1982). Complex formation between thrombin and thrombomodulin inhibits both thrombin-catalyzed fibrin formation and factor V activation. J. Biol. Chem. *257*, 7944-7.

Esmon, C. T., and Lollar, P. (1996). Involvement of thrombin anion-binding exosites 1 and 2 in the activation of factor V and factor VIII. J. Biol. Chem. *271*, 13882-7.

Esmon, C. T., and Owen, W. G. (1981). Identification of an endothelial cell cofactor for thrombin-catalyzed activation of protein C. Proc. Natl Acad. Sci. USA *78*, 2249-52.

Esmon, C. T., Owen, W. G., and Jackson, C. M. (1974). A plausible mechanism for prothrombin activation by factor Xa, factor Va, phospholipid, and calcium ions. J. Biol. Chem. *249*, 8045-7.

Esmon, N. L., Carroll, R. C., and Esmon, C. T. (1983). Thrombomodulin blocks the ability of thrombin to activate platelets. J. Biol. Chem. *258*, 12238-42.

Esmon, N. L., Owen, W. G., and Esmon, C. T. (1982). Isolation of a membrane-bound cofactor for thrombin-catalyzed activation of protein C. J. Biol. Chem. *257*, 859-64.

Evans, P. R. (1993). Data reduction. In Proceedings of the CCP4 study weekend, 1993, on data collection and processing, pp. 114-122.

Evans, S. V. (1990). SETOR: hardware lighted three-dimensional solid model representations of macromolecules. J. Mol. Graphics *11*, 134-8.

Everse, S. J., Spraggon, G., Veerapandian, L., Riley, M., and Doolittle, R. F. (1998). Crystal structure of fragment double-D from human fibrin with two different bound ligands. Biochemistry *37*, 8637-42.

F

Fay, P. F., Chavin, S. I., Meyer, D., and Marder, V. J. (1986). Non-enzymatic cofactors: Factor VIII. In Blood coagulation, R. F. A. Zwaal and H. C. Hemker, eds. (New York: Elsevier), pp. 35.

Fay, P. J. (1988). Reconstitution of human factor VIII from isolated subunits. Arch. Biochem. Biophys. *262*, 525-31.

Fay, P. J., Haidaris, P. J., and Smudzin, T. M. (1991). Human factor VIIIa subunit structure. Reconstruction of factor VIIIa from the isolated A1/A3-C1-C2 dimer and A2 subunit. J. Biol. Chem. *266*, 8957-62.

Fay, P. J., and Koshibu, K. (1998). The A2 subunit of factor VIIIa modulates the active site of factor IXa. J. Biol. Chem. *273*, 19049-54.

Fay, P. J., and Smudzin, T. M. (1992). Characterization of the interaction between the A2 subunit and A1/A3-C1-C2 dimer in human factor VIIIa. J. Biol. Chem. *267*, 13246-50.

Fenton, J. W. d., Ni, F., Witting, J. I., Brezniak, D. V., Andersen, T. T., and Malik, A. B. (1993). The rational design of thrombin-directed antithrombotics. Adv. Exp. Med. Biol. *340*, 1-13.

Fenton, J. W. d., Ofosu, F. A., Moon, D. G., and Maraganore, J. M. (1991). Thrombin structure and function: why thrombin is the primary target for antithrombotics. Blood Coagul. Fibrinolysis *2*, 69-75.

Fernandez, J . A., Hackeng T. M., Kojima, K., and Griffin, J. H. (1997). The carbohydrate moiety of factor V modulates inactivation by activated protein C. Blood *89*, 4348-54.

Flower, D. R. (1996). The lipocalin protein family: structure and function. Biochem. J. *318*, 1-14.

Flower, D. R., North, A. C., and Attwood, T. K. (1993). Structure and sequence relationships in the lipocalins and related proteins. Protein Sci. *2*, 753-61.

Foster, D., and Davie, E. W. (1984). Characterization of a cDNA coding for human protein C. Proc. Natl Acad. Sci. USA *81*, 4766-70.

Foster, P. A., Fulcher, C. A., Houghten, R. A., and Zimmerman, T. S. (1990). Synthetic factor VIII peptides with amino acid sequences contained within the C2 domain of factor VIII inhibit factor VIII binding to phosphatidylserine. Blood *75*, 1999-2004.

Foster, W. B., Nesheim, M. E., and Mann, K. G. (1983). The factor Xa-catalyzed activation of factor V. J. Biol. Chem. *258*, 13970-7.

Fox, J. E., Aggerbeck, L. P., and Berndt, M. C. (1988). Structure of the glycoprotein Ib.IX complex from platelet membranes. J. Biol. Chem. *263*, 4882-90.

Francischetti, I. M. B., Ribeiro, J. M. C., Champagne, D., and Andersen, J. (2000). Purification, cloning, expression, and mechanism of action of a novel platelet aggregation inhibitor from the salivary gland of the blood-sucking bug, *Rhodnius prolixus*. J. Biol. Chem. *275*, 12639-50.

Fredenburgh, J. C., Stafford, A. R., and Weitz, J. I. (1997). Evidence for allosteric linkage between exosites 1 and 2 of thrombin. J. Biol. Chem. *272*, 25493-9.

Freedman, S. J., Blostein, M. D., Baleja, J. D., Jacobs, M., Furie, B. C., and Furie, B. (1996). Identification of the phospholipid binding site in the vitamin K-dependent blood coagulation protein factor IX. J. Biol. Chem. *271*, 16227-36.

Freedman, S. J., Furie, B. C., Furie, B., and Baleja, J. D. (1995). Structure of the calcium ion-bound γ-carboxyglutamic acid-rich domain of factor IX. Biochemistry *34*, 12126-37.

Freedman, S. J., Furie, B. C., Furie, B., and Baleja, J. D. (1995). Structure of the metal-free γ-carboxyglutamic acid-rich membrane binding region of factor IX by two-dimensional NMR spectroscopy. J. Biol. Chem. *270*, 7980-7.

Fryklund, L., Borg, H., and Andersson, L. O. (1976). Amino-terminal sequence of human factor IX: presence of gamma-carboxyl glumatic acid residues. FEBS Lett. *65*, 187-9.

Fuentes-Prior, P., Noeske-Jungblut, C., Donner, P., Schleuning, W. D., Huber, R., and Bode, W. (1997). Structure of the thrombin complex with triabin, a lipocalin-like exosite-binding inhibitor derived from a triatomine bug. Proc. Natl Acad. Sci. USA *94*, 11845-50.

Fujikawa, K., Chung, D. W., Hendrickson, L. E., and Davie, E. W. (1986). Amino acid sequence of human factor XI, a blood coagulation factor with four tandem repeats that are highly homologous with plasma prekallikrein. Biochemistry *25*, 2417-24.

Fujimura, Y., Titani, K., Holland, L. Z., Russell, S. R., Roberts, J. R., Elder, J. H., Ruggeri, Z. M., and Zimmerman, T. S. (1986). von Willebrand factor. A reduced and alkylated 52/48-kDa fragment beginning at amino acid residue 449 contains the domain interacting with platelet glycoprotein Ib. J. Biol. Chem. *261*, 381-5.

Fukudome, K., and Esmon, C. T. (1994). Identification, cloning, and regulation of a novel endothelial cell protein C/activated protein C receptor. J. Biol. Chem. *269*, 26486-91.

Fukudome, K., Ye, X., Tsuneyoshi, N., Tokunaga, O., Sugawara, K., Mizokami, H., and Kimoto, M. (1998). Activation mechanism of anticoagulant protein C in large blood vessels involving the endothelial cell protein C receptor. J. Exp. Med. *187*, 1029-35.

Funakoshi, T., Hendrickson, L. E., McMullen, B. A., and Fujikawa, K. (1987). Primary structure of human placental anticoagulant protein. Biochemistry *26*, 8087-92.

Furie, B., and Furie, B. C. (1988). The molecular basis of blood coagulation. Cell *53*, 505-18.

Furie, B. C., and Furie, B. (1997). Structure and mechanism of action of the vitamin K-dependent γ-glutamyl carboxylase: recent advances from mutagenesis studies. Thromb. Haemost. *78*, 595-8.

Furman, M. I., Liu, L., Benoit, S. E., Becker, R. C., Barnard, M. R., and Michelson, A. D. (1998). The cleaved peptide of the thrombin receptor is a strong platelet agonist. Proc. Natl Acad. Sci. USA *95*, 3082-7.

G

Gaboriaud, C., Rossi, V., Fontecilla-Camps, J. C., and Arlaud, G. J. (1998). Evolutionary conserved rigid module-domain interactions can be detected at the sequence level: the examples of complement and blood coagulation proteases. J. Mol. Biol. *282*, 459-70.

Gailani, D., and Broze, G. J., Jr. (1991). Factor XI activation in a revised model of blood coagulation. Science *253*, 909-12.

Gardner, J. M., and Hynes, R. O. (1985). Interaction of fibronectin with its receptor on platelets. Cell *42*, 439-48.

Gerads, I., Govers-Riemslag, J. W. P., Tans, G., Zwaal, R. F. A., and Rosing, J. (1990). Prothrombin activation on membranes with anionic phospholipids containing phosphate, sulfate and/or carboxyl groups. J. Biol. Chem. *29*, 7967-74.

Gerlitz, B., and Grinnell, B. W. (1996). Mutation of protease domain residues Lys37-39 in human protein C inhibits activation by the thrombomodulin-thrombin complex without affecting activation by free thrombin. J. Biol. Chem. *271*, 22285-8.

Gerrard, A. J., Hudson, D. L., Brownlee, G. G., and Watt, F. M. (1993). Towards gene therapy for haemophilia B using primary human keratinocytes. Nature Gen. *3*, 180-3.

Gerszten, R. E., Chen, J., Ishii, M., Ishii, K., Wang, L., Nanevicz, T., Turck, C. W., Vu, T. K., and Coughlin, S. R. (1994). Specificity of the thrombin receptor for agonist peptide is defined by its extracellular surface. Nature *368*, 648-51.

Giancotti, F. G., and Ruoslahti, E. (1999). Integrin signaling. Science *285*, 1028-32.

Gibbs, C. S., Coutre, S. E., Tsiang, M., Li, W. X., Jain, A. K., Dunn, K. E., Law, V. S., Mao, C. T., Matsumura, S. Y., Mejza, S. J., and et al. (1995). Conversion of thrombin into an anticoagulant by protein engineering. Nature *378*, 413-6.

Gilbert, G. E., and Drinkwater, D. (1993). Specific membrane binding of factor VIII is mediated by *O*-phospho-L-serine, a moiety of phosphatidylserine. Biochemistry *32*, 9577-85.

Gill, F. M. (1984). The natural history of factor VIII inhibitors in patients with hemophilia A. In Factor VIII inhibitors, L. W. Hoyer, ed. (New York: Liss), pp. 19.

Gitschier, J., Kogan, S., Diamond, C., and Levinson, B. (1991). Genetic basis of hemophilia A. Thromb. Haemost. *66*, 37-9.

Glaser, C. B., Morser, J., Clarke, J. H., Blasko, E., McLean, K., Kuhn, I., Chang, R. J., Lin, J. H., Vilander, L., Andrews, W. H., et al. (1992). Oxidation of a specific methionine in thrombomodulin by activated neutrophil products blocks cofactor activity. A potential rapid mechanism for modulation of coagulation. J. Clin. Invest. *90*, 2565-73.

Glusa, E., Bretschneider, E., Daum, J., and Noeske-Jungblut, C. (1997). Inhibition of thrombin-mediated cellular effects by triabin, a highly potent anion-binding exosite thrombin inhibitor. Thromb. Haemost. *77*, 1196-200.

Godden, J. W., Turley, S., Teller, D. C., Adman, E. T., Liu, M. Y., Payne, W. J., and LeGall, J. (1991). The 2.3 Å X-ray structure of nitrite reductase from *Achromobacter cycloclastes*. Science *253*, 438-42.

Godowski, P. J., Mark, M. R., Chen, J. A., Sadick, M. D., Raab, H., and Hammond, R. G. (1995). Reevaluation of the roles of protein S and Gas6 as ligands for the receptor tyrosine kinase Rse/Tyro 3. Cell *82*, 355-8.

Goto, S., Ikeda, Y., Saldivar, E., and Ruggeri, Z. M. (1998). Distinct mechanisms of platelet aggregation as a consequence of different shearing flow conditions. J. Clin. Invest. *101*, 479-86.

Gralnick, H. R., Williams, S., McKeown, L. P., Hansmann, K., Fenton, J. W., 2nd, and Krutzsch, H. (1994). High-affinity α-thrombin binding to platelet glycoprotein Ib α: identification of two binding domains. Proc. Natl Acad. Sci. USA *91*, 6334-8.

Greenberg, C. S., Birckbichler, P. J., and Rice, R. H. (1991). Transglutaminases: multifunctional cross-linking enzymes that stabilize tissues. FASEB J. *5*, 3071-7.

Greer, J. (1990). Comparative modeling methods: application to the family of the mammalian serine proteases. Proteins *7*, 317-34.

Grinnell, B. W., Gerlitz, B., and Berg, D. T. (1994). Identification of a region in protein C involved in thrombomodulin-stimulated activation by thrombin: potential repulsion at anion-binding site I in thrombin. Biochem. J. *303*, 929-33.

Grinnell, B. W., Walls, J. D., and Gerlitz, B. (1991). Glycosylation of human protein C affects its secretion, processing, functional activities, and activation by thrombin. J. Biol. Chem. *266*, 9778-85.

Grundmann, U., Amann, E., Zettlmeissl, G., and Kupper, H. A. (1986). Characterization of cDNA coding for human factor XIIIa. Proc. Natl Acad. Sci. USA *83*, 8024-8.

Grütter, M. G., Priestle, J. P., Rahuel, J., Grossenbacher, H., Bode, W., Hofsteenge, J., and Stone, S. R. (1990). Crystal structure of the thrombin-hirudin complex: a novel mode of serine protease inhibition. EMBO J. *9*, 2361-5.

Gunzler, W. A., Steffens, G. J., Otting, F., Kim, S. M., Frankus, E., and Flohe, L. (1982). The primary structure of high molecular mass urokinase from human urine. The complete amino acid sequence of the A chain. Hoppe-Seylers Zeitschrift fur Physiologische Chemie *363*, 1155-65.

H

Hall, S. W., Nagashima, M., Zhao, L., Morser, J., and Leung, L. L. (1999). Thrombin interacts with thrombomodulin, protein C, and thrombin-activatable fibrinolysis inhibitor *via* specific and distinct domains. J. Biol. Chem. *274*, 25510-6.

Han, X., Huang, Z. F., Fiehler, R., and Broze, G. J., Jr. (1999). The protein Z-dependent protease inhibitor is a serpin. Biochemistry *38*, 11073-8.

Harlos, K., Martin, D. M., O'Brien, D. P., Jones, E. Y., Stuart, D. I., Polikarpov, I., Miller, A., Tuddenham, E. G., and Boys, C. W. (1994). Crystal structure of the extracellular region of human tissue factor. Nature *370*, 662-6.

Harris, R. J., and Spellman, M. W. (1993). *O*-linked fucose and other post-translational modifications unique to EGF modules. Glycobiology *3*, 219-24.

Harris, R. J., van Halbeek, H., Glushka, J., Basa, L. J., Ling, V. T., Smith, K. J., and Spellman, M. W. (1993). Identification and structural analysis of the tetrasaccharide NeuAc $\alpha(2\rightarrow6)$Gal $\beta(1\rightarrow4)$GlcNAc $\beta(1\rightarrow3)$Fuc α 1→O-linked to serine 61 of human factor IX. Biochemistry *32*, 6539-47.

Harris, T. J. (1987). Second-generation plasminogen activators. Protein Eng. *1*, 449-58.

Harris, T. J., Patel, T., Marston, F. A., Little, S., Emtage, J. S., Opdenakker, G., Volckaert, G., Rombauts, W., Billiau, A., and De Somer, P. (1986). Cloning of cDNA coding for human tissue-type plasminogen activator and its expression in *Escherichia coli*. Mol. Biol. Med. *3*, 279-92.

Hase, S., Kawabata, S., Nishimura, H., Takeya, H., Sueyoshi, T., Miyata, T., Iwanaga, S., Takao, T., Shimonishi, Y., and Ikenaka, T. (1988). A new trisaccharide sugar chain linked to a serine residue in bovine blood coagulation factors VII and IX. J. Biochem. *104*, 867-8.

Hayes, K. L., and Tracy, P. B. (1999). The platelet high affinity binding site for thrombin mimics hirudin, modulates thrombin-induced platelet activation, and is distinct from the glycoprotein Ib-IX-V complex. J. Biol. Chem. *274*, 972-80.

Healy, A. M., Rayburn, H. B., Rosenberg, R. D., and Weiler, H. (1995). Absence of the blood-clotting regulator thrombomodulin causes embryonic lethality in mice before development of a functional cardiovascular system. Proc. Natl Acad. Sci. USA *92*, 850-4.

Heeb, M. J., Kojima, Y., Greengard, J. S., and Griffin, J. H. (1995). Activated protein C resistance: molecular mechanisms based on studies using purified Gln506-factor V. Blood *85*, 3405-11.

Heeb, M. J., Mesters, R. M., Tans, G., Rosing, J., and Griffin, J. H. (1993). Binding of protein S to factor Va associated with inhibition of prothrombinase that is independent of activated protein C. J. Biol. Chem. *268*, 2872-7.

Heeb, M. J., Rosing, J., Bakker, H. M., Fernandez, J. A., Tans, G., and Griffin, J. H. (1994). Protein S binds to and inhibits factor Xa. Proc. Natl Acad. Sci. USA *91*, 2728-32.

Herrick, S., Blanc-Brude, O., Gray, A., and Laurent, G. (1999). Fibrinogen. Intern. J. Biochem. Cell Biol. *31*, 741-6.

Hertzberg, M. S., Ben-Tal, O., Furie, B., and Furie, B. C. (1992). Construction, expression, and characterization of a chimera of factor IX and factor X. The role of the second epidermal growth factor domain and serine protease domain in factor Va binding. J. Biol. Chem. *267*, 14759-66.

Herzyk, P., and Hubbard, R. E. (1998). Combined biophysical and biochemical information confirms arrangement of transmembrane helices visible from the three-dimensional map of frog rhodopsin. J. Mol. Biol. *281*, 741-54.

Hickey, M. J., Deaven, L. L., and Roth, G. J. (1990). Human platelet glycoprotein IX. Characterization of cDNA and localization of the gene to chromosome 3. FEBS Lett. *274*, 189-92.

Hickey, M. J., Hagen, F. S., Yagi, M., and Roth, G. J. (1993). Human platelet glycoprotein V: characterization of the polypeptide and the related Ib-V-IX receptor system of adhesive, leucine-rich glycoproteins. Proc. Natl Acad. Sci. USA *90*, 8327-31.

Ho, G., Toomey, J. R., Broze, G. J., Jr., and Schwartz, A. L. (1996). Receptor-mediated endocytosis of coagulation factor Xa requires cell surface-bound tissue factor pathway inhibitor. J. Biol. Chem. *271*, 9497-502.

Hoekema, L., Nicolaes, G. A., Hemker, H. C., Tans, G., and Rosing, J. (1997). Human factor Va1 and factor Va2: properties in the procoagulant and anticoagulant pathways. Biochemistry *36*, 3331-5.

Hofsteenge, J., Braun, P. J., and Stone, S. R. (1988). Enzymatic properties of proteolytic derivatives of human α-thrombin. Biochemistry *27*, 2144-51.

Hofsteenge, J., Taguchi, H., and Stone, S. R. (1986). Effect of thrombomodulin on the kinetics of the interaction of thrombin with substrates and inhibitors. Biochem. J. *237*, 243-51.

Hogg, P. J., Ohlin, A. K., and Stenflo, J. (1992). Identification of structural domains in protein C involved in its interaction with thrombin-thrombomodulin on the surface of endothelial cells. J. Biol. Chem. *267*, 703-6.

Hohenester, E., Maurer, P., and Timpl, R. (1997). Crystal structure of a pair of follistatin-like and EF-hand calcium-binding domains in BM-40. EMBO J. *16*, 3778-86.

Holden, H. M., Rypniewski, W. R., Law, J. H., and Rayment, I. (1987). The molecular structure of insecticyanin from the tobacco hornworm *Manduca sexta* L. at 2.6 Å resolution. EMBO J. *6*, 1565-70.

Honda, G., Masaki, C., Zushi, M., Tsuruta, K., and Sata, M. (1995). The roles played by the D2 and D3 domains of recombinant human thrombomodulin in its function. J. Biochem. *118*, 1030-6.

Hopfner, K. P., Lang, A., Karcher, A., Sichler, K., Kopetzki, E., Brandstetter, H., Huber, R., Bode, W., and Engh, R. A. (1999). Coagulation factor IXa: the relaxed conformation of Tyr99 blocks substrate binding. Structure with Folding & Design *7*, 989-96.

Hortin, G. L. (1990). Sulfation of tyrosine residues in coagulation factor V. Blood *76*, 946-52.

Howard, P. R., Bovill, E. G., Pike, J., Church, W. R., and Tracy, R. P. (1994). Factor VII antigen levels in a healthy blood donor population. Thromb. Haemost. *72*, 21-7.

Hoyer, L. W., and Scandella, D. (1994). Factor VIII inhibitors: structure and function in autoantibody and hemophilia A patients. Semin. Hematol. *31*, 1-5.

Huang, Z. F., Higuchi, D., Lasky, N., and Broze, G. J., Jr. (1997). Tissue factor pathway inhibitor gene disruption produces intrauterine lethality in mice. Blood *90*, 944-51.

Hubbard, S. J., Campbell, S. F., and Thornton, J. M. (1991). Molecular recognition: Conformational analysis of limited proteolytic sites and serine proteinase protein inhibitors. J. Mol. Biol. *220*, 507-30.

Huber, R., and Bode, W. (1978). Structural basis of the activation and action of trypsin. Acc. Chem. Res. *11*, 114-22.

Huber, R., and Carrell, R. W. (1989). Implications of the three-dimensional structure of α1-antitrypsin for structure and function of serpins. Biochemistry *28*, 8951-66.

Huber, R., Kukla, D., Bode, W., Schwager, P., Bartels, K., Deisenhofer, J., and Steigemann, W. (1974). Structure of the complex formed by bovine trypsin and bovine

pancreatic trypsin inhibitor. II. Crystallographic refinement at 1.9 Å resolution. J. Mol. Biol. *89*, 73-101.

Huber, R., Römish, J., and Pâques, E.-P. (1990). The crystal and molecular structure of human annexin V, an anticoagulant protein that binds to calcium and phospholipid membranes. EMBO J. *9*, 3867-74.

Huber, R., Schneider, M., Mayr, I., Muller, R., Deutzmann, R., Suter, F., Zuber, H., Falk, H., and Kayser, H. (1987). Molecular structure of the bilin binding protein (BBP) from *Pieris brassicae* after refinement at 2.0 Å resolution. J. Mol. Biol. *198*, 499-513.

Huizinga, E. G., Martijn van der Plas, R., Kroon, J., Sixma, J. J., and Gros, P. (1997). Crystal structure of the A3 domain of human von Willebrand factor: implications for collagen binding. Structure *5*, 1147-56.

Hynes, R. O. (1992). Integrins: versatility, modulation, and signaling in cell adhesion. Cell *69*, 11-25.

I

Ichinohe, T., Takayama, H., Ezumi, Y., Yanagi, S., Yamamura, H., and Okuma, M. (1995). Cyclic AMP-insensitive activation of c-Src and Syk protein-tyrosine kinases through platelet membrane glycoprotein VI. J. Biol. Chem. *270*, 28029-36.

Iiri, T., Farfel, Z., and Bourne, H. R. (1998). G-protein diseases furnish a model for the turn-on switch. Nature *394*, 35-8.

Inoue, K., and Morita, T. (1993). Identification of *O*-linked oligosaccharide chains in the activation peptides of blood coagulation factor X. The role of the carbohydrate moieties in the activation of factor X. Eur. J. Biochem. *218*, 153-63.

Isawa, H., Yuda, M., Yoneda, K., and Chinzei, Y. (2000). The insect salivary protein, prolixin-S, inhibits factor IXa generation and Xase complex formation in the blood coagulation pathway. J. Biol. Chem. *275*, 6636-41.

Ishimoto, Y., and Nakano, T. (2000). Release of a product of growth arrest-specific gene 6 from rat platelets. FEBS Lett. *466*, 197-9.

Ito, N., Phillips, S. E. V., Stevens, C., Ogel, Z. B., McPherson, M. J., Keen, J. N., Yadav, K. D. S., and Knowles, P. F. (1991). Novel thioether bond revealed by a 1.7 Å crystal structure of galactose oxidase. Nature *350*, 87-90.

Ito, N., Phillips, S. E. V., Yadav, K. D. S., and Knowles, P. F. (1994). Crystal structure of a free radical enzyme, galactose oxidase. J. Mol. Biol. *238*, 794-814.

J

Jakubowski, H. V., Kline, M. D., and Owen, W. G. (1986). The effect of bovine thrombomodulin on the specificity of bovine thrombin. J. Biol. Chem. *261*, 3876-82.

Jalbert, L. R., Rosen, E. D., Moons, L., Chan, J. C., Carmeliet, P., Collen, D., and Castellino, F. J. (1998). Inactivation of the gene for anticoagulant protein C causes lethal perinatal consumptive coagulopathy in mice. J. Clin. Invest. *102*, 1481-8.

Jandrot-Perrus, M., Bouton, M. C., Lanza, F., and Guillin, M. C. (1996). Thrombin interaction with platelet membrane glycoprotein Ib. Semin. Thromb. Hemost. *22*, 151-6.

Jenny, R. J., Pittman, D. D., Toole, J. J., Kriz, R. W., Aldape, R. A., Hewick, R. M., Kaufman, R. J., and Mann, K. G. (1987). Complete cDNA and derived amino acid sequence of human factor V. Proc. Natl Acad. Sci. USA *84*, 4846-50.

Jin, J., Chang, J., Chang, J. Y., Kelley, R. F., Stafford, D. W., and Straight, D. L. (1999). Factor VIIa's first epidermal growth factor-like domain's role in catalytic activity. Biochemistry *38*, 1185-92.

Jin, L., Abrahams, J. P., Skinner, R., Petitou, M., Pike, R. N., and Carrell, R. W. (1997). The anticoagulant activation of antithrombin by heparin. Proc. Natl Acad. Sci. USA *94*, 14683-8.

Johnson, J. D., Edman, J. C., and Rutter, W. J. (1993). A receptor tyrosine kinase found in breast carcinoma cells has an extracellular discoidin I-like domain. Proc. Natl Acad. Sci. USA *90*, 5677-81.

Jorgensen, M. J., Cantor, A. B., Furie, B. C., Brown, C. L., Shoemaker, C. B., and Furie, B. (1987). Recognition site directing vitamin K-dependent γ-carboxylation resides on the propeptide of factor IX. Cell *48*, 185-91.

Jung, S. M., and Moroi, M. (2000). Signal-transducing mechanisms involved in activation of the platelet collagen receptor integrin α2β1. J. Biol. Chem. *275*, 8016-26.

K

Kahn, M. L., Zheng, Y. W., Huang, W., Bigornia, V., Zeng, D., Moff, S., Farese, R. V., Jr., Tam, C., and Coughlin, S. R. (1998). A dual thrombin receptor system for platelet activation. Nature *394*, 690-4.

Kalafatis, M., Bertina, R. M., Rand, M. D., and Mann, K. G. (1995). Characterization of the molecular defect in factor V R506Q. J. Biol. Chem. *270*, 4053-7.

Kalafatis, M., Egan, J. O., van 't Veer, C., Cawthern, K. M., and Mann, K. G. (1997). The regulation of clotting factors. Crit. Rev. Eukaryot. Gene Expression *7*, 241-80.

Kalafatis, M., Rand, M. D., Jenny, R. J., Ehrlich, Y. H., and Mann, K. G. (1993). Phosphorylation of factor Va and factor VIIIa by activated platelets. Blood *81*, 704-19.

Kalafatis, M., Rand, M. D., and Mann, K. G. (1994). Factor Va-membrane interaction is mediated by two regions located on the light chain of the cofactor. Biochemistry *33*, 486-93.

Kalafatis, M., Rand, M. D., and Mann, K. G. (1994). The mechanism of inactivation of human factor V and human factor Va by activated protein C. J. Biol. Chem. *269*, 31869-80.

Kamata, K., Kawamoto, H., Honma, T., Iwama, T., and Kim, S. H. (1998). Structural basis for chemical inhibition of human blood coagulation factor Xa. Proc. Natl Acad. Sci. USA *95*, 6630-5.

Kane, W. H., and Davie, E. W. (1988). Blood coagulation factors V and VIII: structural and functional similarities and their relationship to hemorrhagic and thrombotic disorders. Blood *71*, 539-55.

Kane, W. H., and Davie, E. W. (1986). Cloning of a cDNA coding for human factor V, a blood coagulation factor homologous to factor VIII and ceruloplasmin. Proc. Natl Acad. Sci. USA *83*, 6800-4.

Kane, W. H., Ichinose, A., Hagen, F. S., and Davie, E. W. (1987). Cloning of cDNAs coding for the heavy chain region and connecting region of human factor V, a blood coagulation factor with four types of internal repeats. Biochemistry *26*, 6508-14.

Kao, Y. H., Lee, G. F., Wang, Y., Starovasnik, M. A., Kelley, R. F., Spellman, M. W., and Lerner, L. (1999). The effect of *O*-fucosylation on the first EGF-like domain from human blood coagulation factor VII. Biochemistry. *38*, 7097-110.

Kasai, S., Arimura, H., Nishida, M., and Suyama, T. (1985). Primary structure of single-chain pro-urokinase. J. Biol. Chem. *260*, 12382-9.

Kato, T., Oda, A., Inagaki, Y., Ohashi, H., Matsumoto, A., Ozaki, K., Miyakawa, Y., Watarai, H., Fuju, K., Kokubo, A., Kadoya, T., Ikeda, Y., and Miyazaki, H. (1997). Thrombin cleaves recombinant human thrombopoietin: one of the proteolytic events that generates truncated forms of thrombopoietin. Proc. Natl Acad. Sci. USA *94*, 4669-74.

Keller, F. G., Ortel, T. L., Quinn-Allen, M. A., and Kane, W. H. (1995). Thrombin-catalyzed activation of recombinant human factor V. Biochemistry *34*, 4118-24.

Keller, P. M., Waxman, L., Arnold, B. A., Schultz, L. D., Condra, C., and Connolly, T. M. (1993). Cloning of the cDNA and expression of moubatin, an inhibitor of platelet aggregation. J. Biol. Chem. *268*, 5450-6.

Kelley, R. F., Costas, K. E., O'Connell, M. P., and Lazarus, R. A. (1995). Analysis of the factor VIIa binding site on human tissue factor: effects of tissue factor mutations on the kinetics and thermodynamics of binding. Biochemistry *34*, 10383-92.

Kemball-Cook, G., Johnson, D. J., Tuddenham, E. G., and Harlos, K. (1999). Crystal structure of active site-inhibited human coagulation factor VIIa (des-Gla). J. Struct. Biol. *127*, 213-23.

Kemball-Cook, G., and Tuddenham, E. G. (1997). The factor VIII mutation database on the World Wide Web: the haemophilia A mutation, search, test and resource site. HAMSTeRS update (version 3.0). Nucl. Acid. Res. *25*, 128-32.

Kim, S. W., Ortel, T. L., Quinn-Allen, M. A., Yoo, L., Worfolk, L., Zhai, X., Lentz, B. R., and Kane, W. H. (1999). Partial glycosylation at asparagine-2181 of the second C-type domain of human factor V modulates assembly of the prothrombinase complex. Biochemistry *38*, 11448-54.

Kim, S. W., Quinn-Allen, M. A., Camp, J. T., Macedo-Ribeiro, S., Fuentes-Prior, P., Bode, W., and Kane, W. H. (2000). Identification of functionally important amino acid residues within the C2-domain of human factor V using alanine-scanning mutagenesis. Biochemistry *39*, 1951-58.

Kleywegt, G. J., and Jones, A. T. (1994). Detection, delineation, measurement and display of cavities in macromolecular structures. Acta Crystallogr. D *50*, 178-85.

Kluft, C., Dooijewaard, G., and Emeis, J. J. (1987). Role of the contact system in fibrinolysis. Semin. Thromb. Hemost. *13*, 50-68.

Knight, S. (1989). Ribulose 1,5-Biphosphate carboxylase/oxygenase- A structural study, Swedish University of Agricultural Sciences, ed. (Uppsala, Sweden).

Knobe, K. E., Berntsdotter, A., Shen, L., Morser, J., Dahlbäck, B., and Villoutreix, B. O. (1999). Probing the activation of protein C by the thrombin-thrombomodulin complex using structural analysis, site-directed mutagenesis, and computer modeling. Proteins *35*, 218-34.

Koedam, J. A., Meijers, J. C., Sixma, J. J., and Bouma, B. N. (1988). Inactivation of human factor VIII by activated protein C. Cofactor activity of protein S and protective effect of von Willebrand factor. J. Clin. Invest. *82*, 1236-43.

Koesling, D., and Friebe, A. (1999). Soluble guanylyl cyclase: structure and regulation. Rev. Physiol. Biochem. Pharmacol. *135*, 41-65.

Kokame, K., Zheng, X., and Sadler, J. E. (1998). Activation of thrombin-activable fibrinolysis inhibitor requires epidermal growth factor-like domain 3 of thrombomodulin and is inhibited competitively by protein C. J. Biol. Chem. *273*, 12135-9.

Kolkman, J. A., Christophe, O. D., Lenting, P. J., and Mertens, K. (1999). Surface loop 199-204 in blood coagulation factor IX is a cofactor-dependent site involved in macromolecular substrate interaction. J. Biol. Chem. *274*, 29087-93.

Kolkman, J. A., Lenting, P. J., and Mertens, K. (1999). Regions 301-303 and 333-339 in the catalytic domain of blood coagulation factor IX are factor VIII-interactive sites involved in stimulation of enzyme activity. Biochem. J. *339*, 217-21.

Kondo, S., Noguchi, M., Funakoshi, T., Fujikawa, K., and Kisiel, W. (1987). Inhibition of human factor VIIa-tissue factor activity by placental anticoagulant protein. Thromb. Res. *48*, 449-59.

Koppaka, V., Talbot, W. F., Zhai, X., and Lentz, B. R. (1997). Roles of factor Va heavy and light chains in protein and lipid rearrangements associated with the formation of a bovine factor Va-membrane complex. Biophys. J. *73*, 2638-52.

Korrel, S. A., Clemetson, K. J., Van Halbeek, H., Kamerling, J. P., Sixma, J. J., and Vliegenthart, J. F. (1984). Structural studies on the *O*-linked carbohydrate chains of human platelet glycocalicin. Eur. J. Biochem. *140*, 571-6.

Kraut, J. (1988). How do enzymes work? Science *242*, 533-40.

Kraut, J. (1977). Serine proteases: structure and mechanism of catalysis. Annu. Rev. Biochem. *46*, 331-58.

Krishnaswamy, S., Church, W. R., Nesheim, M. E., and Mann, K. G. (1987). Activation of human prothrombin by human prothrombinase. Influence of factor Va on the reaction mechanism. J. Biol. Chem. *262*, 3291-9.

Krishnaswamy, S., and Mann, K. G. (1988). The binding of factor Va to phospholipid vesicles. J. Biol. Chem. *263*, 5714-23.

Krishnaswamy, S., Mann, K. G., and Nesheim, M. E. (1986). The prothrombinase-catalyzed activation of prothrombin proceeds through the intermediate meizothrombin in an ordered, sequential reaction. J. Biol. Chem. *261*, 8977-84.

Kuhn, L. A., Griffin, J. H., Fisher, C. L., Greengard, J. S., Bouma, B. N., Espana, F., and Tainer, J. A. (1990). Elucidating the structural chemistry of glycosaminoglycan recognition by protein C inhibitor. Proc. Natl Acad. Sci. USA *87*, 8506-10.

Kulman, J. D., Harris, J. E., Haldeman, B. A., and Davie, E. W. (1997). Primary structure and tissue distribution of two novel proline-rich γ-carboxyglutamic acid proteins. Proc. Natl Acad. Sci. USA *94*, 9058-62.

Kumada, T., Dittman, W. A., and Majerus, P. W. (1988). A role for thrombomodulin in the pathogenesis of thrombin-induced thromboembolism in mice. Blood *71*, 728-33.

Kundu, R. K., Sangiorgi, F., Wu, L. Y., Kurachi, K., Anderson, W. F., Maxson, R., and Gordon, E. M. (1998). Targeted inactivation of the coagulation factor IX gene causes hemophilia B in mice. Blood *92*, 168-74.

Kurachi, K., Kurachi, S., Furukawa, M., and Yao, S. N. (1993). Biology of factor IX. Blood Coagul. Fibrinolysis *4*, 953-73.

Kurachi, S., Deyashiki, Y., Takeshita, J., and Kurachi, K. (1999). Genetic mechanisms of age regulation of human blood coagulation factor IX. Science *285*, 739-43.

Kurachi, S., Hitomi, E., and Kurachi, K. (1996). Age and sex dependent regulation of the factor IX gene in mice. Thromb. Haemost. *76*, 965-9.

Kurosawa, S., Galvin, J. B., Esmon, N. L., and Esmon, C. T. (1987). Proteolytic formation and properties of functional domains of thrombomodulin. J. Biol. Chem. *262*, 2206-12.

Kurosawa, S., Stearns, D. J., Jackson, K. W., and Esmon, C. T. (1988). A 10-kDa cyanogen bromide fragment from the epidermal growth factor homology domain of rabbit thrombomodulin contains the primary thrombin binding site. J. Biol. Chem. *263*, 5993-6.

L

Lai, T. S., Slaughter, T. F., Peoples, K. A., and Greenberg, C. S. (1999). Site-directed mutagenesis of the calcium-binding site of blood coagulation factor XIIIa. J. Biol. Chem. *274*, 24953-8.

Lamba, D., Bauer, M., Huber, R., Fischer, S., Rudolph, R., Kohnert, U., and Bode, W. (1996). The 2.3 Å crystal structure of the catalytic domain of recombinant two-chain human tissue-type plasminogen activator. J. Mol. Biol. *258*, 117-35.

Lanza, F., Morales, M., de La Salle, C., Cazenave, J. P., Clemetson, K. J., Shimomura, T., and Phillips, D. R. (1993). Cloning and characterization of the gene encoding the human platelet glycoprotein V. A member of the leucine-rich glycoprotein family cleaved during thrombin-induced platelet activation. J. Biol. Chem. *268*, 20801-7.

Lapan, K. A., and Fay, P. J. (1998). Interaction of the A1 subunit of factor VIIIa and the serine protease domain of factor X identified by zero-length cross-linking. Thromb. Haemost. *80*, 418-22.

Lapan, K. A., and Fay, P. J. (1997). Localization of a factor X interactive site in the A1 subunit of factor VIIIa. J. Biol. Chem. *272*, 2082-8.

Laskowski, R., MacArthur, M., Hutchinson, E., and Thorton, J. (1993). PROCHECK: a program to check the stereochemical quality of protein structures. J. Appl. Cryst. *26*, 283-91.

Laue, T. M., Lu, R., Krieg, U. C., Esmon, C. T., and Johnson, A. E. (1989). Ca^{2+}-dependent structural changes in bovine blood coagulation factor Va and its subunits. Biochemistry *28*, 4762-71.

Law, D. A., DeGuzman, F. R., Heiser, P., Ministri-Madrid, K., Killeen, N., and Phillips, D. R. (1999). Integrin cytoplasmic tyrosine motif is required for outside-in αIIbβ3 signalling and platelet function. Nature *401*, 808-11.

Law, D. A., Nannizzi-Alaimo, L., and Phillips, D. R. (1996). Outside-in integrin signal transduction. αIIbβ3-(GP IIbIIIa) tyrosine phosphorylation induced by platelet aggregation. J. Biol. Chem. *271*, 10811-5.

Lawrence, D. A., Ginsburg, D., Day, D. E., Berkenpas, M. B., Verhamme, I. M., Kvassman, J. O., and Shore, J. D. (1995). Serpin-protease complexes are trapped as stable acyl-enzyme intermediates. J. Biol. Chem. *270*, 25309-12.

Le Bonniec, B. F., and Esmon, C. T. (1991). Glu−192Gln substitution in thrombin mimics the catalytic switch induced by thrombomodulin. Proc. Natl Acad. Sci. USA *88*, 7371-5.

Le Bonniec, B. F., MacGillivray, R. T., and Esmon, C. T. (1991). Thrombin Glu-39 restricts the P3' specificity to nonacidic residues. J. Biol. Chem. *266*, 13796-803.

Lee, T. H., Rhim, T., and Kim, S. S. (1998). Prothrombin kringle-2 domain has a growth inhibitory activity against basic fibroblast growth factor-stimulated capillary endothelial cells. J. Biol. Chem. *273*, 28805-12.

LeMosy, E. K., Hong, C. C., and Hashimoto, C. (1999). Signal transduction by a protease cascade. Trends Cell Biol. *9*, 102-7.

Lenting, P. J., Donath, M. J., van Mourik, J. A., and Mertens, K. (1994). Identification of a binding site for blood coagulation factor IXa on the light chain of human factor VIII. J. Biol. Chem. *269*, 7150-5.

Lenting, P. J., Neels, J. G., van den Berg, B. M., Clijsters, P. P., Meijerman, D. W., Pannekoek, H., van Mourik, J. A., Mertens, K., and van Zonneveld, A. J. (1999). The light chain of factor VIII comprises a binding site for low density lipoprotein receptor-related protein. J. Biol. Chem. *274*, 23734-9.

Lenting, P. J., van de Loo, J. W., Donath, M. J., van Mourik, J. A., and Mertens, K. (1996). The sequence Glu1811-Lys1818 of human blood coagulation factor VIII comprises a binding site for activated factor IX. J. Biol. Chem. *271*, 1935-40.

Lentz, S. R., Chen, Y., and Sadler, J. E. (1993). Sequences required for thrombomodulin cofactor activity within the fourth epidermal growth factor-like domain of human thrombomodulin. J. Biol. Chem. *268*, 15312-7.

Leslie, A. (1991). Macromolecular Data Processing. In Crystal. Computing V, D. Moras, A. D. Podjarny and J. C. Thierry, eds. (Oxford, UK: Oxford University Press), pp. 27-38.

Lessel, U., and Schomburg, D. (1994). Similarities between protein 3-D structures. Protein Eng. *7*, 1175-87.

Leyte, A., van Schijndel, H. B., Niehrs, C., Huttner, W. B., Verbeet, M. P., Mertens, K., and van Mourik, J. A. (1991). Sulfation of Tyr1680 of human blood coagulation factor VIII is essential for the interaction of factor VIII with von Willebrand factor. J. Biol. Chem. *266*, 740-6.

Leyte, A., Verbeet, M. P., Brodniewicz-Proba, T., Van Mourik, J. A., and Mertens, K. (1989). The interaction between human blood-coagulation factor VIII and von Willebrand

factor. Characterization of a high-affinity binding site on factor VIII. Biochem. J. *257*, 679-83.

Leytus, S. P., Kurachi, K., Sakariassen, K. S., and Davie, E. W. (1986). Nucleotide sequence of the cDNA coding for human complement C1r. Biochemistry *25*, 4855-63.

Li, X., Bokman, A. M., Llinas, M., Smith, R. A., and Dobson, C. M. (1994). Solution structure of the kringle domain from urokinase-type plasminogen activator. J. Mol. Biol. *235*, 1548-59.

Liaw, P. C. Y., Fredenburgh, J. C., Stafford, A. R., Tulinsky, A., Austin, R. C., and Weitz, J. I. (1998). Localization of the thrombin-binding domain on prothrombin fragment 2. J. Biol. Chem. *273*, 8932-9.

Liaw, P. C. Y., Neuenschwander, P. F., Smirnov, M. D., and Esmon, C. T. (2000). Mechanisms by which soluble endothelial cell protein C receptor modulates protein C and activated protein C function. J. Biol. Chem. *275*, 5447-52.

Light, D. R., Glaser, C. B., Betts, M., Blasko, E., Campbell, E., Clarke, J. H., McCaman, M., McLean, K., Nagashima, M., Parkinson, J. F., et al. (1999). The interaction of thrombomodulin with Ca^{2+}. Eur. J. Biochem. *262*, 522-33.

Lin, J. H., Wang, M., Andrews, W. H., Wydro, R., and Morser, J. (1994). Expression efficiency of the human thrombomodulin-encoding gene in various vector and host systems. Gene *147*, 287-92.

Lin, Y., Harris, R. B., Yan, W., McCrae, K. R., Zhang, H., and Colman, R. W. (1997). High molecular weight kininogen peptides inhibit the formation of kallikrein on endothelial cell surfaces and subsequent urokinase-dependent plasmin formation. Blood *90*, 690-7.

Liu, D., Bienkowska, J., Petosa, C., Collier, R. J., Fu, H., and Liddington, R. (1995). Crystal structure of the ζ isoform of the 14-3-3 protein. Nature *376*, 191-4.

Liu, L., Freedman, J., Hornstein, A., Fenton, J. W., 2nd, Song, Y., and Ofosu, F. A. (1997). Binding of thrombin to the G-protein-linked receptor, and not to glycoprotein Ib, precedes thrombin-mediated platelet activation. J. Biol. Chem. *272*, 1997-2004.

Liu, L. W., Rezaie, A. R., Carson, C. W., Esmon, N. L., and Esmon, C. T. (1994). Occupancy of anion binding exosite 2 on thrombin determines Ca^{2+} dependence of protein C activation. J. Biol. Chem. *269*, 11807-12.

Liu, L. W., Vu, T. K., Esmon, C. T., and Coughlin, S. R. (1991). The region of the thrombin receptor resembling hirudin binds to thrombin and alters enzyme specificity. J. Biol. Chem. *266*, 16977-80.

Lombardi, A., De Simone, G., Galdiero, S., Staiano, N., Nastri, F., and Pavone, V. (1999). From natural to synthetic multisite thrombin inhibitors. Biopolymers *51*, 19-39.

Lopez, J. A. (1994). The platelet glycoprotein Ib-IX complex. Blood Coagul. Fibrinolysis *5*, 97-119.

Lopez, J. A., Andrews, R. K., Afshar-Kharghan, V., and Berndt, M. C. (1998). Bernard-Soulier syndrome. Blood *91*, 4397-418.

Lopez, J. A., Chung, D. W., Fujikawa, K., Hagen, F. S., Davie, E. W., and Roth, G. J. (1988). The α and β chains of human platelet glycoprotein Ib are both transmembrane proteins containing a leucine-rich amino acid sequence. Proc. Natl Acad. Sci. USA *85*, 2135-9.

Lopez, J. A., Chung, D. W., Fujikawa, K., Hagen, F. S., Papayannopoulou, T., and Roth, G. J. (1987). Cloning of the α chain of human platelet glycoprotein Ib: a transmembrane protein with homology to leucine-rich α2-glycoprotein. Proc. Natl Acad. Sci. USA *84*, 5615-9.

Lopez, J. A., and Dong, J. F. (1997). Structure and function of the glycoprotein Ib-IX-V complex. Curr. Opin. Hematol. *4*, 323-9.

Lougheed, J. C., Bowman, C. L., Meininger, D. P., and Komives, E. A. (1995). Thrombin inhibition by cyclic peptides from thrombomodulin. Protein Sci. *4*, 773-80.

Lowe, G. D. O., Rumley, A., Woodward, M., Morrison, C. E., Philippou, H., Lane, D. A., and Tunstallpedoe, H. (1997). Epidemiology of coagulation factors, inhibitors and activation markers - the third Glasgow Monica survey. 1. Illustrative reference ranges by age, sex and hormone use. British J. Haematol. *97*, 775-84.

Lu, R. L., Esmon, N. L., Esmon, C. T., and Johnson, A. E. (1989). The active site of the thrombin-thrombomodulin complex. A fluorescence energy transfer measurement of its distance above the membrane surface. J. Biol. Chem. *264*, 12956-62.

Lu, Z. L., and Hulme, E. C. (2000). A network of conserved intramolecular contacts defines the off-state of the transmembrane switch mechanism in a seven-transmembrane receptor. J. Biol. Chem. *275*, 5682-6.

Lundwall, A., Dackowski, W., Cohen, E., Shaffer, M., Mahr, A., Dahlbäck, B., Stenflo, J., and Wydro, R. (1986). Isolation and sequence of the cDNA for human protein S, a regulator of blood coagulation. Proc. Natl Acad. Sci. USA *83*, 6716-20.

M

Ma, S. F., Garcia, J. G., Reuning, U., Little, S. P., Bang, N. U., and Dixon, E. P. (1997). Thrombin induces thrombomodulin mRNA expression *via* the proteolytically activated thrombin receptor in cultured bovine smooth muscle cells. J. Lab. Clin. Med. *129*, 611-9.

Macfarlane, R. G. (1964). An enzyme cascade in the blood clotting mechanism, and its function as a biochemical amplifier. Nature *202*, 498-9.

Magnusson, S., Sottrup-Jensen, L., Petersen, T. E., Dudek-Wojciechowska, G., and Claeys, H. (1976). Homologous "Kringle" structures common to plasminogen and prothrombin. Substrate specificity of enyzmes activating prothrombin and plasminogen. pp. 203-38. In: Ribbons DW, Brew K, ed. Proteolysis and physiological regulation. New York, Academic Press *11*.

Mahasandana, C., Suvatte, V., Marlar, R. A., Manco-Johnson, M. J., Jacobson, L. J., and Hathaway, W. E. (1990). Neonatal purpura fulminans associated with homozygous protein S deficiency. Lancet *335*, 61-2.

Manfioletti, G., Brancolini, C., Avanzi, G., and Schneider, C. (1993). The protein encoded by a growth arrest-specific gene (gas6) is a new member of the vitamin K-dependent proteins related to protein S, a negative coregulator in the blood coagulation cascade. Mol. Cell. Biol. *13*, 4976-85.

Mann, K. G., Lawler, C. M., Vehar, G. A., and Church, W. R. (1984). Coagulation factor V contains copper ion. J. Biol. Chem. *259*, 12949-51.

Mann, K. G., and Lorand, L. (1993). Introduction: blood coagulation. Methods Enzymol. *222*, 1-10.

Mannaioni, P. F., Di Bello, M. G., and Masini, E. (1997). Platelets and inflammation: role of platelet-derived growth factor, adhesion molecules and histamine. Inflammation Res. *46*, 4-18.

Marchese, P., Murata, M., Mazzucato, M., Pradella, P., De Marco, L., Ware, J., and Ruggeri, Z. M. (1995). Identification of three tyrosine residues of glycoprotein Ib α with distinct roles in von Willebrand factor and α-thrombin binding. J. Biol. Chem. *270*, 9571-8.

Marchese, P., Saldivar, E., Ware, J., and Ruggeri, Z. M. (1999). Adhesive properties of the isolated amino-terminal domain of platelet glycoprotein Ibα in a flow field. Proc. Natl Acad. Sci. USA *96*, 7837-42.

Markwardt, F. (1994). Coagulation inhibitors from blood-sucking animals. A new line of developing antithrombotic drugs. Pharmazie *49*, 313-6.

Markwardt, F. (1994). The development of hirudin as an antithrombotic drug. Thromb. Res. *74*, 1-23.

Marti, D. N., Hu, C. K., An, S. S. A., von Haller, P., Schaller, J., and Llinas, M. (1997). Ligand preferences of kringle 2 and homologous domains of human plasminogen: canvassing weak, intermediate, and high-affinity binding sites by 1H-NMR. Biochemistry *36*, 11591-604.

Martin, D. M., Boys, C. W., and Ruf, W. (1995). Tissue factor: molecular recognition and cofactor function. FASEB J. *9*, 852-9.

Martin, P. D., Malkowski, M. G., Box, J., Esmon, C. T., and Edwards, B. F. (1997). New insights into the regulation of the blood clotting cascade derived from the X-ray crystal structure of bovine meizothrombin des F1 in complex with PPACK. Structure *5*, 1681-1693.

Martin, P. D., Robertson, W., Turk, D., Huber, R., Bode, W., and Edwards, B. F. (1992). The structure of residues 7-16 of the Aα-chain of human fibrinogen bound to bovine thrombin at 2.3-Å resolution. J. Biol. Chem. *267*, 7911-20.

Mather, T., Oganessyan, V., Hof, P., Huber, R., Foundling, S., Esmon, C., and Bode, W. (1996). The 2.8 Å crystal structure of Gla-domainless activated protein C. EMBO J. *15*, 6822-31.

Matheson, N. R., van Halbeek, H., and Travis, J. (1991). Evidence for a tetrahedral intermediate complex during serpin-proteinase interactions. J. Biol. Chem. *266*, 13489-91.

Mathews, II, Padmanabhan, K. P., Ganesh, V., Tulinsky, A., Ishii, M., Chen, J., Turck, C. W., Coughlin, S. R., and Fenton, J. W., 2nd (1994). Crystallographic structures of thrombin complexed with thrombin receptor peptides: existence of expected and novel binding modes. Biochemistry *33*, 3266-79.

Mathews, II, Padmanabhan, K. P., Tulinksy, A., and Sadler, J. E. (1994). Structure of a nonadecapeptide of the fifth EGF domain of thrombomodulin complexed with thrombin. Biochemistry *33*, 13547-52.

Mathews, II, Vanderhoff-Hanaver, P., Castellino, F. J., and Tulinsky, A. (1996). Crystal structures of the recombinant kringle 1 domain of human plasminogen in complexes with the ligands epsilon-aminocaproic acid and trans-4-(aminomethyl)cyclohexane-1-carboxylic acid. Biochemistry *35*, 2567-76.

Mathur, A., and Bajaj, S. P. (1999). Protease and EGF1 domains of factor IXa play distinct roles in binding to factor VIIIa. Importance of helix 330 (helix 162 in chymotrypsin) of protease domain of factor IXa in its interaction with factor VIIIa. J. Biol. Chem. *274*, 18477-86.

Matsushita, T., Dong, Z., and Sadler, J. E. (1994). von Willebrand's factor and von Willebrand's disease. Curr. Opin. Hematol. *1*, 362-8.

Matthews, B. W., Sigler, P. B., Henderson, R., and Blow, D. M. (1967). Three-dimensional structure of tosyl-α-chymotrypsin. Nature *214*, 652-6.

McCallum, C. D., Su, B., Neuenschwander, P. F., Morrissey, J. H., and Johnson, A. E. (1997). Tissue factor positions and maintains the factor VIIa active site far above the membrane surface even in the absence of the factor VIIa Gla domain. A fluorescence resonance energy transfer study. J. Biol. Chem. *272*, 30160-6.

McCoy, A. J., Chandana Epa, V., and Colman, P. M. (1997). Electrostatic complementarity at protein/protein interfaces. J. Mol. Biol. *268*, 570-84.

McDonald, I. K., and Thornton, J. M. (1994). Satisfying hydrogen bonding potential in proteins. J. Mol. Biol. *238*, 777-93.

McDonald, J. F., Evans, T. C., Jr., Emeagwali, D. B., Hariharan, M., Allewell, N. M., Pusey, M. L., Shah, A. M., and Nelsestuen, G. L. (1997). Ionic properties of membrane association by vitamin K-dependent proteins: the case for univalency. Biochemistry *36*, 15589-98.

McDonald, J. F., Shah, A. M., Schwalbe, R. A., Kisiel, W., Dahlbäck, B., and Nelsestuen, G. L. (1997). Comparison of naturally occurring vitamin K-dependent proteins: correlation of amino acid sequences and membrane binding properties suggests a membrane contact site. Biochemistry *36*, 5120-7.

McMullen, B. A., Fujikawa, K., and Kisiel, W. (1983). The occurrence of β-hydroxyaspartic acid in the vitamin K-dependent blood coagulation zymogens. Biochem. Biophys. Res. Commun. *115*, 8-14.

McMullen, B. A., Fujikawa, K., Kisiel, W., Sasagawa, T., Howald, W. N., Kwa, E. Y., and Weinstein, B. (1983). Complete amino acid sequence of the light chain of human blood coagulation factor X: evidence for identification of residue 63 as β-hydroxyaspartic acid. Biochemistry *22*, 2875-84.

McRae, B. J., Kurachi, K., Heimark, R. L., Fujikawa, K., Davie, E. W., and Powers, J. C. (1981). Mapping the active sites of bovine thrombin, factor IXa, factor Xa, factor XIa, factor XIIa, plasma kallikrein, and trypsin with amino acid and peptide thioesters: development of new sensitive substrates. Biochemistry *20*, 7196-206.

Meers, P. (1990). Location of tryptophans in membrane-bound annexins. Biochemistry *29*, 3325-30.

Meers, P., and Mealy, T. (1993). Relantionship between annexin V tryptophan exposure, calcium and phospholipid binding. Biochemistry *32*, 5411-8.

Meininger, D. P., Hunter, M. J., and Komives, E. A. (1995). Synthesis, activity, and preliminary structure of the fourth EGF-like domain of thrombomodulin. Protein Sci. *4*, 1683-95.

Messerschmidt, A., and Huber, R. (1990). The blue oxidases, ascorbate oxidase, laccase and ceruloplasmin. Modelling and structural relationships. Eur. J. Biochem. *187*, 341-52.

Messier, T. L., Pittman, D. D., Long, G. L., Kaufman, R. J., and Church, W. R. (1991). Cloning and expression in COS-1 cells of a full-length cDNA encoding human coagulation factor X. Gene *99*, 291-4.

Miletich, J. P., and Broze, G. J., Jr. (1990). Beta protein C is not glycosylated at asparagine 329. The rate of translation may influence the frequency of usage at asparagine-X-cysteine sites. J. Biol. Chem. *265*, 11397-404.

Miletich, J. P., Prescott, S. M., White, R., Majerus, P. W., and Bovill, E. G. (1993). Inherited predisposition to thrombosis. Cell *72*, 477-80.

Miller, J. L., Cunningham, D., Lyle, V. A., and Finch, C. N. (1991). Mutation in the gene encoding the α chain of platelet glycoprotein Ib in platelet-type von Willebrand disease. Proc. Natl Acad. Sci. USA *88*, 4761-5.

Mitchell, C. A., Kelemen, S. M., and Salem, H. H. (1988). The anticoagulant properties of a modified form of protein S. Thromb. Haemost. *60*, 298-304.

Molinari, A., Giorgetti, C., Lansen, J., Vaghi, F., Orsini, G., Faioni, E. M., and Mannucci, P. M. (1992). Thrombomodulin is a cofactor for thrombin degradation of recombinant single-chain urokinase plasminogen activator "in vitro" and in a perfused rabbit heart model. Thromb. Haemost. *67*, 226-32.

Moroi, M., and Jung, S. M. (1997). Platelet receptors for collagen. Thromb. Haemost. *78*, 439-44.

Mulichak, A. M., Tulinsky, A., and Ravichandran, K. G. (1991). Crystal and molecular structure of human plasminogen kringle 4 refined at 1.9-Å resolution. Biochemistry *30*, 10576-88.

Muller, Y. A., Ultsch, M. H., Kelley, R. F., and de Vos, A. M. (1994). Structure of the extracellular domain of human tissue factor: location of the factor VIIa binding site. Biochemistry *33*, 10864-70.

Müller-Eberhard, H. J. (1988). Molecular organization and function of the complement system. Annual Review of Biochemistry *57*, 321-47.

Muranyi, A., Finn, B. E., Gippert, G. P., Forsen, S., Stenflo, J., and Drakenberg, T. (1998). Solution structure of the N-terminal EGF-like domain from human factor VII. Biochemistry *37*, 10605-15.

Murphy, M. E., Lindley, P. F., and Adman, E. T. (1997). Structural comparison of cupredoxin domains: domain recycling to construct proteins with novel functions. Protein Sci. *6*, 761-70.

Musci, G., Berliner, L. J., and Esmon, C. T. (1988). Evidence for multiple conformational changes in the active center of thrombin induced by complex formation with thrombomodulin: an analysis employing nitroxide spin-labels. Biochemistry *27*, 769-73.

Muslin, A. J., Tanner, J. W., Allen, P. M., and Shaw, A. S. (1996). Interaction of 14-3-3 with signaling proteins is mediated by the recognition of phosphoserine. Cell *84*, 889-97.

Muszbek, L., Polgar, J., and Boda, Z. (1993). Platelet factor XIII becomes active without the release of activation peptide during platelet activation. Thromb. Haemost. *69*, 282-5.

Muszbek, L., Yee, V. C., and Hevessy, Z. (1999). Blood coagulation factor XIII: structure and function. Thromb. Res. *94*, 271-305.

Myles, T., Church, F. C., Whinna, H. C., Monard, D., and Stone, S. R. (1998). Role of thrombin anion-binding exosite-I in the formation of thrombin-serpin complexes. J. Biol. Chem. *273*, 31203-8.

Myrmel, K. H., Lundblad, R. L., and Mann, K. G. (1976). Characteristics of the association between prothrombin fragment 2 and α-thrombin. Biochemistry *15*, 1767-73.

N

Nagashima, M., Lundh, E., Leonard, J. C., Morser, J., and Parkinson, J. F. (1993). Alanine-scanning mutagenesis of the epidermal growth factor-like domains of human thrombomodulin identifies critical residues for its cofactor activity. J. Biol. Chem. *268*, 2888-92.

Naito, K., and Fujikawa, K. (1991). Activation of human blood coagulation factor XI independent of factor XII. Factor XI is activated by thrombin and factor XIa in the presence of negatively charged surfaces. J. Biol. Chem. *266*, 7353-8.

Nakagaki, T., Foster, D. C., Berkner, K. L., and Kisiel, W. (1991). Initiation of the extrinsic pathway of blood coagulation: evidence for the tissue factor dependent autoactivation of human coagulation factor VII. Biochemistry *30*, 10819-24.

Nakanishi-Matsui, M., Zheng, Y. W., Sulciner, D. J., Weiss, E. J., Ludeman, M. J., and Coughlin, S. R. (2000). PAR3 is a cofactor for PAR4 activation by thrombin. Nature *404*, 609-13.

Nalefski, E. A., and Falke, J. J. (1996). The C2 domain calcium-binding motif: structural and functional diversity. Protein Sci. *5*, 2375-90.

Navaza, J. (1994). An automated package for molecular replacement. Acta Crystallogr. A *50*, 157-63.

Nelsestuen, G. L. (1976). Role of γ-carboxyglutamic acid. An unusual protein transition required for the calcium-dependent binding of prothrombin to phospholipid. J. Biol. Chem. *251*, 5648-56.

Nesheim, M. (1998). Fibrinolysis and the plasma carboxypeptidase. Curr. Opin. Hematol. *5*, 309-13.

Nesheim, M., Wang, W., Boffa, M., Nagashima, M., Morser, J., and Bajzar, L. (1997). Thrombin, thrombomodulin and TAFI in the molecular link between coagulation and fibrinolysis. Thromb. Haemost. *78*, 386-91.

Nesheim, M. E., Abbott, T., Jenny, R., and Mann, K. G. (1988). Evidence that the thrombin-catalyzed feedback cleavage of fragment 1.2 at Arg154-Ser155 promotes the release of thrombin from the catalytic surface during the activation of bovine prothrombin. J. Biol. Chem. *263*, 1037-44.

Nesheim, M. E., Pittman, D. D., Wang, J. H., Slonosky, D., Giles, A. R., and Kaufman, R. J. (1988). The binding of 35S-labeled recombinant factor VIII to activated and unactivated human platelets. J. Biol. Chem. *263*, 16467-70.

Nesheim, M. E., Taswell, J. B., and Mann, K. G. (1979). The contribution of bovine Factor V and Factor Va to the activity of prothrombinase. J. Biol. Chem. *254*, 10952-62.

Neuenschwander, P. F., Fiore, M. M., and Morrissey, J. H. (1993). Factor VII autoactivation proceeds *via* interaction of distinct protease-cofactor and zymogen-cofactor complexes. Implications of a two-dimensional enzyme kinetic mechanism. J. Biol. Chem. *268*, 21489-92.

Neurath, H. (1986). The versatility of proteolytic enzymes. J. Cell. Biochem. *32*, 35-49.

Newcomer, M. E. (1993). Structure of the epididymal retinoic acid binding protein at 2.1 Å resolution. Structure *1*, 7-18.

Newcomer, M. E., Jones, T. A., Aqvist, J., Sundelin, J., Eriksson, U., Rask, L., and Peterson, P. A. (1984). The three-dimensional structure of retinol-binding protein. EMBO J. *3*, 1451-4.

Nguyen, M., Arkell, J., and Jackson, C. J. (2000). Activated protein C directly activates human endothelial gelatinase A. J. Biol. Chem. *275*, 9095-8.

Nicholls, A., Bharadwaj, R., and Honig, B. (1993). GRASP - graphical representation and analysis of surface properties. Biophys. J. *64*, A166.

Nishimura, H., Takao, T., Hase, S., Shimonishi, Y., and Iwanaga, S. (1992). Human factor IX has a tetrasaccharide *O*-glycosidically linked to serine 61 through the fucose residue. J. Biol. Chem. *267*, 17520-5.

Noeske-Jungblut, C., Haendler, B., Donner, P., Alagon, A., Possani, L., and Schleuning, W. D. (1995). Triabin, a highly potent exosite inhibitor of thrombin. J. Biol. Chem. *270*, 28629-34.

Noeske-Jungblut, C., Kratzschmar, J., Haendler, B., Alagon, A., Possani, L., Verhallen, P., Donner, P., and Schleuning, W. D. (1994). An inhibitor of collagen-induced platelet aggregation from the saliva of *Triatoma pallidipennis*. J. Biol. Chem. *269*, 5050-3.

Novokhatny, V. V., Kudinov, S. A., and Privalov, P. L. (1984). Domains in human plasminogen. J. Mol. Biol. *179*, 215-32.

Novokhatny, V. V., Medved, L. V., Mazar, A., and Ingham, K. C. (1993). Effect of tethered peptidylchloromethylketone inhibitors on thermal stability and domain interactions of urokinase and other serine proteases. J. Biol. Chem. *268*, 17211-8.

Nurden, A. T. (1995). Polymorphisms of human platelet membrane glycoproteins: structure and clinical significance. Thromb. Haemost. *74*, 345-51.

Ny, T., Elgh, F., and Lund, B. (1984). The structure of the human tissue-type plasminogen activator gene: correlation of intron and exon structures to functional and structural domains. Proc. Natl Acad. Sci. USA *81*, 5355-9.

Nyberg, P., Dahlbäck, B., and Garcia de Frutos, P. (1998). The SHBG-like region of protein S is crucial for factor V-dependent APC-cofactor function. FEBS Lett. *433*, 28-32.

O

Obert, B., Houllier, A., Meyer, D., and Girma, J. P. (1999). Conformational changes in the A3 domain of von Willebrand factor modulate the interaction of the A1 domain with platelet glycoprotein Ib. Blood *93*, 1959-68.

O'Brien, L. M., Huggins, C. F., and Fay, P. J. (1997). Interacting regions in the A1 and A2 subunits of factor VIIIa identified by zero-length cross-linking. Blood *90*, 3943-50.

Offermanns, S., Toombs, C. F., Hu, Y. H., and Simon, M. I. (1997). Defective platelet activation in $G\alpha_q$-deficient mice. Nature *389*, 183-6.

Ohlin, A. K., and Marlar, R. A. (1995). The first mutation identified in the thrombomodulin gene in a 45-year-old man presenting with thromboembolic disease. Blood *85*, 330-6.

Ohlin, A. K., Norlund, L., and Marlar, R. A. (1997). Thrombomodulin gene variations and thromboembolic disease. Thromb. Haemost. *78*, 396-400.

Olsen, P. H., Esmon, N. L., Esmon, C. T., and Laue, T. M. (1992). Ca^{2+} dependence of the interactions between protein C, thrombin, and the elastase fragment of thrombomodulin. Analysis by ultracentrifugation. Biochemistry *31*, 746-54.

Olson, S. T., and Bjork, I. (1991). Predominant contribution of surface approximation to the mechanism of heparin acceleration of the antithrombin-thrombin reaction. Elucidation from salt concentration effects. J. Biol. Chem. *266*, 6353-64.

Olson, S. T., and Shore, J. D. (1982). Demonstration of a two-step reaction mechanism for inhibition of α-thrombin by antithrombin III and identification of the step affected by heparin. J. Biol. Chem. *257*, 14891-5.

O'Reilly, M. S., Pirie-Shepherd, S., Lane, W. S., and Folkman, J. (1999). Antiangiogenic activity of the cleaved conformation of the serpin antithrombin. Science *285*, 1926-8.

Ortel, T. L., Charles, L. A., Keller, F. G., Marcom, P. K., Oldham, H. N., Jr., Kane, W. H., and Macik, B. G. (1994). Topical thrombin and acquired coagulation factor inhibitors: clinical spectrum and laboratory diagnosis. Am. J. Hematol. *45*, 128-35.

Ortel, T. L., Devore-Carter, D., Quinn-Allen, M., and Kane, W. H. (1992). Deletion analysis of recombinant human factor V. Evidence for a phosphatidylserine binding site in the second C-type domain. J. Biol. Chem. *267*, 4189-98.

Ortel, T. L., Moore, K. D., Quinn-Allen, M. A., Okamura, T., Sinclair, A. J., Lazarchick, J., Govindan, R., Carmagnol, F., and Kane, W. H. (1998). Inhibitory anti-factor V antibodies bind to the factor V C2 domain and are associated with hemorrhagic manifestations. Blood *91*, 4188-96.

Ortel, T. L., Quinn-Allen, M. A., Charles, L. A., Devore-Carter, D., and Kane, W. H. (1992). Characterization of an acquired inhibitor to coagulation factor V. Antibody binding to the second C-type domain of factor V inhibits the binding of factor V to phosphatidylserine and neutralizes procoagulant activity. J. Clin. Invest. *90*, 2340-7.

Ortel, T. L., Quinn-Allen, M. A., Keller, F. G., Peterson, J. A., Larocca, D., and Kane, W. H. (1994). Localization of functionally important epitopes within the second C-type domain of coagulation factor V using recombinant chimeras. J. Biol. Chem. *269*, 15898-905.

O'Toole, T. E., Mandelman, D., Forsyth, J., Shattil, S. J., Plow, E. F., and Ginsberg, M. H. (1991). Modulation of the affinity of integrin αIIbβ3 (GPIIb-IIIa) by the cytoplasmic domain of αIIb. Science *254*, 845-7.

Otwinowski, Z., and Minor, W. (1993). DENZO: a film processing for macromolecular crystallography (New Haven: Yale University).

P

Paborsky, L. R., and Harris, R. J. (1990). Post-translational modifications of recombinant human tissue factor. Thromb. Res. *60*, 367-76.

Padmanabhan, K., Padmanabhan, K. P., Tulinsky, A., Park, C. H., Bode, W., Huber, R., Blankenship, D. T., Cardin, A. D., and Kisiel, W. (1993). Structure of human des(1-45) factor Xa at 2.2 Å resolution. J. Mol. Biol. *232*, 947-66.

Padmanabhan, K., Wu, T. P., Ravichandran, K. G., and Tulinsky, A. (1994). Kringle-kringle interactions in multimer kringle structures. Protein Sci. *3*, 898-910.

Paesen, G. C., Adams, P. L., Harlos, K., Nuttall, P. A., and Stuart, D. I. (1999). Tick histamine-binding proteins: isolation, cloning, and three-dimensional structure. Mol. Cell *3*, 661-71.

Pan, Y., DeFay, T., Gitschier, J., and Cohen, F. E. (1995). Proposed structure of the A domains of factor VIII by homology modelling. Nature Struct. Biol. *2*, 740-4.

Parkinson, J. F., Nagashima, M., Kuhn, I., Leonard, J., and Morser, J. (1992). Structure-function studies of the epidermal growth factor domains of human thrombomodulin. Biochem. Biophys. Res. Commun. *185*, 567-76.

Parkinson, J. F., Vlahos, C. J., Yan, S. C., and Bang, N. U. (1992). Recombinant human thrombomodulin. Regulation of cofactor activity and anticoagulant function by a glycosaminoglycan side chain. Biochem. J. *283*, 151-7.

Parry, M. A., Fernandez-Catalan, C., Bergner, A., Huber, R., Hopfner, K. P., Schlott, B., Guhrs, K. H., and Bode, W. (1998). The ternary microplasmin-staphylokinase-microplasmin complex is a proteinase-cofactor-substrate complex in action. Nature Struct. Biol. *5*, 917-23.

Parry, M. A., Stone, S. R., Hofsteenge, J., and Jackman, M. P. (1993). Evidence for common structural changes in thrombin induced by active-site or exosite binding. Biochem. J. *290*, 665-70.

Patthy, L. (1990). Evolution of blood coagulation and fibrinolysis. Blood Coagul. Fibrinolysis *1*, 153-66.

Pedersen, L. C., Yee, V. C., Bishop, P. D., Le Trong, I., Teller, D. C., and Stenkamp, R. E. (1994). Transglutaminase factor XIII uses proteinase-like catalytic triad to crosslink macromolecules. Protein Sci. *3*, 1131-5.

Pegelow, C. H., Ledford, M., Young, J. N., and Zilleruelo, G. (1992). Severe protein S deficiency in a newborn. Pediatrics *89*, 674-6.

Pellequer, J. L., Gale, A. J., Griffin, J. H., and Getzoff, E. D. (1998). Homology models of the C domains of blood coagulation factors V and VIII - A proposed membrane binding mode for FV and FVIII C2 domains. Blood Cells, Molecules and Diseases *24*, 448-61.

Pemberton, S., Lindley, P., Zaitsev, V., Card, G., Tuddenham, E. G., and Kemball-Cook, G. (1997). A molecular model for the triplicated A domains of human factor VIII based on the crystal structure of human ceruloplasmin. Blood *89*, 2413-21.

Perona, J. J., and Craik, C. S. (1997). Evolutionary divergence of substrate specificity within the chymotrypsin-like serine protease fold. J. Biol. Chem. *272*, 29987-90.

Petersen, T. E. (1988). The amino-terminal domain of thrombomodulin and pancreatic stone protein are homologous with lectins. FEBS Lett. *231*, 51-3.

Petersen, T. E., Martzen, M. R., Ichinose, A., and Davie, E. W. (1990). Characterization of the gene for human plasminogen, a key proenzyme in the fibrinolytic system. J. Biol. Chem. *265*, 6104-11.

Petersen, T. E., Thlgersen, H. C., Sottrup-Jensen, L., Magnusson, S., and Jornvall, H. (1980). Isolation and N-terminal amino acid sequence of protein Z, a gamma-carboxyglutamic acid containing protein from bovine plasma. FEBS Lett. *114*, 278-82.

Phillips, D. R., Charo, I. F., Parise, L. V., and Fitzgerald, L. A. (1988). The platelet membrane glycoprotein IIb-IIIa complex. Blood *71*, 831-43.

Phillips, D. R., Charo, I. F., and Scarborough, R. M. (1991). GPIIb-IIIa: the responsive integrin. Cell *65*, 359-62.

Pike, A. C., Brzozowski, A. M., Roberts, S. M., Olsen, O. H., and Persson, E. (1999). Structure of human factor VIIa and its implications for the triggering of blood coagulation. Proc. Natl Acad. Sci. USA *96*, 8925-30.

Pittman, D. D., Tomkinson, K. N., and Kaufman, R. J. (1994). Post-translational requirements for functional factor V and factor VIII secretion in mammalian cells. J. Biol. Chem. *269*, 17329-37.

Pittman, D. D., Tomkinson, K. N., Michnick, D., Selighsohn, U., and Kaufman, R. J. (1994). Posttranslational sulfation of factor V is required for efficient thrombin cleavage and activation and for full procoagulant activity. Biochemistry *33*, 6952-9.

Plow, E. F., and Ginsberg, M. H. (1989). Cellular adhesion: GPIIb-IIIa as a prototypic adhesion receptor. Progr. Hemost. Thromb. *9*, 117-56.

Plow, E. F., Herren, T., Redlitz, A., Miles, L. A., and Hoover-Plow, J. L. (1995). The cell biology of the plasminogen system. FASEB J. *9*, 939-45.

Polgar, J., Hidasi, V., and Muszbek, L. (1990). Non-proteolytic activation of cellular protransglutaminase (placenta macrophage factor XIII). Biochem. J. *267*, 557-60.

Poncz, M., Eisman, R., Heidenreich, R., Silver, S. M., Vilaire, G., Surrey, S., Schwartz, E., and Bennett, J. S. (1987). Structure of the platelet membrane glycoprotein IIb. Homology to the alpha subunits of the vitronectin and fibronectin membrane receptors. J. Biol. Chem. *262*, 8476-82.

Ponting, C. P., Marshall, J. M., and Cederholm-Williams, S. A. (1992). Plasminogen: a structural review. Blood Coagul. Fibrinolysis *3*, 605-14.

Poole, S., Firtel, R. A., Lamar, E., and Rowekamp, W. (1981). Sequence and expression of the discoidin I gene family in *Dictyostelium discoideum*. J. Mol. Biol. *153*, 273-289.

Potempa, J., Korzus, E., and Travis, J. (1994). The serpin superfamily of proteinase inhibitors: structure, function, and regulation. J. Biol. Chem. *269*, 15957-60.

Pratt, K. P., Shen, B. W., Takeshima, K., Davie, E. W., Fujikawa, K., and Stoddard, B. L. (1999). Structure of the C2 domain of human factor VIII at 1.5 Å resolution. Nature *402*, 439-42.

Pusey, M. L., Mayer, L. D., Wei, G. J., Bloomfield, V. A., and Nelsestuen, G. L. (1982). Kinetic and hydrodynamic analysis of blood clotting factor V-membrane binding. Biochemistry *21*, 5262-9.

Pusey, M. L., and Nelsestuen, G. L. (1984). Membrane binding properties of blood coagulation Factor V and derived peptides. Biochemistry *23*, 6202-10.

Pytela, R., Pierschbacher, M. D., Ginsberg, M. H., Plow, E. F., and Ruoslahti, E. (1986). Platelet membrane glycoprotein IIb/IIIa: member of a family of Arg-Gly-Asp--specific adhesion receptors. Science *231*, 1559-62.

R

Ragni, M. V., Sinha, D., Seaman, F., Lewis, J. H., Spero, J. A., and Walsh, P. N. (1985). Comparison of bleeding tendency, factor XI coagulant activity, and factor XI antigen in 25 factor XI-deficient kindreds. Blood *65*, 719-24.

Ramakrishnan, V., Reeves, P. S., DeGuzman, F., Deshpande, U., Ministri-Madrid, K., DuBridge, R. B., and Phillips, D. R. (1999). Increased thrombin responsiveness in platelets from mice lacking glycoprotein V. Proc. Natl Acad. Sci. USA *96*, 13336-41.

Rand, M. D., Kalafatis, M., and Mann, K. G. (1994). Platelet coagulation factor Va: The major secretory platelet phosphoprotein. Blood *83*, 2180-90.

Rao, S. P., Poojary, M. D., Elliott, B. W., Jr., Melanson, L. A., Oriel, B., and Cohen, C. (1991). Fibrinogen structure in projection at 18 Å resolution. Electron density by co-ordinated cryo-electron microscopy and X-ray crystallography. J. Mol. Biol. *222*, 89-98.

Rao, Z., Handford, P., Mayhew, M., Knott, V., Brownlee, G. G., and Stuart, D. (1995). The structure of a Ca2+-binding epidermal growth factor-like domain - Its role in protein-protein interactions. Cell *82*, 131-41.

Rawlings, N. D., and Barrett, A. J. (1994). Families of serine peptidases. Methods Enzymol. *244*, 19-61.

Read, R. J. (1986). Improved coefficients for map calculation using partial structures with errors. Acta Crystallogr. A *42*, 140-9.

Rebay, I., Fleming, R. J., Fehon, R. G., Cherbas, L., Cherbas, P., and Artavanis-Tsakonas, S. (1991). Specific EGF repeats of Notch mediate interactions with Delta and Serrate: implications for Notch as a multifunctional receptor. Cell *67*, 687-99.

Reed, G. L., Matsueda, G. R., and Haber, E. (1992). Platelet factor XIII increases the fibrinolytic resistance of platelet-rich clots by accelerating the crosslinking of α2-antiplasmin to fibrin. Thromb. Haemost. *68*, 315-20.

Reid, K. B. (1983). Proteins involved in the activation and control of the two pathways of human complement. Biochem. Soc. Transactions *11*, 1-12.

Reitsma, P. H., Bernardi, F., Doig, R. G., Gandrille, S., Greengard, J. S., Ireland, H., Krawczak, M., Lind, B., Long, G. L., Poort, S. R., and et al. (1995). Protein C deficiency: a database of mutations, 1995 update. Thromb. Haemost. *73*, 876-89.

Reitsma, P. H., Poort, S. R., Bernardi, F., Gandrille, S., Long, G. L., Sala, N., and Cooper, D. N. (1993). Protein C deficiency: a database of mutations. Thromb. Haemost. *69*, 77-84.

Rejante, M. R., and Llinas, M. (1994). Solution structure of the epsilon-aminohexanoic acid complex of human plasminogen kringle 1. Eur. J. Biochem. *221*, 939-49.

Renatus, M., Engh, R. A., Stubbs, M. T., Huber, R., Fischer, S., Kohnert, U., and Bode, W. (1997). Lysine 156 promotes the anomalous proenzyme activity of tPA: X-ray crystal structure of single-chain human tPA. EMBO J. *16*, 4797-805.

Reutelingsperger, C. P., Kop, J. M., Hornstra, G., and Hemker, H. C. (1988). Purification and characterization of a novel protein from bovine aorta that inhibits coagulation. Inhibition of the phospholipid-dependent factor-Xa-catalyzed prothrombin activation, through a high-affinity binding of the anticoagulant to the phospholipids. Eur. J. Biochem. *173*, 171-8.

Rezaie, A. R. (1998). Elucidation of the structural basis for the slow reactivity of thrombin with plasminogen activator inhibitor-1. Biochemistry *37*, 13138-42.

Rezaie, A. R., Cooper, S. T., Church, F. C., and Esmon, C. T. (1995). Protein C inhibitor is a potent inhibitor of the thrombin-thrombomodulin complex. J. Biol. Chem. *270*, 25336-9.

Rezaie, A. R., and Esmon, C. T. (1994). Calcium inhibition of the activation of protein C by thrombin. Role of the P3 and P3' residues. Eur. J. Biochem. *223*, 575-9.

Rezaie, A. R., He, X., and Esmon, C. T. (1998). Thrombomodulin increases the rate of thrombin inhibition by BPTI. Biochemistry *37*, 693-9.

Rezaie, A. R., Mather, T., Sussman, F., and Esmon, C. T. (1994). Mutation of Glu-80 → Lys results in a protein C mutant that no longer requires Ca^{2+} for rapid activation by the thrombin-thrombomodulin complex. J. Biol. Chem. *269*, 3151-4.

Ribeiro, J. M., Hazzard, J. M., Nussenzveig, R. H., Champagne, D. E., and Walker, F. A. (1993). Reversible binding of nitric oxide by a salivary heme protein from a bloodsucking insect. Science *260*, 539-41.

Ribeiro, J. M. C., Schneider, M., and Guimaraes, J. A. (1995). Purification and characterization of prolixin S (nitrophorin 2), the salivary anticoagulant of the blood-sucking bug *Rhodnius prolixus*. Biochem. J. *308*, 243-9.

Ribeiro, J. M. C., and Walker, F. A. (1994). High affinity histamine-binding and antihistaminic activity of the salivary nitric oxide-carrying heme protein (nitrophorin) of *Rhodnius prolixus*. J. Exp. Med. *180*, 2251-7.

Ritchie, H., Robbie, L. A., Kinghorn, S., Exley, R., and Booth, N. A. (1999). Monocyte plasminogen activator inhibitor 2 (PAI-2) inhibits u-PA-mediated fibrin clot lysis and is cross-linked to fibrin. Thromb. Haemost. *81*, 96-103.

Rosen, E. D., Chan, J. C., Idusogie, E., Clotman, F., Vlasuk, G., Luther, T., Jalbert, L. R., Albrecht, S., Zhong, L., Lissens, A., Schoonjans, L., Moons, L., Collen, D., Castellino, F. J., and Carmeliet, P. (1997). Mice lacking factor VII develop normally but suffer fatal perinatal bleeding. Nature *390*, 290-4.

Rosenberg, R. D. (1995). The absence of the blood clotting regulator thrombomodulin causes embryonic lethality in mice before development of a functional cardiovascular system. Thromb. Haemost. *74*, 52-7.

Rosing, J., Bakker, H. M., Thomassen, M. C., Hemker, H. C., and Tans, G. (1993). Characterization of two forms of human factor Va with different cofactor activities. J. Biol. Chem. *268*, 21130-6.

Rosing, J., Hoekema, L., Nicolaes, G. A., Thomassen, M. C., Hemker, H. C., Varadi, K., Schwarz, H. P., and Tans, G. (1995). Effects of protein S and factor Xa on peptide bond cleavages during inactivation of factor Va and factor Va R506Q by activated protein C. J. Biol. Chem. *270*, 27852-8.

Rosing, J., Speijer, H., and Zwaal, R. F. (1988). Prothrombin activation on phospholipid membranes with positive electrostatic potential. Biochemistry *27*, 8-11.

Rosing, J., Tans, G., Govers-Riemslag, J. W., Zwaal, R. F., and Hemker, H. C. (1980). The role of phospholipids and factor Va in the prothrombinase complex. J. Biol. Chem. *255*, 274-83.

Roussel, A., and Cambillau, C. (1989). TurboFRODO in Sillicon Graphics geometry (Mountain View, CA: Sillicon Graphics).

Rouvinen, J., Rautiainen, J., Virtanen, T., Zeiler, T., Kauppinen, J., Taivainen, A., and Mantyjarvi, R. (1999). Probing the molecular basis of allergy. Three-dimensional structure of the bovine lipocalin allergen Bos d 2. J. Biol. Chem. *274*, 2337-43.

Ruf, W., and Edgington, T. S. (1994). Structural biology of tissue factor, the initiator of thrombogenesis in vivo. FASEB J. *8*, 385-90.

Ruggeri, Z. M., and Ware, J. (1993). von Willebrand factor. FASEB J. *7*, 308-16.

Ruggeri, Z. M., and Zimmerman, T. S. (1980). Variant von Willebrand's disease: characterization of two subtypes by analysis of multimeric composition of factor VIII/von Willebrand factor in plasma and platelets. J. Clin. Invest. *65*, 1318-25.

Ruoslahti, E., and Engvall, E. (1997). Integrins and vascular extracellular matrix assembly. J. Clin. Invest. *100*, S53-6.

Russell, S. D., and Roth, G. J. (1993). Pseudo-von Willebrand disease: a mutation in the platelet glycoprotein Ib α gene associated with a hyperactive surface receptor. Blood *81*, 1787-91.

Rydel, T. J., Ravichandran, K. G., Tulinsky, A., Bode, W., Huber, R., Roitsch, C., and Fenton, J. W. d. (1990). The structure of a complex of recombinant hirudin and human α-thrombin. Science *249*, 277-80.

Ryden, L. (1988). Evolution of blue copper proteins. Progr. Clin. Biol. Res. *274*, 349-66.

S

Sadler, J. E. (1998). Biochemistry and genetics of von Willebrand factor. Annu. Rev. Biochem. *67*, 395-424.

Sadler, J. E. (1997). Thrombomodulin structure and function. Thromb. Haemost. *78*, 392-5.

Sadler, J. E., and Davie, E. W. (1987). Hemophilia A, hemophilia B and von Willebrand's disease. In The molecular basis of blood diseases, G. Stamatoyannopoulos, A. W. Nienhuis, P. Leder and P. W. Majerus, eds. (Philadelphia: Saunders), pp. 575.

Sadler, J. E., Lentz, S. R., Sheehan, J. P., Tsiang, M., and Wu, Q. (1993). Structure-function relationships of the thrombin-thrombomodulin interaction. Haemostasis *23*, 183-93.

Saenko, E. L., Shima, M., Rajalakshmi, K. J., and Scandella, D. (1994). A role for the C2 domain of factor VIII in binding to von Willebrand factor. J. Biol. Chem. *269*, 11601-5.

Safa, O., Morrissey, J. H., Esmon, C. T., and Esmon, N. L. (1999). Factor VIIa/tissue factor generates a form of factor V with unchanged specific activity, resistance to activation by thrombin, and increased sensitivity to activated protein C. Biochemistry *38*, 1829-37.

Sakata, Y., and Aoki, N. (1980). Cross-linking of α2-plasmin inhibitor to fibrin by fibrin-stabilizing factor. J. Clin. Invest. *65*, 290-7.

Sakata, Y., and Aoki, N. (1982). Significance of cross-linking of α2-plasmin inhibitor to fibrin in inhibition of fibrinolysis and in hemostasis. J. Clin. Invest. *69*, 536-42.

Samis, J. A., Garrett, M., Manuel, R. P., Nesheim, M. E., and Giles, A. R. (1997). Human neutrophil elastase activates human factor V but inactivates thrombin-activated human factor V. Blood *90*, 1065-74.

Sampoli Benitez, B. A., Hunter, M. J., Meininger, D. P., and Komives, E. A. (1997). Structure of the fifth EGF-like domain of thrombomodulin: An EGF-like domain with a novel disulfide-bonding pattern. J. Mol. Biol. *273*, 913-26.

Santoro, S. A., and Zutter, M. M. (1995). The α2β1 integrin: a collagen receptor on platelets and other cells. Thromb. Haemost. *74*, 813-21.

Sauer, C. G., Gehrig, A., Warneke-Wittstock, R., Marquardt, A., Ewing, C. C., Gibson, A., Lorenz, B., Jurklies, B., and Weber, B. H. (1997). Positional cloning of the gene associated with X-linked juvenile retinoschisis. Nature Gen. *17*, 164-70.

Savage, C. R., Jr., Inagami, T., and Cohen, S. (1972). The primary structure of epidermal growth factor. J. Biol. Chem. *247*, 7612-21.

Schechter, I., and Berger, A. (1967). On the size of the active site in proteases. I. Papain. Biochem. Biophys. Res. Commun. *27*, 157-62.

Schmaier, A. H. (1997). Contact activation: a revision. Thromb. Haemost. *78*, 101-7.

Schreuder, H. A., de Boer, B., Dijkema, R., Mulders, J., Theunissen, H. J., Grootenhuis, P. D., and Hol, W. G. (1994). The intact and cleaved human antithrombin III complex as a model for serpin-proteinase interactions. Nature Struct. Biol. *1*, 48-54.

Schwartz, M. A., Schaller, M. D., and Ginsberg, M. H. (1995). Integrins: emerging paradigms of signal transduction. Annu. Rev. Cell Devel. Biol. *11*, 549-99.

Seeler, R. A. (1972). Parahemophilia. Factor V deficiency. Med. Clin. N. Am. *56*, 119-25.

Seigneuret, M., and Devaux, P. F. (1984). ATP-dependent asymmetric distribution of spin-labeled phospholipids in the erythrocyte membrane: relation to shape changes. Proc. Natl Acad. Sci. USA *81*, 3751-5.

Selander-Sunnerhagen, M., Ullner, M., Persson, E., Teleman, O., Stenflo, J., and Drakenberg, T. (1992). How an epidermal growth factor (EGF)-like domain binds calcium. High resolution NMR structure of the calcium form of the NH_2-terminal EGF-like domain in coagulation factor X. J. Biol. Chem. *267*, 19642-9.

Seshadri, T. P., Tulinsky, A., Skrzypczak-Jankun, E., and Park, C. H. (1991). Structure of bovine prothrombin fragment 1 refined at 2.25 Å resolution. J. Mol. Biol. *220*, 481-94.

Sevinsky, J. R., Rao, L. V., and Ruf, W. (1996). Ligand-induced protease receptor translocation into caveolae: a mechanism for regulating cell surface proteolysis of the tissue factor-dependent coagulation pathway. J. Cell Biol. *133*, 293-304.

Shao, X., Davletov, B. A., Sutton, R. B., Südhof, T. C., and Rizo, J. (1996). Bipartite Ca^{2+}-binding motif in C2 domains of synaptotagmin and protein kinase C. Science *273*, 248-51.

Shattil, S. J., and Brugge, J. S. (1991). Protein tyrosine phosphorylation and the adhesive functions of platelets. Curr. Opin. Cell Biol. *3*, 869-79.

Shattil, S. J., Kashiwagi, H., and Pampori, N. (1998). Integrin signaling: the platelet paradigm. Blood *91*, 2645-57.

Sheldrix, G.M. (1984). SHELX-84 - A program system for crystal-structure solution and refinement. Acta Crystallogr. A *40*, C440.

Shelton-Inloes, B. B., Titani, K., and Sadler, J. E. (1986). cDNA sequences for human von Willebrand factor reveal five types of repeated domains and five possible protein sequence polymorphisms. Biochemistry *25*, 3164-71.

Shen, L., and Dahlbäck, B. (1994). Factor V and protein S as synergistic cofactors to activated protein C in degradation of factor VIIIa. J. Biol. Chem. *269*, 18735-8.

Shen, L., Villoutreix, B. O., and Dahlbäck, B. (1999). Interspecies loop grafting in the protease domain of human protein C yielding enhanced catalytic and anticoagulant activity. Thromb. Haemost. *82*, 1078-87.

Shima, M., Scandella, D., Yoshioka, A., Nakai, H., Tanaka, I., Kamisue, S., Terada, S., and Fukui, H. (1993). A factor VIII neutralizing monoclonal antibody and a human inhibitor alloantibody recognizing epitopes in the C2 domain inhibit factor VIII binding to von Willebrand factor and to phosphatidylserine. Thromb. Haemost. *69*, 240-6.

Siess, W. (1989). Molecular mechanisms of platelet activation. Physiol. Rev. *69*, 58-178.

Simon, M. I., Strathmann, M. P., and Gautam, N. (1991). Diversity of G proteins in signal transduction. Science *252*, 802-8.

Sixma, J. J., van Zanten, G. H., Huizinga, E. G., van der Plas, R. M., Verkley, M., Wu, Y. P., Gros, P., and de Groot, P. G. (1997). Platelet adhesion to collagen: an update. Thromb. Haemost. *78*, 434-8.

Sixma, J. J., van Zanten, G. H., Saelman, E. U., Verkleij, M., Lankhof, H., Nieuwenhuis, H. K., and de Groot, P. G. (1995). Platelet adhesion to collagen. Thromb. Haemost. *74*, 454-9.

Skogen, W. F., Esmon, C. T., and Cox, A. C. (1984). Comparison of coagulation factor Xa and des-(1-44)factor Xa in the assembly of prothrombinase. J. Biol. Chem. *259*, 2306-10.

Skrzypczak-Jankun, E., Carperos, V. E., Ravichandran, K. G., Tulinsky, A., Westbrook, M., and Maraganore, J. M. (1991). Structure of the hirugen and hirulog 1 complexes of alpha-thrombin. J. Mol. Biol. *221*, 1379-93.

Smirnova, I. V., Zhang, S. X., Citron, B. A., Arnold, P. M., and Festoff, B. W. (1998). Thrombin is an extracellular signal that activates intracellular death protease pathways inducing apoptosis in model motor neurons. J. Neurobiol. *36*, 64-80.

Soejima, K., Kurihara, Y., Kamiya, K., and Umeyama, H. (1999). Dynamic character of the complex of human blood coagulation factor VIIa with the extracellular domain of human tissue factor: a normal mode analysis. FEBS Lett. *463*, 19-23.

Soff, G. A., and Levin, J. (1981). Familial multiple coagulation factor deficiencies. I. Review of the literature: Differentiation of single hereditary disorders associated with multiple factor deficiencies from coincidental concurrence of single factor deficiency states. Semin. Thromb. Hemost. *7*, 112-48.

Soff, G. A., Levin, J., and Bell, W. R. (1981). Familial multiple coagulation factor deficiencies. II. Combined factor VIII, IX, and XI deficiency and combined factor IX and

XI deficiency: two previously uncharacterized familial multiple factor deficiency syndromes. Semin. Thromb. Hemost. *7*, 149-69.

Sorbara, L. R., Davies-Hill, T. M., Koehler-Stec, E. M., Vannucci, S. J., Horne, M. K., and Simpson, I. A. (1997). Thrombin-induced translocation of GLUT3 glucose transporters in human platelets. Biochem. J. *328*, 511-6.

Spinelli, S., Ramoni, R., Grolli, S., Bonicel, J., Cambillau, C., and Tegoni, M. (1998). The structure of the monomeric porcine odorant binding protein sheds light on the domain swapping mechanism. Biochemistry *37*, 7913-8.

Spraggon, G., Everse, S. J., and Doolittle, R. F. (1997). Crystal structures of fragment D from human fibrinogen and its crosslinked counterpart from fibrin. Nature *389*, 455-62.

Spraggon, G., Phillips, C., Nowak, U. K., Ponting, C. P., Saunders, D., Dobson, C. M., Stuart, D. I., and Jones, E. Y. (1995). The crystal structure of the catalytic domain of human urokinase-type plasminogen activator. Structure *3*, 681-91.

Stearns, D. J., Kurosawa, S., and Esmon, C. T. (1989). Microthrombomodulin. Residues 310-486 from the epidermal growth factor precursor homology domain of thrombomodulin will accelerate protein C activation. J. Biol. Chem. *264*, 3352-6.

Stearns-Kurosawa, D. J., Kurosawa, S., Mollica, J. S., Ferrell, G. L., and Esmon, C. T. (1996). The endothelial cell protein C receptor augments protein C activation by the thrombin-thrombomodulin complex. Proc. Natl Acad. Sci. USA *93*, 10212-6.

Stec, B., Yamano, A., Whitlow, M., and Teeter, M. M. (1997). Structure of human plasminogen kringle 4 at 1.68 Å and 277 K - a possible structural role of disordered residues. Acta Crystallogr. D *53*, 169-78.

Steigemann, W. (1974). Die Entwicklung und Anwendung von Rechenverfahren und Rechenprogrammen zur Strukturanalyse von Proteinen am Beispiel des Trypsin-Trypsin Inhibitor Komplexen, des Freien Inhibitors und der L-Asparagine (München, Germany: TU).

Stein, D., and Nusslein-Volhard, C. (1992). Multiple extracellular activities in *Drosophila* egg perivitelline fluid are required for establishment of embryonic dorsal-ventral polarity. Cell *68*, 429-40.

Steitz, T. A., and Shulman, R. G. (1982). Crystallographic and NMR studies of the serine proteases. Annu. Rev. Biophys. Bioeng. *11*, 419-44.

Stenflo, J. (1999). Contributions of Gla and EGF-like domains to the function of vitamin K-dependent coagulation factors. Crit. Rev. Eukaryot. Gene Expression *9*, 59-88.

Stenflo, J., and Fernlund, P. (1982). Amino acid sequence of the heavy chain of bovine protein C. J. Biol. Chem. *257*, 12180-90.

Stetefeld, J., Mayer, U., Timpl, R., and Huber, R. (1996). Crystal structure of three consecutive laminin-type epidermal growth factor-like (Le) modules of laminin γ-1 chain harboring the nidogen binding site. J. Mol. Biol. *257*, 644-57.

Stitt, T. N., Conn, G., Gore, M., Lai, C., Bruno, J., Radziejewski, C., Mattsson, K., Fisher, J., Gies, D. R., Jones, P. F., et al. (1995). The anticoagulation factor protein S and its relative, Gas6, are ligands for the Tyro 3/Axl family of receptor tyrosine kinases. Cell *80*, 661-70.

Stoylova, S., Gray, E., Barrowcliffe, T. W., Kemball-Cook, G., and Holzenburg, A. (1998). Structural determination of lipid-bound human blood coagulation factor IX. Biochim. Biophys. Acta *1383*, 175-8.

Strader, C. D., Fong, T. M., Graziano, M. P., and Tota, M. R. (1995). The family of G-protein-coupled receptors. FASEB J. *9*, 745-54.

Stratikos, E., and Gettins, P. G. (1999). Formation of the covalent serpin-proteinase complex involves translocation of the proteinase by more than 70 Å and full insertion of the reactive center loop into beta-sheet A. Proc. Natl Acad. Sci. USA *96*, 4808-13.

Stratikos, E., and Gettins, P. G. (1997). Major proteinase movement upon stable serpin-proteinase complex formation. Proc. Natl Acad. Sci. USA *94*, 453-8.

Streusand, V. J., Bjork, I., Gettins, P. G., Petitou, M., and Olson, S. T. (1995). Mechanism of acceleration of antithrombin-proteinase reactions by low affinity heparin. Role of the antithrombin binding pentasaccharide in heparin rate enhancement. J. Biol. Chem. *270*, 9043-51.

Stubbs, J. D., Lekutis, C., Singer, K. L., Bui, A., Yuzuki, D., Srinivasan, U., and Parry, G. (1990). cDNA cloning of a mouse mammary epithelial cell surface protein reveals the existence of epidermal growth factor-like domains linked to factor VIII-like sequences. Proc. Natl Acad. Sci. USA *87*, 8417-21.

Stubbs, M. T., and Bode, W. (1994). Coagulation factors and their inhibitors. Curr. Opin. Struct. Biol. *4*, 823-32.

Stubbs, M. T., and Bode, W. (1993). A player of many parts: the spotlight falls on thrombin's structure. Thromb. Res. *69*, 1-58.

Stubbs, M. T., Oschkinat, H., Mayr, I., Huber, R., Angliker, H., Stone, S. R., and Bode, W. (1992). The interaction of thrombin with fibrinogen. A structural basis for its specificity. Eur. J. Biochem. *206*, 187-95.

Suh, T. T., Holmback, K., Jensen, N. J., Daugherty, C. C., Small, K., Simon, D. I., Potter, S., and Degen, J. L. (1995). Resolution of spontaneous bleeding events but failure of pregnancy in fibrinogen-deficient mice. Genes Dev. *9*, 2020-33.

Sun, J., Yamaguchi, M., Yuda, M., Miura, K., Takeya, H., Hirai, M., Matsuoka, H., Ando, K., Watanabe, T., Suzuki, K., et al. (1996). Purification, characterization and cDNA cloning of a novel anticoagulant of the intrinsic pathway, (prolixin-S) from salivary glands of the blood sucking bug, *Rhodnius prolixus*. Thromb. Haemost. *75*, 573-7.

Sun, W. Y., Witte, D. P., Degen, J. L., Colbert, M. C., Burkart, M. C., Holmback, K., Xiao, Q., Bugge, T. H., and Degen, S. J. (1998). Prothrombin deficiency results in embryonic and neonatal lethality in mice. Proc. Natl Acad. Sci. USA *95*, 7597-602.

Sunnerhagen, M., Forsen, S., Hoffren, A. M., Drakenberg, T., Teleman, O., and Stenflo, J. (1995). Structure of the Ca^{2+}-free Gla domain sheds light on membrane binding of blood coagulation proteins. Nature Struct. Biol. *2*, 504-9.

Sunnerhagen, M., Olah, G. A., Stenflo, J., Forsen, S., Drakenberg, T., and Trewhella, J. (1996). The relative orientation of Gla and EGF domains in coagulation factor X is altered by Ca^{2+} binding to the first EGF domain. A combined NMR-small angle X-ray scattering study. Biochemistry *35*, 11547-59.

Sutton, R. B., Davletov, B. A., Berghuis, A. M., Südhof, T. C., and Sprang, S. R. (1995). Structure of the first C2 domain of synaptotagmin I: a novel Ca^{2+}/phospholipid -binding fold. Cell *80*, 929-38.

Sutton, R. B., and Sprang, S. R. (1998). Structure of the protein kinase Cb phospholipid-binding C-2 domain complexed with Ca^{2+}. Structure *6*, 1395-405.

Suzuki, K., Dahlbäck, B., and Stenflo, J. (1982). Thrombin-catalyzed activation of human coagulation factor V. J. Biol. Chem. *257*, 6556-64.

Suzuki, K., Kusumoto, H., Deyashiki, Y., Nishioka, J., Maruyama, I., Zushi, M., Kawahara, S., Honda, G., Yamamoto, S., and Horiguchi, S. (1987). Structure and expression of human thrombomodulin, a thrombin receptor on endothelium acting as a cofactor for protein C activation. EMBO J. *6*, 1891-7.

Swairjo, M. A., Concha, N. O., Kaetzel, M. A., Dedman, J. R., and Seaton, B. A. (1995). Ca^{2+}-bridging mechanism and phospholipid head group recognition in the membrane-binding protein annexin V. Nature Struct. Biol. *2*, 968-74.

T

Tagliavacca, L., Moon, N., Dunham, W. R., and Kaufman, R. J. (1997). Identification and functional requirement of Cu(I) and its ligands within coagulation factor VIII. J. Biol. Chem. *272*, 27428-34.

Takahashi, N., Takahashi, Y., and Putnam, F. W. (1986). Primary structure of blood coagulation factor XIIIa (fibrinoligase, transglutaminase) from human placenta. Proc. Natl Acad. Sci. USA *83*, 8019-23.

Takahashi, Y., Hosaka, Y., Niina, H., Nagasawa, K., Naotsuka, M., Sakai, K., and Uemura, A. (1995). Soluble thrombomodulin purified from human urine exhibits a potent anticoagulant effect in vitro and in vivo. Thromb. Haemost. *73*, 805-11.

Taneda, H., Andoh, K., Nishioka, J., Takeya, H., and Suzuki, K. (1994). Blood coagulation factor Xa interacts with a linear sequence of the kringle 2 domain of prothrombin. J. Biochem. *116*, 589-97.

Tans, G., and Rosing, J. (1987). Structural and functional characterization of factor XII. Semin. Thromb. Hemost. *13*, 1-14.

Tegoni, M., Ramoni, R., Bignetti, E., Spinelli, S., and Cambillau, C. (1996). Domain swapping creates a third putative combining site in bovine odorant binding protein dimer. Nature Struct. Biol. *3*, 863-7.

Thim, L., Bjoern, S., Christensen, M., Nicolaisen, E. M., Lund-Hansen, T., Pedersen, A. H., and Hedner, U. (1988). Amino acid sequence and posttranslational modifications of human factor VIIa from plasma and transfected baby hamster kidney cells. Biochemistry *27*, 7785-93.

Thomas, D. W., Mannon, R. B., Mannon, P. J., Latour, A., Oliver, J. A., Hoffman, M., Smithies, O., Koller, B. H., and Coffman, T. M. (1998). Coagulation defects and altered hemodynamic responses in mice lacking receptors for thromboxane A2. J. Clin. Invest. *102*, 1994-2001.

Thompson, R. E., Mandle, R., Jr., and Kaplan, A. P. (1977). Association of factor XI and high molecular weight kininogen in human plasma. J. Clin. Invest. *60*, 1376-80.

Thorelli, E., Kaufman, R. J., and Dahlbäck, B. (1998). The C-terminal region of the factor V B-domain is crucial for the anticoagulant activity of factor V. J. Biol. Chem. *273*, 16140-5.

Titani, K., Takio, K., Handa, M., and Ruggeri, Z. M. (1987). Amino acid sequence of the von Willebrand factor-binding domain of platelet membrane glycoprotein Ib. Proc. Natl Acad. Sci. USA *84*, 5610-4.

Tollefsen, D. M., Majerus, D. W., and Blank, M. K. (1982). Heparin cofactor II. Purification and properties of a heparin-dependent inhibitor of thrombin in human plasma. J. Biol. Chem. *257*, 2162-9.

Toole, J. J., Knopf, J. L., Wozney, J. M., Sultzman, L. A., Buecker, J. L., Pittman, D. D., Kaufman, R. J., Brown, E., Shoemaker, C., Orr, E. C., et al. (1984). Molecular cloning of a cDNA encoding human antihaemiphilic factor. Nature *312*, 342-7.

Toomey, J. R., Kratzer, K. E., Lasky, N. M., Stanton, J. J., and Broze, G. J., Jr. (1996). Targeted disruption of the murine tissue factor gene results in embryonic lethality. Blood *88*, 1583-7.

Tracy, P. B., and Mann, K. G. (1987). Abnormal formation of the prothrombinase complex: factor V deficiency and related disorders. Hum. Pathol. *18*, 162-9.

Travis, J., and Salvesen, G. S. (1983). Human plasma proteinase inhibitors. Annu. Rev. Biochem. *52*, 655-709.

Tsiang, M., Jain, A. K., Dunn, K. E., Rojas, M. E., Leung, L. L., and Gibbs, C. S. (1995). Functional mapping of the surface residues of human thrombin. J. Biol. Chem. *270*, 16854-63.

Tsiang, M., Lentz, S. R., Dittman, W. A., Wen, D., Scarpati, E. M., and Sadler, J. E. (1990). Equilibrium binding of thrombin to recombinant human thrombomodulin: effect of hirudin, fibrinogen, factor Va, and peptide analogues. Biochemistry *29*, 10602-12.

Tsiang, M., Lentz, S. R., and Sadler, J. E. (1992). Functional domains of membrane-bound human thrombomodulin. EGF-like domains four to six and the serine/threonine-rich domain are required for cofactor activity. J. Biol. Chem. *267*, 6164-70.

Tsiang, M., Paborsky, L. R., Li, W. X., Jain, A. K., Mao, C. T., Dunn, K. E., Lee, D. W., Matsumura, S. Y., Matteucci, M. D., Coutre, S. E., et al. (1996). Protein engineering thrombin for optimal specificity and potency of anticoagulant activity in vivo. Biochemistry *35*, 16449-57.

Tsopanoglou, N. E., and Maragoudakis, M. E. (1999). On the mechanism of thrombin-induced angiogenesis. Potentiation of vascular endothelial growth factor activity on endothelial cells by up-regulation of its receptors. J. Biol. Chem. *274*, 23969-76.

Tulinsky, A., Park, C. H., and Rydel, T. J. (1985). The structure of prothrombin fragment 1 at 3.5-Å resolution. J. Biol. Chem. *260*, 10771-8.

Tulinsky, A., Park, C. H., and Skrzypczak-Jankun, E. (1988). Structure of prothrombin fragment 1 refined at 2.8 Å resolution. J. Mol. Biol. *202*, 885-901.

Turk, D. (1992). Weiterentwicklung eines Programms für Molekülgraphik und Elektronendichte-Manipulation und seine Anwendung auf verschiedene Protein-Strukturäufklarungen (München: Technische Universität).

U

Ullner, M., Selander, M., Persson, E., Stenflo, J., Drakenberg, T., and Teleman, O. (1992). Three-dimensional structure of the apo form of the N-terminal EGF-like module of blood coagulation factor X as determined by NMR spectroscopy and simulated folding. Biochemistry *31*, 5974-83.

Unger, V. M., Hargrave, P. A., Baldwin, J. M., and Schertler, G. F. (1997). Arrangement of rhodopsin transmembrane α-helices. Nature *389*, 203-6.

V

van de Locht, A., Bode, W., Huber, R., Le Bonniec, B. F., Stone, S. R., Esmon, C. T., and Stubbs, M. T. (1997). The thrombin E192Q-BPTI complex reveals gross structural rearrangements: implications for the interaction with antithrombin and thrombomodulin. EMBO J. *16*, 2977-84.

van de Locht, A., Lamba, D., Bauer, M., Huber, R., Friedrich, T., Kroger, B., Hoffken, W., and Bode, W. (1995). Two heads are better than one: crystal structure of the insect derived double domain Kazal inhibitor rhodniin in complex with thrombin. EMBO J. *14*, 5149-57.

van de Locht, A., Stubbs, M. T., Bode, W., Friedrich, T., Bollschweiler, C., Hoffken, W., and Huber, R. (1996). The ornithodorin-thrombin crystal structure, a key to the TAP enigma? EMBO J. *15*, 6011-7.

van de Waart, P., Bruls, H., Hemker, H. C., and Lindhout, T. (1983). Interaction of bovine blood clotting factor Va and its subunits with phospholipid vesicles. Biochemistry *22*, 2427-32.

van 't Veer, C., Butenas, S., Golden, N. J., and Mann, K. G. (1999). Regulation of prothrombinase activity by protein S. Thromb. Haemost. *82*, 80-7.

van Wijnen, M., Stam, J. G., van't Veer, C., Meijers, J. C., Reitsma, P. H., Bertina, R. M., and Bouma, B. N. (1996). The interaction of protein S with the phospholipid surface is essential for the activated protein C-independent activity of protein S. Thromb. Haemost. *76*, 397-403.

van Willigen, G., Hers, I., Gorter, G., and Akkerman, J. W. (1996). Exposure of ligand-binding sites on platelet integrin αIIb/β3 by phosphorylation of the β3 subunit. Biochem. J. *314*, 769-79.

Vehar, G. A., Keyt, B., Eaton, D., Rodriguez, H., O'Brien, D. P., Rotblat, F., Oppermann, H., Keck, R., Wood, W. I., Harkins, R. N. et al. (1984). Structure of human factor VIII. Nature *312*, 337-42.

Verdaguer, N., Corbalan-Garcia, S., Ochoa, W. F., Fita, I., and Gomez-Fernandez, J. C. (1999). Ca^{2+} bridges the C2 membrane-binding domain of protein kinase Cα directly to phosphatidylserine. EMBO J. *18*, 6329-38.

Verweij, C. L., Diergaarde, P. J., Hart, M., and Pannekoek, H. (1986). Full-length von Willebrand factor (vWF) cDNA encodes a highly repetitive protein considerably larger than the mature vWF subunit. EMBO J. *5*, 1839-47.

Vijayalakshmi, J., Padmanabhan, K. P., Mann, K. G., and Tulinsky, A. (1994). The isomorphous structures of prethrombin2, hirugen-, and PPACK-thrombin: changes accompanying activation and exosite binding to thrombin. Protein Sci. *3*, 2254-71.

Villoutreix, B. O., Blom, A. M., and Dahlbäck, B. (1999). Structural prediction and analysis of endothelial cell protein C/activated protein C receptor. Protein Eng. *12*, 833-40.

Villoutreix, B. O., Bucher, P., Hofmann, K., Baumgartner, S., and Dahlbäck, B. (1998). Molecular models for the two discoidin domains of human blood coagulation factor V. J. Mol. Modelling. *4*, 268-75.

Villoutreix, B. O., and Dahlbäck, B. (1998). Molecular model for the C-type lectin domain of human thrombomodulin. J. Mol. Modelling. *4*, 310-22.

Villoutreix, B. O., and Dahlbäck, B. (1998). Structural investigation of the A domains of human blood coagulation factor V by molecular modelling. Protein Sci. *7*, 1317-25.

Vincenot, A., Gaussem, P., Pittet, J. L., Debost, S., and Aiach, M. (1995). Amino acids 225-235** of the protein C serine-protease domain are important for the interaction with the thrombin-thrombomodulin complex. FEBS Lett. *367*, 153-7.

Vindigni, A., White, C. E., Komives, E. A., and Di Cera, E. (1997). Energetics of thrombin-thrombomodulin interaction. Biochemistry *36*, 6674-81.

Vinogradova, O., Haas, T., Plow, E. F., and Qin, J. (2000). A structural basis for integrin activation by the cytoplasmic tail of the α_{IIb}-subunit. Proc. Natl Acad. Sci. USA *97*, 1450-5.

Vlot, A. J., Koppelman, S. J., Bouma, B. N., and Sixma, J. J. (1998). Factor VIII and von Willebrand factor. Thromb. Haemost. *79*, 456-65.

Vogel, W., Gish, G. D., Alves, F., and Pawson, T. (1997). The discoidin domain receptor tyrosine kinases are activated by collagen. Mol. Cell *1*, 13-23.

Volkman, B. F., Anderson, M. E., Clark, K. D., Hayakawa, Y., Strand, M. R., andMarkley, J. L. (1999). Structure of the insect cytokine peptide plasmatocyte-spreading peptide 1 from *Pseudoplusia includens*. J. Biol. Chem. *274*, 4493-6.

Vu, T. K., Hung, D. T., Wheaton, V. I., and Coughlin, S. R. (1991). Molecular cloning of a functional thrombin receptor reveals a novel proteolytic mechanism of receptor activation. Cell *64*, 1057-68.

W

Wagner, D. D., and Marder, V. J. (1983). Biosynthesis of von Willebrand protein by human endothelial cells. Identification of a large precursor polypeptide chain. J. Biol. Chem. *258*, 2065-7.

Walker, F. J. (1981). Regulation of activated protein C by protein S. The role of phospholipid in factor Va inactivation. J. Biol. Chem. *256*, 11128-31.

Walker, F. J., and Fay, P. J. (1992). Regulation of blood coagulation by the protein C system. FASEB J. *6*, 2561-7.

Walsh, P. N. (1999). Platelets and factor XI bypass the contact system of blood coagulation. Thromb. Haemost. *82*, 234-42.

Walsmann, P., and Markwardt, F. (1985). On the isolation of the thrombin inhibitor hirudin. Thromb. Res. *40*, 563-9.

Walz, D. A., Hewett-Emmett, D., and Seegers, W. H. (1977). Amino acid sequence of human prothrombin fragments 1 and 2. Proc. Natl Acad. Sci. USA *74*, 1969-72.

Wang, W., Hendriks, D. F., and Scharpe, S. S. (1994). Carboxypeptidase U, a plasma carboxypeptidase with high affinity for plasminogen. J. Biol. Chem. *269*, 15937-44.

Wang, X., Lin, X., Loy, J. A., Tang, J., and Zhang, X. C. (1998). Crystal structure of the catalytic domain of human plasmin complexed with streptokinase. Science *281*, 1662-5.

Ware, J. (1998). Molecular analyses of the platelet glycoprotein Ib-IX-V receptor. Thromb. Haemost. *79*, 466-78.

Warren, D. L., Morrissey, J. H., and Neuenschwander, P. F. (1999). Proteolysis of blood coagulation factor VIII by the factor VIIa-tissue factor complex: generation of an inactive factor VIII cofactor. Biochemistry *38*, 6529-36.

Waxman, L., and Connolly, T. M. (1993). Isolation of an inhibitor selective for collagen-stimulated platelet aggregation from the soft tick *Ornithodoros moubata*. J. Biol. Chem. *268*, 5445-9.

Weichsel, A., Andersen, J. F., Champagne, D. E., Walker, F. A., and Montfort, W. R. (1998). Crystal structures of a nitric oxide transport protein from a blood-sucking insect. Nature Struct. Biol. *5*, 304-9.

Weiler-Guettler, H., Christie, P. D., Beeler, D. L., Healy, A. M., Hancock, W. W., Rayburn, H., Edelberg, J. M., and Rosenberg, R. D. (1998). A targeted point mutation in thrombomodulin generates viable mice with a prethrombotic state. J. Clin. Invest. *101*, 1983-91.

Weisel, J. W., Nagaswami, C., Young, T. A., and Light, D. R. (1996). The shape of thrombomodulin and interactions with thrombin as determined by electron microscopy. J. Biol. Chem. *271*, 31485-90.

Weiss, M. S., Abele, U., Weckesser, J., Welte, W., Schiltz, E., and Schulz, G. E. (1991). Molecular architecture and electrostatic properties of a bacterial porin. Science *254*, 1627-30.

Weiss, M. S., Metzner, H. J., and Hilgenfeld, R. (1998). Two non-proline *cis* peptide bonds may be important for factor XIII function. FEBS Lett. *423*, 291-6.

Wen, D. Z., Dittman, W. A., Ye, R. D., Deaven, L. L., Majerus, P. W., and Sadler, J. E. (1987). Human thrombomodulin: complete cDNA sequence and chromosome localization of the gene. Biochemistry *26*, 4350-7.

Wesselschmidt, R., Likert, K., Huang, Z., MacPhail, L., and Broze, G. J., Jr. (1993). Structural requirements for tissue factor pathway inhibitor interactions with factor Xa and heparin. Blood Coagul. Fibrinolysis *4*, 661-9.

Whisstock, J., Skinner, R., and Lesk, A. M. (1998). An atlas of serpin conformations. Trends Biochem. Sci. *23*, 63-7.

White, C. E., Hunter, M. J., Meininger, D. P., Garrod, S., and Komives, E. A. (1996). The fifth epidermal growth factor-like domain of thrombomodulin does not have an epidermal growth factor-like disulfide bonding pattern. Proc. Natl Acad. Sci. USA *93*, 10177-82.

Wilczynska, M., Fa, M., Ohlsson, P. I., and Ny, T. (1995). The inhibition mechanism of serpins. Evidence that the mobile reactive center loop is cleaved in the native protease-inhibitor complex. J. Biol. Chem. *270*, 29652-5.

Wildgoose, P., Nemerson, Y., Hansen, L. L., Nielsen, F. E., Glazer, S., and Hedner, U. (1992). Measurement of basal levels of factor VIIa in hemophilia A and B patients. Blood *80*, 25-8.

Wiman, B., and Wallen, P. (1975). Amino-acid sequence of the cyanogen-bromide fragment from human plasminogen that forms the linkage between the plasmin chains. Eur. J. Biochem. *58*, 539-47.

Wong, M. Y., Gurr, J. A., and Walsh, P. N. (1999). The second epidermal growth factor-like domain of human factor IXa mediates factor IXa binding to platelets and assembly of the factor X activating complex. Biochemistry *38*, 8948-60.

Wright, H. T. (1973). Activation of chymotrypsinogen-A. An hypothesis based upon comparison of the crystal structures of chymotrypsinogen-A and α-chymotrypsin. J. Mol. Biol. *79*, 13-23.

Wright, H. T. (1973). Comparison of the crystal structures of chymotrypsinogen-A and α-chymotrypsin. J. Mol. Biol. *79*, 1-11.

Wu, Q. Y., Sheehan, J. P., Tsiang, M., Lentz, S. R., Birktoft, J. J., and Sadler, J. E. (1991). Single amino acid substitutions dissociate fibrinogen-clotting and thrombomodulin-binding activities of human thrombin. Proc. Natl Acad. Sci. USA *88*, 6775-9.

Wu, S. Y., Perez, M. D., Puyol, P., and Sawyer, L. (1999). β-lactoglobulin binds palmitate within its central cavity. J. Biol. Chem. *274*, 170-4.

Wu, T. P., Padmanabhan, K., Tulinsky, A., and Mulichak, A. M. (1991). The refined structure of the ε-aminocaproic acid complex of human plasminogen kringle 4. Biochemistry *30*, 10589-94.

Wu, T. P., Padmanabhan, K. P., and Tulinsky, A. (1994). The structure of recombinant plasminogen kringle 1 and the fibrin binding site. Blood Coagul. Fibrinolysis *5*, 157-66.

Wun, T. C., Kretzmer, K. K., Girard, T. J., Miletich, J. P., and Broze, G. J., Jr. (1988). Cloning and characterization of a cDNA coding for the lipoprotein-associated coagulation inhibitor shows that it consists of three tandem Kunitz-type inhibitory domains. J. Biol. Chem. *263*, 6001-4.

X

Xu, J., Esmon, N. L., and Esmon, C. T. (1999). Reconstitution of the human endothelial cell protein C receptor with thrombomodulin in phosphatidylcholine vesicles enhances protein C activation. J. Biol. Chem. *274*, 6704-10.

Xu, J., Qu, D. F., Esmon, N. L., and Esmon, C. T. (2000). Metalloproteolytic release of endothelial cell protein C receptor. J. Biol. Chem. *275*, 6038-44.

Xu, W. F., Andersen, H., Whitmore, T. E., Presnell, S. R., Yee, D. P., Ching, A., Gilbert, T., Davie, E. W., and Foster, D. C. (1998). Cloning and characterization of human protease-activated receptor 4. Proc. Natl Acad. Sci. USA *95*, 6642-6.

Xue, J., Kalafatis, M., and Mann, K. G. (1993). Determination of the disulfide bridges in factor Va light chain. Biochemistry *32*, 5917-23.

Xue, J., Wu, Q., Westfield, L. A., Tuley, E. A., Lu, D., Zhang, Q., Shim, K., Zheng, X., and Sadler, J. E. (1998). Incomplete embryonic lethality and fatal neonatal hemorrhage caused by prothrombin deficiency in mice. Proc. Natl Acad. Sci. USA *95*, 7603-7.

Y

Yang, Z., Mochalkin, I., Veerapandian, L., Riley, M., and Doolittle, R. F. (2000). Crystal structure of native chicken fibrinogen at 5.5-Å resolution. Proc. Natl Acad. Sci. USA *97*, 3907-12.

Yau, W. M., Wimley, W. C., Gawrisch, K., and White, S. H. (1998). The preference of tryptophan for membrane interfaces. Biochemistry *37*, 14713-8.

Ye, J., Esmon, C. T., and Johnson, A. E. (1993). The chondroitin sulfate moiety of thrombomodulin binds a second molecule of thrombin. J. Biol. Chem. *268*, 2373-9.

Ye, J., Esmon, N. L., Esmon, C. T., and Johnson, A. E. (1991). The active site of thrombin is altered upon binding to thrombomodulin. Two distinct structural changes are detected by fluorescence, but only one correlates with protein C activation. J. Biol. Chem. *266*, 23016-21.

Yee, V. C., Pedersen, L. C., Bishop, P. D., Stenkamp, R. E., and Teller, D. C. (1995). Structural evidence that the activation peptide is not released upon thrombin cleavage of factor XIII. Thromb. Res. *78*, 389-97.

Yee, V. C., Pedersen, L. C., Le Trong, I., Bishop, P. D., Stenkamp, R. E., and Teller, D. C. (1994). Three-dimensional structure of a transglutaminase: human blood coagulation factor XIII. Proc. Natl Acad. Sci. USA *91*, 7296-300.

Yee, V. C., Pratt, K. P., Cote, H. C., Trong, I. L., Chung, D. W., Davie, E. W., Stenkamp, R. E., and Teller, D. C. (1997). Crystal structure of a 30 kDa C-terminal fragment from the γ chain of human fibrinogen. Structure *5*, 125-38.

Yegneswaran, S., Smirnov, M. D., Safa, O., Esmon, N. L., Esmon, C. T., and Johnson, A. E. (1999). Relocating the active site of activated protein C eliminates the need for its protein S cofactor. A fluorescence resonance energy transfer study. J. Biol. Chem. *274*, 5462-8.

Yegneswaran, S., Wood, G. M., Esmon, C. T., and Johnson, A. E. (1997). Protein S alters the active site location of activated protein C above the membrane surface. A fluorescence resonance energy transfer study of topography. J. Biol. Chem. *272*, 25013-21.

Yuan, Y., Dopheide, S. M., Ivanidis, C., Salem, H. H., and Jackson, S. P. (1997). Calpain regulation of cytoskeletal signaling complexes in von Willebrand factor-stimulated platelets. Distinct roles for glycoprotein Ib-V-IX and glycoprotein IIb-IIIa (integrin αIIbβ3) in von Willebrand factor-induced signal transduction. J. Biol. Chem. *272*, 21847-54.

Z

Zaitseva, I., Zaitsev, V., Card, G., Moshkov, K., Bax, B., Ralph, A., and Lindley, P. (1996). The X-ray structure of human serum ceruloplasmin at 3.1 Å - Nature of the copper centres. JBIC *1*, 15-23.

Zanotti, G., Berni, R., and Monaco, H. L. (1993). Crystal structure of liganded and unliganded forms of bovine plasma retinol-binding protein. J. Biol. Chem. *268*, 10728-38.

Zanotti, G., Ottonello, S., Berni, R., and Monaco, H. L. (1993). Crystal structure of the trigonal form of human plasma retinol-binding protein at 2.5 Å resolution. J. Mol. Biol. *230*, 613-24.

Zanotti, G., Panzalorto, M., Marcato, A., Malpeli, G., Folli, C., and Berni, R. (1998). Structure of pig plasma retinol-binding protein at 1.65 Å resolution. Acta Crystallogr. D *54*, 1049-52.

Zeng, Z. H., Castano, A. R., Segelke, B. W., Stura, E. A., Peterson, P. A., and Wilson, I. A. (1997). Crystal structure of mouse CD1 - an MHC-like fold with a large hydrophobic binding groove. Science. *277*, 339-45.

Zhang, E., St Charles, R., and Tulinsky, A. (1999). Structure of extracellular tissue factor complexed with factor VIIa inhibited with a BPTI mutant. J. Mol. Biol. *285*, 2089-104.

Zhang, Y., Ribeiro, J. M. C., Guimaraes, J. A., and Walsh, P. N. (1998). Nitrophorin-2: A novel mixed-type reversible specific inhibitor of the intrinsic factor-X activating complex. Biochemistry *37*, 10681-90.

Zhang, Y., Weiler-Guettler, H., Chen, J., Wilhelm, O., Deng, Y., Qiu, F., Nakagawa, K., Klevesath, M., Wilhelm, S., Bohrer, H., et al. (1998). Thrombomodulin modulates growth of tumor cells independent of its anticoagulant activity. J. Clin. Invest. *101*, 1301-9.

Zucker, M. B., and Nachmias, V. T. (1985). Platelet activation. Arteriosclerosis *5*, 2-18.

Zucker, S., Conner, C., DiMassmo, B. I., Ende, H., Drews, M., Seiki, M., and Bahou, W. F. (1995). Thrombin induces the activation of progelatinase A in vascular endothelial cells. Physiologic regulation of angiogenesis. J. Biol. Chem. *270*, 23730-8.

Zushi, M., Gomi, K., Honda, G., Kondo, S., Yamamoto, S., Hayashi, T., and Suzuki, K. (1991). Aspartic acid 349 in the fourth epidermal growth factor-like structure of human thrombomodulin plays a role in its Ca^{2+}-mediated binding to protein C. J. Biol. Chem. *266*, 19886-9.

Zushi, M., Gomi, K., Yamamoto, S., Maruyama, I., Hayashi, T., and Suzuki, K. (1989). The last three consecutive epidermal growth factor-like structures of human thrombomodulin comprise the minimum functional domain for protein C-activating cofactor activity and anticoagulant activity. J. Biol. Chem. *264*, 10351-3.

Zwaal, R. F., Comfurius, P., and Bevers, E. M. (1998). Lipid-protein interactions in blood coagulation. Biochim. Biophys. Acta *1376*, 433-53.

Zwaal, R. F., and Schroit, A. J. (1997). Pathophysiologic implications of membrane phospholipid asymmetry in blood cells. Blood *89*, 1121-32.

Die zu der vorliegenden Doktorarbeit zugrundeliegenden experimentelle Arbeit wurde im wesentlichen zwischen März 1996 und November 1999 in der Abteilung Strukturforschung des Max-Planck-Instituts für Biochemie durchgeführt. Es versteht sich von selbst –und soll trotzdem ausdrücklich erwähnt werden– daß diese Arbeit ohne die Mitwirkung von mehreren Personen nicht entstanden wäre. Frau Dr. Christiane Noeske-Jungblut (Research Laboratories of Schering AG, Berlin) hat rekombinantes Triabin überexprimiert und gereinigt. Ihr und Prof. Dr. Wolf-Dieter Schleuning möchte ich für die Zusammenarbeit am Triabin-Projekt danken. Unseren Kollegen in der Duke University, North Carolina, insbesondere Mrs. Mary-Ann Quinn-Allen, Dr. Tom Ortel und Prof. William Kane, danke ich für die langjährige, erfolgreiche Zusammenarbeit an die C2-Domäne von Faktor V. Unseren Kollegen von Berlex Biosciences (Richmond, California), und insbesondere Dr. David Light ist die Lösung der Thrombin-Thrombomodulin Struktur in hohem Maße zu verdanken.

Meinen Kollegen in Martinsried gebührt ein besonderer Dank. Doris Grosse war Jahre lang eine zuverlässige Mitarbeiterin. Viele (Pro)thrombin Präparationen hat sie fast im Alleingang gemacht. Darüber hinaus hat sie FVa-C2 in der ‘offenen’ Form kristallisiert. Frau Dr. Sandra Macedo-Ribeiro hat nicht nur die ‘geschlossene’ Kristallform von FVa-C2 kristallisiert, sondern auch entscheidend bei der Strukturaufklärung mitgewirkt. Frau Dr. Yoriko Iwanaga hat viele Kristallisationsansätze des Thrombin–Thrombomodulin Komplexes durchgeführt – darunter auch die, die zum ersten Mal brauchbare Kristalle brachten. Danke schön! Unseren Sekretärinnen Frau Gina Beckmann und Frau Renate Rüller danke ich für ihre Hilfe beim Einleben in München, für deren Nachfragen nach meinem Wohlergehen –und dafür, daß sie es geschafft haben, auch nicht statthafte Briefumschläge mit der Post wegzuschicken.

Die bearbeiteten Projekte standen bei Anregungen und/oder unter der Leitung von Prof. Wolfram Bode –und sind zweifelsohne ein Tribut zu seiner langjährigen Tätigkeit auf diesem Gebiet. Ihm möchte ich an dieser Stelle für die offene, fruchtbare Zusammenarbeit ganz herzlich danken.

Ein gewisser, selbst ernannter Journalist hat einmal geschrieben, daß er in die Vereinigten Staaten auswandern mußte, um einen Professor zu erleben, der selbst im Labor arbeitete. Da mußte ich lächeln – und nochmals bedenken,

was für einen unglaublichen Ansporn die ständige Mitwirkung eines Menschen darstellt, der schon alle Ruhm und Ehre erreicht hat, was die wissenschaftliche Welt anbieten kann. Prof. Robert Huber danke ich auch für die ständige Unterstützung – und dafür, daß er immer wieder die Fragen stellt, die den Kern eines wissenschaftlichen Problemes treffen / mögliche Unregelmäßigkeiten aufdecken. Aus einem anderen Grund gebührt ihm mein besonderer Dank – er hat an mir geglaubt, und mir (kann man es anders sagen?) ein zweites Lebens ermöglicht. Meine Dankberkeit dafür teilt er mit dem ehemaligen Mitarbeiter des deutschen Konsulats in Havanna, Herr Herbert Quelle. Damals ...

“Para el tigre, ¿qué es una raya más?”

(Dicho cubano, en la voz de Abel Poveda Tudela)